University of Bath

PHD

A study of the genetic control of photoenzymatic repair in Escherichia coli K-12

Smith, Anthony W.

Award date:
1987

Awarding institution:
University of Bath

Link to publication

Alternative formats
If you require this document in an alternative format, please contact:
openaccess@bath.ac.uk

Copyright of this thesis rests with the author. Access is subject to the above licence, if given. If no licence is specified above, original content in this thesis is licensed under the terms of the Creative Commons Attribution-NonCommercial 4.0 International (CC BY-NC-ND 4.0) Licence (https://creativecommons.org/licenses/by-nc-nd/4.0/). Any third-party copyright material present remains the property of its respective owner(s) and is licensed under its existing terms.

Take down policy
If you consider content within Bath's Research Portal to be in breach of UK law, please contact: openaccess@bath.ac.uk with the details. Your claim will be investigated and, where appropriate, the item will be removed from public view as soon as possible.

Download date: 05. May. 2023

A STUDY OF THE GENETIC CONTROL OF PHOTOENZYMATIC REPAIR IN *ESCHERICHIA COLI* K-12

THESIS

Submitted by Anthony W. Smith, B. Pharm., M.P.S.

for the degree of

Doctor of Philosophy of the University of Bath

1987

This research has been carried out in the School of Pharmacy and Pharmacology of the University of Bath under the supervision of

S. H. Moss, M.Sc., Ph.D., M.P.S.

COPYRIGHT

Attention is drawn to the fact that copyright of this thesis rests with its author. This copy of the thesis has been supplied on condition that anyone who consults it is understood to recognise that its copyright rests with its author and that no quotation from the thesis and no information derived from it may be published without the prior written consent of the author.

This thesis may be made available for consultation within the University Library and may be photocopied or lent to other libraries for the purpose of consultation.

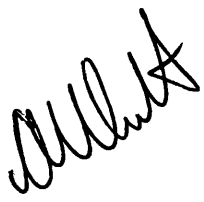

UMI Number: U000937

All rights reserved

INFORMATION TO ALL USERS
The quality of this reproduction is dependent upon the quality of the copy submitted.

In the unlikely event that the author did not send a complete manuscript
and there are missing pages, these will be noted. Also, if material had to be removed,
a note will indicate the deletion.

UMI U000937
Published by ProQuest LLC 2014. Copyright in the Dissertation held by the Author.
Microform Edition © ProQuest LLC.
All rights reserved. This work is protected against
unauthorized copying under Title 17, United States Code.

ProQuest LLC
789 East Eisenhower Parkway
P.O. Box 1346
Ann Arbor, MI 48106-1346

S015622

UNIVERSITY OF BATH
LIBRARY

23 - 5 JAN 1988

PHD

TO MY PARENTS

ACKNOWLEDGEMENTS

The author wishes to express his gratitude for the encouragement and guidance received from Dr. S. H. Moss throughout all stages of the work. His sincere thanks are due to Professor J. E. Rees for providing facilities for the research and to Dr. S. P. Moore and D. A. Vinicombe for their interest and advice.

The work was carried out with the aid of a Quota award from the Science and Engineering Research Council to whom the author also wishes to express gratitude.

His thanks are also due to Dr. P. Christie for his advice concerning the statistics, to the technical staff in the Media Preparation Laboratory and to Miss D. Sexton for typing the manuscript.

SUMMARY

In the work described in this thesis the photoreactivable responses of a series of strains mutated at one or both of the proposed *phr* loci have been determined after 254 nm UV inactivation and acetophenone-sensitized 313 nm UV inactivation in an attempt to determine if there are multiple genes and/or photolyase molecules present in *Escherichia coli* K-12.

The introduction includes a review of ultraviolet light-induced DNA damage and the repair mechanisms which act upon it. The experimental work is divided into four parts. The first section is concerned with the construction and mapping of mutants by bacteriophage P1-mediated transduction. In the second section the photoreactivable responses of excision-deficient strains mutated at one or both of the proposed *phr* loci have been compared. A Δ*phrA* mutant photoreactivated 254 nm UV-induced damage at a rate 40 per cent that of a *phr*$^+$ strain, whilst PR was demonstrated in a *phrB* which was absent when the mutation was transduced into a Δ*phrA* background. In Section III, the photoreactivable responses of totally dark-repair-deficient strains were compared. The *phr*$^+$ and *phrA* strains both exhibited biphasic repair kinetics after 254 nm UV- and acetophenone-sensitised 313 nm UV-induced damage, suggesting the existence of two repair activites. The temperature- and wavelength- dependence of the the photorepair in the *phrB* mutant suggested that the repair was mediated by a photolyase-like molecule. The Δ*phrA* *phrB* mutant did not exhibit a photoreactivable response after growth at 37^{o}C, but growth at 26^{o}C resulted in measurable photorepair. These data suggested that the Δ*phrA* *phrB* mutant could not be regarded as totally photoreactivation-deficient

and implicated the existence of another photolyase molecule from an unknown locus, or a temperature-dependent activity from the mutant *phrB* gene product. In the final section of the experimental work an attempt has been made to clone the proposed *phrA* gene. It was shown that a plasmid carrying a gene from the region purported to include the *phrA*$^+$ gene did increase the rate of photoreactivation in a Δ*phrA* strain.

The findings of these four experimental sections have been discussed in relation to the current concept of photoenzymatic repair *in vivo* and *in vitro* and suggest that the proposed *phrA*$^+$ gene does affect the rate of photoenzymatic repair but probably does not code for a photolyase molecule. However, the data do support the hypothesis that there is a second photolyase molecule, the locus of which is not known.

TABLE OF CONTENTS

		Page No.
INTRODUCTION		
1.1	Background	1
1.2	Ultraviolet radiation induced photoproducts	2
1.3	Ultraviolet-induced non-DNA damage	9
2.	DNA repair and damage tolerance	10
2.1.1	Enzymatic photoreactivation	11
2.1.2	Sensitized photoreversal	14
2.1.3	Indirect photoreactivation	14
2.1.4	Occurrence of PRE activity	15
2.1.5	Assay methods for PRE activity	16
2.1.6	The properties of DNA photolyases	18
2.2	Nucleotide excision repair	51
2.3	DNA damage tolerance and post-replication repair	57
2.4	The SOS regulatory system of *E. coli*	60
GENERAL METHODOLOGY		
1	Storage of organisms	65
2	Glassware	66
3	Water	66
4	Growth of organisms	67
5	Harvesting of organisms	68
6	Assessment of viability	70
7	Irradiation procedures	72
8	Radiation sources	74
9	Arrangement of optical bench	76
10	Analysis of emitted radiation	80
11	Procedure for UV irradiation	80

12 Determination of fluence rate 82

13 Acetophenone 84

14 Photoreactivation procedures 84

RESULTS AND DISCUSSION - PART I

1.1 Isolation of a P1::Tn9 lysogen 91

1.2 Lysogen induction 91

1.3 Determination of bacteriophage titer 92

1.4 Transduction 93

2. Construction of *phrB* derivatives 94

3. Construction of *recA* derivatives 95

4. Transduction mapping of *phrB* 97

5. Deletion analysis of the *chlA* to *gal* region 99

RESULTS AND DISCUSSION - PART II

2.1 Inactivation at 254 nm 100

2.2 Liquid holding recovery 108

2.3 Photoreactivation experiments 109

RESULTS AND DISCUSSION - PART III

3.1 Introduction 124

3.2 Inactivation with 254 nm radiation and high-intensity flash photolysis 125

3.3 Photoreactivation with continuous illumination 140

3.4 The dependence of photoenzymatic repair on temperature 159

3.5 The dependence of photoenzymatic repair on the wavelength of photoreactivating light 167

3.6 The dependence of photoenzymatic repair on pre-irradiation growth conditions 174

3.7 Photoreactivation after acetophenone-sensitised 313 nm UV radiation 205

SUMMARY 212

RESULTS AND DISCUSSION - PART IV

4.1 Isolation and selection protocol 224

4.2 Preparation of stock solutions 226

4.3 Preparation of organic reagents 229

4.4 Preparation of dialysis tubing 229

4.5 Enzymes 230

4.6 Agarose gel electrophoresis 232

4.7 Preparation of pBR322 plasmid DNA 235

4.8 Construction of a λ*dgal*λ specialised transducing 'phage 239

4.9 Cloning the *phrA* gene 251

4.10 Photoreactivation of AS46/pAS01 and DY326/pAS01 *in vivo* 257

4.11 Photoreactivation of AS44/pAS01 and AS44/pBR322 *in vivo* 265

CONCLUDING DISCUSSION 278

APPENDIX 1 289

APPENDIX 2 291

APPENDIX 3 293

APPENDIX 4 297

APPENDIX 5 374

BIBLIOGRAPHY 378

INTRODUCTION

1.1 Background

The environment presents a continual challenge to the integrity of our genetic material and so one of the principle functions of any cell is the prevention of an unacceptably high mutation rate. Many enzymatic mechanisms exist to ensure that the genetic material, deoxyribonucleic acid (DNA), is replicated with high fidelity and that repair activities recognise various alterations in DNA arising from ionizing radiations, ultraviolet from the sun and chemical agents. The study of ultraviolet radiation effects is of particular interest because organisms have always had to respond to the genotoxic effects of solar UV radiation.

The ultraviolet region of the electromagnetic spectrum is conveniently divided into far- (190-290 nm), mid- (290-320 nm) and near-UV (320-400 nm), and this terminology will be used throughout this work. However, the terms UVC (far-UV), UVB (mid-UV) and UVA (near-UV), are encountered in the literature (discussed by Jagger, 1985). Unlike gamma radiation and X-rays, the energy of ultraviolet radiation above 190 nm is insufficient to bring about electron ejection and hence ionization, but is sufficient to cause molecular excitation by promotion of electrons to higher-energy orbitals. The description of light as an electromagnetic wave is not adequate to explain the absorption and emission of light by molecules, and so is regarded as being quantized into discrete packets of energy called photons. The energy (E) of a photon is given by:-

$$E = hc/\lambda$$

where h is Planck's constant (6.624×10^{-34} J.s), λ is the

wavelength (m) and c is the velocity of light (3×10^8 $m.s.^{-1}$). Thus, the energy of a photon is inversely proportional to the wavelength, with the consequence that far-UV is considerably more energetic than near-UV.

1.2 Ultraviolet Radiation-Induced Photoproducts

The work of this thesis is primarily concerned with UV-induced DNA damage and this will be reviewed in detail here. However, it is important to remember that DNA is not the only target for UV damage so a brief review of non-DNA damage has been included for completeness.

In contrast to the earlier hypothesis that the cytotoxic effects of UV radiation increased with decreasing wavelength, Gates (1930) recognised that bacteria exhibited a maximum UV absorption at approximately 260 nm which, was associated with a concomitant increase in cell lethality. This suggested an interaction with a specific target molecule, which was later shown to be DNA. Many of the biological effects of UV radiation have now been attributed to the formation of specific photoproducts in DNA.

1.2.1 Cyclobutane-Type Dipyrimidine Dimers

When DNA is exposed to radiation at wavelengths approaching its absorption maximum (about 260 nm), adjacent pyrimidines become covalently linked through their 5,6 double-bonds to form a cyclobutane ring (Beukers and Berends, 1960). Although there are twelve possible isomeric cyclobuta- dipyrimidines, the cis-syn form is thought to predominate in B DNA (Kittler and Lober, 1977).

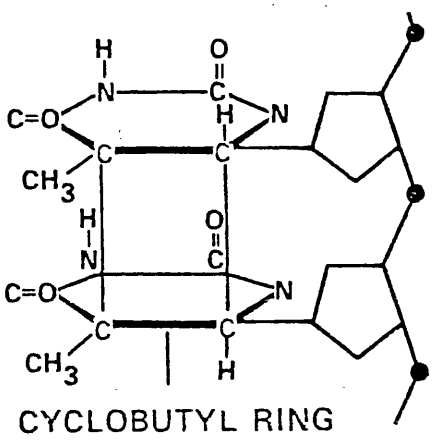

Figure 1. A cis-syn Cyclobutadipyrimidine dimer.

In addition to thymine-thymine (T-T) dimers, uracil-uracil (U-U), thymine-cytosine (T-C), uracil-thymine (U-T), cytosine-cytosine (C-C), and uracil-cytosine (U-C) dimers are also formed. Setlow and Carrier (1966) found that in 260 nm-irradiated E. coli, which has an approximately equal G-C and A-T content, the percentage ratio of cytosine-cytosine, cytosine-thymine and thymine-thymine dimers was 6, 26 and 68 per cent, respectively. Gordon and Haseltine (1982) have studied dimer formation in an end-labelled 117-bp segment of the E. coli lacI gene and found the steady-state value for formation of C-C dimers was reached at a 254 nm fluence of 500 Jm^{-2} , whilst the steady-state level for T-T dimers was not reached until the DNA had been exposed to fluences of about 2000 Jm^{-2}. In addition, the absolute level of dimerization varied at individual dimer sites. The level varied from less than 1 per cent at sites of potential C-C dimers to as high as 10 per cent for some T-T sites. In double-stranded DNA, the flanking nucleotides also had an effect on the steady-state level of dimer formation. The plateau level of dimerization was

greater for TT sequences flanked on both sides by adenosines than it was for TT sequences that were flanked on the 5' side by adenosine and on the 3' side by guanosine. While these studies show that pyrimidine dimer contents in a particular sequence of UV-irradiated DNA cannot necessarily be extrapolated to other irradiation conditions, the pyrimidine dimer remains the classic test lesion against which the effects of other UV-induced photoproducts are measured.

1.2.2 The Pyrimidine [6-4] Pyrimidone Photoproduct.

Lippke et al. (1981) reported the detection of alkali-labile sites in a defined sequence of UV-irradiated human DNA where a cytidine was 3' to a pyrimidine nucleoside. These sites were refractory to an apyrimidinic (AP) endonuclease and to *Micrococcus luteus* pyrimidine dimer endonuclease. The [6-4] photoproduct structure was suggested and is shown in Fig.2.

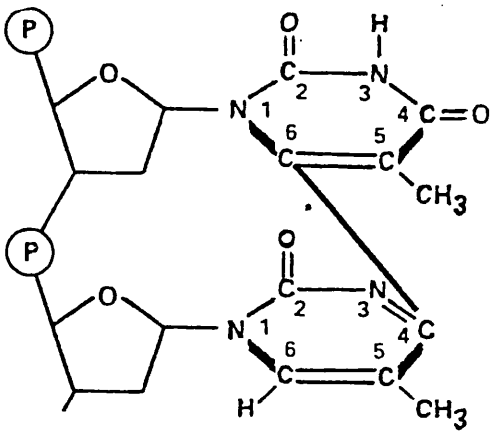

Figure 2. The Pyrimidine [6-4] Pyrimidone photoproduct

Lippke et al. (1981) found that the T-C [6-4] photoproduct was formed preferentially, followed by formation at C-C and T-T sites. In double-stranded DNA, [6-4] photoproduct formation was not

evident at C-T sequences (Franklin et al., 1982). Although the cyclobutane-type pyrimidine dimer is formed in approximately 10-fold greater abundance than the [6-4] photoproduct upon exposure of DNA to low fluences of 254 nm radiation (Lippke et al., 1981), the frequency distribution of dimers did not correlate with the frequency distribution of mutations observed in the lacI gene of E. coli (Brash and Haseltine, 1982). At certain sequences the rate of formation of the [6-4] photoproduct exceeded that of the cyclobutane pyrimidine dimer, even at very low UV fluences in the range 10-50 Jm^{-2}. Chan et al. (1986) measured the action spectrum for formation of [6-4] photoproducts and found it to be indistinguishable from the pyrimidine dimer-formation action spectrum. Below 300 nm, both action spectra closely paralleled the DNA absorption spectrum. More cyclobutane pyrimidine dimers were formed by far-UV than [6-4] photoproducts, but the ratio varied according to the site.

The correlation of [6-4] photoproducts with mutation hot-spots has heightened speculation that this photoproduct may be the most significant pre-mutagenic lesion (reviewed by Franklin and Haseltine, 1986). Tang et al. (1986) have compared the relative cytotoxicity and mutagenicity of cyclobutane-type pyrimidine dimers and [6-4] photoproducts in E. coli uvrA cells. Using photo-reactivation to remove all pyrimidine dimers they found that, at the same survival levels, photoreactivated cells had a higher mutation frequency than non-photoreactivated cells. They calculated that pyrimidine dimers and [6-4] photoproducts were equitoxic, but the latter were more mutagenic. Glickman et al. (1986) found that most mutations occurring at dipyrimidine lesions are recovered as G-C ⟶ A-T transitions. They proposed the

following explanation to account for this observation. The 5'-pyrimidine ring of the [6-4] photoproduct can still pair normally, but because the 3'-amino group of the pyrimidone ring has been transferred to the 5'-pyrimidine ring, the planar angle of this ring will not permit base-pairing in B DNA. The local distortion at the 3'-pyrimidone ring is similar to that envisaged at an apyrimidinic site, under which circumstances E. coli DNA polymerase preferentially inserts an adenine residue which causes a G-C $\longrightarrow$ A-T transition.

1.2.3 Pyrimidine Hydrates

The addition of a molecule of water across the 5-6 double bond of a pyrimidine base results in the formation of a 5,6-dihydro-6-hydroxy derivative (Fig. 3). Kittler and Lober (1977) found that the quantum yield for formation of cytosine hydrates in UV irradiated DNA was greater in single-stranded DNA compared with duplex DNA.

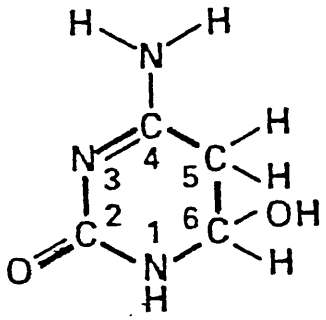

Figure 3. A 5,6-dihydro-6-hydroxycytosine.

These photoproducts have short-half lives and readily dehydrate to the parent form, leading to the conclusion that they are probably only of biological significance in areas of

single-strandedness, such as during replication and/or transcription of the DNA (Kittler and Lober, 1977).

1.2.4 Thymine Glycols

These lesions result from the saturation of the 5-6 double-bond of some pyrimidines (Fig. 4). This is one of the major forms of DNA base damage induced by ionizing radiation, but it can result from UV radiation (Demple and Linn, 1982).

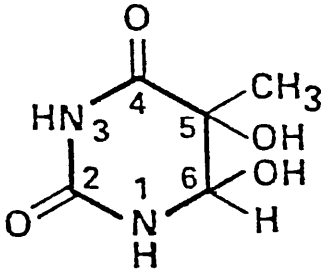

Figure 4. A 5,6-dihydroxy-5,6-dihydrothymine.

Clark and Beardsley (1986) found that cis-thymine glycols induced in single stranded M13mp9 DNA by osmium tetroxide, blocked DNA synthesis when using the Klenow fragment of DNA polymerase I or T4 DNA polymerase. Sequence analysis revealed that synthesis was halted after addition of the correct nucleotide (i.e. A opposite T), suggesting that the lesion may not be premutagenic.

1.2.5 DNA-Protein Crosslinks

There is a fluence-dependent decrease in the amount of DNA that can be extracted free of protein from both prokaryotic and eukaryotic cells. However, treatment with trypsin yields free DNA, suggesting that the DNA has become cross-linked with protein. The mechanism is not known, but may result from photoproduct formation

between thymine and cysteine. Peak et al. (1985) have constructed an action spectrum for the induction of DNA-protein cross-links in human cells. Below 290 nm the spectrum coincides with the DNA absorption spectrum, suggesting a direct photon-absorption event. However, deviation from the DNA spectrum above 290 nm implies the participation of as-yet-unidentified chromophores other than DNA. Below 320 nm, Peak et al. (1985) estimated that there was approximately 1 DNA-protein cross-link per 2 x 10^4 dimers, or about 40 DNA-protein cross-links per lethal event. The authors were unable to conclude whether DNA- protein cross-links are lethal lesions.

1.2.6 Miscellaneous UV-induced DNA Photoproducts

Other photoproducts which have been proposed include a lesion formed between two or more adjacent adenine residues in polyadenylic acid (Porsche, 1973) and a photoaddition product between adjacent adenine and thymine bases (Bose and Davies, 1984). Recently, Gallagher and Duker (1986) have reported the detection of purine photoproducts in a defined sequence of human DNA irradiated with a broad band mercury light source (250-400 nm). Incubation of the irradiated DNA with endonuclease V (the *denV* gene product of 'phage T4 infected *E. coli*), produced incision at purine loci, suggesting the existence of purine photoproducts, possibly dimers.

1.2.7 Sensitized UV-Induced Base Damage

The most important photosensitized reactions are those resulting in the formation of thymine dimers in DNA by triplet

excitation transfer. Lamola and Yamane (1967) reported that 313 nm irradiation of deoxygenated aqueous solutions containing DNA and acetophenone lead to the efficient formation of thymine dimers. The lowest triplet state of acetophenone is slightly higher than that of thymine, but lower than the triplet states of the other bases. Hence the triplet energy of the excited photosensitizer is transferred to thymine, facilitating the formation of T-T dimers. Lamola (1969) found the initial rates of production of T-T and C-C dimers to be 1.00 and 0.03, respectively. Lamola (1969) concluded that whilst 254 nm irradiation of DNA results in a steady state of approximately 7 per cent of thymine dimerized, irradiation at 313 nm in the presence of acetophenone can yield T-T dimers at a level close to the theoretic maximum. Using photoreactivation as a measure of the extent of pyrimidine dimer damage, Hodges et al. (1980) found the photoreactivation sector (PRS) of the UV-sensitive mutant E. coli K-12 AB2480 to be 0.98 after acetophenone-sensitized 313 nm radiation compared with 0.818 after 254 nm irradiation, indicating a significantly greater proportion of photoreactivable damage after sensitized irradiation.

1.3. Ultraviolet-induced Non-DNA Damage

Whilst the action spectra for lethality in many species have been shown to closely follow the absorbance of DNA up to 313 nm, beyond this many of the lethal responses are probably due to photon absorption by other chromophores causing either DNA molecular alterations or other effects lethal to the cell. The targets for near-UV killing have been reviewed by Jagger (1985) and include DNA itself, DNA repair systems and membranes. To amplify briefly on one of these points, Tyrrell et al. (1973) have demonstrated

destruction of the E. coli photoreactivating enzyme by 365 nm radiation. Similarly, Tyrrell and Webb (1973) found the ability of E. coli B/r to excise 254 nm-radiation-induced pyrimidine dimers from its DNA was also progressively reduced as a function of the fluence of 365 nm radiation. Both of these findings, and the observation that near-UV radiation survival curves exhibit large shoulders before dropping off steeply at higher fluences, suggests that damage to DNA repair systems may be an important factor in determining ultraviolet radiation lethality.

2 DNA Repair and Damage Tolerance

DNA repair mechanisms can be separated into two classes; those which recognise and repair damage prior to replication, namely photoreactivation and nucleotide excision repair, and those which facilitate tolerance of persisting damage during and after replication. This latter process is referred to as post-replication repair. The nature of this thesis demands a comprehensive review of the literature concerning photoenzymatic repair, so the processes of excision repair and post-replication repair can only be treated briefly. However, it must be remembered that these processes respond to a variety of damaging agents in addition to UV radiation, and so their overall importance as DNA repair mechanisms should be emphasised.

2.1 Enzymatic Photoreactivation

Introduction and Background

Enzymatic photoreactivation (EPR) may be conveniently defined as the repair of UV-induced photoproducts *in situ* by the combined action of a photoreactivating enzyme (PRE) and visible light. This definition does, however, have to be broadened to include the EPR of UV-type damage induced by ionizing radiation (reviewed by Redpath, 1986).

Although the antagonism of UV-radiation and visible light had already been recognised (Whittaker, 1942), the systematic study of EPR did not begin until the late 1940s with the simultaneous publications by Albert Kelner and Renato Dulbecco. Whilst investigating the effect of post-irradiation temperature on the UV-survival of *Streptomyces griseus* conidia, Kelner (1949) reported that exposure of UV-irradiated suspensions to visible light resulted in an increase in survival rate, whereas controls kept in the dark did not. Dulbecco (1949) reported a similar observation with UV-irradiated T-bacteriophages in *E. coli* and coined the term 'photoreactivation'.

Rupert et al. (1958) used crude cell extracts and the *Haemophilus influenzae* transformation assay to measure PRE activity *in vitro*. These data suggested the photorepairable lesion was situated in the DNA and that the agent was enzymatic in nature.

Claud Rupert developed a reaction scheme for the photoreactivating enzyme complexing with the substrate based on Michaelis-Menten kinetics (Rupert, 1962a,b). A schematic illustration of the reaction is shown in Fig. 5.

At this time the nature of the substrate was not known. Beukers and Berends (1960) and Wang (1960) found that UV-

1). Pyrimidine dimer in UV-irradiated DNA

2). Complex of DNA with photoreactivating enzyme

3). Absorption of light

4). Release of enzyme to restore native DNA

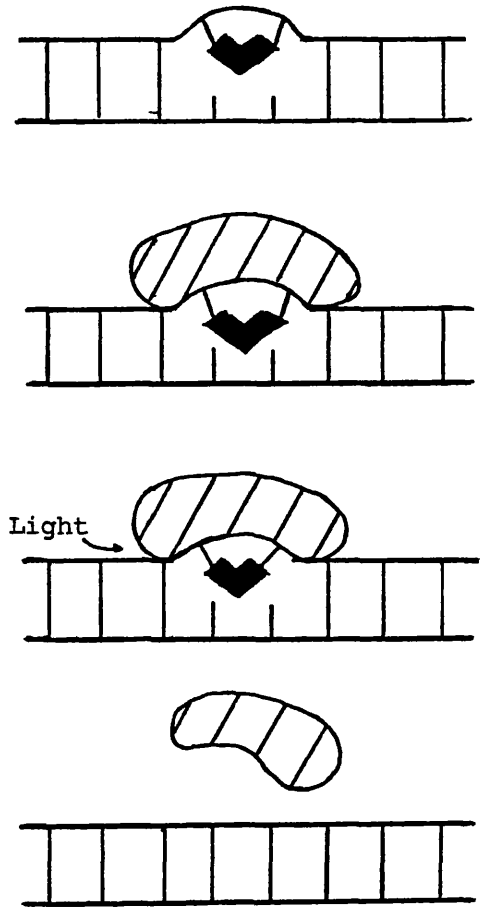

FIG.5. Schematic illustration of the photoreactivation of ultraviolet-induced pyrimidine dimers in DNA.

irradiation of a frozen thymine solution yielded a dimeric thymine photoproduct which was identical to the main photoproduct in UV-irradiated DNA. Subsequent irradiation of the thawed solution led to the reappearance of the characteristic thymine absorption spectrum. The authors suggested this reversible alteration of DNA by UV-radiation might be related to biological photoreactivation, however, Wang (1960) showed that irradiation of thymine dimers in solution with 370 nm photoreactivating light did not lead to the reappearance of thymine monomers. Wulff and Rupert (1962) were able to show loss of thymine dimers from ^{3}H-thymine-labelled DNA by the combined action of a cell-free extract of bakers' yeast and photoreactivating light. This suggested that enzymatic photoreactivation involved the splitting of pyrimidine dimers into their constituent monomers, and was proven by the work of Setlow and Setlow (1962).

At this point a distinction should be drawn between enzymatic photoreactivation (Fig. 5) and other examples of light-dependent recovery including direct photoreversal, sensitized photoreversal and indirect photoreactivation. As discussed above, direct or short-wavelength reactivation, in which transforming DNA inactivated with 280 nm light is partially reactivated by irradiation with 239 nm UV, occurs due to a shift in the equilibrium between the thymine monomer and cyclobutane-type dimer in favour of the monomer (see Fig. 6 and Section 1.2.1).

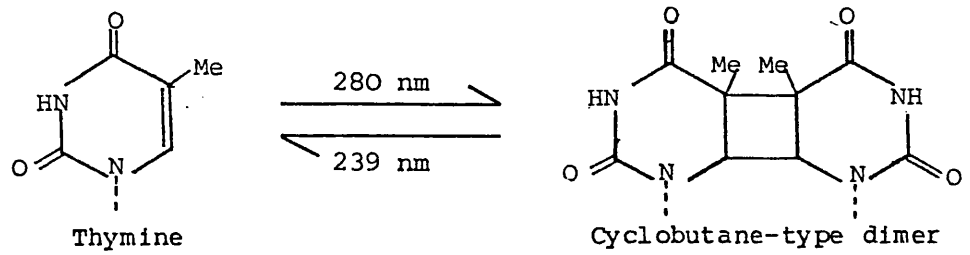

Thymine — Cyclobutane-type dimer

Figure 6. Reversible photodimerization of thymine.

2.1.2 Sensitized Photoreversal

This process has been observed with tryptophan and tryptophan-containing oligopeptides such as lys-trp-lys, as well as the tryptophan-rich protein coded by gene 32 of 'phage T4 (reviewed by Helene et al., 1978). The mechanism is thought to proceed via a base-stacking interaction of the tryptophanyl residue with a pyrimidine dimer, which facilitates electron transfer from the excited indole ring to the dimer. This phenomenon is not observed with wavelengths above 300 nm and is thus distinguished from 'true' EPR.

2.1.3 Indirect Photoreactivation

This phenomenon became apparent when photoreactivation was observed with 254 nm UV irradiated E. coli Bphr, a strain lacking photoreactivating enzyme. The effect did not occur with 405 nm photoreactivating light and was not due to splitting of thymine dimers (Jagger et al., 1969). In contrast to EPR, these workers suggested that this 'indirect' photoreactivation resulted from enhancement of dark repair processes. This was subsequently proven by Ramabhadran and Jagger (1976) who demonstrated that near-UV irradiation induced a growth delay which facilitated the excision repair process. The mechanism of near-UV radiation-induced growth delay has been reviewed Jagger (1985). Briefly, near-UV radiation induces a photoadduct between 4-thiouridine in the 8-position and a cytidine in the 13-position of certain rare forms of tRNA. This lowers the rate at which the tRNA accepts amino acids, which in turn decreases the rate of protein synthesis. The presence of uncharged tRNAs in the cell leads to an increase in the levels of guanosine tetraphosphate (ppGpp), and guanosine pentaphosphate

(ppGppp) and a decrease in the rate of stable RNA accumulation with consequent growth delay.

This phenomenon should not be confused with the light enhancement of PRE activity in Saccharomyces cerevisiae, discussed in Section 2.1.6.1.

2.1.4 Occurrence of DNA Photoreactivating Enzyme Activity

Photoreactivating enzyme (PRE) or DNA photolyase (EC 4.1.99.3) has been detected in many organisms by a variety of assay methods (discussed below). Considering the role of UV radiation as a source of genetic damage in biological evolution it is not surprising that organisms have developed specific methods for the repair of pyrimidine dimers. This is reflected in the near ubiquity of PRE. The phylogenetic distribution of PRE has been reviewed by Rupert (1975). Specific examples include the blue-green alga, Anacystis nidulans (Saito and Werbin, 1970); the colon bacterium Escherichia coli (Rupert et al., 1958); the soil actinomycete Streptomyces griseus (Eker, 1978), bakers' yeast, Saccharomyces cerevisiae (Rupert, 1960a,b) and in several mammalian species including the American opossum Didelphis marsupialis (Cook and Regan, 1969); the rabbit, Oryctolagus cuniculus (H. Harm, unpublished), and human cells (Sutherland and Sutherland, 1975). Whilst evidence has been published for the presence of DNA photolyase in cell extracts of placental mammals, the phenomenon of enzymatic photoreactivation in human cells is controversial. Detailed consideration of the evidence for photoreactivation in human cells will be given later. Interestingly, PRE activity has been demonstrated in tissues which are not normally exposed to light, including a report by Woodhead and Achey (1979) that PRE is

present in the blind cavefish Anoptichthys jordani, which lost the eyes in a degenerative adaptation to the dark environment. This raises the question whether it is possible that PRE has another function in the cell besides photoreactivation. With the exception of the finding of Yamamoto et al. (1983a) that PRE enhances excision repair in recA strains of E. coli (discussed in Section 2.2), no definite clues have been found for this supposition.

2.1.5 Assay Methods for Photoreactivating Enzyme Activity

Besides various biological criteria used for in vivo studies, several methods have been developed for the measurement of photoreactivating enzyme activity in vitro.

2.1.5.1 Transformation Assay

In this assay a purified transforming DNA, often from Haemophilus influenzae, carrying a known genetic marker (e.g. streptomycin resistance), is UV irradiated and incubated with preparations of DNA photolyase in the presence of photoreactivating light in vitro. The cells of a streptomycin-sensitive strain are made competent (i.e. able to take up, incorporate and express exogenous DNA) and the number of streptomycin-resistant transformants determined. The PRE activity is quantified by the increase in number of transformants compared with the control incubated in the dark.

2.1.5.2 Membrane-Binding Assay

Madden et al. (1973) developed the membrane-binding assay based on the fact that whilst photoreactivating wavelengths of

light are required for the splitting of pyrimidine dimers by all known DNA photolyases, the binding of the PRE to dimers in duplex DNA occurs in the dark. They incubated UV-irradiated [^{3}H]-labelled bacteriophage T7 DNA with purified yeast photolyase in the dark, and filtered the mixture through a nitrocellulose membrane filter. The PRE-UV-DNA complex is retained on the filter and the amount of radioactivity bound to the filter is proportional to the PRE concentration. Whilst this assay is useful for purified photolyase preparations, it has the disadvantage that in cruder preparations other proteins having non-specific DNA-binding activity may cause significant interference.

2.1.5.3 Oligonucleotide Assay

Sutherland and Chamberlin (1973) developed the oligonucleotide assay based on the unique resistance of the intra-dimer nucleotide phosphate bond to hydrolysis by pancreatic DNaseI, snake venom phosphodiesterase and alkaline phosphatase. Bacteriophage T7 DNA, labelled with ^{32}P, was UV-irradiated and incubated with cell extracts containing PRE in the light or dark. The DNA was digested to completion with the three enzymes discussed above, and passed through activated charcoal. Only ^{32}P-labelled, dimer-containing oligonucleotides were retained, and so the amount of bound ^{32}P radioactivity was representative of the concentration of pyrimidine dimers. DNA photolyase activity was determined from the loss of charcoal-bound ^{32}P oligonucleotides due to dimer monomerization. Farland and Sutherland (1979) modified the technique to measure the radioactivity of ^{3}H-oligonucleotides bound to DEAE-substituted paper discs.

2.1.5.4 RNA Polymerase Assay

Pyrimidine dimers in UV-irradiated DNA reduce the template activity for RNA transcription by *E. coli* RNA polymerase *in vitro*. Piessens and Eker (1975) demonstrated that enzymatic photoreactivation of the dimer-containing DNA resulted in increased ribonucleotide incorporation into RNA, and quantified this as an assay for DNA photolyase activity.

2.1.5.5 UV-Endonuclease Assay

The existence of nucleases which introduce single-strand breaks at the sites of specific damage has been recognised (Patrick and Harm, 1973). An example is the *Micrococcus luteus* UV-endonuclease which is specific for *cis-syn* pyrimidine dimers (Ahmed and Setlow, 1979). The number of pyrimidine dimers in UV-irradiated DNA can be quantified by treatment with the UV-endonuclease and analysis by alkaline gel-electrophoresis (Achey et al, 1979). DNA photolyase activity can be detected as a decrease in the number of UV-endonuclease sensitive sites (ESS) in UV-irradiated DNA.

2.1.6 The Properties of DNA Photolyases

DNA photolyase activity has been determined in many organisms (Section 2.1.4), but much of our knowledge is based on the characterisation of photoenzymatic repair in *S. cerevisiae* (bakers' yeast), *Streptomyces griseus*, *E. coli* and human cells. It is pertinent to discuss these studies in greater detail.

2.1.6.1 *Saccharomyces cerevisiae* enzyme.

Saccharomyces cerevisiae was one of the first organisms in which DNA photolyase activity was studied using crude cell

extracts. This was in part due to the relatively low cellular levels of nucleases which allowed the use of the transforming DNA assay (Rupert, 1960) and the advantages of using a commercially available source of bakers' yeast for large scale preparation of cell extracts.

However, problems appeared in the purification procedures resulting in enzyme preparations with apparently different activities and spectral properties. This has led to the suggestion that yeast cells have multiple photoreactivating enzymes, and the literature supports the hypothesis that there are two species of PRE molecules. Before reviewing the *in vitro* properties of these enzymes it is pertinent to discuss the *in vivo* data which are indicative of two molecules.

Fukui and Laskowski (1984a,b,1985) have adduced indirect evidence for the existence of three distinct types of photolyase molecules in cells of an excision-deficient haploid strain. Using the flash-photolysis method of Harm et al. (1971) they determined the number of PRE molecules per cell after growth at different temperatures, with or without illumination, by holding cells in buffer with or without illumination, and with or without cycloheximide present. These results led Fukui and Laskowski (1985) to conclude that yeast cells may contain three classes of PRE molecules, PRE_A normally active; PRE_B, normally inactive but which becomes activated by pre-illumination with light flashes or by buffer-holding in the dark, and PRE_C which requires buffer holding with continuous illumination for at least 24 hours to become active. Activation of PRE_C was prevented by cycloheximide. Johnson and Haynes (1986a) developed a method for analyzing the kinetics of survival-enhancement by continuous illumination and

used this to check the findings of Fukui and Laskowski (Johnson and Haynes, 1986b). Their analyses supported the hypothesis that there are three PRE species in a sensitive haploid strain. MacQuillan et al. (1981) isolated a mutant of S. cerevisiae which had a low capacity for photoreactivation of UV-induced lethal damage. In vivo complementation was shown in crosses with phr1 strains, whilst tetrad analysis and back crosses suggested the new mutation defined a second gene phr2, which is loosely linked to the phr1 gene.

Bakers' Yeast Enzyme I

A photoreactivating enzyme from bakers' yeast was purified 70,000-fold by Minato and Werbin (1971), the final preparative procedure being chromatography on far-UV-irradiated DNA non-covalently bound to cellulose. The enzyme preparation absorbed near-UV light between 350 and 420 nm with a maximum absorbance at 380 nm. Maxima at 385 and 485-490 nm appeared in its excitation and fluorescence spectra, respectively. The fluorescent material was not removed from the enzyme by chromatography on either hydroxylapatite or Sephadex G-100, providing that during the latter procedure the salt concentration of the buffer was maintained at 0.4 M. The molecular weight of the enzyme, determined by gel filtration, was 53,000. In a modified purification procedure Iwatsuki et al. (1980) used affinity chromatography with UV-irradiated DNA supported on cellulose, followed by chromatography on activated thiol-sepharose 4B, which yielded a single protein band having a molecular weight of 51,000 when analyzed by sodium dodecylsulphate polyacrylamide gel electrophoresis. Upon denaturation by heat or 8M urea, oxidized flavin adenine dinucleotide (FAD) was isolated from the mixture and identified by

thin-layer chromatography. In contrast to flavoproteins to which FAD is bound, which generally exhibit two absorbance maxima between 300 and 500 nm, photolyase had only one maximum at 380 nm. These findings, and the similar characteristics of the absorption and emission spectra of native photolyase with those of flavoproteins in which the chromophore is a 4a, 5-reduced flavin, led the authors to suggest this configuration for the photolyase chromophore.

Schild et al. (1984) isolated a plasmid containing a 6 kilobase-pair (kbp) insert of S. cerevisiae DNA including the phr1 gene. Subcloning experiments indicated that the phr1 gene was situated in a 3.3 kbp PvuII fragment of this insert. Both Sancar (1985b) and Yasui and Langeveld (1985) have subcloned this fragment and sequenced the phr1 gene. Sancar (1985b) sequenced a 2301 bp region, and found a single open reading frame (ORF) of 1695 bp. The sequence of the 565 amino acid long polypeptide, predicted from the nucleotide sequence was compared with the sequence of E. coli DNA photolyase determined by Sancar et al. (1984c). Overall the sequence homology was 36.5 per cent, although short regions near the amino- and carboxy-termini showed significantly greater homology. Yasui and Langeveld (1985) found a similar 1695 bp intronless ORF coding for a polypeptide of 564 amino acids, which gave a predicted Mr of 66,123. The nucleotide sequence had a G + C content of 36.2 per cent compared with 53.7 per cent in E. coli DNA photolyase (Sancar et al., 1984c). However, despite the difference in G + C content, the amino acid sequences of the two photolyases were 35 per cent homologous, in agreement with the data of Sancar (1985b).

Bakers' Yeast Enzyme II

Boatwright et al. (1975) purified a DNA photolyase by affinity chromatography, which ran as a single component when analysed by either polyacrylamide gradient gel electrophoresis or sedimentation velocity through 5-20 per cent sucrose gradients containing 0.4 M KCl. The molecular weights determined by these methods were 130,000 and 136,000, respectively. Two bands were resolved on sodium dodecyl sulphate polyacrylamide gels, corresponding to molecular weights of 60,000 and 85,000, whilst sucrose gradient sedimentation in the presence of 1.0 M KCl revealed polypeptides of 54,000 and 82,500 in the fractions collected. Boatwright et al. (1975) concluded that the enzyme consisted of two dissimilar subunits, which when mixed together resulted in a time-dependent increase in photolyase activity, indicating that an active enzyme could be regenerated from these subunits. This purified enzyme did not show absorbance of light in the photoreactivating wavelength range, but did show an excitation maximum at 358 nm for a fluorescence emission maximum at 440 nm. When enhancement of photolyase activity was used as an assay, activators of the enzyme activity were isolated from acidified cell-free extracts of yeast (Madden et al., 1976; Werbin and Madden, 1977). The photolyase activity was enhanced by a compound referred to as Activator III, which emitted at 350 and 440 nm when excited at 290 nm, and emitted at 440 nm when excited at 358 nm. After acid hydrolysis, emission was produced only by excitation at 358 nm, indicating two separate chromophoric moieties. Maximal enhancement of the photolyase activity was obtained from approximately equimolar amounts of enzyme and Activator III suggesting that the latter may be the chromophore of the enzyme, but their excitation spectra do not

reflect the action spectrum for enzymatic photoreactivation (Harm, 1975). However, this must be weighed against the relative cellular roles of the two enzymes identified, which is at present not known.

Kinetics of Dimer Monomerization By Yeast DNA Photolyase

The relative ease with which photolyase activity could be isolated from cell-free extracts has resulted in a full characterization of the *in vitro* rate constants associated with the reaction scheme described by Equation 1, proposed by Rupert (1962a,b).

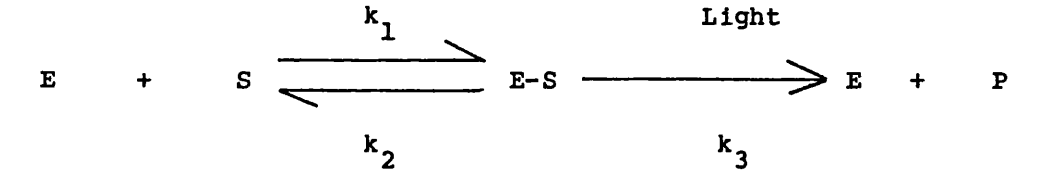

...1

Much of the work has been done by the flash-photolysis method developed and reviewed by Harm et al. (1971). The importance of the technique in the study of enzymatic photoreactivation merits further discussion at this juncture. It is based upon the observation that the light-dependent step is preceded by a light-independent step during which the enzyme interacts with the pyrimidine dimer substrate to form an enzyme-substrate [ES] complex. Harm et al. (1971) found that a single intense flash of photoreactivating light of millisecond duration was sufficient to permit photoreactivation of all the [ES] complexes existing at that time. The number of [ES] complexes can be estimated by measuring

the disappearance of pyrimidine dimers, which can be conveniently determined from the increased survival of UV-irradiated bacteria or 'phage, or the increased activity of UV-irradiated transforming DNA. This biological effect can be expressed quantitatively by the parameter ΔD (the difference between the UV fluence D actually applied and a smaller UV fluence D' that would have led to the same survival without subsequent photoreactivation) (Fig. 7).

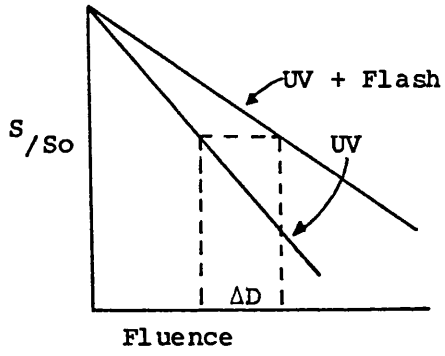

Figure 7. Derivation of the parameter ΔD.

Therefore, ΔD reflects the amount of radiation which is reversed by a single light flash. Under conditions in which the substrate is in excess of the enzyme, and hence all enzyme molecules are complexed, the maximal level of ΔD obtained by a single light flash is a measure of the maximum number of DNA photolyase molecules. Similarly, when light flashes are given in rapid sequence only a few enzyme-substrate complexes can be formed between flashes and so the concentration of free enzyme (E) is roughly constant and approximately equal to the concentration of the enzyme.

The rate of [ES] complex formation is described by the equation:

$$d[ES]/dt = k_1[E][S] - k_2[ES] \qquad \ldots 2$$

As described above, [E] is aproximated to [E]o, the initial enzyme concentration, $k_2[ES]$ is negligibly small and d[ES] is replaced by -d[S], the change in substrate concentration,

$$-d[S]/_{dt} = k_1[E]o[S] \qquad ...3$$

$$-d[S]/_{[S]} = k_1[E]dt \qquad ...4$$

$$[S]t/_{[S]o} = e^{-k_1[E]ot} \qquad ...5$$

where $[S]t/_{[S]o}$ is the experimentally determined value of $(1-\Delta D/\Delta D_{max})$, with [S]t = substrate concentration at time t and [S]o = starting substrate concentration. In this instance ΔD is the fluence reduction obtained after photoreactivation for time t, and ΔD_{max} corresponds to complete photoreactivation ([S]t = 0). This analysis assumes that pyrimidine dimers are produced in proportion to the UV fluence and that all photorepairable, inactivating photoproducts contribute with equal probability to the decrease in survival, and that their photorepair contributes to the increase in surviving fraction with equal probability. The k_1 value for yeast enzyme <u>in vitro</u> is 6×10^7 $L.mol^{-1}.s^{-1}$ at room temperature (Harm and Rupert, 1968), based on 1.5×10^{12} molecules per ml or 2.5×10^{-9} $mol.L^{-1}$. The rate constant k_2 was determined by introducing an excess of UV irradiated competing DNA which was not measured by the <u>H. influenzae</u> transforming assay. The PRE molecules which dissociated from the transforming DNA became complexed with the competing DNA. Therefore, the decrease in the number of [ES] complexes was measured as a decrease in biological effect by a single light flash. Harm and Rupert (1968) determined

values of 10^{-2} to $10^{-3}s^{-1}$ for k_2 resulting in a dark equilibrium for [ES] formation of approximately 10^{10} $L.mol^{-1}$, indicating that the complex is very stable in the dark. Harm and Rupert (1970a) determined the effect of temperature on the [ES] complex formation reaction in vitro, which when expressed by the Arrhenius relationship gave values of 1.6×10^{14} $L.mol^{-1}.sec^{-1}$ for the frequency factor and an activation energy (E_A) of 9.3 $kcal.mol^{-1}$ for the forward reaction (k_1). The concentration ratio k_1/k_2 showed two maxima at ionic strengths of 0.12 and 0.18.

The photolytic rate costant k_3 (equation 1) for the photolysis of pyrimidine dimers from the [ES] complex can be expressed by the product k_pI, where I is the intensity of the photoreactivating light and k_p is the 'photolytic constant'. Under conditions where all the available substrate is complexed (achieved by having excess PRE), the application of light results in the loss of [ES] complexes as a function of light fluence (L). Therefore:-

$$[ES]_L/[ES]o = e^{-kpL} \qquad ...6$$

Harm and Rupert (1970b) suggested that the parameter k_p is a measure of the efficiency of the use of light in the reaction and reflects the extent to which complexes absorb incident photons (molar extinction coefficient, ϵ) and the probability with which an absorbed photon leads to monomerization of a dimer (quantum yield, ϕ). At the optimal wavelength for photoreactivation, 355-385 nm, k_p was found to be approximately 10^4 $L.mol^{-1}.cm^{-1}$. The authors postulated that it was unlikely that the quantum yield would be less than 10^{-1}, hence the absorption of light and its use in dimer monomerization must be very efficient. There was no ionic strength effect on k_p.

Using the flash photolysis method, Fukui et al. (1978) found

that the number of PRE molecules in a stationary phase culture of an excision-defective strain S. cerevisiae XS 774-6A (αrad 1-1) was approximately 180 per cell, but decreased to 30 per cent of that value in the logarithmic phase. Similarly, Fukui et al. (1981) used light-flash analysis to determine the rate constant (k_1) for formation of the [ES] complex and its activation energy term in vivo. At 30°C, k_1 was 1.1×10^5 $L.mol^{-1}.sec^{-1}$, assuming a nuclear volume of 3×10^{-15} L. The rate constant k_1 showed positive temperature-dependence, as described by the Arrhenius expression with an activation energy of 11.8 $kcal.mol^{-1}$, in reasonable agreement with the figure of 9.3 $kcal.mol^{-1}$ determined by Harm and Rupert (1970a) in vitro.

Using the same haploid excision-repair-defective strain, Fukui and Laskowski (1984a) found that the number of PRE molecules in cells grown at 37° was about 13 per cent of that grown at 23°C, although the total amount of protein per cell remained the same. In addition, they found the number of PRE molecules in cells grown in light conditions was about 2.8-fold greater than those grown in the dark, but the number of PRE molecules in cells grown in the light decreased more rapidly during holding in buffer in the dark than in the light. They concluded that cells have stable as well as unstable PRE molecules and that the percentage of unstable PRE molecules grown in the light is larger than in cells grown in the dark and that light has a stabilizing effect on PRE molecules. Furthermore, Fukui and Laskowski (1984b) reported the fluence decrement ΔD_{PRE} obtained by one high-intensity flash became larger when dark-grown cells were pre-illuminated with light flashes prior to UV-irradiation. They suggested that there existed PRE molecules in yeast cells which may occur in an active condition as well as an

inactive condition, but that the latter become active after pre-illumination. Harm and Rupert (1976) reported a similar observation with a yeast PRE in vitro. A semi-crude extract or highly purified form of the yeast enzyme showed increased activity if it was illuminated with near-UV or short-wave visible light prior to its use in the transforming DNA assay. The action spectrum for pre-illumination had a maximum in the 355-385 nm region, but wavelengths up to 546 nm were also effective. Pre-illuminated enzyme was more stable to thermal inactivation at 65°C than untreated enzyme, but the light-induced activation was slowly lost by dark storage. However, the effect could be recovered repeatedly by renewed pre-illumination. Harm (1979) showed that with [ES] complexes formed from non-pre-illuminated PRE the repair probability per incident photon was only 25 per cent of that in complexes formed from pre-illuminated PRE. However, the repair probability increased to greater than 50 per cent if a high-intensity flash was given. Harm (1979) suggested a 'two- photon photolysis' theory in which the repair probability per incident photon increases if two or more photons are absorbed within a millisecond time period; the first absorption yields a metastable excited state of the complex, during which the repair probability is increased by absorption of another photon.

2.1.6.2 Streptomyces griseus Enzyme

Eker and Fichtinger-Shepman (1975) have described the isolation of a DNA photolyase from S. grisues. The enzyme had a molecular weight of 43,000 and appeared to consist of a single protein chain (Eker, 1978). An optimal pH of 7.0, an optimal ionic strength of 0.04, and an isoelectric point at pH 4.7 were found

(Eker, 1978). The enzyme consists of a high molecular weight protein and a low molecular weight chromophore which can be released by heat denaturation. The chromophore has an absorption maximum at 420 nm and a fluorescence emission maximum at 460 nm upon excitation at 400 nm (Eker, 1980). However, the fluorescence is almost completely quenched when the chromophore is bound to native enzyme, but an additional absorption band at 445 nm is observed (Eker, 1980). Depending on the pH, absorption maxima were found at 420 (pH 8.3), 396 (pH 5.2) and 375 nm (pH 1). These spectra were found to be very similar to the spectra of the substance of SF 420 (Eker et al., 1981). Eker et al. (1981) concluded that the cofactor of S. griseus PRE is a 7,8-didemethyl-8-hydroxy-5-deazaflavin derivative. SF420 alone sensitized the splitting of thymine dimers when irradiated with blue light, supporting the structure proposed for the PRE cofactor. Eker (1985) has suggested that the enzyme has an essential arginine residue based on the inhibition of PRE activity by butane-2,3-dione. However, UV-irradiated DNA protected the enzyme against inactivation, as did non-irradiated DNA at higher concentrations, indicating that PRE can form non-specific complexes. Using the H. influenzae transformation assay, Eker et al. (1986) have determined an action spectrum for the enzyme. A high similarity was noted between the action spectrum (max at 445 nm) and the long wavelength absorption band (max at 443 nm) of the PRE. In addition to the 400 to 470 nm region, considerable enzymatic photoreactivation was found between 280 and 320 nm. No photoreactivation was found above 500 nm. Kinetic studies yielded values of 2.1×10^{8} $L.mol^{-1}.s^{-1}$ for the dark complexation of the enzyme with the substrate (k_1) and $0.48 s^{-1}$ for the dissociation rate constant (k_2) (Eker et al.,1986).

2.1.6.3 Escherichia coli Enzyme

Although E. coli was the first organism in which DNA photolyase activity was demonstrated in vitro (Rupert et al. 1958), the high cellular nuclease activities made purification of the enzyme difficult. Thus much of the early characterisation was of the in vivo process using the flash photolysis method reviewed by Harm et al. (1971).

Harm et al. (1968) estimated the number of PRE molecules per cell to be 20 in E. coli B_{s-1} using the figure of 65 pyrimidine dimers per genome per erg/mm^2 incident at 254 nm. The rate constant k_1 for the complexation of the enzyme with the substrate was found to be 1.1×10^6 L.mol^{-1}.s^{-1}, whilst the dissociation rate constant of the enzyme-substrate complex in the dark (k_2) was 1.9×10^{-3} s^{-1}; determined by infection of cells with irradiated bacteriophage T1 and then irradiating the infected cells (Harm, 1970). At the most effective wavelength (385 nm), the product $\epsilon\phi$ was found to be 2.4*L.mol^{-1}.s^{-1}. Both k_1 and k_2 showed temperature-dependence over the range 5° to 37°C, resulting in an activation energy of 11 kcal.mol^{-1} for k_1 derived from the Arrhenius relationship (Harm, 1970). Tyrrell and Davies (1974) investigated PR kinetics in the UV-sensitive mutant K-12 AB2480 and found the photoreactivable sector to be 0.82 (defined as $(1-[k_1/k_2])$ where k_1 is the UV inactivation constant and k_2 is the inactivation constant after maximum PR). Developing the (1-P) method of analysis, Tyrrell and Davies (1974) estimated two different rate processes involved in photoenzymatic repair. They found that approximately 50 per cent of the lesions were repaired at a faster rate, the exponential rate constant k_{fast} being 7.9×10^{-3} s^{-1}. Saturating irradiance conditions for this faster

component of the process were reached at approximately 60 erg.mm^{-2} s^{-1} (6 Wm^{-2}), using broad-band photoreactivating light. The temperature-dependence of k_{fast} resulted in an activation energy of 9 kcal.mol^{-1}, compared with 11 kcal.mol^{-1} measured by Harm (1970) using E. coli B_{s-1}. Tyrrell et al. (1972) studied the number of PRE molecules in AB2480 as a function of the stage of growth. They found that cells have a minimum number of PRE molecules in exponential phase which rises to a maximum in late stationary phase. However, this was not attributable to a change in the photoreactivable sector. In addition, Tyrrell (1973b) has shown that production of PRE molecules in K-12 strains of E. coli is suppressed under anaerobic growth conditions, but the number of PRE molecules estimated by flash-photolysis could not be reduced below an average of one per cell.

Harm (1969) isolated a PRE overproducing strain E. coli B_{s-1}-160, by nitrosoguanidine mutagenesis of B_{s-1} and estimated the number of PRE molecules per cell to be 110. Nishioka and Harm (1972) found that this strain was an adenine auxotroph (purA), lacking adenylosuccinate synthetase (EC 6.3.4.4). Excess PRE production was only exhibited by cells entering the stationary phase of growth, whilst supplementation of the growth medium with adenine or adenine analogues decreased the number of PRE molecules in stationary phase B_{s-1}-160, but had no effect on the parent strain B_{s-1}. It was concluded that excess PRE production occurs only under conditions of severe adenine restriction, suggesting that adenine or some related compound is involved in a regulatory mechanism responsible for the low level of PRE production that is characteristic of E. coli.

As discussed above, early attempts to isolate the E. coli

photoreactivating enzyme *in vitro* were hindered by the low copy number per cell. It was necessary, therefore, to increase the amount of enzyme in the cell. Sutherland et al. (1972) achieved this by isolating a Lambda transducing 'phage carrying the gene for this enzyme, which upon induction of a lysogenic strain resulted in a 2000-fold increase in PRE activity in cell extracts. A *phr* mutant of *E. coli*, lacking active PRE, was isolated by Harm and Hillebrandt (1962), and found to map near *gal* on the *E. coli* chromosome by Van de Putte et al. (1965) (Fig. 8).

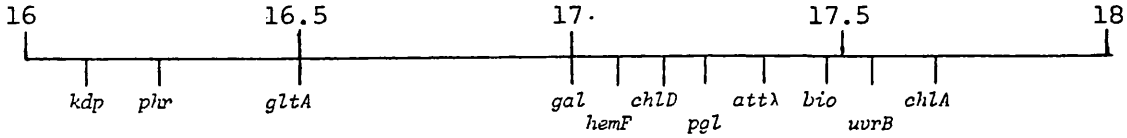

Figure 8. The 16- to 18-minute region of the *E. coli* chromosome (adapted from Bachmann, 1983).

Sutherland et al. (1972) studied PER in mutants with deletions extending from *chlA* to either *attλ*, or through to *gal*, and concluded that the *phr* locus was between *gal* and *attλ*. An *E. coli* strain lysogenic for a Lambda specialised transducing 'phage carrying the *gal*-*attλ* region was constructed, and a 2000-fold increase in PRE activity was obtained upon induction, using the oligonucleotide assay developed by Sutherland and Chamberlin (1973). An enzyme with apparent PRE activity was isolated and characterized (Sutherland et al., 1973). However, Youngs and Smith (1978) and Sancar and Rupert (1978a) presented data which conclusively placed the *phr* gene counter-clockwise of *gal*, contradicting the findings of Sutherland et al. (1972). Youngs and Smith (1978) investigated PR in strains with deletions extending through

the gal-attλ region and found them to be PHR^+. These were checked against known phr strains, carrying the phr mutation isolated by Harm and Hillebrandt (1962), which proved to be phenotypically PHR^-. Co-transduction data clearly placed the phr locus between kdp and gltA (Fig. 8). Sancar and Rupert (1978a) also measured PR in mutants which had the gal-attλ region missing, and found them to be PHR^+, both as regards colony formation and survival of UV-inactivated T4vl 'phage. A phr mutant of AB1886 was isolated by penicillin selection (Sancar and Rupert, 1979) and derivatives of this strain were transformed with a λdvgal plasmid. The GAL^+ transformants retained their PHR^- phenotype. These results were in conflict with the conclusion of Sutherland et al. (1972) that λ dgal transducing particles carry the phr gene. In addition, Sancar and Rupert (1978a) mapped the phr locus between supE and tolAB. Sutherland and Hausrath (1979) investigated PR in deletion mutants lacking the gal-attλ region and found them to be PHR^+, in contrast to the findings of Sutherland et al. (1972). Strains with a Δ(gal-chlA) deletion photoreactivated 254 nm UV-induced damage at a rate 20 per cent that of Δ(attλ-chlA) strains. Photoreactivating enzymes isolated from Δ(gal-chlA) strains had an apparent Km approximately 2-3-fold higher than normal enzyme and showed markedly increased heat lability. They suggested that a gene, termed phrA, situated in the gal-attλ interval, contained information affecting the functional properties of the phrB product mapped at 16.2 minutes on the recalibrated E. coli linkage map (Bachmann, 1983) by Youngs and Smith (1978) and Sancar and Rupert (1978a).

Sancar et al. (1983) have cloned and amplified the phrB gene product and have isolated, purified and sequenced the photolyase

gene and protein (Sancar et al., 1984b; Sancar et al., 1984c) whilst Snapka and Sutherland (1980) have reported the purification to apparent homogeneity of a PRE obtained from induction of an E. coli strain lysogenic for a lambda 'phage carrying the gal-attλ region.

Hence a conflict in the literature can be envisaged; Snapka and Sutherland (1980) have purified a protein which is presumably the proposed phrA gene product, its proposed function being to interact with the phrB gene product (Sutherland and Hausrath, 1979), and yet it has apparent photoreactivating enzyme properties in its own right. This must raise the question of the existence of multiple photolyase molecules in E. coli. The presentation of in vivo data to address this question is the subject of this thesis.

Because of the lack of published in vivo data to support the existence of two photolyase molecules it is pertinent to review the in vitro data for the two individual photolyase molecules which has led to the present controversy regarding the 40-kDa DNA photolyase (phrA gene product). Indeed, it has been suggested that the PRE activity associated with this protein may be due to low level contamination with the phrB gene product (Sancar et al., 1984b).

40-kDa DNA Photolyase

Sutherland et al. (1973) purified a DNA photoreactivating enzyme from induced cells of an E. coli strain having a lysogenic Lambda bacteriophage carrying the gal-attλ chromosomal region (Sutherland et al., 1972). The enzyme, which eluted from hydroxyl-apatite/ammonium sulphate gradients in a constant fraction and appeared as a single band on polyacrylamide gels at pH 9.5 under non-denaturing conditions, has a molecular weight of 43,000

determined by sedimentation through glycerol gradients, and a pH optimum for photoreactivating enzyme activity at pH 7.2. The purified enzyme tended to form aggregates. Snapka and Sutherland (1980) developed a purification procedure to minimise aggregation. In addition to the streptomycin and ammonium sulphate precipitation steps reported by Sutherland et al. (1973), the fraction was further purified by isoelectric focusing and chromatography on Bio-Gel P30. The final fraction (fraction V) contained about 2500 units/mg of PRE activity, where one unit is defined as the amount of photolyase required to reverse 1 ng of dimers in 1 hour at 37°C.

Sodium dodecylsulphate polyacrylamide gel electrophoresis of dansyl-labelled enzyme gave bands corresponding to a molecular weight of 35,200 $\pm$ 200 and its multiples (due to aggregate formation). Amino acid analysis of the apoprotein revealed an arginine residue at the N-terminus, no detectable tryptophan residues and a low overall incidence of aromatic amino acids. The presence of mannose, glucose, galactose and N-acetylglucosamine associated with the apoprotein were detected by gas liquid chromatography. The enzyme exhibited absorption at 250 nm and had approximately 10 nucleotides of RNA associated with each PRE molecule. Neither the cofactor, apoenzyme, nor holoenzyme showed any absorption between 300 and 400 nm and yet the isolated enzyme had an action spectrum which peaked at 360 nm (Snapka and Fuselier, 1977). However, Wun et al. (1977) used absorption difference spectroscopy to demonstrate the appearance of a new absorption in the spectral analysis when the enzyme was incubated with UV-irradiated DNA. There was a concomitant decrease in the absorption of the mixture below 300 nm. Both the hyperchromicity above 300 nm and hypochromicity below 300 nm could be reversed with identical

first-order kinetics by irradiation with 365 nm light. This led to the suggestion that the enzyme does not possess a distinct chromophore, but instead a new absorption results when it binds to dimer-containing DNA.

Although the isolated enzyme lacked absorption in its actinic wavelength region, there was an absorption maximum near 260 nm that was due primarily to an RNA cofactor (Cimino and Sutherland, 1982). Both A-U and G-C base pairs were present in equal concentrations and about 20 per cent were in a double-stranded conformation in the native enzyme.

Substrate Range of the 40-kDa DNA-Photoreactivating Enzyme

Sutherland et al. (1986) found that the isolated enzyme quantitatively monomerized cis-syn pyrimidine dimers in DNA but not RNA. The pyrimidine [6-4] pyrimidone photoproduct (Lippke et al., 1981) was not a substrate for the enzyme. Sutherland et al. (1986) also constructed pyrimidine dimer substrates in DNA having the two pyrimidines and the cyclobutane ring characteristic of the cis-syn dimer, but without individual bonds in the immediate vicinty of the dimer. The enzyme did not photoreactivate dimers lacking an N-glycosyl bond linking one of the pyrimidine moieties to the deoxyribose backbone and only bound the DNA very poorly. Similarly, the enzyme did not monomerize dimers in which the phosphodiester bond joining the two deoxyribose moieties was not intact. Sutherland et al. (1980) showed that M. luteus UV endonuclease could displace the PRE already bound to dimer sites, resulting in nicking at these sites. In contrast, the yeast enzyme preparation used by Patrick and Harm (1973) was not displaced by M. luteus UV endonuclease, suggesting that the yeast PRE had a relatively greater affinity for

the dimer site than the 40-kDa E. coli PRE.

50-kDa DNA Photolyase

As a consequence of the controversy regarding the map location of the phr gene discussed above, Sancar and Rupert (1978b) developed a method to clone the phrB gene using chromosomal DNA as the gene source. Three phr strains, including the original photoreactivation-deficient mutant E. coli Bphr (Harm and Hillebrandt, 1962), were transformed to the PHR^+ phenotype by the cloned phrB gene, carried on plasmid pCSR604. This plasmid, pCSR604, was subcloned and the phrB gene put under the control of the tac promoter in pUNC09 resulting in pMS969 (Sancar et al., 1983). Two proteins of molecular weights 49,000 and 20,000 were identified on SDS-polyacrylamide gels after plasmid induction with IPTG. The Mr 49,000 protein was identified as being the phrB gene product, using the technique of Tn1000 insertional inactivation described by Guyer (1978). The gene product repaired UV irradiated pBR322 DNA in vitro (Sancar et al., 1983). Sancar et al. (1984b) have described a purification procedure in which the final fraction elutes as a single peak from a phenyl-sepharose column having an Mr of 49,000. They calculated a specific activity of 4×10^6 units per mg of enzyme in contrast to the approximately 1000-fold lower value obtained by Snapka and Sutherland (1980) for the purified 40-kDa protein. Sancar et al. (1984b) measured a turnover rate of 2.4 dimers/photolyase molecule/minute, in reasonable agreement with the in vivo turnover rate of 4.5 dimers/molecule/minute for E. coli B_{s-1} (Harm, 1970). Sancar et al. (1984c) have sequenced a 2039-bp segment containing the phrB gene. Two open reading frames were found, one of which encodes a polypeptide of 53,994-Da based on the

amino acid composition predicted from the nucleotide sequence. The transcriptional promoters identified had only limited homology with the canonical -35 sequence TTGACA and the Pribnow box TATAATG, which may in part explain the low cellular copy number of PRE molecules. A Shine and Dalgarno ribosome binding site showed good homology with the consensus sequence originally proposed by Shine and Dalgarno (1974). The amino acid composition derived from the nucleotide sequence revealed a bias in favour of rare and infrequent codons. Twenty five per cent of the codons in the gene were rare, leading Sancar et al. (1984c) to conclude that the low cellular copy number of PRE molecules may be attributable to regulation at the level of transcription and/or translation. Ihara et al. (1987) have compared the promoter sequence of the phrB gene with those of several SOS-inducible genes, and found a limited degree of homology. Furthermore, these workers have used a phrB-lacZ fusion to show induction of the phr gene with UV-radiation, 4-nitroquinoline and mitomycin C. Their results suggest that the gene is SOS-inducible. Sancar and Sancar (1984) reported that the enzyme had an intrinsic chromophore with the spectral properties of flavin adenine dinucleotide (FAD). This was found to be a blue neutral FAD radical (Jorns et al.,1984). Disproportionation of the radical observed upon anaerobic denaturation was consistent with an N-5 unsubstituted radical. The photolyase exhibited absorption maxima at 580, 475 and 384 nm. The absorbance of the enzyme at wavelengths above 500 nm is due only to the FAD radical,whereas the band at 384 nm reflects contributions from both the FAD radical and a second chromophore. Native photolyase is fluorescent, having an emission maximum at 470 nm and an excitation maximum at 398 nm. The enzyme fluorescence has been attributed to the second chromophore

(SC) (Jorns et al., 1984). Evidence for this arose by studying the denaturation of the enzyme with sodium dodecylsulphate. The initial absorption spectrum after addition of SDS showed an intense band at 360 nm which slowly decayed in a first-order reaction. The stability of the SC was pH-dependent. Jorns et al. (1984) have calculated that 50 per cent of the absorption in the actinic region is attributable to the second chromophore. Jorns et al. (1987) have shown that oxidation of the flavin radical in photolyase is accompanied by a reversible loss of enzyme activity, whilst reduction of the radical to the fully reduced flavin resulted in a 3-fold increase in turnover, suggesting that reduced flavin may act as an electron donor in catalysis. Jorns et al. (1987) report a significant difference between the absorption spectrum calculated for the protein-bound second chromophore (λmax = 390 nm) compared with the protein-free second chromophore (λmax = 360 nm) (Jorns et al., 1984). The authors conclude that the binding site of the second chromophore in photolyase may provide an environment which differs from the bulk solvent. The available evidence suggests that the flavin binds at a hydrophobic site. In an attempt to determine the efficiency with which the enzyme converts light energy into chemical energy (i.e. the quantum yield) and the roles of the chromophores in photosensitization, Sancar et al. (1987a) measured the extinction coefficient at 384 nm (ε_{384}) of pure blue photolyase and found it to be 1.8×10^4 $M^{-1}.cm^{-1}$ in good agreement with the value predicted by Harm (1970). However, these workers found the photoreactivation cross-section $\varepsilon_{384}\phi$ = 1209 resulting in a quantum yield ϕ= 0.065, which indicated a very inefficient process. This disagreed with the prediction of Harm (1970) that the quantum yield should have a value between 0.1 and 1.0. Sancar

et al. (1987a) repeated the measurements with the fully reduced enzyme and determined ε_{384} = 16,100 and $\varepsilon_{384}\phi$ = 16,250, from which ϕ = 1.0. The authors concluded that the enzyme contains a fully reduced flavin *in vivo* and acts as a very efficient photosensitizer with a quantum efficiency of about 1.0. They suggest two pathways for the mechanism of photosensitization depending on whether a photon is absorbed by the reduced flavin or the second chromophore. When the second chromophore acts as the sensitizer, it donates an electron to the dimer to form a radical cation and pyrimidine dimer anion; the cation is reduced by electron transfer from $FADH_2$. The pyrimidine dimer radical anion is unstable and spontaneously monomerizes to yield pyrimidine plus pyrimidine radical anion; the latter donates an electron to the flavin radical, regenerating $FADH_2$. Alternatively, when $FADH_2$ acts as sensitizer, it donates an electron directly to the dimer.

Substrate Range of the 50-kDa DNA Photolyase

Brash et al. (1985) treated UV-irradiated, end-labelled DNA with either *M. luteus* UV endonuclease or hot alkali and detected the presence of cyclobutane pyrimidine dimers and pyrimidine [6-4] pyrimidone photoproducts, respectively. Incubation of irradiated DNA with photolyase in the dark did not alter the frequency or distribution of cyclobutane dimers. However, after 30 minutes incubation in the presence of visible light, no dimers could be detected. This treatment did not alter the distribution of hot alkali labile sites, leading the authors to conclude that DNA photolyase specifically reverses cyclobutane-type pyrimidine dimers, but not pyrimidine [6-4] pyrimidone photoproducts. Brash et al. (1985) pointed out that, unlike the cyclobutane pyrimidine

dimer, the [6-4] photoproduct cannot be reversed to its parent pyrimidine moieties by the simple breakage of covalent bonds.

Sancar et al. (1985) have studied the binding of DNA photolyase to dimer-containing DNA in vitro using the purified enzyme preparation (Sancar et al. 1984b). The enzyme bound specifically to UV-irradiated DNA, and only at the highest enzyme concentration could any non-specific binding be detected. The binding reaction had pH and ionic strength optima at 7.4-7.6 and 0.125 - 0.150, respectively. The enzyme bound UV-irradiated superhelical, relaxed circular and linear DNA equally well, suggesting that it does not possess DNA-unwinding activity. The enzyme also bound to UV-irradiated, single-stranded and double-stranded DNA with equal affinity. The finding that the secondary and higher-order structure of UV-irradiated DNA has no apparent effect on the binding of DNA photolyase strongly suggests that it is the dimer, rather than a helical deformity, which is specifically recognised. Jorns et al. (1985) found that DNA photolyase exhibits the same turnover number (3.4 min^{-1}) for the repair of dimers in oligothymidylates [oligo (dT)n] containing 4-18 residues, as with native DNA. Photolyase can repair internal dimers and dimers at the 5' end where the terminal ribose is phosphorylated, but not at unphosphorylated 5' or 3' ends. This explains why the enzyme is inactive with oligo $(dT)_2$, since the only dimer possibility involves an unphosphorylated 3' end. The results reported by Jorns et al. (1985) support the conclusion of Sancar et al. (1985) that it is the dimer itself which is specifically recognised, as opposed to the DNA helical deformation produced by the dimer. In a recent study, Sancar et al. (1987b) used the techniques of nitrocellulose filter binding and flash photolysis to determine the rate constants

for the formation of the enzyme-substrate complex. The association (k_1) and dissociation (k_2) rate constants were estimated to be 1-4 x 10^6 $M^{-1}.s^{-1}$ and 2-3 x 10^{-2} s^{-1}, respectively, in reasonable agreement with the *in vivo* data published by Harm (1970). The equilibrium association constant (K_A) was found to be approximately 6 x 10^7 M^{-1}. From the dependence of the association constant on ionic strength the authors concluded that the enzyme contacts no more than two phosphodiester bonds upon binding, in agreement with the findings of the substrate study of Jorns et al. (1985).

2.1.6.4 *DNA Photolyase From Human Cells*

Cook and Regan (1969) described photoreactivation in the marsupial *Potorus triadactylus,* but it was several years later before any further work was reported. Ley (1984) reported photo-repair of pyrimidine dimers in the epidermis of the marsupial *Monodelphis domestica* using the *M. luteus* UV-endonuclease sensitive sites assay, whilst Ley and Applegate (1985) found that post-UV radiation exposure of skin to photoreactivating light suppressed the induction of sunburn cells and epidermal hyperplasia by 75 per cent. These data suggested a causal link between pyrimidine dimers and induction of sunburn cells and epidermal hyperplasia in *M. domestica*. Ley (1985) found a similar relationship between UV-induced pyrimidine dimers and erythema in the same species. Sabourin and Ley (1987) have isolated and purified a photolyase from *M. domestica* which shows activity in the range 325-475 nm with a peak at 375 nm.

Initially, photoreactivation could not be demonstrated in rodent cells (Cleaver, 1966; Cook and McGrath, 1967; Ley et al., 1978), however, Ananthaswamy and Fisher (1981) observed

photoreactivation in the dermis of new born, but not adult mice. Similarly, photoreactivation could not be demonstrated in human cells (Cleaver, 1966), but Sutherland (1974) described the isolation of a photoreactivating enzyme from human leukocytes; detection being by the nuclease digestion method. The enzyme had similar properties to the 40-kDa photolyase from E. coli (Snapka and Sutherland, 1980) with respect to aggregate formation and lacking an intrinsic chromophore. However, the 40-kDa human leukocyte PRE had pH and ionic strength optima at 7.2 and 0.5 respectively (Sutherland, 1974). In contrast to other photoreactivating enzymes, the actinic wavelength range extended to 600 nm (Sutherland et al., 1974). The enzyme was detected in monocytes and polymorphonuclear leukocytes, but serum and erythrocytes had no significant activity (Sutherland et al., 1974). In addition, PRE activity was also detected in extracts of bovine bone marrow (Sutherland et al., 1974), suggesting that the PRE activity measured in leukocytes was not attributable to phagocytic engulfment of bacteria containing PRE. Sutherland and Oliver (1976) reported that the level of PRE activity in fibroblasts cultured in Eagle's minimal essential medium supplemented with foetal bovine serum was very low, whereas parallel cultures grown in Dulbecco's modified Eagle's essential medium (DMEM) contained higher levels of enzyme. A similar phenomenon was reported by Mortelmans et al. (1978) with human fibroblasts cultured in DMEM, but the authors suggested that the observed photoreactivable response could not be distinguished between true photoenzymatic repair and a medium-dependent photosensitization phenomenon. It has been suggested that patients suffering from the inherited disorder Xeroderma pigmentosum (XP) have low levels of PRE (Sutherland and Oliver,

1975; Sutherland et al., 1975), with values ranging from 0 to 40 per cent of normal.

The demonstration of photoenzymatic repair in human cells *in vivo* has been particularly controversial. Sutherland et al. (1980) have used the *M. luteus* UV endonuclease/alkaline agarose gel electrophoresis technique to demonstrate the presence of cyclobutadipyrimidine dimers in the DNA of human skin following *in vivo* irradiation with sub-erythemal fluences of UV radiation from FS-20 sunlamp fluorescent tubes. Even fewer endonuclease-sensitive sites were detected after 20 minutes post-UV irradiation with visible light than when the area was kept in the dark, suggesting that photoreactivation can make a contribution to the total repair process. Similar results were obtained by D'Ambrosio et al. (1981) using the UV-endonuclease/alkaline sedimentation technique, and with lupus erythematosus cells (D'Ambrosio, 1983). However, Zwetsloot et al. (1985) did not detect any PR-light-induced reduction in unscheduled DNA synthesis (UDS) in repair proficient human fibroblasts, suggesting that there was no light-induced repair of pyrimidine dimers in this cell line. Using the micro-injection technique, Zwetsloot et al. (1985) demonstrated that PRE from *S. cerevisiae* and the cyanobacteria *Anacystis nidulans* significantly reduces the level of UV-induced UDS after exposure to photoreactivating light. Purified yeast PRE was able to reduce UDS to 20-25 per cent of the value found in non-injected cells, whereas PRE from *A. nidulans* gave a reduction to only 70 per cent, suggesting that the eukaryotic enzyme is more efficient in the removal of pyrimidine dimers from mammalian chromatin than its prokaryotic equivalent. Furthermore, Zwetsloot et al. (1986) found that the reduction of UDS afforded by micro-injection of purified

yeast PRE was less in fibroblasts from XP complementation groups C,F and I compared with wild-type and XP-variant cell lines, whereas no reduction in UDS was seen in fibroblasts belonging to groups A,D, E and H. The authors suggested these data indicated that the genetic repair defect in some XP-strains may be attributable to altered accessibility to the UV-damaged sites.

2.1.6.5 Comparative Homology

Meechan et al. (1986) evaluated the degree of homology between the cloned E. coli and yeast DNA photolyase genes and human genomic DNA and mRNA sequences by hybridization analysis. The cloned sequences failed to hybridize to each other, even under non-stringent conditions and they only showed weak hybridization with human DNA or mRNA under similar non-stringent conditions. The authors were unable to conclude whether this indicates sequence divergence for prokaryotic and eukaryotic photoreactivation genes, or the absence of such genes from the mammalian genome.

As discussed before, Yasui and Langeveld (1985) and Sancar (1985b) have compared the cloned yeast phrl and E. coli phrB DNA photolyase genes and have found a 35 per cent homology between the deduced amino acid sequences, suggesting that both genes may have a common ancestral origin. In addition, Sancar (1985a) has cloned the 3.3 kb PvuII fragment carrying the S. cerevisiae phrl gene into an E. coli expression vector and demonstrated complementation of the E. coli phrB mutation. This finding indicates that there are no introns in the yeast phrl sequence and the chromophore of the enzyme can be substituted by a chromophoric entity present in E. coli. Similarly, Langeveld et al. (1985) have expressed the E.

coli phrB gene in S. cerevisiae, indicating that the prokaryotic PRE can gain access to and repair the eukaryotic DNA, notwithstanding the different chromosomal structure.

Table 1 summarises the principle properties of the DNA photolyases characterized to date.

Mechanism of Action

Although a great deal of elegant biochemical and photobiological work has resulted in the characterization of DNA photolyase activities in many species, little is still known about the nature of the binding reaction with the dimer and the mechanism of dimer-splitting.

Helene and Charlier (1977) have described the photosensitized splitting of dimers by indoles and indole derivatives, but only with wavelengths up to 350 nm. These moieties donate an electron to the dimer during the monomerization process via a stacked indole-dimer structural intermediate. However, despite the wavelength being outside the actinic region for PER, it is interesting to note that both the 50-kDa E. coli photolyase and the phrl photolyase from S. cerevisiae are unusually rich in tryptophan (Sancar, 1985b). The positions of nine tryptophans are conserved in both enzymes, including six tryptophans in the highly conserved carboxy terminal regions (50 per cent) compared with 30-35 per cent overall homology (Sancar, 1985b; Yasui and Langeveld, 1985). The secondary structure suggested by this homology is indicative of alternating α-helices and β-sheets, such as are found in FAD binding domains (Sancar, 1985b). No tryptophan residues were detected in the 40-kDa E. coli DNA photolyase (Snapka and Sutherland, 1980).

Table 1. COMPARISON OF IN VITRO PROPERTIES OF SOME DNA PHOTOLYASES

	NUMBER OF ENZYMES		MOLECULAR WEIGHT OF PROTEIN SUB-UNIT	CHROMOPHORE/ COFACTOR	ACTINIC WAVE-LENGTH REGION [MAXIMUM] nm
Saccharomyces cerevisiae	2	I	53,000	4A,5,-reduced Flavin	350-[380]-420
		II	130,000 (85,000+60,000)	Activator III	Not Published
Streptomyces griseus	1		43,000	7,8-didemethyl-8-hydroxy-5-deazaflavin	400-[445]-470
Escherichia coli	2	A	35,200	RNA	320-[360]-420
		B	49,000	Neutral Flavin Radical + 'Second chromophore'	350-[384]-420
Homo sapiens	1		40,000	None identified	300-[405]-600

Pac et al. (1982) have suggested a mechanism of dimer-splitting via a cation or anion radical intermediate, which is formed by photochemical electron transfer between the photolyase molecule and the pyrimidine dimer. In their study they demonstrated catalytic dimer-splitting by a photogenerated cation radical of aromatic hydrocarbons. Pac et al. (1982) postulated that oxidation potential should be taken into consideration as one of the essential factors determining the feasibility of photo-sensitized dimer splitting. Syn dimers, which are all reactive to redox photosensitization, have lower oxidation potentials than the unreactive anti dimers. They found that the oxidation potential of N-N'-dimethyl-5,6-dihydrothymine (DMT) was very similar to those of 'anti' dimers and considerably higher than the reactive 'syn' dimers; suggesting that when a dimer between two DMT molecules is formed with 'syn' chemistry, there must be significant electron perturbation which is not observed in the 'anti' conformation. Such perturbations can be explained in part by 'through-bond' interactions between the 'n' orbital, N (1) and N (1') involving the C(6)- C(6') bond (Fig. 9). Syn dimers are structurally favourable for 'through-bond' interactions because of the relatively small dihedral angles between the C(6)-C(6') bond and each n orbital of N(1) and N(1').

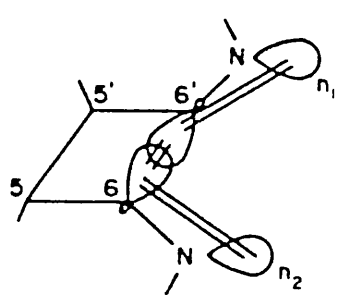

Fig. 9. 'Through-bond' interaction in a 'syn' dimer.

Pac et al. (1982) suggested that when a charge transfer complex is formed between a dimer and a cation radical of the photosensitizer, the partial positive charge can be populated on the dimer by charge resonance, probably on the N(1)-C(6)-C(6')-N(1') array for the most part since the n orbitals of N(1) and N(1') largely contribute to, or constitute the highest occupied molecular orbital. The net result is to increasingly elongate the C(6)-C(6') bond by the development of a partial positive charge. Thus, by this mechanism, dimers which lack 'through-bond' interaction are inherently incapable of splitting via a charge-transfer complex. Cis-syn pyrimidine dimers are more strained than trans-syn, because of the cis location of the two pyrimidine rings. Similarly, steric considerations may be used to explain the rate of dimer splitting observed by Setlow and Carrier (1966), the order being T-T > C-T > C-C.

In a recent study, Heelis and Sancar (1986) have investigated the effect of illumination on the flavin neutral blue radical associated with the 50-kDa E. coli DNA photolyase. Laser flash photolysis at 532 nm reduced the flavin and produced a transient absorption band at 420 nm, probably representing the lowest excited doublet state of the radical. Heelis and Sancar (1986) suggest that the primary step in photoreduction involves an electron donor that is a constituent of the enzyme itself.

$$\begin{array}{l} E \\ | \\ DH \end{array} \!\!\!\

unlikely. However, Heelis and Sancar (1986) suggest that a mechanism involving electron photoreduction of E-$FADH^{\bullet *}$ followed by electron-donation by E-$FADH_2$ to the pyrimidine dimer would seem plausible.

Concluding Remarks

The isolation of highly purified photoreactivating enzymes has led to the elucidation of the chromophoric entities and reaction kinetics in many species. However, it is a sobering thought that despite being the first DNA repair mechanism to be discovered and probably the simplest, much has yet to be learned about the mechanism of specific binding of PRE to UV-irradiated DNA; the nature of the photochemical reaction; the regulation of PRE activity and the interaction between photoenzymatic repair and other DNA and cellular repair mechanisms.

2.2 Nucleotide Excision Repair

Nucleotide excision repair was initially recognised by the ability of UV-irradiated E. coli strains to undergo recovery during post-UV incubation in the dark. Both Setlow and Carrier (1964) and Boyce and Howard-Flanders (1964) showed that in most UV-irradiated E. coli strains, thymine-containing pyrimidine dimers were lost from the acid-insoluble fraction of the DNA and appeared in the acid-soluble phase during post-UV incubation. However, this phenomenon was not seen in strains unable to undergo host-cell reactivation such as B_{s-1}, nor in K-12 strains defective at the uvrA locus. Furthermore, genetic loci termed uvrB and uvrC were also implicated in excision repair in K-12 strains.

The uvrA, uvrB and uvrC genes have been cloned and the proteins isolated in vitro (for a review see Sancar and Rupp, 1983; Thomas et al., 1985).

The uvrA gene codes for a single polypeptide of Mr 103,866 of which there are approximately 20 copies per cell (Sancar et al., 1981c). Sancar et al. (1982a) have sequenced the uvrA gene and found a LEXA binding site overlapping the -35 sequence of the promoter. LEXA protein markedly inhibited transcription of the uvrA gene in vitro, suggesting that excision repair is under SOS control (see Section 2.4).

The cloned uvrB gene codes for a polypeptide of Mr 76,118 of which there are 150-200 copies in uninduced cells (Sancar et al., 1981a). The sequence of the UVRB protein shows some homology with the UVRC protein and to the ATP binding site of the UVRA protein. The regulation of the uvrB gene is complex and not fully understood, having three promoters on the 5' side, only one of which is under LEXA control (Sancar et al., 1982b). In addition, there is a

repetitive extragenic palindrome on the 3' side, implicating a further unknown regulatory mechanism, possibly involving mRNA stability (Arikan et al., 1986). Sancar et al. (1981b) have identified the uvrC gene product as being a single polypeptide of Mr 66,038, which has DNA binding activity. However, the gene is not UV-inducible (Moolenaar et al., 1987).

Using these purified proteins, Sancar and Rupp (1983) reconstituted the UVR ABC nuclease activity in vitro. The nuclease had an absolute requirement for ATP and Mg^{2+} ions. Using UV-irradiated pBR322 DNA, Maxam-Gilbert sequence analysis indicated that the UVR ABC nuclease hydrolyses the eighth phosphodiester bond 5' to a pyrimidine dimer or [6-4] photoproduct and at the fourth phosphodiester bond 3' to T-C, C-C and C-T dimers, but at the fourth or fifth phosphodiester bond from potential T-T dimers. Thus the UVR ABC excision nuclease removes a 12- or 13-nucleotide long single-stranded DNA fragment to produce a gap of that size, which is then filled and sealed by DNA polymerase I and ligase.

It was found that the UVR ABC excision nuclease did not dissociate from DNA in the absence of other proteins implicated in excision repair. Husain et al. (1985) found that when used alone, neither the purified DNA polymerase I (polA gene product) or helicase II (uvrD gene product) had any significant effect on the initial rate of excision nuclease activity or turnover of the enzyme. However, when used togther, the rate of incision was not increased, suggesting that they do not assist in substrate recognition and nucleolytic activity, but the turnover rate of the enzyme in vitro approached that measured in vivo.

Husain et al. (1985) and Yeung et al. (1986) have proposed a model for nucleotide excision repair which is shown in Fig. 10.

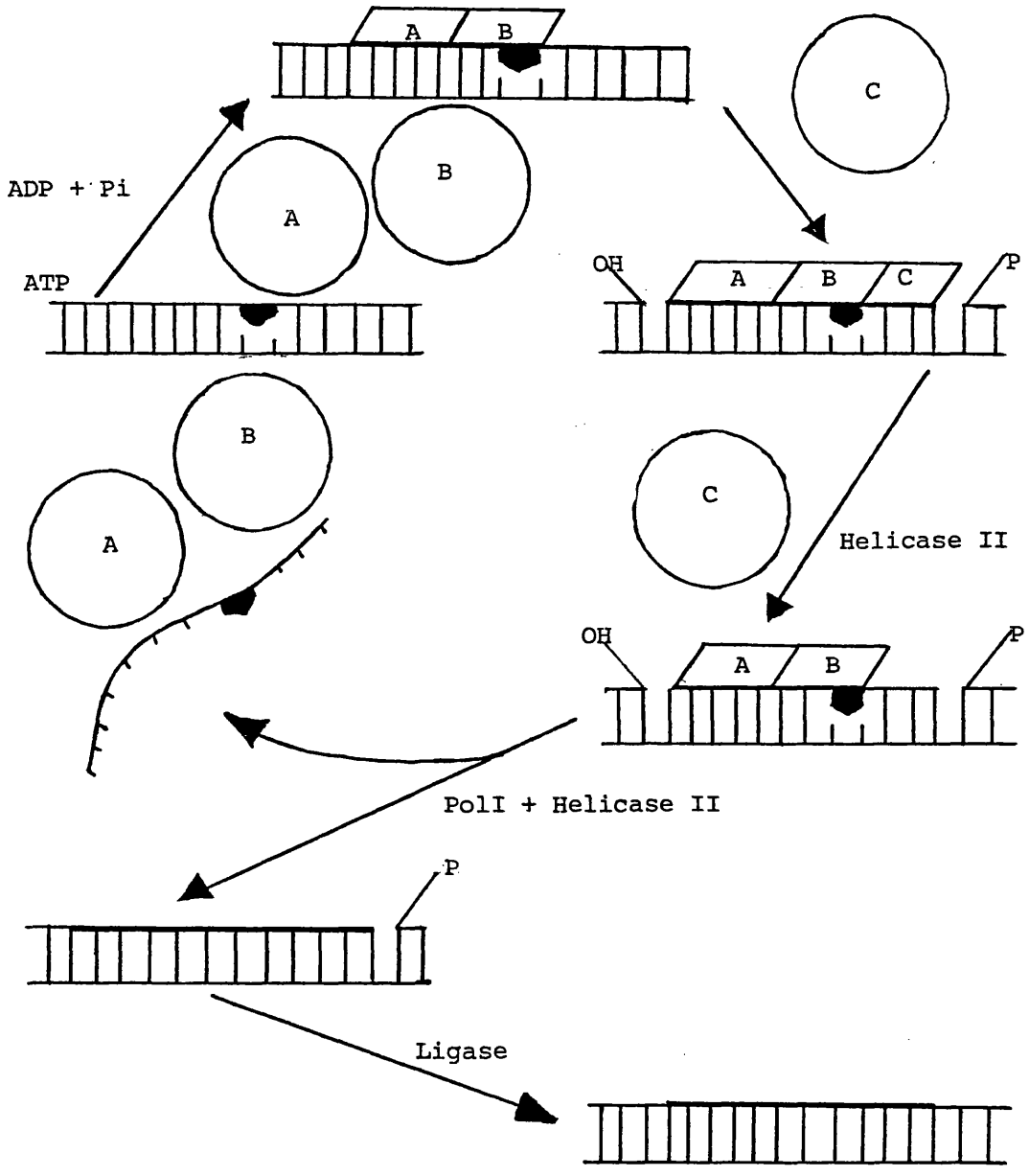

Fig.10. Schematic illustration of the model for Nucleotide Excision Repair proposed by Husain and Sancar (1985)

Briefly, the UVRA protein is an ATPase which scans DNA and stops when it encounters a nucleotide adduct. The UVRB protein binds to and stabilizes the UVRA protein-DNA complex, resulting in a 2 to 3-fold stimulation of UVRA ATPase activity. UVRC protein binds to the UVRA-UVRB-DNA ternary complex to constitute UVR ABC excision nuclease, which cuts the 8th phosphodiester bond 5' and the 4th (or 5th) phosphodiester bond 3' to the adduct. After incision, UVRC protein may be released by helicase II; however, the other two subunits remain at the cutting site. The UVRA and UVRB proteins, together with the excised oligonucleotide, are displaced by the combined action of DNA polymerase I and helicase II. The excision gap is filled in by the polymerase as the displacement occurs and ligase seals the resulting nick. Caron et al. (1985) found that DNA polymerase I cannot initiate nucleotide incorporation into nicked DNA in the absence of helicase II. The authors suggested the UVR ABC protein may protect nicks from exonuclease attack until the rest of the repair machinery arrives. Matson (1986) found the helicase activity of the uvrD gene product translocates along DNA in a 3' $\rightarrow$ 5' direction and is maintained on the template strand, consistent with the hypothesis that it displaces the incised fragment. It is intriguing that a similar incision pattern is obtained using differing damage substrates, even though each causes different topological configurations. Oh and Grossman (1986) postulated that this constancy of breakage sites is probably imposed on DNA by the UVR proteins. Using DNA unwinding studies, these workers found that it was ATP binding to UVRA protein and not its hydrolysis which imposes conformational changes in the latter and so 'locks' the protein-DNA complex into a productive conformation.

Effects of DNA Photolyase on UVRABC Excision Nuclease Activity

Yamamoto et al. (1983b) have reported the observation that when a recA strain of E. coli is transformed with a multicopy plasmid pKY1 carrying the phr gene of E. coli, its extreme UV sensitivity is decreased in yellow light, which is not effective in photoreactivation. This was not seen in strains carrying phr:: Tn1000 plasmids, in which phr gene function was inactivated by transposon insertion. Yamamato et al. (1983a) reported similar results using E. coli recA purA strains, and concluded that PRE participates in the process of dark repair of UV-damaged DNA. Hays et al.(1985) drew a similar conclusion from studies with the Lambda 'phage-repressed infection system.

In a further study using strains transformed with plasmid pKY1, Yamamoto et al. (1984) found that the increased UV-resistance was not apparent in uvrA, uvrB, uvrC, lexA, recBC or recF backgrounds. The sensitivity of recA lexA and recA recBC multiple mutants to UV irradiation was suppressed by the plasmid, but that of recA uvrA, recA uvrB and recA uvrC was not. These results indicated that the REC BC nuclease does not have any function in the dark repair capacity of photolyase. The plasmid had no effect on Hfr-mediated genetic recombination efficiency nor did it influence the level of spontaneous Lambda 'phage induction in a lysogenic recA strain. The authors concluded that the dark-repair capacity of photolyase is associated with excision repair.

Using UV-irradiated pBR322 DNA and the reconstituted UVR ABC excision nuclease system in vitro, Sancar et al. (1984a) found that addition of highly purified E. coli DNA photolyase stimulated both the initial rate and extent of the cutting reaction 2-fold. However, no stimulation was observed using a cis-platinum damaged

substrate, indicating that the effect of photolyase on the activity of UVR ABC excision nuclease is specific for pyrimidine dimers. The same rate and extent of photoreactivation was observed irrespective of whether UVRA and UVRB proteins were present or absent in the reaction mixture, suggesting that the binding of these subunits does not affect the binding of photolyase. DNA photolyase was found to inhibit T4 endonuclease V, an enzyme which repairs only pyrimidine dimers by cleaving the N-glycosyl bond of the 5' pyrimidine and then the phosphodiester bond 3' to the newly generated apyrimidinic deoxyribose. These data implicate the pyrimidine dimer itself as being the important structure for recognition by both T4 endonuclease V and DNA photolyase. Sancar et al. (1984a) concluded that since the incision sites generated by UVR ABC nuclease are apart by about one turn of the helix, the enzyme binds to DNA on one face that does not include the two pyrimidines forming the dimer. Therefore, the excinuclease does not interfere with photolyase binding, which recognises the dimer, but instead recognises the helical distortion caused by the damage. In a study using various damage substrates, the authors found that psoralen-pyrimidine mono- and di-adducts were the best substrates, followed by [6-4] photoproducts, certain cis-Platinum$(NH_3)_2Cl_2$ adducts and then pyrimidine dimers.

In a recent study, Myles et al. (1987) have used DNA photolyase and alkali hydrolysis to investigate non-standard incision by UVRABC excision nuclease. They found that both pyrimidine dimers and [6-4] photoproducts could result in cutting at the 7th rather than the 8th phosphodiester bond 5' to the damage. By measuring the photolyase-induced stimulation of UVRABC excision nuclease activity, the authors were able to conclude that photolyase does

not bind to [6-4] photoproducts. However, T-T dimers are good substrates for both binding and photolysis whilst T-C, C-T and in particular C-C dimers are neither bound nor repaired efficiently.

2.3 DNA Damage Tolerance and Post-replication Repair

Several lines of evidence indicated that nucleotide excision repair was not the only DNA repair mechanism occurring in the dark in E. coli. Firstly, bacterial strains deficient in both excision repair and genetic recombination were more sensitive to killing by UV radiation than were strains carrying either mutation alone, suggesting that genetic recombination may have some function in DNA repair. Secondly, Rupp and Howard-Flanders (1968) demonstrated that in an excision-repair-deficient strain, newly synthesized DNA from UV irradiated cells sedimented more slowly than DNA from non-UV irradiated cells, suggesting the presence of daughter-strand discontinuities; but after further incubation, the sedimentation rate of the UV-irradiated DNA approached that of the control DNA. The authors hypothesized that the advancing replicative machinery temporarily halted when it encountered a UV-induced photoproduct, and recommenced synthesis some way downstream of the damage, resulting in a daughter strand gap opposite the damage. A re-combination event between homologous sister strands was postulated to fill the gaps. The concepts of strand exchange and post-replication repair were derived from this work. The published work resulting in the model shown in Fig. 11. has been reviewed by Howard-Flanders (1981). Briefly, a lesion in a parental strand DNA results in the formation of a post-replicative daughter-strand gap (1). RECA protein, the product of the recA gene at 58 minutes on

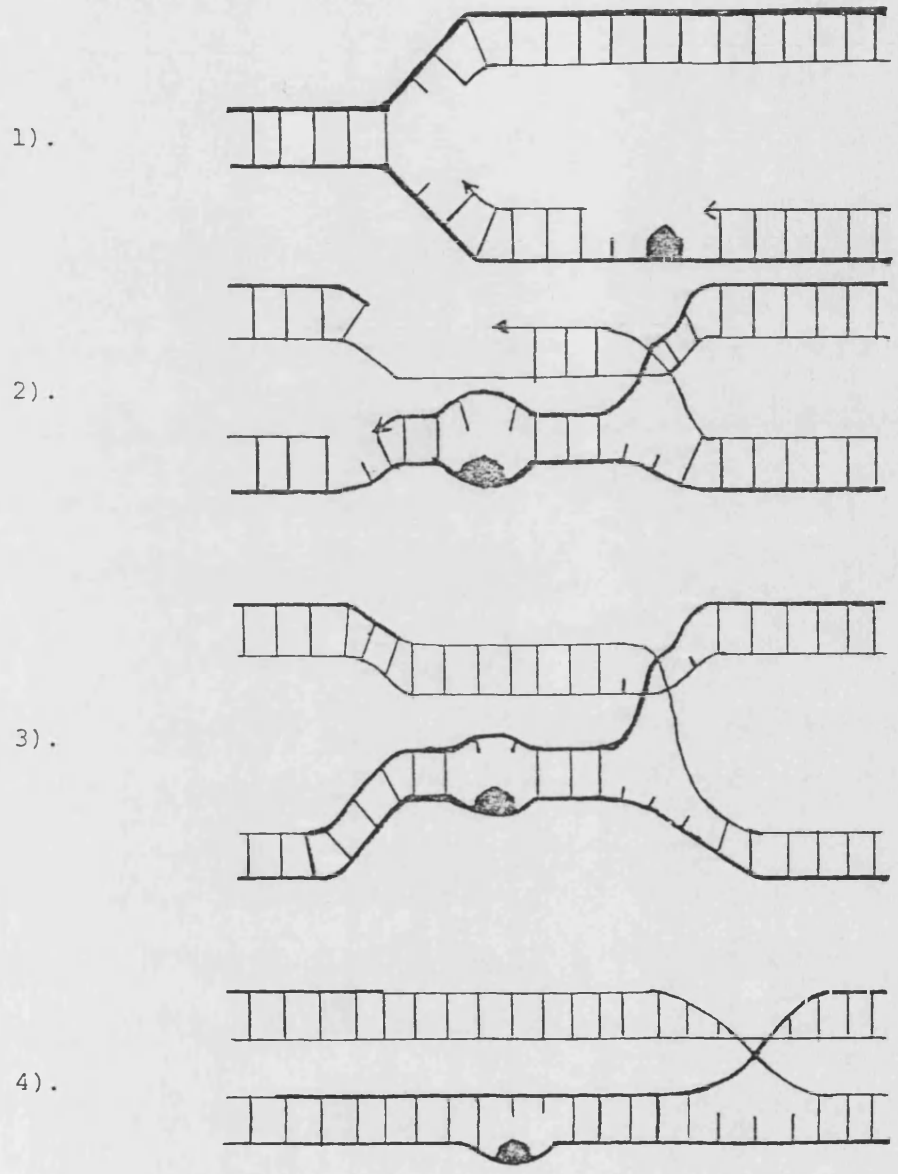

Fig. 11. Schematic illustration of discontinuous semi-conservative DNA replication with gap filling. See text for explanation. (Adapted from Friedberg, 1984).

the chromosomal map (Bachmann, 1983), binds to the single-stranded region and aligns it with an homologous region of the sister duplex. The interaction of RECA protein with single-stranded DNA is stabilized by the ssb gene product, DNA single-stranded binding protein. When homologous pairing is achieved, an enzyme nicks the duplex and the free end now crosses with the isologous newly synthesized daughter strand, producing a crossed-strand exchange (2). The gaps in the heteroduplexes are repaired by repair synthesis and DNA ligation (3). The two strands are then cut and rejoined (4). It must be remembered that the primary lesion is still present.

There are two main pathways for post-replication repair in E. coli. The recF$^+$-dependent pathway promotes the repair of daughter-strand gaps, whereas the recBC$^+$-dependent pathway repairs DNA double-strand breaks arising from unrepaired daughter-strand gaps (discussed by Wang and Smith, 1986). However, Wang and Smith (1985a) demonstrated that the sbcB suppression of recBC deficiency is attributable to inactivation of DNA exonuclease I, the sbcB gene product. This enzyme degrades single-stranded DNA from the 3' end. The authors suggested that the preservation of 3' single-stranded ends of DNA double-strand breaks may provide an intermediate for the recF$^+$-dependent pathway, whilst in the sbcB$^+$ recBC$^+$ background the combined exonuclease I and exonuclease V (recBC$^+$ gene product) activities produce blunt ends which are a substrate for the helicase activity of the recBC$^+$ gene product. Wang and Smith (1985b) studied the effect of the umuC mutation on post-replication repair in E. coli B. They noted that umuC decreased the ability of uvrB, uvrB recF, uvrB recB, and uvrB recF recB strains to repair daughter-strand gaps, but did not significantly affect the repair

of double-strand breaks arising from unrepaired daughter-strand gaps. The umuC mutation interacted most additively in the uvrB recB recF background suggesting that the two repair processes act on different types of DNA damage. The authors calculated the frequency of overlapping daughter-strand gaps in uvrB cells and found it to be greater than the number of lethal hits. They postulated a role for umuC gene product in a minor pathway in the repair of daughter-strand gaps, possibly overlapping regions. However, uvrB recB recF umuC strains can still undergo gap filling.

2.4 The SOS Regulatory System of Escherichia Coli

E. coli exhibits a complex and diverse response to many conditions which damage DNA or inhibit DNA replication. Phenomena such as enhanced capacity for DNA repair and mutagenesis, inhibition of cell division (filamentation), and Lambda prophage induction have been recognised. The existence of the SOS system was hypothesised to account for these seemingly unrelated phenomena, under the co-ordinate control of two genes termed recA and lexA. The physiology of the SOS responses and the early work on the genetics of lexA and recA have been reviewed by Witkin (1976), whilst later work has been reviewed by Little and Mount (1982) and Walker (1984). In an uninduced cell, the product of the lexA gene acts as a repressor for many unlinked genes including uvrA, uvrB, umuCD, sfiA and the regulatory genes recA and lexA, by binding to similar operator sequences upstream of each gene. The number of operator sites varies according to the gene, as does the affinity of LEXA protein binding, thus facilitating differential expression depending on the cellular level of LEXA repressor protein. When the DNA is damaged or its replication is inhibited,

an inducing signal is generated. This inducing signal, which may be single-stranded DNA, serves to activate the protease activity of RECA protein. This activated RECA protein cleaves the LEXA protein at an alanine-glycine peptide bond, rendering it ineffective as an operator-repressor, and so the various SOS genes begin to be expressed at an increased level. Simple overproduction of RECA protein does not result in LEXA protein cleavage, indicating that activation is essential.

As the cell begins to recover from the inducing treatment, the inducing signal is eliminated, and the RECA molecules return to their proteolytically inactive state. In the absence of RECA protease, the continued synthesis of LEXA molecules leads to repression of the SOS genes and a return to the uninduced state. Sedgwick and Goodwin (1985) introduced a plasmid carrying the *E. coli lexA* gene into six *Enterobacteria* spp. and measured decreased RECA protein levels in *E. coli*, *Klebsiella* sp. and *Citrobacter* sp., whilst *Shigella sonnei* exhibited UV-sensitization without decreased RECA protein levels. The results suggested that the SOS regulatory mechanism is widespread amongst *Enterobacteria* and functionally conserved.

2.4.1 SOS Induction and Mutagenesis

A comprehensive review of mutagenic repair is beyond the scope of this work; however, it is apposite to briefly discuss some recent work which has used enzymatic photoreactivation to probe the mechanisms of UV-induced mutagenesis.

Bridges and Woodgate (1984) tested the hypothesis that the *umuC* gene product is required for DNA strand elongation past photo-

products in the template strand. They found that application of photoreactivating light immediately after UV radiation in a umuC$^+$ strain resulted in a decrease in the mutation frequency, whereas if the bacteria were allowed to metabolise on nutrient plates for 4 hours before photoreactivating light treatment, the decrease in mutation frequency was still significant but considerably smaller. This indicated that as the mutation became fixed, photo-reversibility was lost. However, in the umuC strain, the initial photoreactivating light treatment did not alter the mutation frequency from the spontaneous level, but delayed PR treatment resulted in an increase in the mutation frequency. This failure to fix lethal damage up to 4 hours after irradiation led the authors to suggest that the presence of pyrimidine dimers maintains the replication fork in a configuration which neither allows replication nor DNA degradation. The increase in mutability of the umuC strain after photoreactivation indicates that the umuC$^+$ gene product is involved in strand elongation past damage, rather than the misincorporation event. In a further study using photo-reactivation to dissect the processes of mutagenesis, Bridges and Woodgate (1985) established that the RECA protein must have a role in addition to derepressing umuCD genes since in a lexA51 (no LEXA repressor activity), recA430 (no protease activity) strain, the mutation frequency was similar to recA430 alone. Perry et al. (1985) have compared the homology of the umuD and lexA gene products and found 31 per cent overall homology. In addition they found a cysteine-glycine cleavage site in UMUD protein corresponding to the alanine-glycine cleavage site of LEXA repressor. This suggests that proteolytic cleavage of UMUD protein, by activated RECA protein, may be necessary for SOS

mutagenesis. Bridges and Woodgate (1985) have developed a 'two-step' model to describe bacterial UV mutagenesis.

STEP 1. DNA polymerase III (*polC* gene product) proceeds until it encounters a photoproduct. Activated RECA protein facilitates insertion of bases opposite the lesion by decreasing the fidelity of the 3' ⟶ 5' proof-reading activity of the polymerase.

STEP 2. UMUCD protein modifies the configuration of the lesion-mismatch terminus so that it is a suitable primer for continued chain elongation.

As discussed in Section 1.2.2, there is a growing body of evidence to suggest that the photoreactivable *cis-syn* cyclobutadipyrimidine dimer may not be the major pre-mutagenic UV-induced lesion (reviewed by Franklin and Haseltine, 1986). Brash and Haseltine (1985) found that photoreactivation treatment reduced the induction of the *umuC*$^+$ gene to that corresponding to a seven-fold lower UV-fluence, whilst the extent of photoreversal of *umuC*$^+$ induction was the same as the decrease in mutation frequency. Therefore, the cyclobutane dimer may be the significant SOS-inducing lesion whilst other lesions are pre-mutagenic. Ruiz-Rubio et al. (1986) found that UV mutagenesis in a *uvrB5 lexA51* mutant was photoreversible to the same extent as the *lex*$^+$ partner, indicating that dimers must have some function in addition to SOS induction. To test the hypothesis that dimers activate RECA protein to the 'second mechanism' expressed constitutively by the *recA441* allele or whether dimers are the target lesion, they measured the effect of photoreactivation treatment on a UV-irradiated *uvrB5 lexA51 recA441* strain. They found that whilst survival was photoreversible, mutagenesis was not, indicating that dimers are not target lesions for UV mutagenesis in the mutational system

studied.

Yamamoto et al. (1985) measured the effect of photoreactivation on killing, induction of RECA and UMUC proteins, and *his-4* to *his*$^+$ mutation in *E. coli uvrA6*. The PR dose-modification factor for killing was 7, but only 2.5 for RECA protein induction. Indeed, RECA protein was still induced to 60 per cent of its maximum level even after full PR treatment, suggesting that non-dimer photoproducts are more significant pre-mutagenic lesions and more effective at SOS induction. However, Yamamoto (1985) found photoreactivation treatment repaired lethal damage, and damage leading to *trpE9777* frameshift mutation to *trp*$^+$ to the same extent. This work appeared to contradict the finding of Yamamoto et al. (1985), but Yamamoto (1985) pointed out that the *trpE9777* frameshift mutation results from the addition of an A-T base pair to a run of five A-T base pairs and is thus a potential target for T-T dimers, whereas the *his-4* to *his*$^+$ mutation is probably a base subsitution which is more likely to result from a [6-4] photoproduct.

Thus it will be concluded that UV mutagenesis is complex and the effect of photoreactivation depends both on the locus and the mutation-type assayed.

GENERAL METHODOLOGY

The principal organisms used in this study were E. coli K-12 AB2480, DY326, AS44 and AS46. A list describing the genotypes and source of all the organisms used in this study is included in Appendix A1.

1. Storage of Organisms

Stock cultures of all strains were sealed in sterile plastic tubes, packed in plastic vials and stored in the vapour phase of a liquid nitrogen refrigerator (Union Carbide Ltd) at -196°C. These were subcultured into nutrient agar stabs which were prepared by dispensing 5 ml aliquots of molten nutrient agar into 7 ml screw-capped glass vials (Hoslab, Ilford, Essex). The nutrient agar was prepared by adding 22.4g of Oxoid CM3 nutrient agar (Oxoid Ltd., Basingstoke) to 800 ml of glass-distilled water in a 1 litre flat-bottomed flask and allowing to stand for 10 minutes. The agar was dissolved by bringing to the boil. These were then sterilized by autoclaving at 121°C for 15 minutes. After allowing to set in an upright position, the stabs were inoculated and incubated for 48 hours at either 30° or 37°C (as appropriate) in a LEEC PCF2 incubator (LEEC, Nottingham) . Approximately 0.4 ml of sterilized liquid paraffin BP (Thornton and Ross, Huddersfield) was aseptically added to each vial to reduce evaporation. The liquid paraffin was prepared by sealing 1 ml aliquots in 1 ml nominal capacity glass ampoules and sterilized at 160°C in a hot air oven for 4 hours. These stabs were kept in the dark at room temperature.

For strains carrying antibiotic resistance plasmids, the appropriate antibiotic was added to the nutrient agar. In such cases, 100 ml of sterilized nutrient agar was prepared and allowed

to cool to 55°C. The antibiotic was then added and 5 ml aliquots dispensed into pre-sterilized vials.

For routine use, an inoculum from the stab culture was streaked out onto a nutrient agar plate using a sterile wire loop. The agar for these plates was prepared as described above and 20 ml volumes of molten agar were poured into 9 cm sterile petri dishes (Sterilin Ltd, Feltham). After inoculation and incubation, the plates were sealed with parafilm (Nescofilm) and stored in an inverted position at 4°C. These plates were discarded after two weeks. The phenotype of each strain was routinely verified by assessing growth on appropriate defined media plates.

2. Glassware

Glassware was decontaminated where necessary by autoclaving at 121°C for 30 minutes. All glassware was washed in glass distilled water and then rinsed three times before drying overnight in an oven. Sterilization was performed by heating at 160°C for 4 hours.

3. Water

The water used for all preparative work throughout this study was single glass distilled.

4. Growth of Organisms

4.1 Media Used for the Growth of Organisms

Nutrient broth was used as the growth medium for all UV-survival and photoreactivation experiments. Thirteen g of Oxoid CM1 nutrient broth was added to 1 litre of glass distilled water and allowed to stand for 15 minutes. One hundred ml volumes, in 150 ml medical screw-cap flat bottles, (Beatson-Clarke) were autoclaved at 121°C for 15 minutes. The final pH was 7.2-7.4 at 20°C. These were stored in the dark at room temperature prior to use.

A full list of the other media used in this study is included in the Appendix A2.

4.2 Incubation Water Bath

This was a Gallenkamp BKS 350 immersion water bath set at a temperature of 37° ± 0.5°C (unless otherwise stated) and shaking at 100 cycles per minute. The safety 'cut-out' thermostat was set at 45°C. Both the temperature and number of cyles per minute were monitored routinely.

4.3 Aeration Apparatus

A forced aeration system was used to standardize the amount of air to each culture vessel. Compressed air was passed through a course cotton wool filter connected to a Rotameter flow meter (Rotameter, Croydon) which regulated the flow-rate to 10 ml per minute to each culture vessel. The air was sterilized by passage through a 25 mm diameter, 0.45 μm pore-size Sartorius membrane filter (Sartorius membrane filters, GMBH, West Germany) positioned immediately before the entrance port to the culture vessel. This

apparatus has been described previously (Hodges, 1979).

4.4 Method

A loopful of surface-grown culture was inoculated into a 250 ml pyrex-screw-top conical flask containing 100 ml of pre-warmed growth medium. This was connected to the aeration apparatus, aeration checked and set at 10 ml per minute, and incubated in the shaking water bath for 24 hours. A secondary liquid culture was prepared by inoculating 99 ml of pre-warmed nutrient broth with 1 ml of the primary culture, and incubated as described above for 24 hours. Growth curves for strains AB2480, AS44, DY326 and AS46 are included in Appendix A3. These culture conditions were adhered to strictly to minimise the variation in photoreactivability measured by Tyrrell et al. (1972).

5. Harvesting of Organisms

5.1 Washing/Dilution Fluid

M9 salts solution (Anderson, 1946) was used to wash and resuspend cells, and also as the diluting fluid. M9 salts solution was prepared from two stock concentrates as follows:

M9 A (50 x concentrate)		M9 B (12.5 x concentrate)	
NH_4Cl	50 g	KH_2PO_4	37.5 g
$MgSO_4.7H_2O$	10 g	$Na_2HPO_4 2H_2O$	75 g
Water to	1 litre	NaCl	6.25 g
		Water to	1 litre

All chemicals were 'Analar' grade obtained from BDH Ltd. (Poole). The stock concentrates were autoclaved in 500 ml MRC bottles at

121°C for 30 minutes. M9 salts solution ('M9') was prepared by mixing 180 ml of M9A concentrate and 720 ml of M9B concentrate and made up to 9 litres with glass distilled water. Approximately 200 ml volumes of this solution were transferred to 250 ml flasks, sealed with aluminium foil and sterilized by autoclaving at 121°C for 15 minutes. The pH of this solution was 6.9 at 20°C.

5.2 Filtration Method

Apparatus. This was a negative-pressure Sartorius apparatus incorporating a sintered-glass supporting bed (Sartorius GMBH, West Germany). The filters used were 25 mm diameter Sartorius membranes with a pore size of 0.45 μm. Prior to use, they were placed between two pieces of Whatman filter paper, sealed in DHSS specification bags (J. Dickenson and Sons Ltd) and sterilized by autoclaving at 121°C for 15 minutes. The filter was rinsed three times prior to and three times after filtration of the cell suspension with 10 ml volumes of ice-cold M9 salts solution. Normally, 1.0 ml of cell suspension was filtered. The vacuum was then released and the filter aseptically transferred to a sterile 50 ml flask containing 10 ml of M9.

After harvesting, an estimate of the viability of the cell suspension was provided by measurement of the optical density of the suspension and referring to a previously determined calibration curve for the particular organism. Such a calibration curve (optical density : viable count) is shown in Appendix A3.

The optical density of the cell suspension was measured against a blank of M9 salts solution in matched 1 cm pathlength glass cuvettes in a Unicam SP 600 spectrophotometer set at a wavelength of 470 nm. The Beer-Lambert relationship does not apply to

optical densities greater than 0.35, so cell suspensions exceeding this value were diluted prior to reading.

6. Assessment of Viability

Cell viability was determined by relative colony forming ability on Oxoid nutrient agar plates.

6.1 Materials

a) Pipettes

Two Gilson pipettes (Gilson Medical Electronics, France) with volume ranges 0.1-1.0ml (model P1000) and 1.0-5.0 ml (model P5000) were used, in conjunction with the appropriate plastic tips. After use, the tips were washed and boiled in glass distilled water, dried, and packed into DHSS specification autoclave bags (J. Dickenson and Sons Ltd.) before sterilization at 132°C for 5 minutes in a Drayton-Castle high vacuum autoclave.

b) Dilution tubes

All serial dilutions were performed in 15cm x 1.9cm rimless thick-walled pyrex glass tubes, fitted with Oxoid aluminium caps. The tubes were prepared as described under 'glassware', dried, and sterilized by holding at 160°C for 4 hours.

c) Spreaders

These were prepared from glass quill, sealed at each end and having a 60° bend approximately two thirds along its length. They were prepared as described above, placed in 250 ml glass beakers, covered with aluminium foil, and sterilized by dry heat at 160°C for 4 hours.

d) Dilution medium

All dilutions were performed in M9 salts solution.

6.2 Plating Media

Unless otherwise stated, Oxoid CM3 nutrient agar was used throughout this study. The method of preparation is given under the 'Storage of Strains' section.

All plates were stored inverted at 4°C in the dark for up to 4 days. Immediately before use they were 'overdried' by placing in an inverted position at 37°C for 60 minutes under ventilated conditions.

6.3 Method of Assessment of Viability

The viable count of the bacteria was determined by an initial 20-fold dilution, effected by transferring 0.2 ml of the test suspension into 3.8 ml of M9 solution in a dilution tube. When survival was low after UV treatment, a 2-fold dilution was prepared by adding 0.4 ml of the test suspension to 0.4 ml of M9 solution. A subsequent series of 10-fold dilutions were performed as necessary by taking 0.5 ml of the diluted test solution and transferring it to 4.5 ml of M9 solution. Each dilution was thoroughly mixed using a Whirlimix (Fisons Ltd). A 0.2 ml aliquot of the required dilution was pipetted onto the surface of each of three nutrient agar plates, and spread uniformly with a sterile glass spreader. A range of dilutions were plated to yield colony counts in the 20-200 range. The plates were incubated in an inverted position at 37°C for 48 hours in the dark. The number of visible colonies (without magnification) on each plate was counted.

The mean value of the three plates, together with the dilution factor, was used to determine the number of viable bacteria in the test suspension.

6.4 Estimation of the Errors involved in Viable Count (VC) Assessment by this technique

The two principle sources of error which may be introduced arise from 1) the pipettes may not deliver accurate or precise volumes, and 2) the mixing of the bacterial suspension after each dilution stage may be insufficient for the count to truly reflect the viability of the suspension.

The error arising from the pipettes was assessed periodically by weighing volumes of glass-distilled water delivered under experimental conditions (Table 1). The conditions used simulated 'in-use' conditions, the pipettes were reset on each occasion and a fresh tip fitted. The glass-distilled water was equilibrated to room temperature (22^{o}C) in a Dewar flask, and the balance chamber was similarly equilibrated to constant humidity.

The efficiency of mixing of the bacterial suspension was assessed by performing six individual serial dilutions and determining the viability by plating a 0.2 ml aliquot onto the surface of each of four nutrient agar plates per dilution series. The experimental results and the analysis of the coefficient of variation are given in Table 2.

7. Irradiation Procedures

General

All ultraviolet light experiments were carried out in a "dark room" under illumination from red fluorescent tubes (Atlas Ltd.

Table 1 Summary of errors introduced in V.C. assessment by Gilson pipettes

Volume (ml)	Pipette	Mean(g)	Standard Deviation of Mean	Coeff. of Variation	%Differance from Theor. Value
0.2	P1000	0.1959	1.05×10^{-3}	0.536	-2.05
0.5	P1000	0.4920	4.792×10^{-3}	0.974	-1.6
3.8	P5000	3.7677	1.126×10^{-2}	0.298	-0.85
4.5	P5000	4.4831	1.165×10^{-2}	0.260	-0.376

Table 2 Analysis of error introduced during serial dilution and plating of the bacterial suspension.

Sample	Plate Counts	Dilution Factor	Viable Count
1	54,63,45,48	10^5	5.25×10^6
2	53,61,49,43	10^5	5.15×10^6
3	56,60,53,56	10^5	5.63×10^6
4	64,50,57,46	10^5	5.425×10^6
5	61,55,60,50	10^5	5.65×10^6
6	54,57,69,48	10^5	5.70×10^6

$\bar{x} = 5.468 \times 10^6$

$\sigma_n = 2.1 \times 10^5$

$\sigma_{n-1} = 2.3 \times 10^5$

$$\text{Coefficient of variation} = \frac{\sigma_{n-1} \times 100}{\bar{x}} = \frac{2.3 \times 10^5 \times 100}{5.468 \times 10^6} = 4.21\%$$

80W) which do not emit at wavelengths below 540 nm. This did not cause concurrent photoreactivation of damage to DNA and was further confirmed by action spectra studies for photoreactivation (see section 3.5).

8. Radiation Sources

8.1 Far-UV Radiation (254 nm)

The source used was a 5 cm Penray lamp (Ultraviolet Products Inc, San Gabriel C.A. JnC SC-1) fitted with a G-275 filter, which results in 95 per cent of the emission at 254 nm. Mains electricity to the lamp was supplied through a voltage stabilizer (Advanced Electronics CV 100A). The lamp was used in a horizontal position in the apparatus shown in Fig. 1. The irradiation vessel was positioned 20 cm directly beneath the UV source, with a shutter regulating exposure, positioned between. This was an iris camera shutter (G.B. Kershaw 630) with a 2 cm aperture and fitted with a cable release. Exposures were timed using a stopwatch. Where exposure times below 10 seconds were required, the shutter was electronically tripped using a relay switch and the exact exposure recorded on a millisecond timer (Marconi Instruments Ltd). The irradiation vessel was a jacketed, straight-sided glass bowl, with an internal diameter of 5.2 cm. Adequate stirring was ensured by passing a stream of filtered, humidified air onto the surface of the test suspension through a side jet. Nine ml of the bacterial test suspension was irradiated. The fractional increase in the distance between the source and the surface of the suspension after removal of each 0.2 ml aliquot was considered to be insignificant. A flow of compressed air was directed over the source filter to

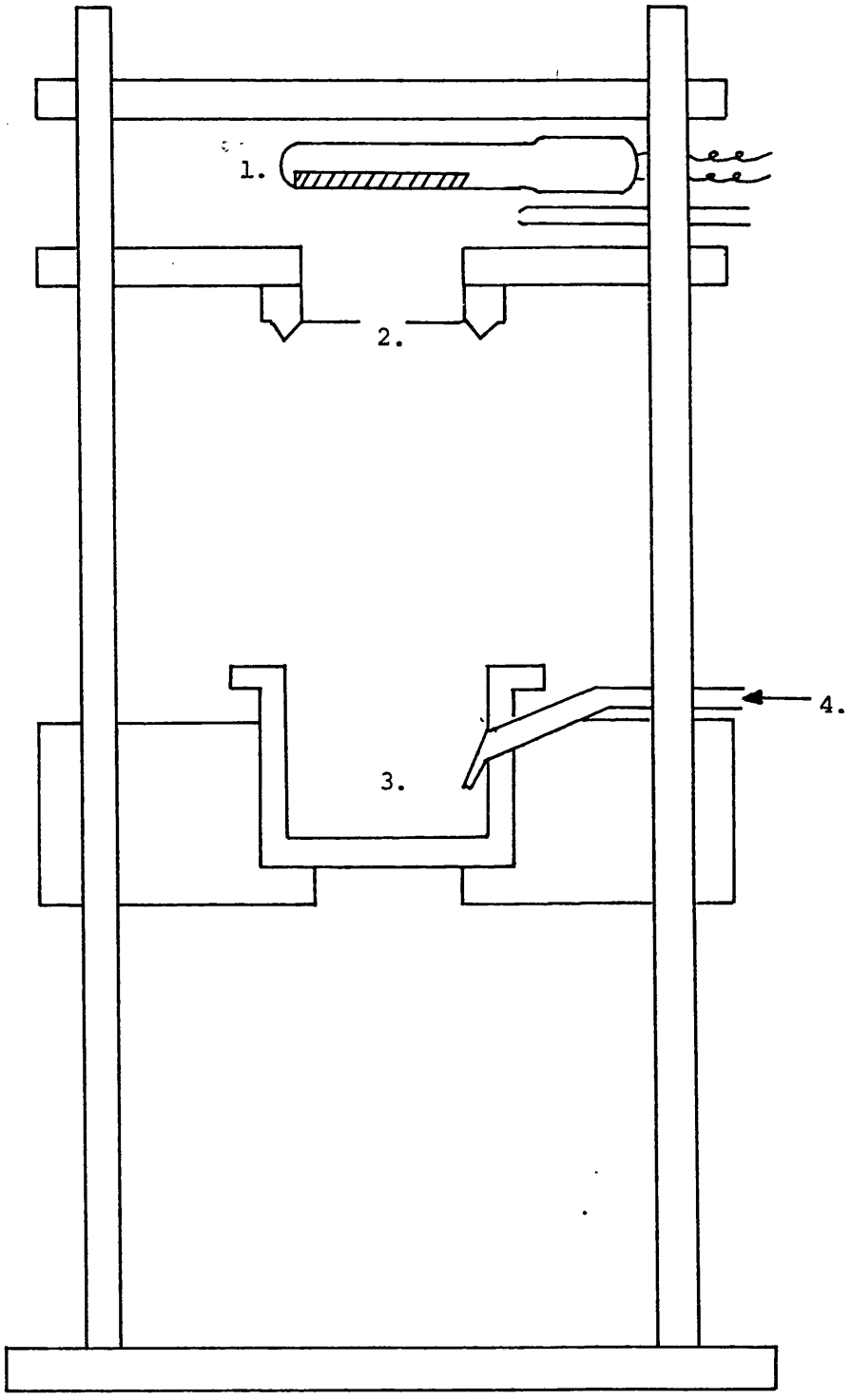

Fig. 1. Diagram of apparatus for 254 nm irradiation.

UV Source (1) Irradiation Vessel (3)

Shutter (2) Air Inlet (4)

prevent any build up of ozone. The bacterial test suspension was equilibrated to 25°C prior to irradiation,which was subsequently carried out at room temperature, 23-27°C.

8.2 Mid-UV Radiation (313nm)

The radiation source was a Bausch and Lomb SP200 super-pressure mercury lamp (Bausch and Lomb, Rochester, New York). This was a 200-W super pressure Mercury vapour lamp with a fused-silica envelope and an appropriate fused-silica condensing lens system. A 2 hour burn-off of newly fitted lamps was allowed prior to use, and each lamp was replaced after 100 hours use. The light source was used in conjunction with a Bausch and Lomb high-intensity grating monochromator which was fitted with a UV-visible diffraction grating of 1350 lines per millimeter for maximum efficiency at 300 nm. Operation is over a wavelength range of 200-800 nm with a stated reciprocal dispersion of 6.4 nm/mm. Matched fixed slit discs were used; the entrance and exit slits being 2.68 mm and 1.5 mm, respectively.

9. Arrangement of Optical Bench for Monochromatic Irradiation of the Cells

All optical components were arranged on an Ealing Beck optical bench and associated supports, thus allowing vertical and horizontal adjustments. The arrangement of the apparatus is shown in Fig. 2.

9.1 The Shutter: This was of the same type as that described in the previous section.

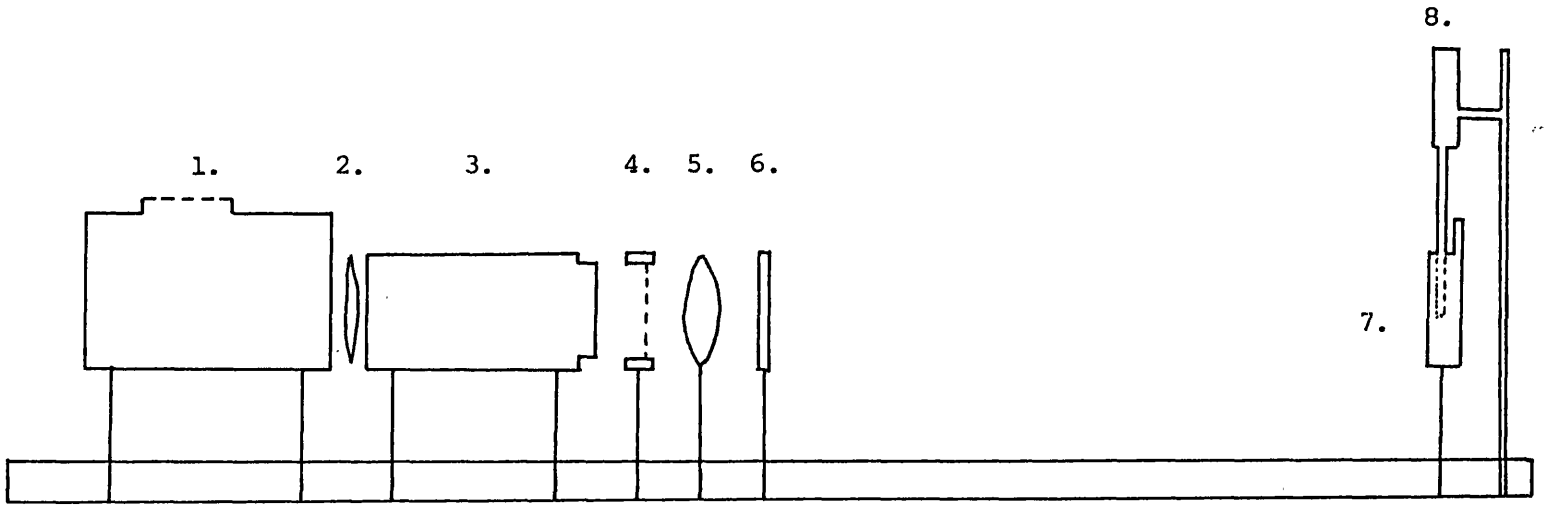

Fig. 2. Diagram of apparatus for 313 nm irradiation.

Mercury UV Source	(1)	Focusing Lens	(5)
Quartz Collective Lens	(2)	Mylar-C Filter	(6)
Monochromator	(3)	Irradiation Cuvette	(7)
Shutter	(4)	Stirrer	(8)

9.2 The Focusing Lens: This was a 40 mm diameter spectrosil biconvex lens having a focal length of 55 mm. This produced an inverted magnified image of the exit slit of the monochromator 3 cm high and 1 cm wide, allowing complete illumination of the irradiation cuvette.

9.3 Stray Light Filters: To eliminate stray light of shorter wavelengths which would contribute significantly to cell inactivation because of their higher energy properties, a 2.5 μm film of Mylar C (Dupont Ltd) was used. A period of approximately 2 hours exposure to 313 nm was required to 'age' the film, after which the transmission of the filter remained stable. A UV transmission spectrum, relative to air, obtained using a Perkin-Elmer 550S scanning spectrophotometer is shown in Fig. 3.

9.4 The Irradiation Cuvette: A jacketed 10 mm internal width, 10 mm pathlength quartz cuvette (Thermal Syndicate Ltd) was used and has been described by Kelland (1984). The temperature of the cell suspension was maintained at $0^{o}C \pm 0.5^{o}C$ (monitored periodically with a Comark probe thermometer) by circulation of a 50 per cent ethylene glycol : water solution through the jacketed cuvette. An insulated reservoir of the ethylene glycol solution was cooled by a U-cool refrigeration unit (Neslab Instruments Ltd) and the temperature regulated by a heating coil pump (Grant Instruments Ltd). The solution was then circulated at a high flow-rate through rubber tubing by a peristaltic pump (Watson Marlow Ltd). Any condensation forming on the cuvette faces was removed at the sampling intervals with absorbent tissue.

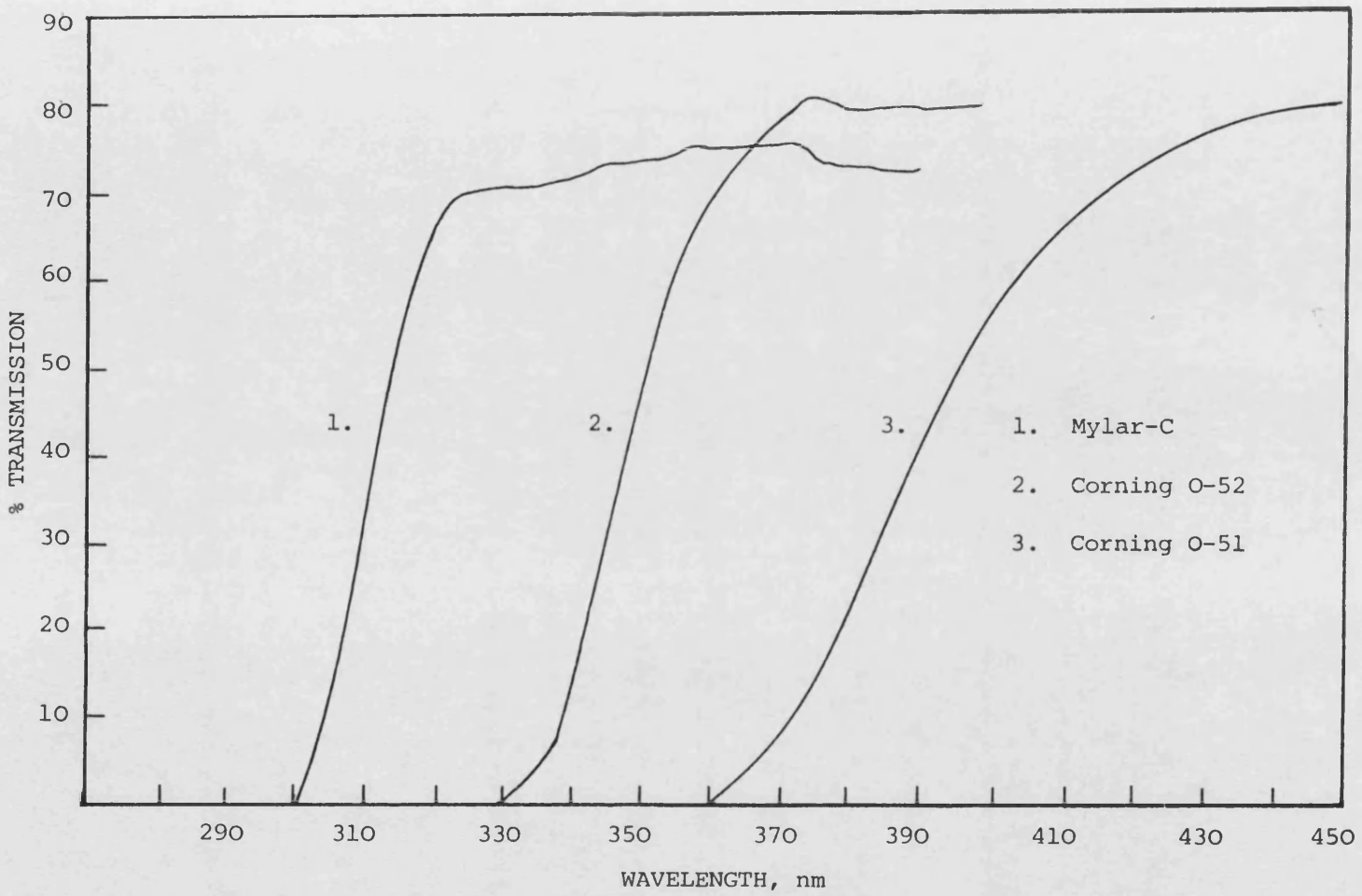

Fig. 3. Transmission characteristics of stray light filters.

9.5 The Stirrer: Cell suspensions were stirred during irradiation by means of a quartz paddle rotating in a laboratory stirrer (Stanhope Seta Ltd) at approximately 1200 rpm.

10. Analysis of Emitted Radiation

A second monochromator was used to scan the spectrum emitted from the monochromator system and Mylar C filter. This second analysing monochromator was an Oriel 7240 grating monochromator with 2400 lines per mm. The entrance and exit slits were set at 0.75 mm. It was positioned on the optical bench between the stray-light filter and the irradiation cuvette. The emitted radiation was focussed onto the entrance slit and dosimetry measurements of the light passing through it made using a calibrated thermopile (see under dosimetry section). The measurements were made at 1 nm intervals at $\pm$ 10 nm from the maximum emission wavelength or until no emitted radiation could be detected. An emission spectrum is shown in Fig. 4.

11. General Procedure for UV Irradiation of Bacterial Suspensions

After the appropriate growth period the bacterial cells were harvested and resuspended in ice-cold M9 salts solution to give a final viable count of approximately 1×10^7 colony forming units per ml. The period of time between harvesting and irradiation of the bacterial suspension was standardized at 12 minutes.

11.1 Penray Lamp (254 nm)

The lamp was switched on 20 minutes before use. The bacterial suspension was equilibrated to $25^{\circ}C$ in a water bath for 5 minutes

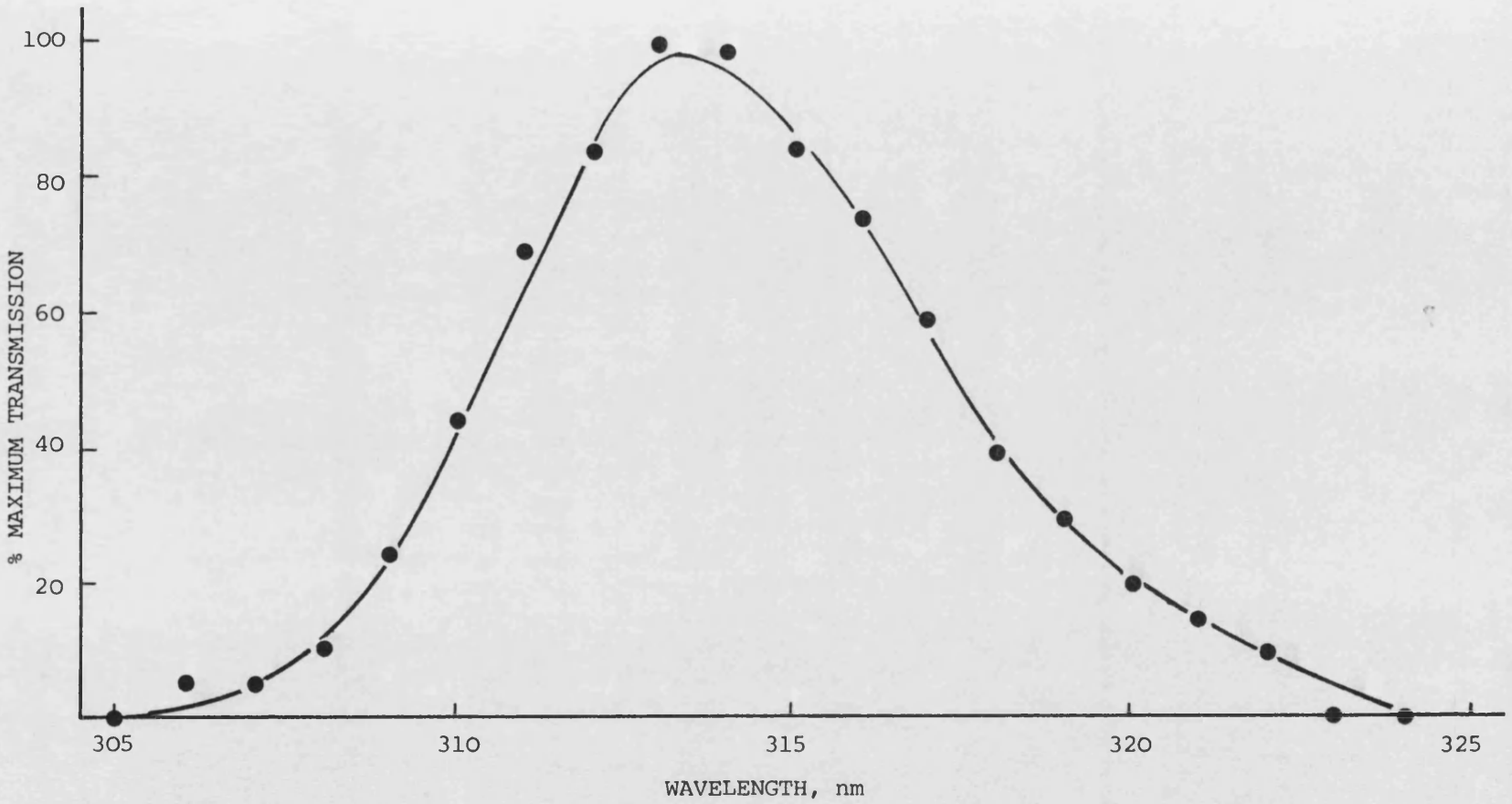

Fig. 4. An analysis of the emitted spectrum at 313 nm of the Bausch and Lomb monochromator fitted with a Mylay-C filter

and 9 ml transferred to the irradiation vessel which had been sterilized by holding at 160°C for at least one hour. A 0.2 ml aliquot was removed for initial viable count assessment and after each subsequent fluence to determine the surviving fraction.

11.2 Bausch and Lomb Lamp (313nm)

The lamp was switched on 40 minutes prior to irradiation or until the thermopile reading was steady (see Determination of Fluence Rate). The irradiation cuvette was aligned on the optical bench such that the beam covered its entire face. A thermopile (Oriel products Model 7102), mounted in a sliding saddle adjacent to the cuvette was moved into the beam and adjusted such that the distance between it and the lamp was equal to that of the face of the cuvette and the lamp. A series of microvolt readings were taken using the focal plane shutter. The irradiation cuvette was moved back into position, rinsed twice with sterile M9 salts solution, the stirring paddle introduced and switched on and the whole assembly sterilized by 15 minutes exposure to 254 nm irradiation from a Penray lamp. A 3 ml volume of the test suspension was introduced into the sterilized cuvette. The circulation of coolant through the jacket surrounding the cuvette was switched on, and a 5 minute period allowed for the suspension to reach 0°C.

12. Determination of the Fluence Rate of Ultraviolet Radiation

12.1 254nm source

The fluence rate was determined by routine chemical actinometry (Hatchard and Parker, 1956). The method uses potassium

ferrioxalate as the actinometer and relies on the light-catalysed production of Fe^{2+} ions in a solution of $K_3Fe(C_2O_4)_3$. The solution absorbs light completely in the UV region, the yield is independent of the fluence rate and the quantum yield of the reaction is constant.

Actinometry was performed under red light according to the method of Jagger (1967), by irradiation of 8.8 ml of actinometer in the irradiation vessel. It was intended that this method would take into account any internal reflection arising from the use of the glass irradiation vessel. A calibration curve of optical density at 510 nm against amount of ferrous ion (shown in the appendix A3) was constructed and used to determine the amount of ferrous ion formed by the radiation. The fluence rate was calculated from this, using the constant pertaining to 254nm (see Jagger, 1967).

12.2 313nm Source

The fluence rate was determined using an Oriel 7102 thermopile (Oriel Scientific Ltd., Kingston-upon-Thames). As described earlier, the thermopile was mounted in a sliding saddle beside the irradiation cuvette and adjusted such that the lamp and detector were equi-distant to that of the lamp and the inside front face of the irradiation cuvette. Output voltages were measured with a Keithley 181 nanovoltmeter (Keithley Instruments, Cleveland OH). The fluence rate was determined again after each irradiation.

12.3 Calibration of the Thermopile

Conversion of the incident energy from microvolts to fluence rate was made by reference to the calibration for the thermopile

determined by potassium ferrioxalate actinometry. A number of fluence rates obtained at different distances from the UV source were determined by chemical actinometry and plotted against the thermopile reading for the Oriel 7102 detector. This graph is shown in Fig. 5. The slope, fitted by least squares linear regression analysis, resulted in a conversion factor for microvolts to Wm^{-2} of 0.02273.

13. Acetophenone

Acetophenone (Aldridge Chemical Co) was stored as a 10 per cent solution in dimethylsulphoxide (DMSO) (BDH, Analar grade, Poole) in sterile 25 ml McCartney Bottles. The bottles were wrapped in foil and kept at room temperature for up to one month.

14. Photoreactivation Procedures

14.1 Apparatus

The apparatus is shown diagrammatically in Fig. 6. All fittings were mounted on an optical bench.

14.2 Light Sources

14.2.1 Continuous broad-band illumination. A 500-Watt quartz halogen lamp (FFX Sylvania Electric Products Inc. USA) in an Anscomatic 604 slide projector (GAF GB Ltd) was used. The projector assembly included a cooling fan and a condensing-focusing system.

14.2.2 High intensity millisecond flash. When determining the number of enzyme substrate complexes and investigating the kinetics of photoreactivation, the millisecond flash photolysis technique

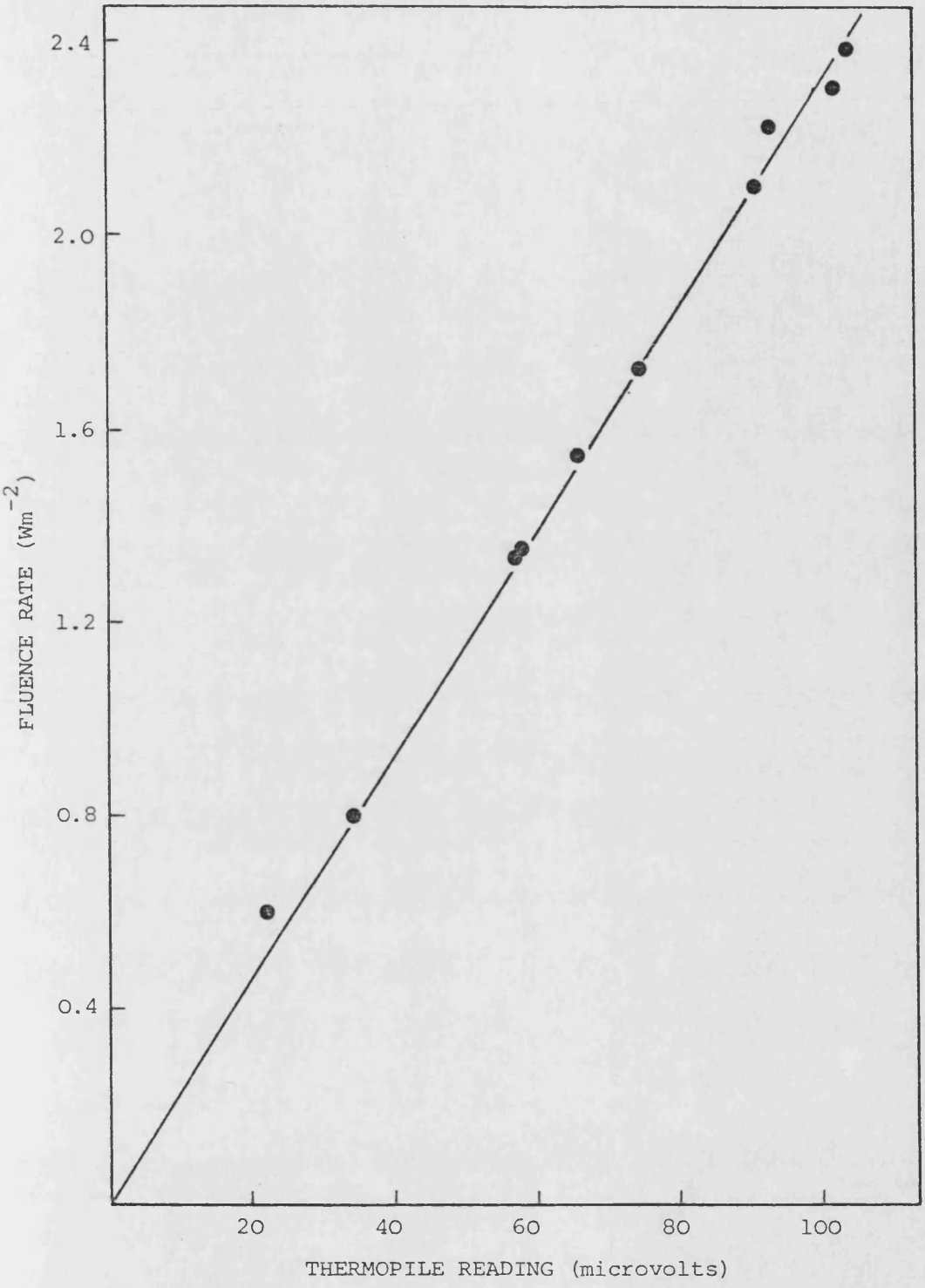

Fig. 5. Calibration curve for the Oriel 7102 thermopile, plotting fluence rate determined by actinometry against the thermopile reading in microvolts (r = 0.998).

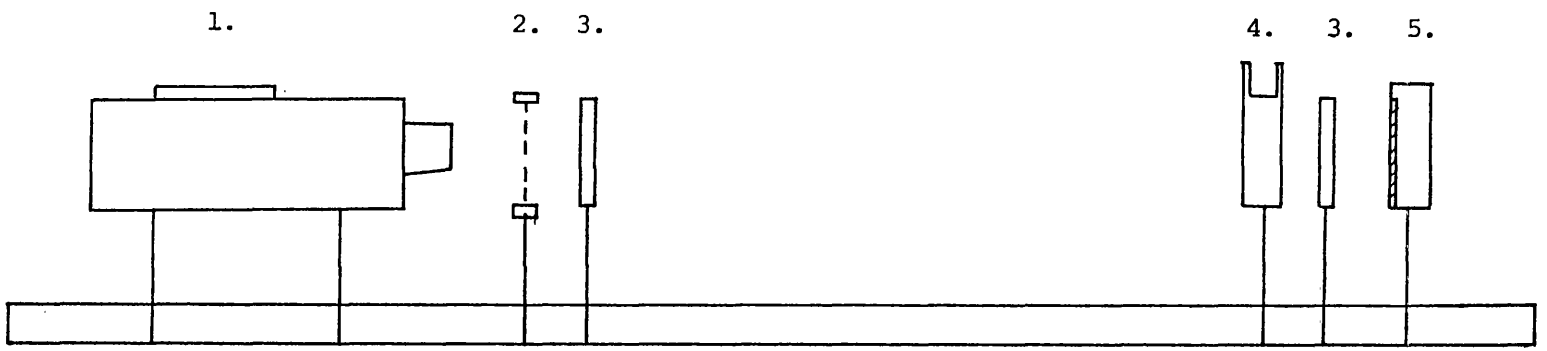

Fig. 6. Diagram of apparatus used for photoreactivation.

G.A.F. Projector	(1)	Temperature Control Unit/ Illumination Vessel	(4)
Shutter	(2)		
Filter Holders	(3)	Flash Gun	(5)

developed by Harm and Rupert (1968) was used. A battery-powered National PE-3064 flash gun was used, which had a recharging time of approximately 15 seconds. The gun was triggered manually.

14.3 Filters

The continuous broad-band light was filtered through a 2 cm pathlength solution containing 1.2% copper sulphate and 1.4% cobaltous sulphate and a purple glass filter (Ealing 26-3384). The resulting transmission spectrum is shown in Fig. 7. The transmitted light was a continuous band of wavelengths between 350 and 420 nm, which is the biologically effective region for photoreactivation (this work; Jagger et al., 1969).

14.4 Illumination Vessel

The bacterial suspension for photoreactivation was placed in a 1 cm pathlength glass cuvette fitted with a plastic lid. These were stored in 70% ethanol, dried by a stream of compressed air and sterilized by 254 nm radiation from a Penray lamp for 10 minutes.

14.5 Temperature Control Unit

This consisted of a rectangular glass vessel 10 cm x 10 cm x 2.5 cm with two optically flat surfaces (Ealing Ltd) and an aluminium lid assembly incorporating an insert to hold the illumination vessel in the light path. A continuous flow of water was supplied to the jacket through one tube from a water bath (Gallenkamp) fitted with a thermostatic pump-heater (Shandon, London), and removed by a constant-level syphon tube. For experiments requiring the temperature to be below ambient

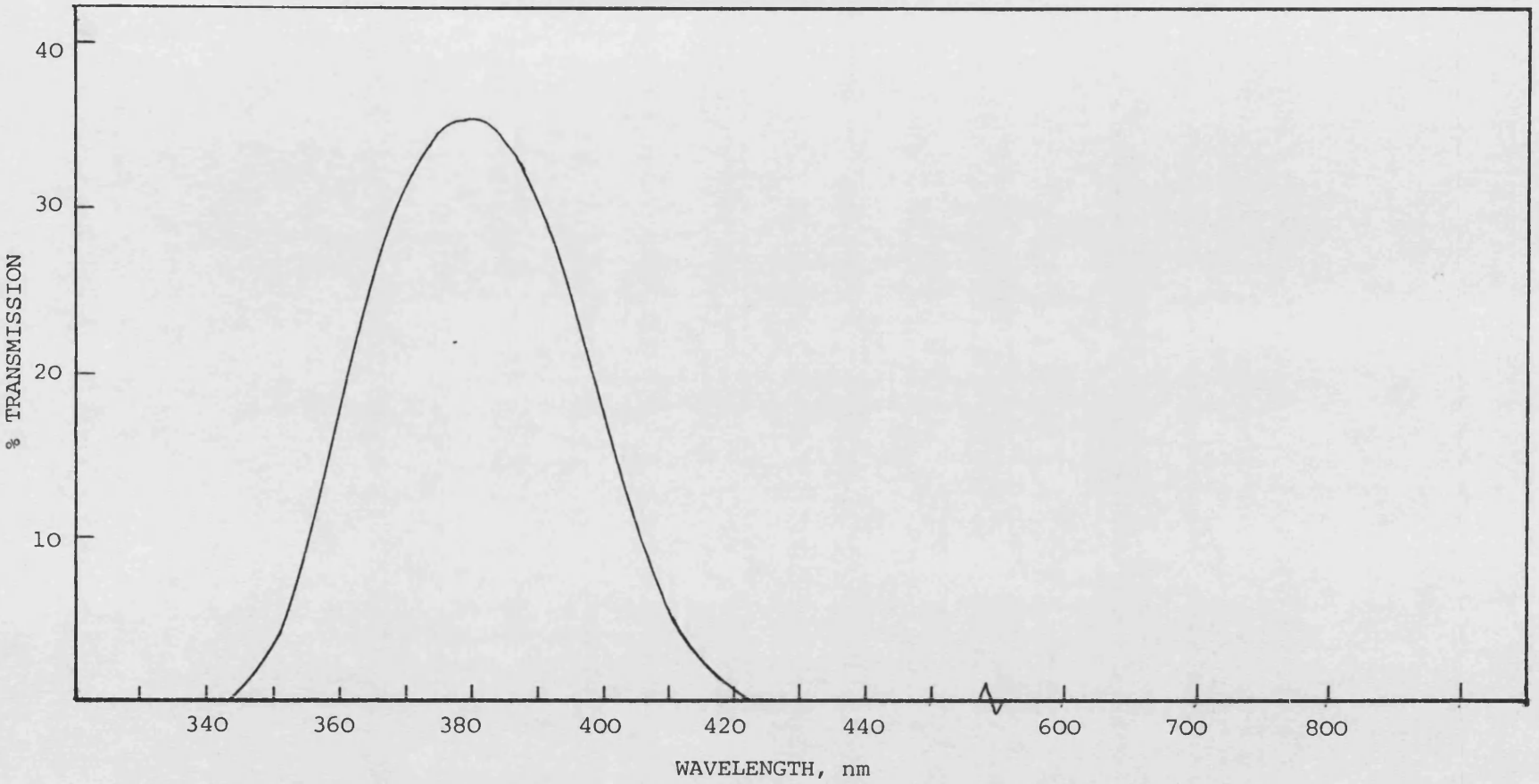

Fig. 7. Transmission properties of the filters used in the photoreactivation experiments.

temperature, a bath-cooler was used (U-cool, Neslab Instruments Ltd). Temperature equilibration was achieved in approximately 4 minutes and maintained throughout within $\pm$ 0.1^{o}C. Routine temperature measurements were made throughout each experiment using a Comark probe thermometer.

14.6 Photoreactivation with Monochromatic Illumination

The illumination vessel and temperature control unit were fitted to the Bausch and Lomb SP200 Mercury lamp and high intensity gating monochromator described previously (see '313nm irradiation'). The stray-light filters listed in Table 3 have been used by Kelland (1984) for the determination of UV inactivation action spectra and were considered appropriate for this study. The transmission properties of these filters are included in Fig. 3.

Table 3. Details of Stray Light Filters used in Monochromatic Photoreactivation Experiments.

STRAY LIGHT FILTER	EXPERIMENTAL RANGE (nm)
MYLAR-C 2.5 μm	313-340
CORNING O-52	350-390
CORNING O-51	400-600

14.7 Method of Photoreactivation

After UV irradiation the suspension to be photoreactivated was held in a 25°C water bath for 20 minutes to allow for the formation of the photoreactivating enzyme-substrate complexes. The cuvette was then placed in the temperature control unit. Unless otherwise stated, all photoreactivation experiments were carried out at 25°C. However, for the temperature studies, a 20 minute period at 25°C was always allowed to elapse prior to equilibration to the required temperature.

A piece of opaque material was placed between the projector assembly and the irradiation vessel, after which the lamp was switched on. This screen was removed at the same instant as the triggering of the flash gun (it was estimated that the time involved was approximately 1 second). A piece of opaque material was then placed in front of the flash gun to minimise errors arising due to reflection. The period of illumination was timed using a stop watch.

Separate UV irradiated samples were used for each photoreactivating exposure, since it has been shown that fractionated doses have an increased effect (Tyrrell, 1971).

A comparative estimate of the fluence rate was made using the calibrated thermopile, which was positioned such that its window corresponded to the front face of the glass cuvette.

RESULTS AND DISCUSSION - PART I

The four principle test organisms used in this study were AB2480, DY326, AS44 and AS46 (see Appendix 1). All of these organisms are uvr recA, and are thus deficient in excision repair and genetic recombination. In this section the isolation of AS44 (a recA derivative of SA206) and AS46 (a recA phrB derivative of SA206) is described.

Strain construction was performed by the bacteriophage transduction method first described by Lennox (1955) and by the general procedure of Miller, 1972. The temperature-sensitive 'phage P1::Tn9, isolated by Rosner (1972), was used. This mutant of P1, which carries the chloramphenicol-resistance transposon Tn9 and makes clear plaques at high temperature (42°C), but turbid plaques at low temperature (32°C), is of particular value because donor-strain lysogens can be isolated at 32° by the acquisition of chloramphenicol resistance, and then heat induced at 42°C to produce a transducing lysate.

1.1 Isolation of a P1::Tn9 Lysogen of the Donor Strain

One drop of P1::Tn9 lysate was added to 1 ml of an overnight culture of the donor strain grown at 37°C in LB medium (see Appendix 2) supplemented with 10 µg/ml thymine and 5×10^{-3} M $CaCl_2$ (LBt). After incubation at 30°C for 20 minutes, one inoculating loopful was streaked onto an L-CAP plate (see Appendix 2) and incubated at 30°C for 24 hours. Colonies were replicated onto L-CAP plates and incubated at 30° and 42°C. Those unable to grow at 42°C were identified as P1::Tn9 lysogens.

1.2 Lysogen Induction

Lysogens were grown overnight at 30°C in lysogen broth

(Appendix 2). One hundred ml of pre-warmed lysogen broth, inoculated with 1 ml of the overnight culture, was shaken at 30° for 2 hours until reaching early logarithmic phase, before being transferred to a 40°C water bath (Gallenkamp Ltd) and shaken for 40 minutes. After chilling on ice for 10 minutes and centrifugation at 4000 rpm (2500g, MSE Chilspin) for 15 minutes at 4°C, 90 per cent of the supernatant was removed and the pellet resuspended in the remaining broth, thus effecting a 10-fold concentration of the bacterial cells. The bacterial suspension was shaken at 37°C for 3 hours until lysis occurred due to 'phage liberation.

Ten drops of chloroform per 100 ml culture were added and shaking continued at 37°C for a further 15 minutes. The cell debris was removed by centrifugation at 4000 rpm for 20 minutes at 4°C. The supernatant was stored in 25 ml glass, screw-topped bottles (McCartney bottles), with a few drops of chloroform, at 4°C. The 'phage titer of lysates stored in this way remained constant over several months.

1.3 Determination of the Bacteriophage titer

The lysate titer was determined by the method described by Miller (1972). Serial dilutions of the lysate were prepared in MC buffer (10 mM $MgSO_4$, 5 mM $CaCl_2$). Pre-adsorption of the 'phage was effected by mixing 0.1 ml of 10^{-1} to 10^{-8} dilutions of the 'phage suspension with 0.1 ml of an overnight culture of a sensitive strain of bacteria in LBt broth (normally the 'recipient' strain used in subsequent transduction experiments). After 10 minutes at 37°C, each pre-adsorption mixture was plated in 3.5 ml of molten R-top agar (Appendix 2) at 42°C over R-plates (Appendix 2). After allowing to dry, the plates were incubated overnight at 37°C. On

day 2, the plaques were counted and the number of 'phage per ml of the original lysate computed. Typical results from four experiments are shown in Table 1.1.

Table 1.1 Result of Plaque Assays of Pl::Tn9 Transducing Lysates

EXPERIMENT NUMBER	PLAQUE COUNTS per 0.1ml	MEAN	DILUTION FACTOR	PFU/ml
1	122, 131, 72	108.0	10^6	1.00×10^9
2	124, 156,112	131.0	10^5	1.31×10^8
3	20, 14, 25	19.67	10^7	2.00×10^9
4	52, 47, 69	56.0	10^7	5.60×10^9

1.4 Transduction

Transduction was performed by the method described by Miller (1972). An overnight culture of the recipient strain, grown in LBt broth at 37°C, was centrifuged at 4000 rpm (2500g, MSE Chilspin) for 15 minutes, resuspended in MC buffer and shaken at 37°C for 30 minutes. Ten- to one-thousand fold dilutions of the 'phage lysate were prepared by serial dilution in MC buffer, and equilibrated to 37°C. A 0.1 ml aliquot of the lysate (or dilution) was incubated with 0.1 ml of recipient cells in a pre-warmed test-tube at 37°C for 30 minutes, after which 0.2 ml of 1M sodium citrate was added to chelate the Mg^{2+} ions necessary for 'phage adsorption. The pre-adsorption mixture was plated in 3.5 ml F-top agar (Appendix 2) at 42°C over the appropriate selective medium. The plates were

incubated at 37°C for 48-72 hours.

2. Construction of phrB Derivatives

E. coli K-12 DY314 (Appendix 1) was used as the source of the phrB mutation. This was the original phr mutation isolated by Harm and Hillebrandt (1962) as a photoreactivation-deficient mutant of E. coli B, and transduced into DY314 (see Appendix 1). A lysate was prepared as described above. The close proximity of phrB to the galKTE locus on the genetic map (Bachmann, 1983) indicated that selection of transductants on M9 minimal media supplemented with 0.2% galactose (Appendix 2) and scoring these for the phr phenotype, would be an appropriate selection protocol. In their phr mapping studies, Youngs and Smith (1978) reported a 28 per cent co-transduction frequency between gal and phrB.

In this work, 52 GAL^+ transductants were picked and replicated onto 4 nutrient agar plates fitted over a grid template. Each plate was treated in the following way:

PLATE NUMBER	TREATMENT
1	Control
2	80 Jm^{-2} 254 nm UV
3	80 Jm^{-2} 254 nm UV followed by 1 hour photoreactivation under a spotlight
4	Control

After 48 hours incubation at 37°C, 14 colonies were selected as potentially PHR^-. An inoculating loopful of each colony was resuspended in 5 ml of M9 salts solution. Ten µl of this suspension was pipetted onto the surface of each of four nutrient

agar plates, and the selection treatment described above repeated, except the 254 nm fluences were reduced to 40 Jm^{-2}. Seven (50 per cent) of the transductants were found to be PHR$^-$. Strain AS45 was selected for full UV survival and photoreactivation studies. The 14 per cent co-transduction of gal and phr was approximately 50 per cent lower than that reported by Youngs and Smith (1978). However, in this study the recipient strain, SA206, had a deletion extending through gal, and so the absence of partially homologous DNA may be expected to significantly reduce the transduction of this marker.

In the phrB mapping studies reported in this work (see Transduction Mapping of phrB), the transduction frequencies reported by Youngs and Smith (1978) have been confirmed using a strain having a point-mutation in gal.

3. Construction of recA Derivatives

Csonka and Clarke (1980) have constructed JC10240, an Hfr strain carrying the tetracycline resistance transposon (Tn10) inserted into the srlA gene (D-glucitol-specific enzyme II of the phosphotransferase system), in addition to the recA56 mutation. Since the srlA::Tn10 marker is approximately 0.1 minute from recA on the K-12 chromosome (Bachmann, 1983), a high frequency of co-transduction would be expected; selection being for acquisition of tetracycline-resistance and screening for increased sensitivity to 254 nm UV radiation. However, Yamamoto et al. (1983b) failed to isolate recA transductants using JC10240 as the donor, and attributed this to low titer P1 lysates. To obtain higher titer lysates, they mated JC10240 with AB1157 and screened AB1157 srlA300::Tn10 exconjugants for increased 254 nm UV sensitivity. P1 lysates from these UV sensitive exconjugants gave satisfactory

transduction of the recA mutation. Similarly, Plakidou et al. (1984) attributed recA transduction problems to persistently low titer P1 lysates, and reported convenient transduction with 'phage T4GT7, a derivative of 'phage T4, capable of generalised transduction.

To obtain high titer lysates, emphasis was placed on the method of lysogen-induction. Rosner (1972) has shown the number of P1 'phage per input cell decreases as the temperature of induction increases, and attributed this to less efficient 'phage production, rather than less efficient induction. Similarly, the yield of 'phage per input cell in a recA lysogen was 14 per cent that of a $recA^+$ lysogen. This was also thought to be due to a smaller burst size (Rosner, 1972). In these experiments, the temperature of induction was decreased from 42° to $40^{\circ}C$ for 40 minutes, and the cells were concentrated 10-fold prior to lysis as described previously. This method routinely resulted in 'phage titers of $0.5\text{-}1.0 \times 10^9$ PFU/ml (Table 1.1). Transduction of the recA mutation was performed by the general method described above. Tetracycline-resistant colonies, selected on YENB plates (Appendix 2) supplemented with tetracycline HCl 15 µg/ml, were replicated onto three nutrient agar plates. Plate number 2 was given a 254 nm fluence of 30 Jm^{-2}, after which they were incubated in the dark at $37^{\circ}C$ for 24 hours. The fluence given had to be sufficiently large to counter the screening effect of the transferred colonies.

The co-transduction frequencies from four typical experiments are given in Table 1.2.

Table 1.2 Co-transduction frequency of recA56 with srlA300::Tn10

EXPT. NUMBER	NUMBER OF TETRACYCLINE RESISTANT COLONIES SCREENED	NUMBER OF UV SENSITIVE COLONIES	% COTRANSFREQUENCY
1	52	39	75.0
2	27	16	59.3
3	50	38	76.0
4	48	35	72.9

4. Transduction Mapping of phrB

The experimental procedure of Youngs and Smith (1978) was repeated using X9170 kdp gal (Appendix 1) as the recipient strain infected with a P1 transducing lysate prepared on DY314 (Appendix 1). The selective media were as described by Youngs and Smith (1978).

The average co-transduction frequencies between the various genes were calculated from the results in Table 1.3, and are shown in Fig. 1.1. The figures in parentheses are the corresponding values obtained by Youngs and Smith (1978).

Table 1.3 Co-transduction of phrB with kdp, gal and uvrB

	UNSELECTED MARKER			
SELECTED MARKER	kdp$^+$	phr$^+$	gal$^+$	uvrB$^+$
kdp$^+$	-	15/23	4/23	0/23
gal$^+$	7/41	15/41	-	15/41
kdp$^+$ gal$^+$	-	7/9	-	0/9

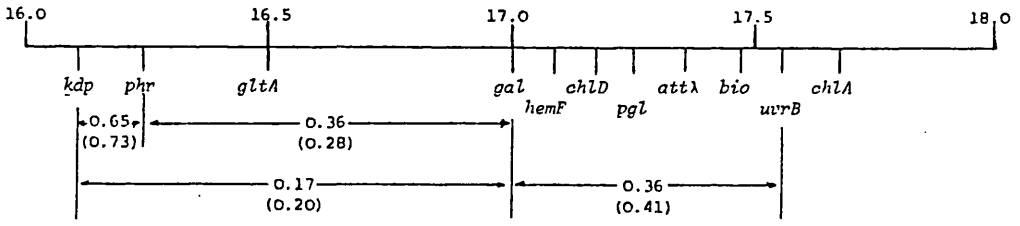

Fig. 1.1. Map positions within the kdp-chlA chromosomal region determined by cotransduction analysis.

These results clearly indicated that the phr mutation isolated by Harm and Hillebrandt (1962) lies counterclockwise of gal at approximately 16.2 minutes on the recalibrated linkage map (Bachmann, 1983).

5. Deletion Analysis of the chlA to gal Region

In an attempt to construct new strains having deletions in the region of the putative phrA gene, the methodology of Adhya et al. (1968) was attempted. Strain C600 (Appendix 1) was grown in nutrient broth (Oxoid Ltd) to mid-logarithmic phase and aliquots plated on chlorate agar (Appendix 2). The plates were incubated anaerobically (Gas-Pak Anaerobic Generating Kit) at 37°C overnight and then aerobically for a further 24 hours. Adhya et al. (1968) found that the surviving colonies did so as a result of a mutation in the chlA gene (nitrate reductase and formate dehydrogenase activity). These workers obtained a 10^{-5} mutation frequency, and of the 400 colonies tested, 39 were deletions.

In this study using C600, the mutation frequency was found to be 5×10^{-5}. However, of the 802 colonies tested, none were GAL^-. This indicated that, if present at all, no deletion had extended into the region of the proposed phrA gene. This methodology was not pursued any further.

RESULTS AND DISCUSSION - PART II

In this section the results of preliminary investigations to establish whether there was any further evidence to support the hypothesis of Sutherland and Hausrath (1979) in favour of two photoreactivation loci, *phrA* and *phrB*, in *E. coli* K-12 are reported. Several excision-deficient strains have been used, including SA446 (Δ(*attλ* -*chlA*) including *uvrB*), SA206 (Δ(*gal*-*chlA*) including *uvrB* and proposed *phrA*), AS45 (Δ(*gal*-*chlA*) *phrB*), DY314 (*uvrA uvrB phrB*) and the isogenic series AB1886 (*uvrA*), AB1885 (*uvrB*) and AB1884 (*uvrC*). The responses of these strains have been compared after 254 nm UV inactivation and exposure to broad-band photoreactivating light, to determine if there was i) altered photoreactivation kinetics in a strain deleted at the proposed *phrA* locus and ii) any evidence of photoreactivation in a strain mutated at the *phrB* locus.

1. Inactivation at 254nm

A 24 hour stationary phase culture of the strain was grown, harvested, and resuspended in M9 salts solution. A suspension was prepared containing 10^7 viable organisms per ml, by reference to the absorbance : viability calibration curve shown in Appendix 3. The suspension was exposed to graded fluences of 254 nm UV radiation; aliquots withdrawn and assessed for viability on nutrient agar plates (Oxoid). Two or three experiments were carried out on the same day for each strain. These survival data have been expressed graphically by plotting the surviving fraction ($^N/No$) on a logarithmic scale against the fluence (D) of radiation received.

Various models have been put forward to mathematically describe the survivor curve (reviewed by Haynes et al., 1984). In

classical hit theory it is assumed that cell killing is the direct result of the accumulation of a number (n) of physical "hits" in the cell. Hits are considered to be randomly distributed in a uniformly irradiated, homogeneous cell population, and so the surviving fraction can be calculated by application of Poisson statistics to the average number of physical hits per cell expected at any given fluence. Thus, in the 'single-hit' case, the predicted fluence-response relationship is exponential for cell survival. If more than one hit is required to produce the observed effect, there will be a threshold for the biological response at the cellular level. However, because of the random distribution of the number of hits per cell in the irradiated population, the fluence-survival curve exhibits a smooth shoulder bending away from the origin, rather than a discontinuous threshold response.

Target theory is similar to hit theory, but in this model it is assumed that cells contain sensitive "target" structures, within which the physical hits must occur to be relevant to the measured end-point. Haynes et al. (1984) claim that these classical approaches are unsatisfactory, because the observed effect is a biological event. Poisson distribution should be applied to these observed, randomly distributed, biological events. The biological events with respect to cell survival are called lethal hits. On average, one biological lethal hit is said to have occurred per cell after a fluence which leaves a surviving fraction of e^{-1}. In this 'repair' theory, lethal hits are assumed to be unrepaired lesions in DNA (Haynes, 1966).

Assuming the 'all-or-none' character of the measured end-point (i.e. survivor vs non-survivor), and denoting the average number of lethal hits per cell by the function H(x), the

probability of survival based on single-event Poisson statistics is exp[-H(x)], then the surviving fraction(s) ($^{N}/No$) of the cells can be written as:-

$$^{N}/No = e^{-H(x)} \quad \ldots\ 1$$

If the relevant physical lesions are formed in direct proportion to the fluence, and no fluence-dependent processes are involved in the conversion of these lesions into biological hits, then the hit function will be linear as in classic, single-hit theory. For single 'hit' kinetics where, according to target theory, a cell can be killed by inactivating just one target, survival curves may be mathematically described by the follow equaton:-

$$^{N}/No = e^{-kD} \quad \ldots\ 2$$

A plot of log $^{N}/No$ against fluence (D) produces a straight line relationship of slope:-

$$^{-k}/_{2.303}$$

However, some survival curves in this study exhibited an initial shoulder indicating a threshold in the cellular response to produce the observed effect as discussed previously. In these instances a 'multi-target' expression may be used:-

$$^{N}/No = 1-(1-e^{-kD})^{n} \quad \ldots\ 3$$

or

$$^{N}/No = ne^{-kD} \quad \ldots\ 4$$

where 'k' is the slope of the linear portion of the survival curve

in reciprocal fluence units (the 'inactivation constant') and n is the extrapolation number, numerically equal to the y-axis intercept of the extrapolation of the exponential part of the survival curve. As discussed earlier, the mathematical and mechanistic approach to the modelling and interpretation of survival curves no longer relies on classical target theory, but the parameters 'k' and 'n' may still be used for empirical determination of the inactivation efficiency of a particular radiation treatment and the response of different strains.

The survivor curves are shown in Figs 2.1 to 2.3, and the data pertaining to them are shown in Tables A4.1-6 (Appendix 4). The linear portions of the curves were fitted by least-squares linear regression analysis. The inactivation parameters obtained from analysis of the linear portion of the curve (obtained at fluences above 5 Jm^{-2}) are given in Table 2.1, together with their associated errors. Each set of data for each strain has been cumulated ('GA' in Table 2.1), and an analysis of covariance carried out to determine if inter-experimental variation was statistically significant. The inactivation parameters obtained from this analysis are also shown in Table 2.1. For each strain, the survival data from each experiment was compared to the cumulated data, to determine if the change in F-ratio was significant when the individual data were compared with the regression model (see Appendix 5). This would determine whether the differences in inactivation parameters represented a statistically significant variation in sensitivity. For each strain, the change in F-ratio arising from analysis of intercept or slope location was not significant at the 5 per cent confidence interval ($p>0.05$). It was considered important to determine if there were any differences

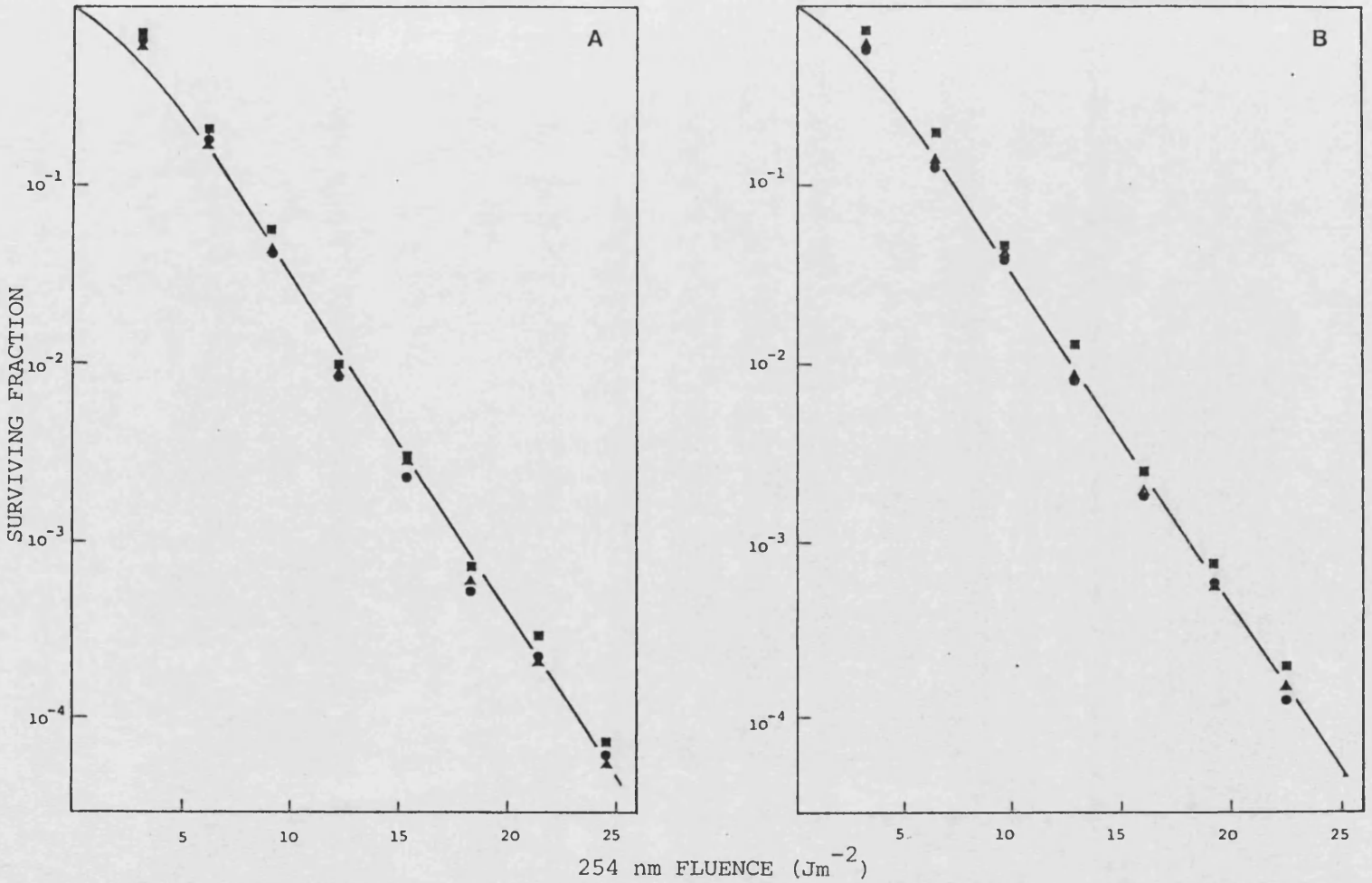

Fig. 2.1. Replicate 254 nm UV inactivation curves for 24 hour stationary phase AB1886 (Panel A) and SA206 (Panel B) at 25°C.

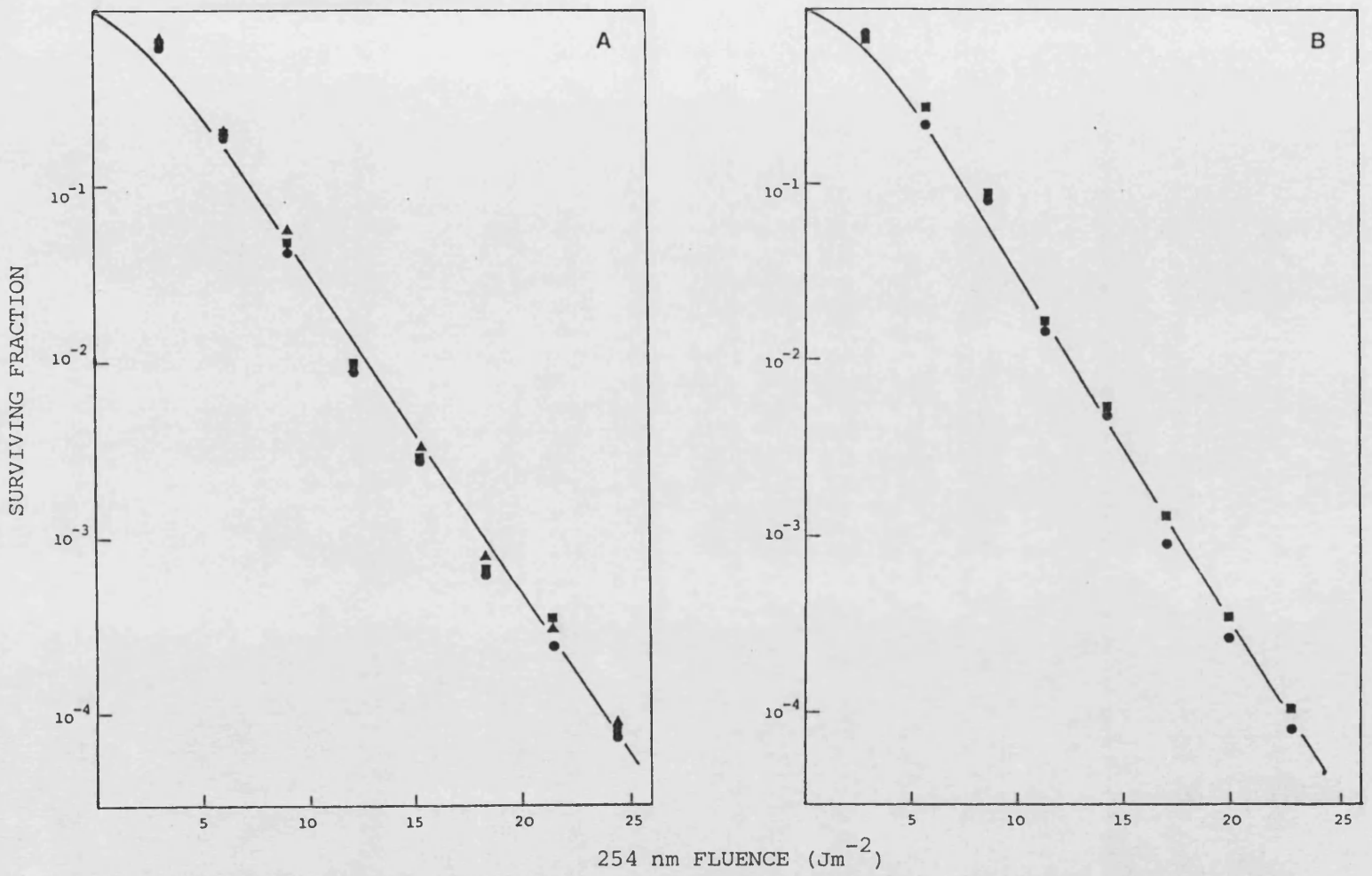

Fig. 2.2. Replicate 254 nm UV inactivation curves for 24 hour stationary phase AB1885 (Panel A) and AB1884 (Panel B) at 25°C.

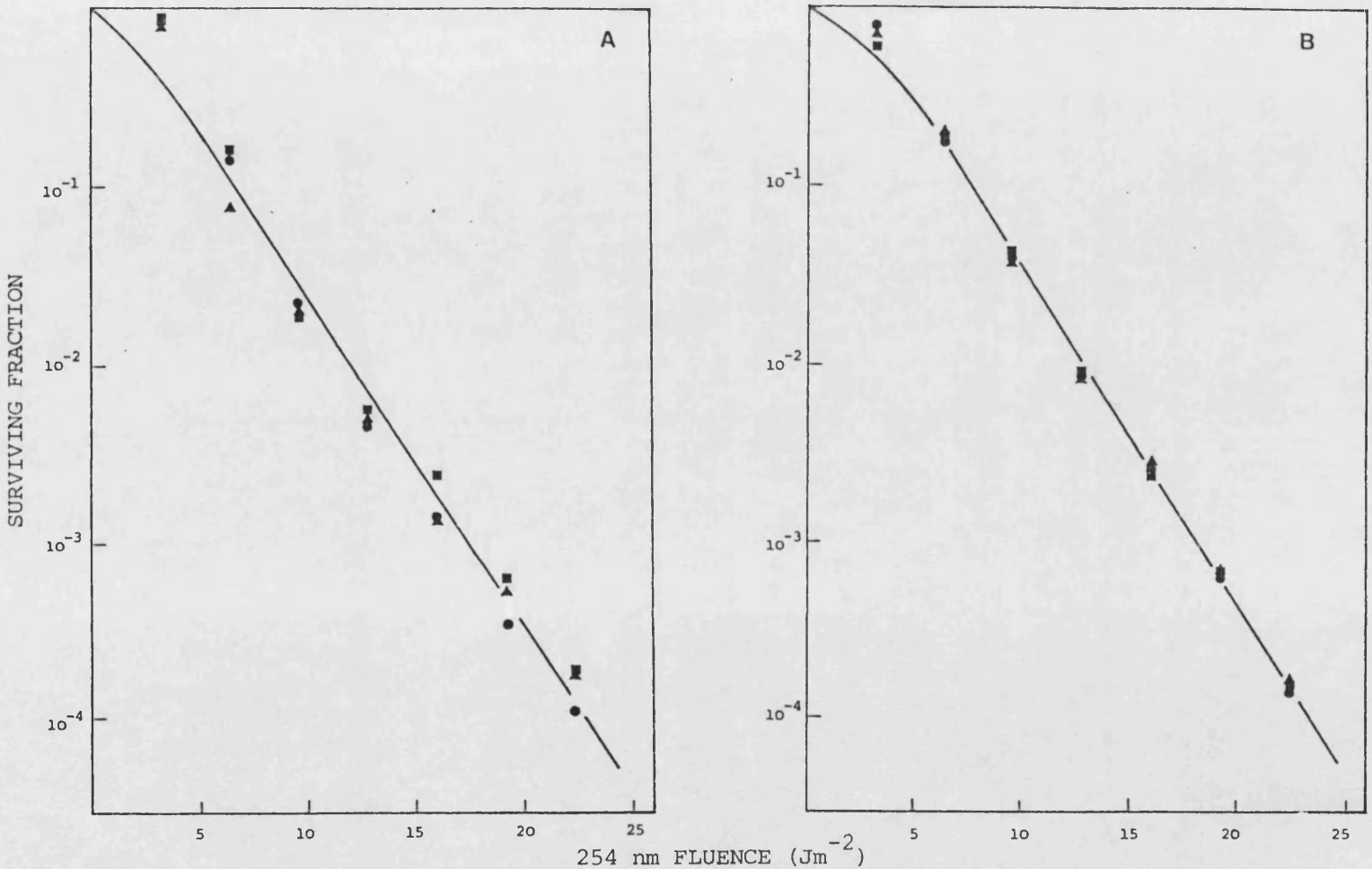

Fig. 2.3. Replicate 254 nm UV inactivation curves for 24 hour stationary phase DY314 (Panel A) and AS45 (Panel B) at 25°C.

Table 2.1 INACTIVATION PARAMETERS FROM THE 254 nm UV INACTIVATION CURVES OF 24h STATIONARY PHASE RECOMBINATION PROFICIENT STRAINS

ORGANISM	EXPT NO.	SLOPE (log 10)	STANDARD ERROR OF SLOPE	INTERCEPT	STANDARD ERROR OF INTERCEPT	'k' $(J.m^{-2})^{-1}$	'n'
	1a	-0.1895	6.6207×10^{-3}	0.33	1.089×10^{-1}	0.116	2.14
AB1886	1b	-0.1893	3.7304×10^{-3}	0.34	6.138×10^{-2}	0.436	2.19
(*uvrA*)	1c	-0.1881	5.5515×10^{-3}	0.41	9.134×10^{-2}	0.433	2.57
	GA	-0.1889	3.3178×10^{-3}	0.36	5.459×10^{-2}	0.435	2.30
	2a	-0.1884	3.900×10^{-3}	0.34	6.055×10^{-2}	0.434	2.20
SA206	2b	-0.1885	3.690×10^{-3}	0.37	5.696×10^{-2}	0.434	2.34
Δ(*gal-chlA*)	2c	-0.1878	2.960×10^{-3}	0.38	4.576×10^{-2}	0.433	2.40
	GA	-0.1883	3.540×10^{-3}	0.37	5.463×10^{-2}	0.434	2.37
	3a	-0.1923	8.146×10^{-3}	0.26	1.255×10^{-1}	0.443	1.81
DY314	3b	-0.1632	6.315×10^{-3}	0.14	9.731×10^{-2}	0.376	1.38
uvrA, *uvrB*,	3c	-0.1742	1.119×10^{-2}	0.135	1.724×10^{-1}	0.401	1.36
phrB	GA	-0.1766	6.029×10^{-3}	0.159	9.291×10^{-2}	0.407	1.44
	4a	-0.1934	5.636×10^{-3}	0.487	5.6033×10^{-2}	0.445	3.07
AS45	4b	-0.1893	4.903×10^{-3}	0.446	7.5556×10^{-2}	0.436	2.79
Δ(*gal-chlA*)	4c	-0.1927	2.136×10^{-3}	0.486	3.2922×10^{-2}	0.443	3.06
phrB	GA	-0.1918	1.941×10^{-3}	0.473	2.9917×10^{-2}	0.442	2.97
	5a	-0.1859	5.274×10^{-3}	0.34	8.6787×10^{-2}	0.428	2.17
AB1885	5b	-0.1837	6.024×10^{-3}	0.36	9.9124×10^{-2}	0.423	2.30
uvrB	5c	-0.1810	9.894×10^{-3}	0.27	1.6280×10^{-1}	0.417	1.86
	GA	-0.1835	3.922×10^{-3}	0.32	0.4543×10^{-2}	0.423	2.10
	6a	-0.2029	4.686×10^{-3}	0.53	7.9549×10^{-2}	0.467	3.41
AB1884	6b	-0.1993	2.603×10^{-3}	0.56	4.4307×10^{-2}	0.459	3.64
uvrC	GA	-0.2010	3.052×10^{-3}	0.547	5.1883×10^{-2}	0.463	3.52

in UV sensitivity between AB1886, SA206, DY314 and AS45, because the recA derivatives of these strains form the major part of this work. To this end, the grouped data for each strain were compared to a regression model formed from the cumulated grouped data. Strains AB1886, SA206 and AS45 were not significantly different ($p>0.05$). However, DY314 was significantly different. Inspection of its survivor curve (Fig 2.3 panel A) reveals it to be slightly more 'tailed' than the other strains, which would account for the change in slope and location of intercept. Moss (1972) has shown that this effect is attributable to post-irradiation incubation time at 37°C and arises due to the appearance of smaller colonies after 48 hours incubation. Moss (1972) observed no 'tailing' when the colonies were counted 16 hours after UV irradiation.

2. Liquid Holding Recovery (LHR)

It was necessary to demonstrate the absence of liquid holding recovery in these strains. All were either deleted or point-mutated in one of the three principle uvr loci, uvrA, uvrB and uvrC, and so we would not expect to observe LHR.

A suspension of 24 hour stationary phase cells of each strain was prepared in M9 salts solution and reduced to approximately $1x10^{-4}$ surviving fraction by an appropriate 254 nm fluence. The suspension was held at 25°C in the dark for 6 hours, with sampling at one-hourly intervals. There was no evidence of LHR or loss of viability when held for up to 6 hours (data not shown). As a further control, irradiated cell samples were kept in the dark and assessed for viability during all photoreactivation experiments.

3. Photoreactivation Experiments

Cell suspensions were prepared in the usual way and reduced to a surviving fraction of 1×10^{-4}. A survival curve was constructed for each photoreactivation experiment to ensure that there were no changes in UV sensitivity. None were detected throughout the duration of the study. The irradiated cell suspensions were held in the dark at 25°C for 20 minutes to enable the PRE molecules to become fully complexed with the dimer substrate. The suspension was then distributed into sterile glass cuvettes and exposed to broad band photoreactivating light for periods of time between 1 minute and 2 hours, at 25°C. A fluence rate of 70 Wm^{-2} was used. Tyrrell (1971) found no increase in the rate of photoreactivation of 254 nm UV-inactivated AB1886, beyond a fluence rate of 60 Wm^{-2}, indicating that saturating irradiation conditions had been reached. Beyond this point, the rate of photoreactivation was dependent only on the rate at which the PRE molecules complex with the substrate. The increase in surviving fraction resulting from exposure to photoreactivating light for the strains tested are shown in Figs. 2.4 to 2.9. The dark controls for DY314 and AS45 are included for reference (closed symbols).

Analysis of Photoreactivation Data

Several attempts have been made to develop mathematical models to linearise photoreactivation data, and so facilitate the derivation of kinetic parameters (Davies et al., 1970; Tyrrell and Davies, 1974; Harm, 1975; Johnson and Haynes, 1986a). In this work, the models of Tyrrell and Davies (1974) and Johnson and Haynes (1986a) have been used. The former method has been used to analyse the data in this section, and so will be discussed here.

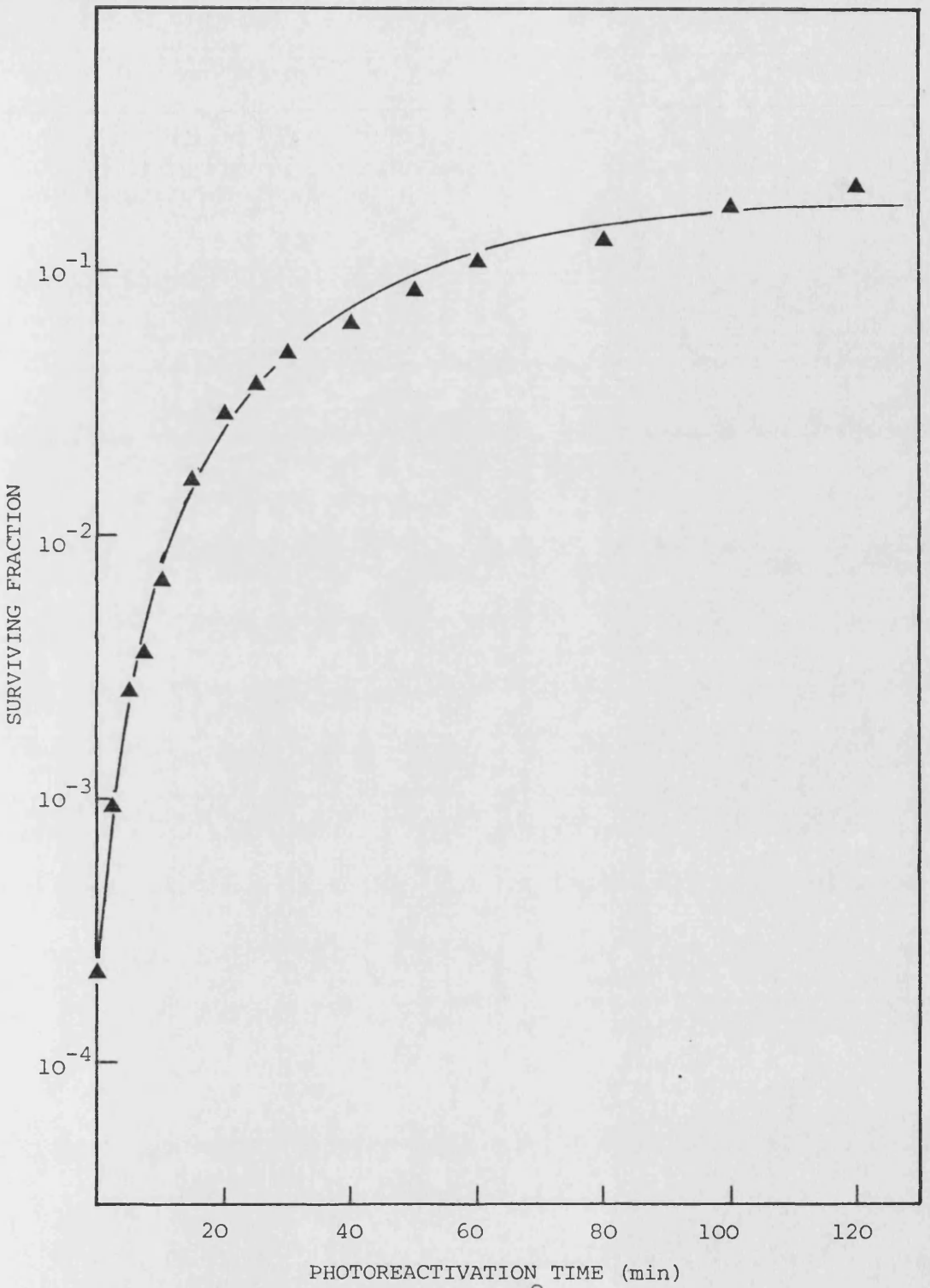

Fig. 2.4. Photoreactivation at 25°C of 254nm UV inactivated AB1886.

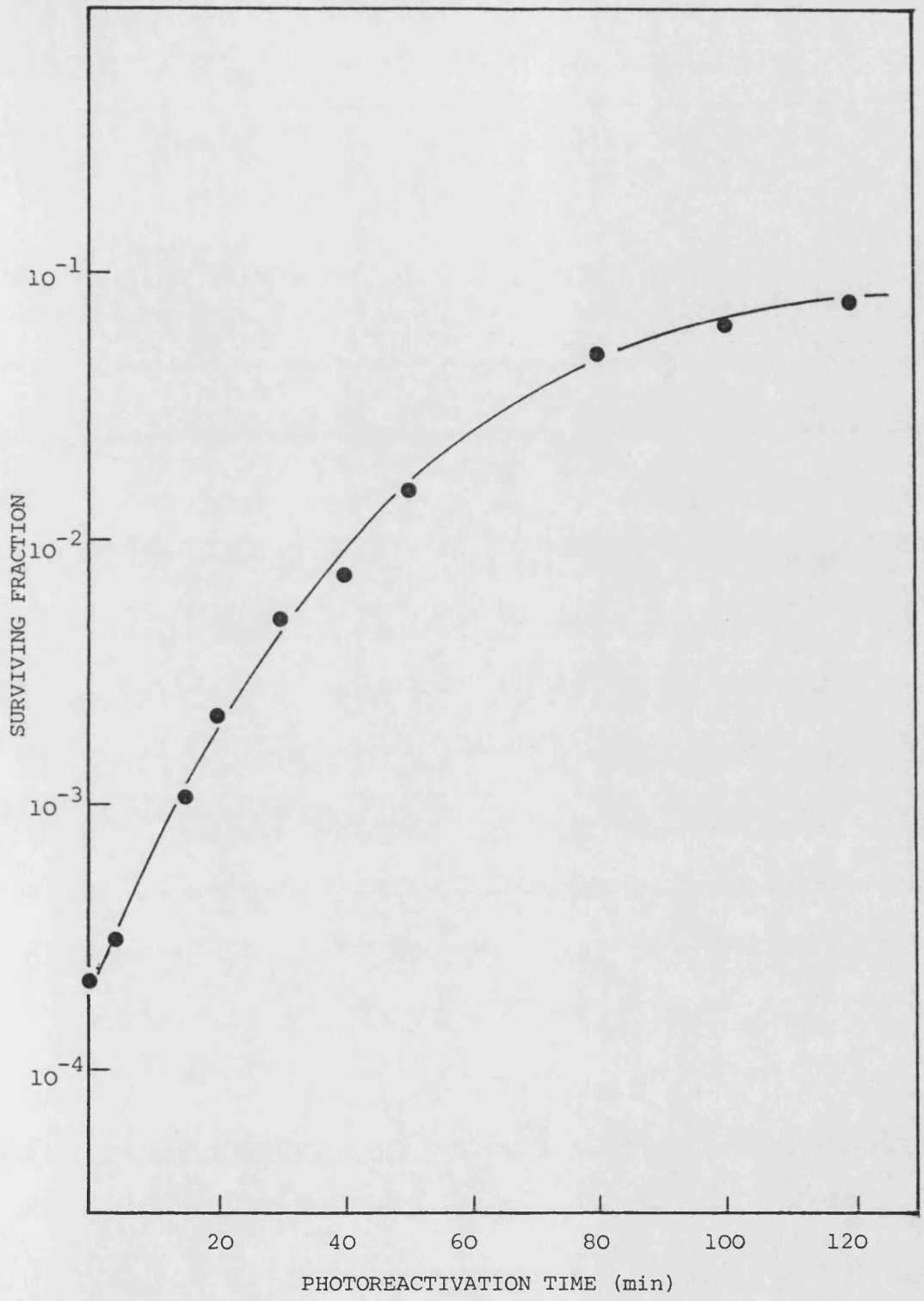

Fig. 2.5. Photoreactivation at 25°C of 254 nm UV inactivated SA206.

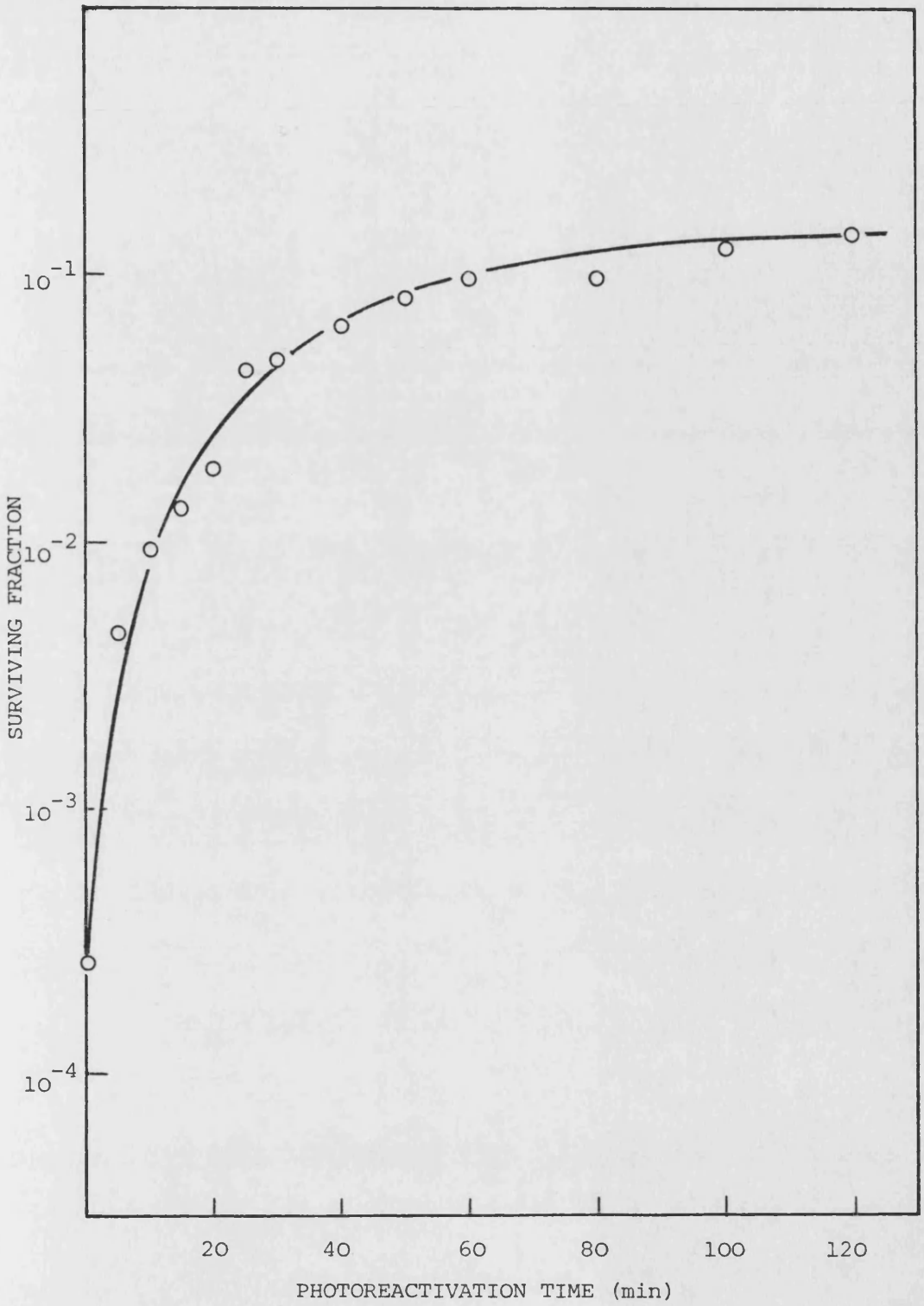

Fig. 2.6. Photoreactivation at 25°C of 254 nm UV inactivated AB1885.

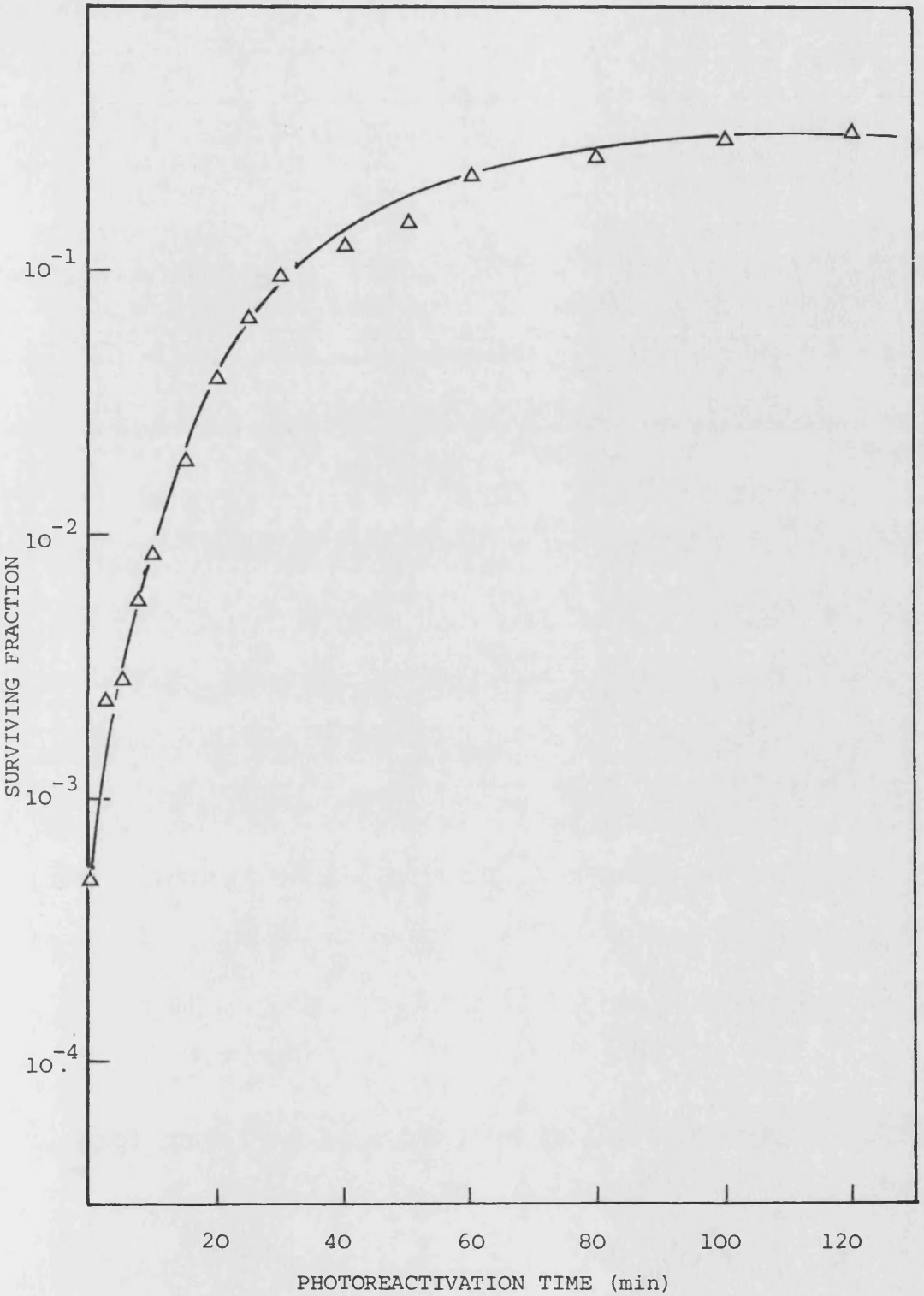

Fig. 2.7. Photoreactivation at 25°C of 254 nm UV inactivated AB1884.

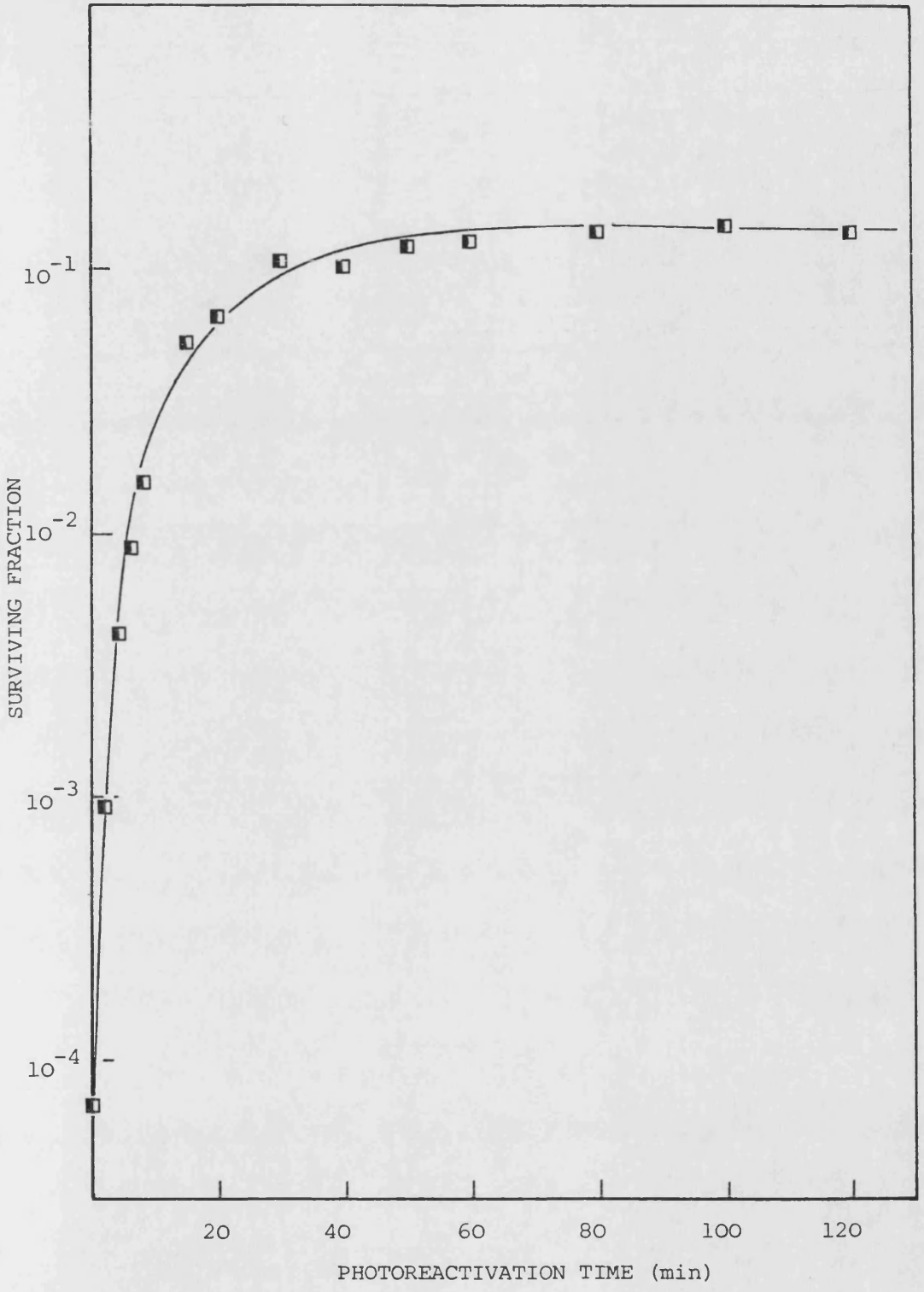

Fig. 2.8. Photoreactivation at 25°C of 254 nm UV inactivated SA446.

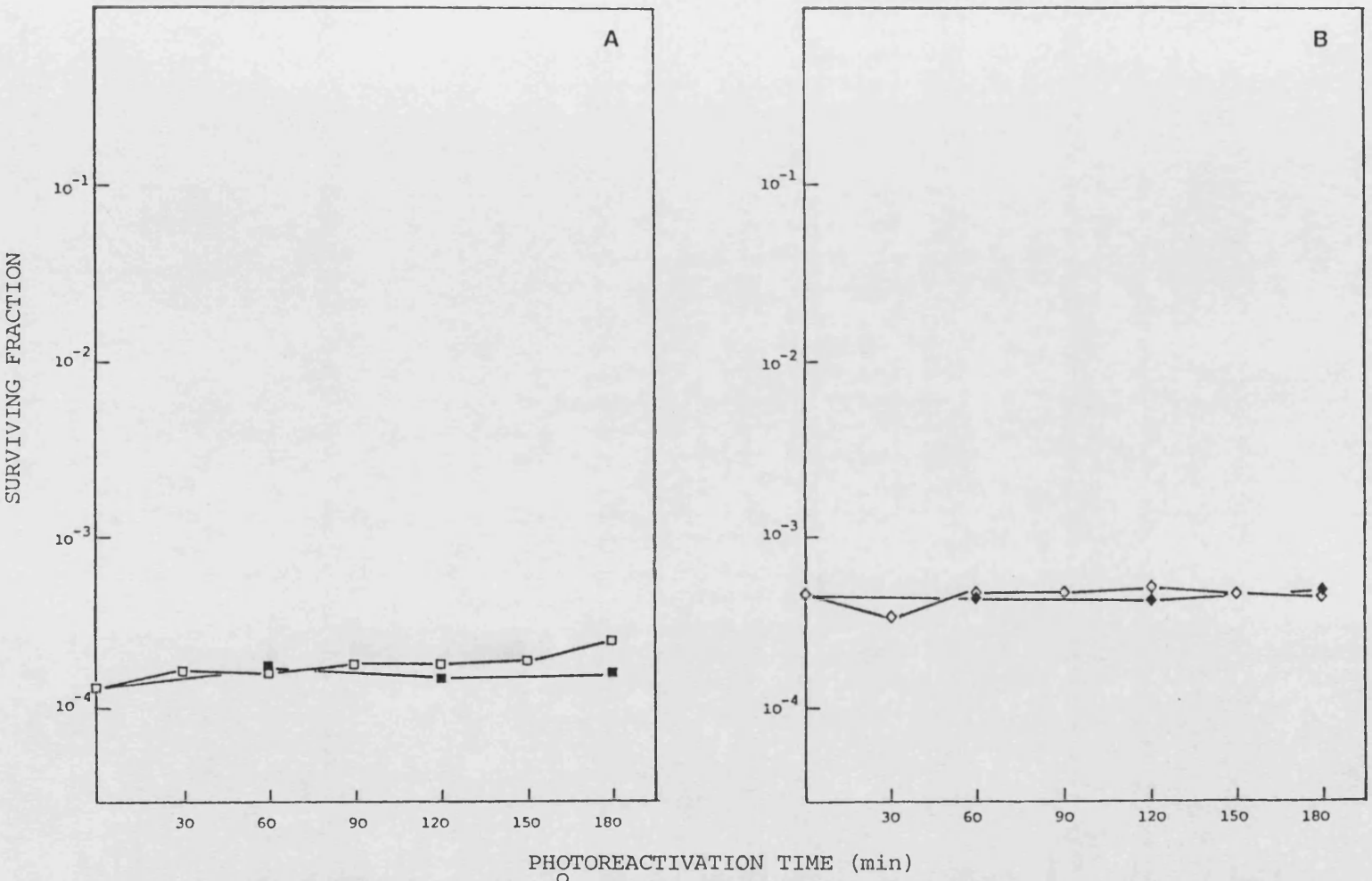

Fig. 2.9. Photoreactivation at 25°C of 254 nm UV inactivated DY314 (Panel A) and AS45 (Panel B).

The Random Photoreactivation Model (1-P)

The model is based on the following assumptions:

1) UV radiation induces lethal events in cells, only one of which is necessary to inactivate a cell. The mean number per cell is given by kD in the equation:-

$$N/No = e^{-kD} \qquad ....2.1$$

The average number of 'lethal hits' per cell is said to be 1 when the surviving fraction of the cell population has been reduced to 0.37.

2) The reversal of all lethal events within a cell results in cell survival.

3) The mean number of UV-induced, photoreversible events per cell is a direct linear function of the UV fluence and these events are Poisson-distributed throughout the cell population.

4) The fraction of the UV-induced events which are not photoenzymatically reversible are mechanistically different to the photoreversible events and so do not represent a limit of photoreactivability.

Tyrrell and Davies (1974) described a dose-reduction situation in which the ratio (P_r) of the survival with no photoreactivation (P_t) to the survival with maximum photoreactivation (P_i) represents the probability of non-occurrence of reversible UV-induced events. Thus, the mean number of reversible events (μ) is a function of P_r and the inactivating fluence (D):

$$\mu = -\ln P_r D \qquad ....2.2$$

If the elimination of photoreversible events is random and follows first-order kinetics, then after any one photoreactivation time, a constant fraction (P) of the UV-induced events will have been reversed. The mean number of reversible events remaining after a given photoreactivation time resulting in a surviving fraction ($^{N}/_{No}$) is given by:

$$\mu(1-P) \qquad \ldots.2.3$$

Thus:

$$^{N}/_{No} = P_i e^{-(1-P)\mu} \qquad \ldots.2.4$$

from which P values may be calculated:

$$1-P = \frac{\ln {}^{Ps}/_{Pi}}{\ln {}^{Pt}/_{Pi}} \qquad \ldots.2.5$$

where P_t is the survival after the inactivating UV fluence, P_i is the experimentally determined survival after maximum photoreactivation treatment and P_s is the survival after photoreactivation treatment for time t. The photoreactivation data from Figs. 2.4 to 2.9 are shown in the (1-P) form in Fig. 2.10. The data pertaining to these analyses are included in Tables A4.7-10. The initial linear portion of each curve has been fitted by regression analysis and the slopes and their associated errors are given in Table 2.2.

It will be seen from the 't' values given in Table 2.2 that the fit of each slope was significant at the 5 per cent level. The critical values for one-tailed probabilities for the student's t-distribution with 3,5,6 or 7 residual degrees of freedom are

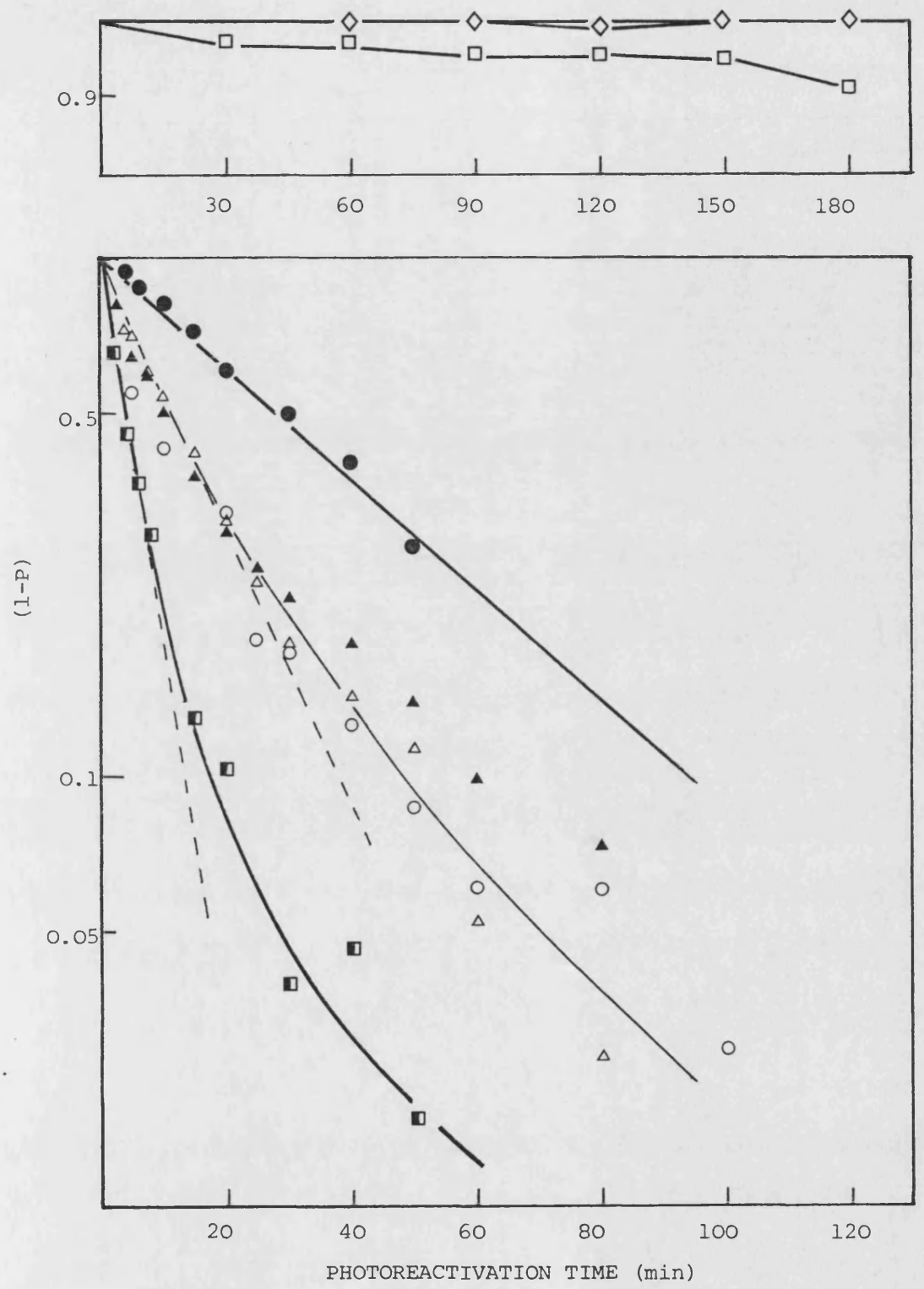

Fig. 2.10. 1-P analysis of the photoreactivation rate at 25°C of AS45 (◇), DY314 (□), SA206 (●), AB1884 (▲), AB1885 (△), AB1886 (▲) and SA446 (◧) after 254 nm UV inactivation.

Table 2.2 SLOPES AND ASSOCIATED ERRORS OF THE (1-P) ANALYSIS OF PHOTOREACTIVATION DATA IN FIGURES 2.4 TO 2.9

STRAIN	SLOPE (min^{-1})	STANDARD ERROR OF SLOPE	NUMBER OF DEGREES OF FREEDOM	't' VALUE	CORRELATION COEFFICIENT
AB1886 *uvrA*	-2.5884×10^{-2}	1.2856×10^{-3}	5	-20.13	0.9939
AB1885 *uvrB*	-2.5227×10^{-2}	3.314×10^{-3}	5	-7.61	0.9671
AB1884 *uvrC*	-2.3445×10^{-2}	9.8771×10^{-4}	6	-23.74	0.9947
SA206 Δ(*gal-chlA*)	-1.0794×10^{-2}	3.6750×10^{-4}	7	-29.37	0.9895
SA446 Δ(*attλ-chlA*)	-6.6067×10^{-2}	5.5768×10^{-3}	3	-11.85	0.9895
DY314 *uvrA,uvrB phrB*	-1.8427×10^{-4}	6.6759×10^{-5}	6	-14.26	0.9258
AS45 Δ(*gal-chlA*) *phrB*	-	-	-	-	-

2.35, 2.02, 1.94 and 1.90, respectively. The magnitude of the slope of the (1-P) plot may be taken as an indication of the relative rate of photoreactivation. Comparison of the slopes of the (1-P) plots obtained with K-12 strains AB1886, AB1885 and AB1884 reveals essentially similar rates of photorepair. These data have been subjected to an analysis of covariance. Strains AB1886 and AB1885 were statistically similar at the 5 per cent confidence interval ($p>0.05$). Strain AB1884 photoreactivated at a slightly lower rate, which was statistically different at the 5 per cent interval but not at the 1 per cent level ($p>0.01$).

Strain SA206 photoreactivated at a rate approximately 42 per cent that of AB1886, whilst the very small photorepair observed with DY314 occurred at an approximately 100-fold lower rate. No measurable photorepair was detected with AS45.

In addition to the strains already discussed, photoreactivation data for strain SA446 are shown in Fig. 2.8 and the (1-P) analysis is included in Fig. 2.10. As will be seen from Appendix 1, this is closely related (but not isogenic) with SA206. However, SA446 has a deletion extending from *chlA* to *attλ* (including *uvrB*), whilst SA206 has a deletion extending from *chlA* through *attλ* and beyond to *gal*. Strain SA446 was acquired during the latter stages of this work and is less well characterised. The rate of photorepair was approximately 2.5-fold greater than AB1886, whilst the rate of photorepair of SA206 was 16 per cent of this value.

Control Experiments

During each photoreactivation experiment, a sample of unirradiated cell suspension was exposed to the photoreactivating

light for the maximum time period. In no case did the surviving fraction fall below 90 per cent, indicating that the light treatment was not exerting a lethal effect (data not shown).

Discussion

The 254 nm inactivation data presented in this section suggest that the presence of different mutated *uvr* loci did not make a biologically significant difference to their UV-sensitivity. A similar result was reported by Tang and Ross (1985), when they transduced mutated *uvrA*, *uvrB* and *uvrC* loci into an isogenic background.

Strains AB1886, AB1885 and AB1884, which are mutated at the *uvrA*, *uvrB* and *uvrC* loci, respectively, showed essentially similar rates of photoreactivation after 254 nm UV inactivation. Therefore, it may be concluded that the presence of different *uvr* mutations does not affect the rate of photorepair. Whilst it is important to make this comparison here, because much of the later work presented in this thesis involves comparison of *uvrA* strains with Δ*uvrB* strains, the result is not surprising since Sancar et al. (1984a) reported that the same rate of photoreactivation was observed *in vitro* regardless of whether purified UVRA or UVRB proteins were present or not. These workers concluded that the presence and/or binding of the excinuclease subunits did not affect the binding of DNA photolyase.

Comparing the rates of photorepair observed with SA446 and SA206 (Table 2.2) is of interest because these two strains differ only in the extent of the deletion in the critical area of the proposed *phrA* locus (see Introduction, *Escherichia coli* Enzyme).

The rate of photorepair of SA206 was 16 per cent that of SA446, in close agreement with the 20 per cent figure obtained by Sutherland and Hausrath (1979) in their publication proposing two loci controlling photoreactivation in E. coli K-12. This strongly suggests that there is a locus in the region between gal and attλ which significantly affects the rate of photoenzymatic repair. In addition, the rate of photoenzymatic repair of SA206 was only 40 per cent that of AB1886, AB1885 and AB1884, once again suggesting that SA206 is significantly deficient in photoreactivation capability.

To further support the suggestion that there might be two phr loci in E. coli K-12, a very small light-dependent recovery was detected in DY314, an excision-deficient strain carrying the original photoreactivation-deficient phr mutation isolated by Harm and Hillebrandt (1962). Although the rate of repair was approximately 100-fold lower than either AB1886 or SA206, and goes against the consensus that such strains should be totally photoreactivation-deficient, it does suggest that there may be a second protein with slight photolyase activity, in addition to the principle DNA photolyase coded by the phrB gene. This would possibly provide a role for the 40-kDa photolyase isolated by Snapka and Sutherland (1980) from the gal- attλ region, or suggest the existence of another photolyase from an unknown locus.

To further support the former hypothesis, no repair was observed in strain AS45, which is deleted at the proposed phrA locus and carries the phrB mutation transduced from DY314.

These preliminary data indicated that there was evidence for two phr loci in E. coli. To further characterise this response, recombination-deficient (recA) derivatives of these strains were

studied, wherein the action of a single photolyase molecule has a significant effect on survival because of the small fluences required for inactivation. These data are presented in the next section.

RESULTS AND DISCUSSION - PART III

3.1 Introduction

The experimental work reported in this thesis is directed primarily towards establishing whether there is any evidence in favour of the existence of multiple photolyase molecules in *Escherichia coli* K-12. In this section, four recombination-deficient derivatives of strains AB1886, SA206, DY314 and AS45 described in Part II have been used, namely AB2480 (*uvr*$^-$ *rec*$^-$), AS44 (Δ(gal-chlA) *rec*$^-$), DY326 (*uvr*$^-$ *rec*$^-$ *phrB*$^-$) and AS46 (Δ(gal-chlA) *rec*$^-$ *phrB*$^-$), representing the four possibilities, *phr*$^+$, *phrA*$^-$, *phrB*$^-$ and *phrA*$^-$ *phrB*$^-$, respectively. Reference to Appendix 1 will indicate that only strains AS44 and AS46 are isogenic with each other and so some caution must be exercised in making quantitative comparisons and drawing conclusions concerning the functions of the proposed *phrA* and *phrB* gene products. However, it was felt that detailed comparisons of the strains were justified, based on the data presented in Part II which suggested that a gene in the *gal-attλ* interval may have an effect on photo-reactivating enzyme activity. The detailed characterisation of the four strains presented in this section has involved several irradiation and photoreactivation procedures in the hope that they might indicate a selection protocol for isolating a point-mutation in the proposed *phrA* locus and so facilitate the construction of an isogenic series of photoreactivation-deficient derivatives.

Before making a detailed study of the kinetics of photo-reactivation, it was necessary to first establish the 254 nm UV sensitivity of the four strains and to determine the time required for the photoreactivating enzyme to complex with the dimer.

3.2. Inactivation with 254 nm UV radiation

Twenty four hour stationary-phase secondary cultures, grown at 37°C, were used throughout this work unless otherwise stated. Cells were harvested and resuspended in M9 salts solution to give a suspension containing 1 x 10^7 colony forming units per ml. Each cell suspension was given graded fluences of 254 nm UV, after each of which a sample was removed, serially diluted, and assayed for viability on three nutrient agar plates as described previously. Three survival curves determined on the same day are shown in Fig. 3.1 (AB2480), Fig. 3.2 (AS44), Fig. 3.3 (DY326) and Fig. 3.4 (AS46). The survival parameters derived from regression analysis of the linear portion of each curve (beyond a fluence of 0.1 Jm^{-2}) are included in Table 3.1, as are the results of several other replicate experiments conducted during this study. The data pertaining to these parameters are included in Tables A4.10-13. In addition, these data have been grouped into a 'total' regression analysis giving average 'k' and 'n' parameters, from which an analysis of covariance has been carried out (see Appendix 5). The results of the analysis of covariance, which was based on a regression model derived from the data points for all four strains, and reflects the change in F-ratio for AS44, DY326, and AS46 with respect to AB2480, are shown in Table 3.2. It will be seen from Table 3.2 that the change in F-ratio resulting from both slope and intercept location fell below the critical value of 3.84 with 1 and ∞ degrees of freedom of the F-distribution at the 5 per cent confidence interval, indicating that the survival parameters of the strains were not significantly different ($p>0.05$). The statistical similarity of both the intercepts and slopes of the four strains is of interest because it indicates that the fluence required for one

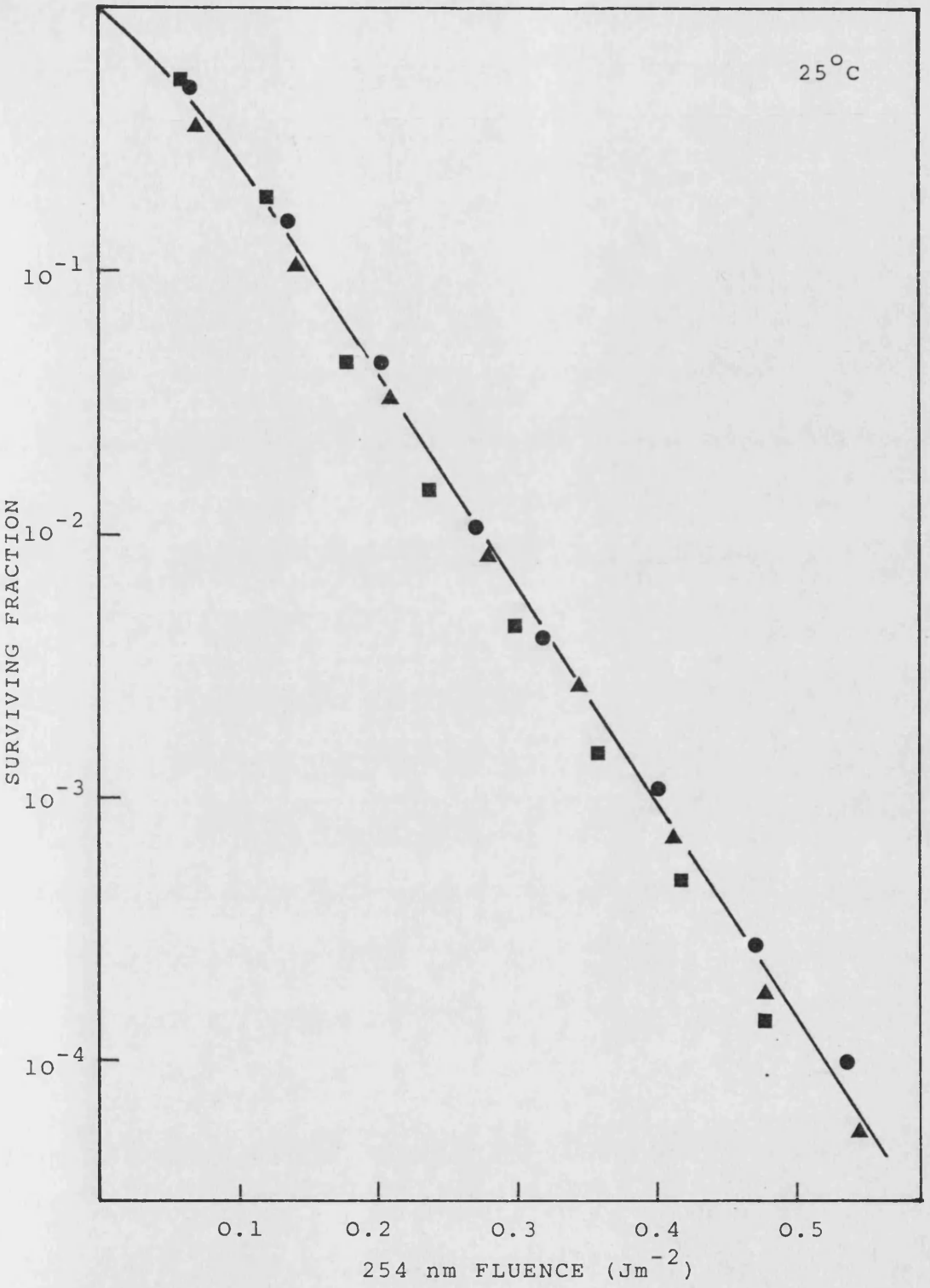

Fig. 3.1 Three 254 nm UV inactivation curves for 24 hour stationary phase AB2480 grown at 37°C.

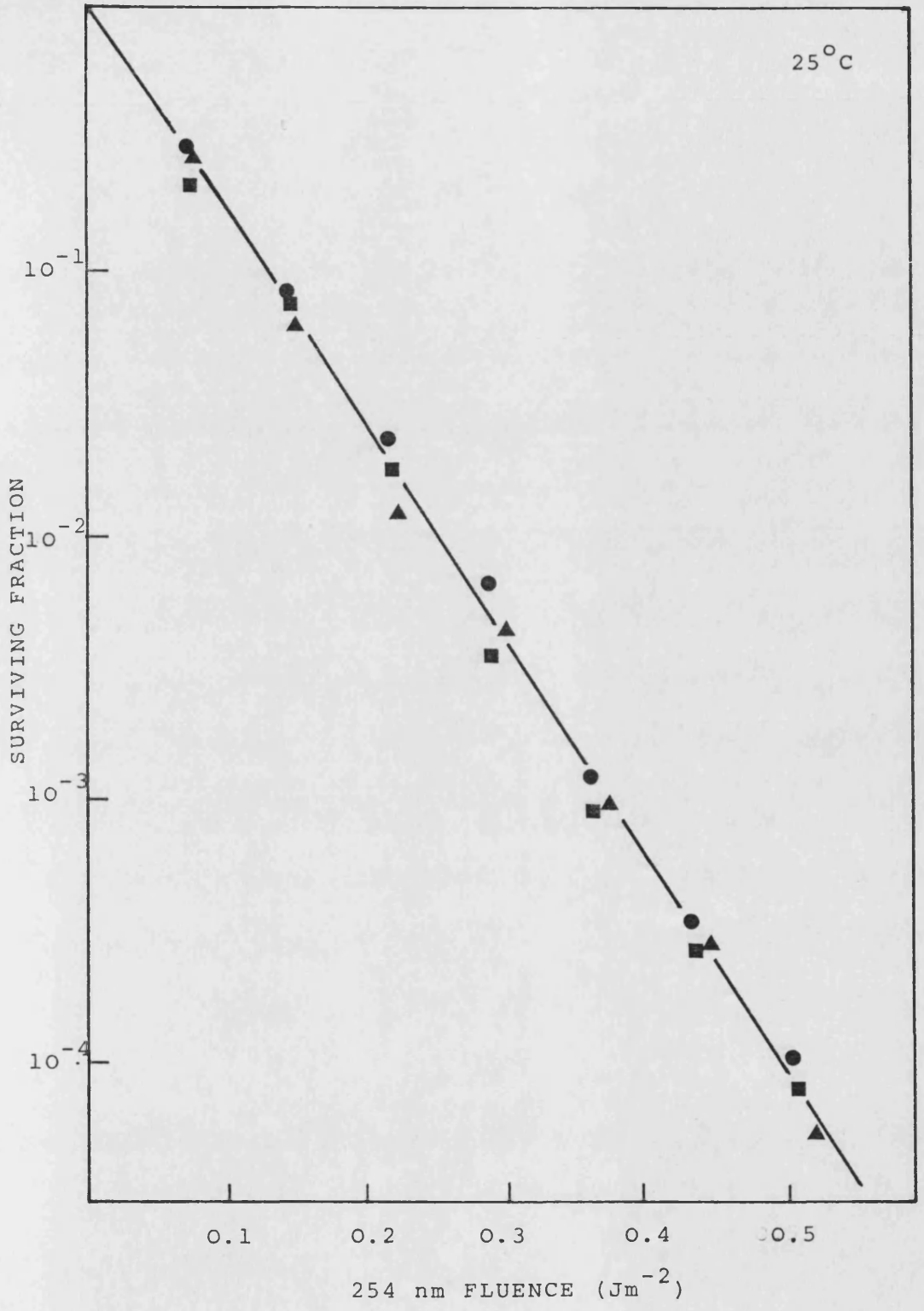

Fig. 3.2. Three 254 nm UV inactivation curves for 24 hour stationary phase AS44 grown at 37°C.

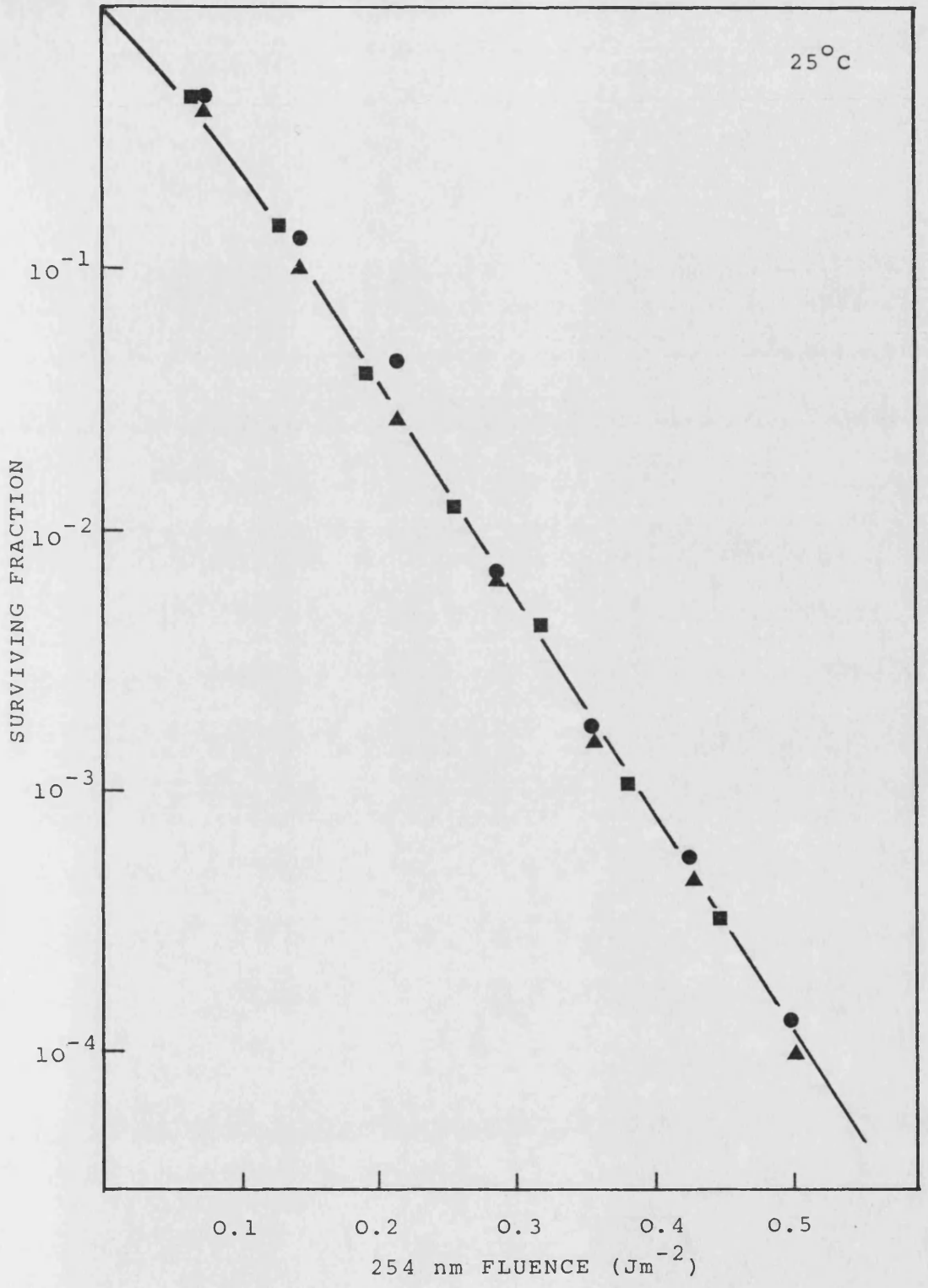

Fig. 3.3. Three 254 nm UV inactivation curves for 24 hour stationary phase DY326 grown at 37°C.

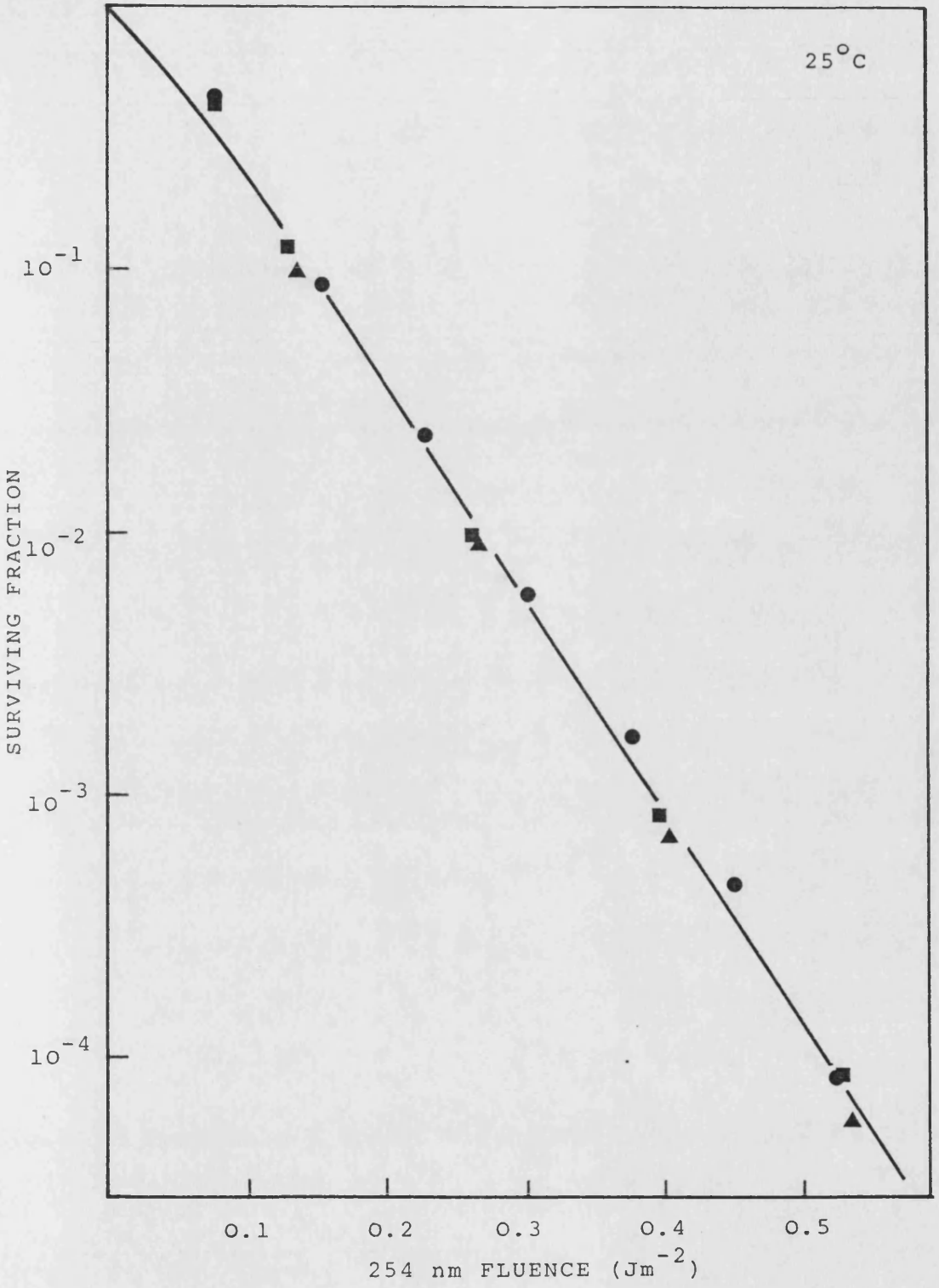

Fig. 3.4. Three 254 nm UV inactivation curves for 24 hour stationary phase AS46 grown at 37°C.

Table 3.1a 254nm UV INACTIVATION PARAMETERS FOR AEROBICALLY GROWN AB2480 AND AS44 AT 25°C

STRAIN	EXPT. NO.	SLOPE (log 10)	Std. Error OF SLOPE	INTERCEPT	STANDARD ERROR OF INTERCEPT	'k' $(Jm^{-2})^{-1}$	'n'
AB2480 (phr$^+$)	10a*	-7.7648	1.9141×10^{-1}	0.2380	7.3606×10^{-2}	17.879	1.730
	10b*	-7.9863	1.3470×10^{-1}	0.2526	4.8753×10^{-2}	18.3891	1.788
	10c*	-8.1981	8.4387×10^{-2}	0.2070	3.1149×10^{-2}	18.8768	1.610
	10d	-8.2705	1.1316×10^{-1}	0.2353	4.1960×10^{-2}	19.043	1.719
	10e	-7.660	2.2473×10^{-2}	0.2627	7.9470×10^{-3}	17.637	1.830
	10f	-7.8062	1.0020×10^{-1}	0.2464	3.5839×10^{-2}	17.974	1.764
	10g	-7.392	6.6442×10^{-2}	0.2652	2.3982×10^{-2}	17.021	1.842
	10h	-7.9736	2.6442×10^{-1}	0.2404	7.7765×10^{-2}	18.360	1.739
	TOTAL	-7.772	1.3717×10^{-1}	0.2383	4.9141×10^{-3}	18.368	1.731
AS44 (phrA)	11a*	-8.4456	9.0350×10^{-2}	0.1251	3.235×10^{-2}	19.4467	1.334
	11b*	-8.3101	1.8720×10^{-1}	0.1521	6.473×10^{-2}	19.134	1.419
	11c	-8.2032	2.2252×10^{-1}	0.0550	7.754×10^{-2}	19.221	1.135
	11d	-8.2032	4.6932×10^{-1}	0.1522	1.804×10^{-2}	18.888	1.419
	11e	-8.6796	1.3129×10^{-1}	0.1767	4.727×10^{-2}	19.985	1.502
	11f	-8.2709	1.1146×10^{-1}	0.076	4.130×10^{-2}	19.044	1.190
	11g	-8.343	1.7617×10^{-1}	0.1280	6.249×10^{-2}	19.21	1.342
	11h	-8.8003	2.2352×10^{-1}	0.1442	8.045×10^{-2}	20.26	1.393
	TOTAL	-8.4519	8.3712×10^{-2}	0.1252	3.017×10^{-2}	19.46	1.334

Table 3.1b 254nm UV INACTIVATION PARAMETERS FOR AEORBICALLY GROWN DY326 AND AS46 AT 25°C

STRAIN	EXPT. NO.	SLOPE (log 10)	Std. ERROR OF SLOPE	INTERCEPT	STANDARD ERROR OF INTERCEPT	'K' $(JM^{-2})^{-1}$	'n'
DY326	12a*	-8.3976	9.218×10^{-2}	0.2167	3.171×10^{-2}	19.336	1.647
(phrB)	12b*	-8.6252	2.801×10^{-1}	0.3741	9.560×10^{-2}	19.86	2.366
	12c*	-8.2789	1.468×10^{-2}	0.2189	4.501×10^{-2}	19.03	1.656
	12d	-8.0033	6.175×10^{-1}	0.0653	6.137×10^{-2}	18.423	1.162
	12e	-8.5932	1.985×10^{-2}	0.1103	6.501×10^{-2}	19.786	1.289
	12f	-8.0385	5.826×10^{-1}	0.1526	2.286×10^{-2}	18.509	1.421
	12g	-8.9202	1.201×10^{-1}	0.1315	3.600×10^{-2}	20.540	1.354
	12h	-8.7026	1.789×10^{-1}	0.2680	5.419×10^{-2}	20.04	1.85
	TOTAL	-8.3395	1.268×10^{-1}	0.1639	4.2456×10^{-2}	19.20	1.458
AS46	13a*	-7.9416	5.2762×10^{-2}	0.1285	2.0530×10^{-1}	18.224	1.344
(phrA,phrB)	13b*	-8.1157	4.5048×10^{-2}	0.1451	1.7519×10^{-2}	18.687	1.385
	13c*	-8.0555	1.8387×10^{-1}	0.1156	7.1017×10^{-2}	18.548	1.305
	13d	-7.9257	1.3145×10^{-1}	0.0878	4.7293×10^{-2}	18.250	1.224
	13e	-7.8413	9.0695×10^{-2}	0.1517	3.5294×10^{-2}	18.055	1.418
	13f	-8.0743	5.7593×10^{-2}	0.1630	2.0741×10^{-2}	18.592	1.455
	13g	-8.0762	8.1723×10^{-1}	0.0862	2.9945×10^{-2}	18.596	1.222
	13h	-7.9686	1.9211×10^{-1}	0.177	6.9562×10^{-2}	18.348	1.506
	TOTAL	-8.0224	1.2087×10^{-1}	0.1161	4.5384×10^{-2}	18.472	1.307

Table 3.2 ANALYSIS OF COVARIANCE OF 254 nm SURVIVAL DATA FOR AS44, DY326 AND AS46 GROWN AT 25°C

STRAIN	INTERCEPT LOCATION			SLOPE LOCATION		
	CHANGE OF F- RATIO	DEGREES OF FREEDOM	PROBABILITY	CHANGE OF F- RATIO	DEGREES OF FREEDOM	PROBABILITY
AS44	2.54	1,177	0.1127	1.337	1,180	0.2489
DY326	0.010	1,178	0.9205	2.50	1,181	0.1155
AS46	0.987	1,179	0.3218	2.975	1,182	0.0862

lethal hit, and hence the number of pyrimidine dimers per lethal hit, is the same for each strain. The calculated values for the number of pyrimidine dimers per lethal hit for AB2480, AS44, DY326 and AS46 were 4.45, 3.5, 3.82 and 3.64, respectively, based on a value of 53 pyrimidine dimers per Jm^{-2} induced in the E. coli genome determined by Ellison and Childs (1981).

3.2 High-Intensity Flash Photolysis

Reference to the kinetic equation for photoreactivation derived by Rupert (1962a,b) reveals that the reaction may be experimentally divided into light and dark periods. During the dark period, the photoreactivating enzyme complexes with the dimer substrate. The rate of complexation in this instance is dependent principally on temperature, whereas during the light-dependent photolysis step, the rate is dependent on the fluence-rate of the photoreactivating light. However, under conditions of saturating fluence-rate of photoreactivating light, whereby a PRE-dimer complex is photolysed as soon as it is formed, the overall rate of photoreactivation becomes dependent only on the dark complexation reaction. As discussed in the Introduction to this work, Harm et al. (1971) developed the high-intensity single flash photolysis method to separate the dark and light components of the reaction. This technique has been used extensively throughout this work, both to estimate the number of photoreactivating enzyme-substrate complexes and to monomerize all pre-formed PRE-substrate complexes prior to kinetic studies. This technique can be used to measure the kinetics of the 'first-round' of complexation, but there are inherent manipulative difficulties in giving a sufficient inactivating fluence quickly enough and then distributing the

sample for flash treatment. Therefore, the kinetic measurements in this work represent the 'second round' of complexation resulting from the complete photolysis of all pre-formed PRE-substrate complexes. However, despite the difficulties previously alluded to, it was necessary to make a crude estimate of the time required for maximal PRE complexation. This would establish the holding time necessary between UV inactivation and photoreactivating light treatments.

Cell suspensions were equilibrated to 25°C for 5 minutes and given a 254 nm fluence of approximately 0.5 Jm^{-2}, sufficient to reduce the surviving fraction to 1 x 10^{-4}. The suspension was then divided into 0.3 ml portions, and each sample given an intense flash of light at times varying from 1 to 40 minutes after UV inactivation. Preliminary experiments had revealed that a single synchronised flash from two photographic flash guns was sufficient to monomerize all pre-existing PRE-substrate complexes (data not shown). The results of these 'flash-complexation' experiments for AB2480 and AS44 are shown in Fig. 3.5. The time required for maximal complexation with AB2480 was approximately 5 minutes, approached at a high initial rate, whereas AS44 exhibited a similar time for maximal complexation, but which was approached at a somewhat slower rate. Both Tyrrell (1971) and Harm et al. (1968) report similar results for *E. coli* K-12 AB2480 and B_{s-1}, respectively.

3.2.1. Estimation of the Number of Photoreactivating Enzyme-Substrate Complexes

Having established that a holding time of 20 minutes at 25°C would be sufficient for all available PRE molecules to become

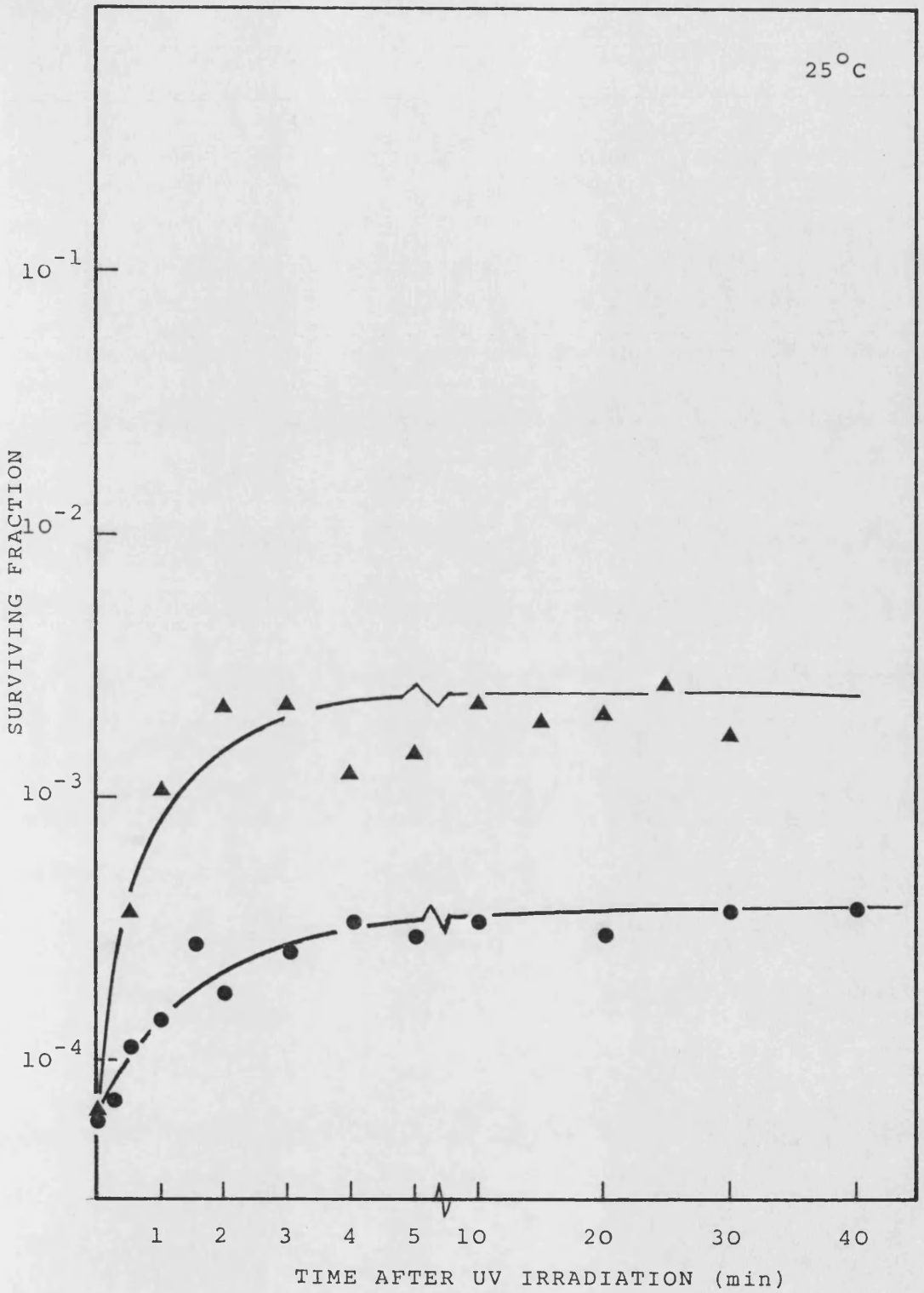

Fig. 3.5. Single flash photolysis of AB2480 (▲) and AS44 (●) at various time periods after 254 nm UV inactivation.

complexed, a number of experiments were performed to determine the 'fluence-decrement' resulting from a single flash of light. Knowing the number of pyrimidine dimers per Jm^{-2} induced in the E. coli genome, the fluence decrement can be used to make a crude estimate of the average number PRE-substrate complexes per cell present at the instant of the flash.

Cell suspensions were given graded fluences of 254 nm UV, after which a sample was removed. The sample was split into two portions, one being assayed for cell survival. The remainder was held at 25°C for 20 minutes, given a single high intensity-flash and then assayed for survival. Duplicate results for AB2480 and AS44 are shown in Fig. 3.6. The survival parameters are included in Table 3.3. The data pertaining to Fig. 3.6 are included in Tables A4.14 and A4.15. The fluence decrement, that is the fluence which results in the same survival as a larger fluence of UV combined with one high-intensity flash, obtained for both AB2480 and AS44 were not constant. Probability theory predicts that where 'lethal hits' are Poisson distributed throughout the population, only those cells having n or less lethal hits will survive after UV inactivation plus one photoreactivating flash; where n is the number of PRE molecules required to reverse the pyrimidine dimers constituting one lethal hit. Thus as the UV fluence increases, the fraction of the cell population having n or less lethal hits becomes constant, resulting in a constant fluence decrement. However, in this study this situation was not reached and so the fluence-decrement must reflect the lower limit of the number of PRE-substrate complexes. The measured fluence-decrements for AB2480 and AS44 were approximately 0.275 and 0.14 Jm^{-2}, respectively, which resulted in a calculated value of 14.6 $\pm$ 0.83

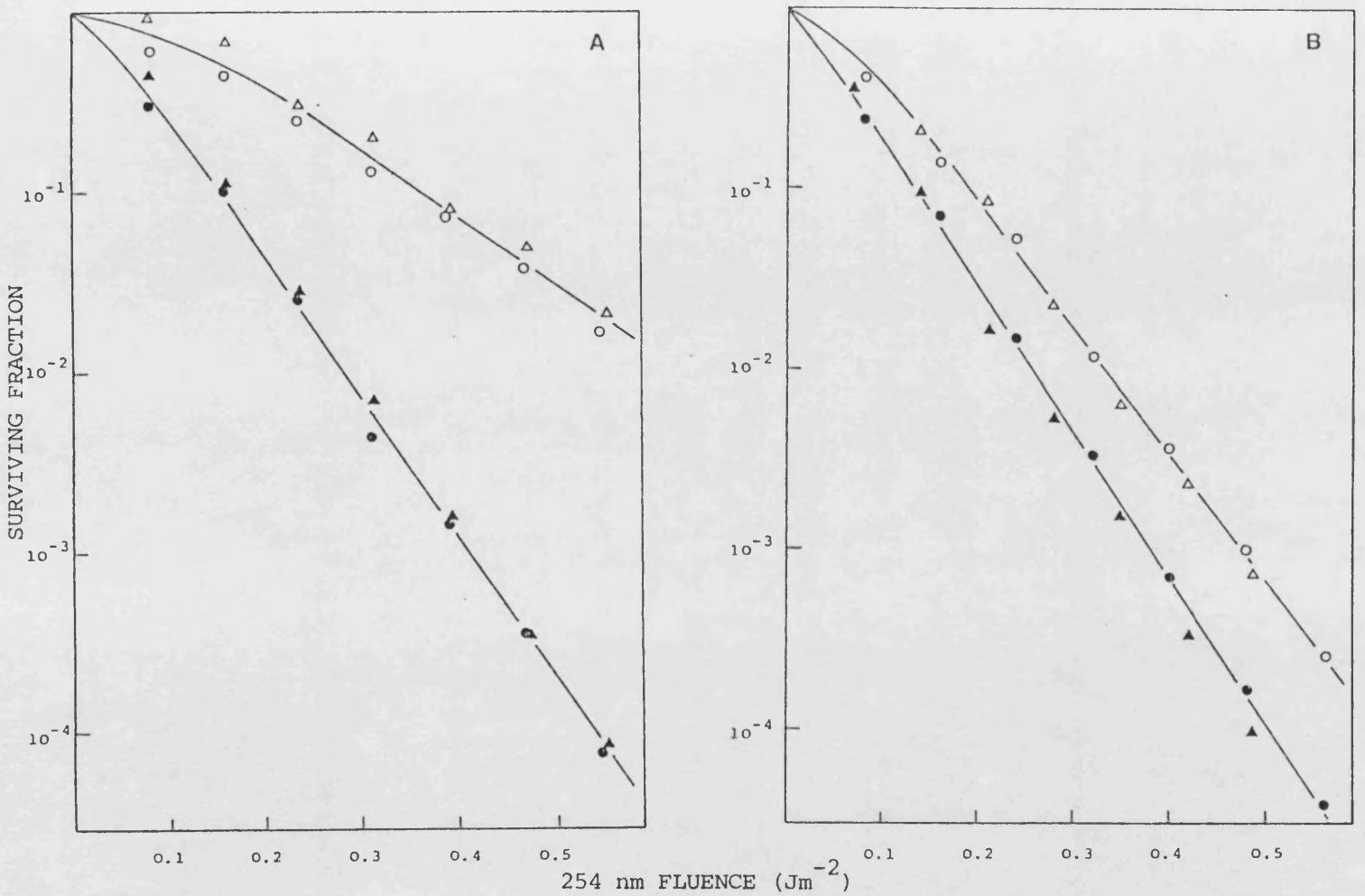

Fig. 3.6. Replicate survival curves for AB2480 (Panel A) and AS44 (Panel B) grown at 37°C after 254 nm UV inactivation (closed symbols) and a single light flash (open symbols) at 25°C.

Table 3.3 SURVIVAL DATA FOR AB2480, AS46, DY326 AND AS46 AFTER 254 nm UV IRRADIATION AND MAXIMUM FLASH PHOTOLYSIS AT 25°C

STRAIN	TREATMENT	INTERCEPT 'n'	(k) $(Jm^{-2})^{-1}$
AB2480	254 nm	1.73 ± 0.073	18.36 ± 0.14
(*phr*$^+$)	FLASH	2.18 ± 0.49	8.28 ± 0.31
AS44	254 nm	1.33 ± 0.03	19.46 ± 0.084
(*phrA*)	FLASH	1.67 ± 0.148	14.23 ± 1.175
DY326	254 nm	1.46 ± 0.042	19.20 ± 0.13
(*phrB*)	FLASH	1.51 ± 0.104	18.26 ± 0.13
AS46	254 nm	1.31 ± 0.04	18.47 ± 0.12
(*phrA*,*phrB*)	FLASH	1.34 ± 0.11	17.05 ± 0.26

and 7.4 ± 0.67 PRE-substrate complexes per cell, based on 53 pyrimidine dimers per Jm^{-2} per genome (Ellison and Childs, 1981). There was no measurable fluence decrement with either DY326 or AS46. The values obtained in this study contrast with the value of 20 determined by Harm et al. (1968) for an overnight culture of *E. coli* B_{s-1}. Tyrrell and Davies (1974) used photoreactivation kinetics to derive a value of 4-5 PRE molecules per cell in a 16 h culture of AB2480 grown in nutrient broth.

Before proceeding to determine the kinetics of photoreactivation in the four strains, it is important to consider why AS44 should have such a markedly decreased flash response compared with AB2480. It could be argued that the production of PRE molecules as a function of the stage of growth could be slower, but the flash response of 48 hour cells remained less than 48 hour AB2480 (data not shown). Similarly, Resnick and Setlow (1972) found that the amount of PRE in tetraploid cells of *S. cerevisiae* was directly proportional to the number of gene copies per cell involved in the synthesis of PRE. An analogous 'gene-dosage' effect in the strains used in this study does seem unlikely, because such genome multiplicity would be reflected in a significant variation in the shoulder of the survival curves. Reference to Figs. 3.1 to 4 and Table 3.2 indicates that this situation does not exist. Finally, Sutherland and Hausrath (1979) reported a 2 to 3 fold-greater apparent Michaelis-Menton constant Km for PRE isolated from strains with a Δ(*gal-attλ*) deletion than from normal strains, leading them to suggest that the enzyme in these cells has a reduced affinity for its substrate, the pyrimidine dimer. From the data obtained in this study, such a hypothesis can neither be confirmed nor rejected. However, the

suggestion that with strain AS44, which is deleted between gal and chlA, the dark equilibrium between complexed PRE and free PRE may be shifted in favour of the latter does seem plausible, but experiments using competing substrate molecules would be needed to confirm this. Preliminary experiments using a recA derivative of strain SA446 (a related, but not isogenic strain to SA206, having a deletion extending from chlA to attλ - see Appendix 1) gave a flash response comparable with AB2480 (data not shown). The fluence decrement was approximately 0.237 Jm^{-2}, giving an estimate of 12.5 PRE molecules per cell. Similarly, and to rule out any effects on photoreactivability resulting from the deletion including the uvrB locus, the fluence decrement was determined for a recA derivative of AB1885 (Appendix 1). The value obtained was 0.233 Jm^{-2}, resulting in an estimate of 12.4 PRE molecules per cell (data not shown). Taken together, these data strongly indicate that there is a locus within the gal- attλ interval which contributes either to the production of PRE molecules or the activity/affinity of those molecules.

3.3 Photoreactivation with Continuous Illumination

In order to determine both the rate and extent of photoenzymatic repair, irradiated cell suspensions were exposed to continuous broad-band photoreactivating light. However, it was first necessary to determine under what fluence-rate conditions the overall rate of the reaction became dependent only on the dark complexation of the PRE with the substrate. Considering the reaction scheme proposed by Rupert (1962a,b) (see equation 1, Introduction) the rate constant k_3 for the photolytic repair reaction can be expressed by the product $k_p I$, where I is the light

intensity and k_p is the 'photolytic constant' which varies essentially with the wavelength. Therefore, when the fluence rate of the light (I) is sufficiently large, causing all [ES] complexes to be split as soon as they are formed, the rate of the reaction becomes dependent on the ability of the PRE to complex with the substrate i.e. the 'dark' reaction.

3.3.1. Determination of Saturating Fluence-Rate Conditions

Cell suspensions were reduced to about 1×10^{-4} surviving fraction with a fluence of 254 nm UV, held at 25°C for 20 minutes and then given a single high-intensity flash at the same instant as commencement of continuous illumination. Cell samples were assayed for survival at times between 15 seconds and 60 minutes. The experiments were repeated at PR fluence rates varying from 0.28 to 31.8 Wm^{-2}. The photoreactivation data of AB2480, AS44 and DY326 at three fluence rates are shown in Fig. 3.7. The data pertaining to this figure are included in Tables A4.16-18. These data have been analysed by the (1-P) method discussed in Results and Discussion - Part II, and are shown in this form in Fig. 3.8. The (1-P) values for AB2480 and AS44 have been corrected such that the value of the single flash recovery alone (equivalent to t=0 min) is 1, by dividing all the values by the (1-P) value calculated for the flash recovery alone. This removes the 'initial-rate-bias' which would become apparent at short time intervals due to summation of the increase in survival resulting from both the first and second rounds of flash complexation. This was adopted throughout the remainder of this work, whenever a flash response was obtained. The initial slopes of the (1-P) plots were fitted by least squares linear regression analysis and the gradients of these slopes have

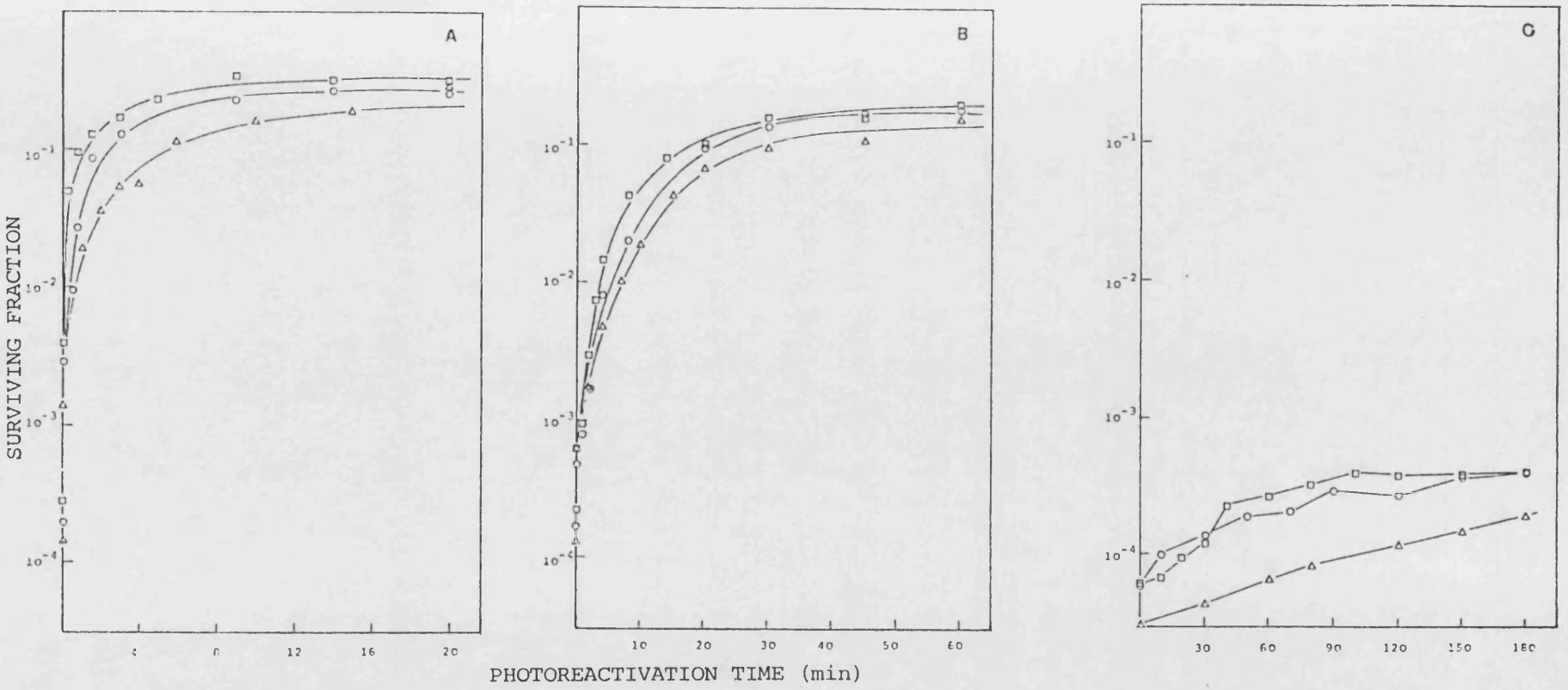

Fig. 3.7. Photoreactivation at 25°C of 254 nm inactivated AB2480 (Panel A), AS44 (Panel B) and DY326 (Panel C) at photoreactivating fluence rates of 1.1 (Δ), 4.55 (O) and 17.6 Wm^{-2} (□).

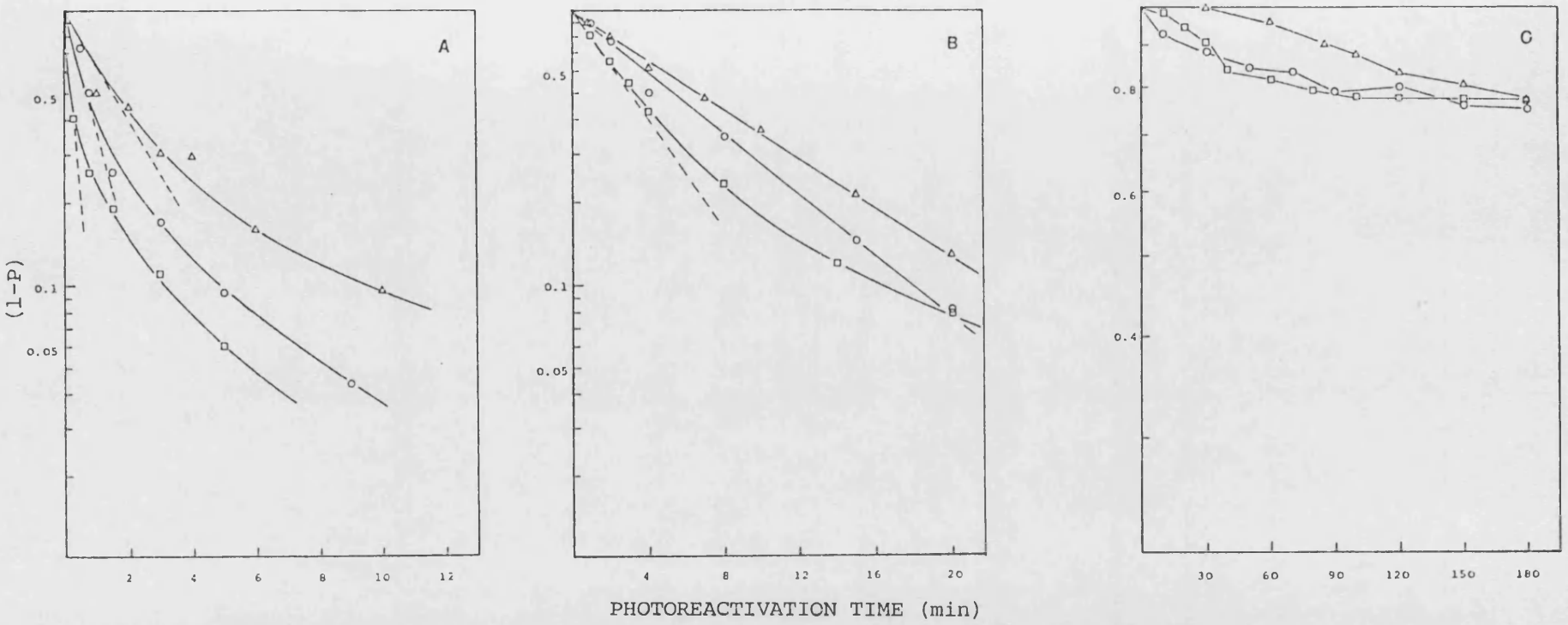

Fig. 3.8. 1-P analysis of the photoreactivation rate at 25°C of AB2480 (Panel A), AS44 (Panel B) and DY326 (Panel C) at photoreactivating fluence rates of 1.1 (Δ), 4.55 (O) and 17.6 Wm^{-2} (□).

been plotted against the photoreactivating light fluence rate (Fig. 3.9). Where the initial portion of the curve was not linear, the slope was calculated from the time required to remove 50 per cent of the photoreactivable lesions. These data indicate that the rate of photoreactivation became independent of fluence rate beyond 7 to 8 Wm^{-2}, and are in good agreement with the value of 60 $erg.mm^{-2}.s^{-1}$ (6 Wm^{-2}) reported by Tyrrell and Davies (1974) for AB2480. Jorns et al. (1987) report unpublished results showing that 70 ergs. $mm^{-2}s^{-1}$ (7 Wm^{-2}) is saturating for E. coli photolyase in vitro.

3.3.2. Kinetics of Dark-Complexation Under Saturating Irradiance Conditions of Broad-Band Light

The same experimental procedure as discussed above was used, except the fluence rate of photoreactivating light was maintained at approximately 17 Wm^{-2}. The photoreactivation data for the four strains are shown in Fig. 3.10 and the (1-P) analyses are included in Fig. 3.11. The rate constant i.e. gradient of the (1-P) plot (Table 3.4) reflects the product of the rate constant for enzyme-substrate complexation and the number of PRE molecules per cell. Using a value of 1.8×10^{-3} cell vol. $mole.^{-1}s^{-1}$ for the rate constant measured by Harm et al. (1971), an estimate of the number of PRE molecules can be made. These estimates are also included in Table 3.4

Concomitant control experiments indicated that the surviving fraction of non-irradiated cells exposed to photoreactivating light did not fall below 0.8 over the time periods studied. The data from a series of experiments to demonstrate the effect of photoreactivating light on unirradiated cells and absence of dark repair are shown in Table 3.5.

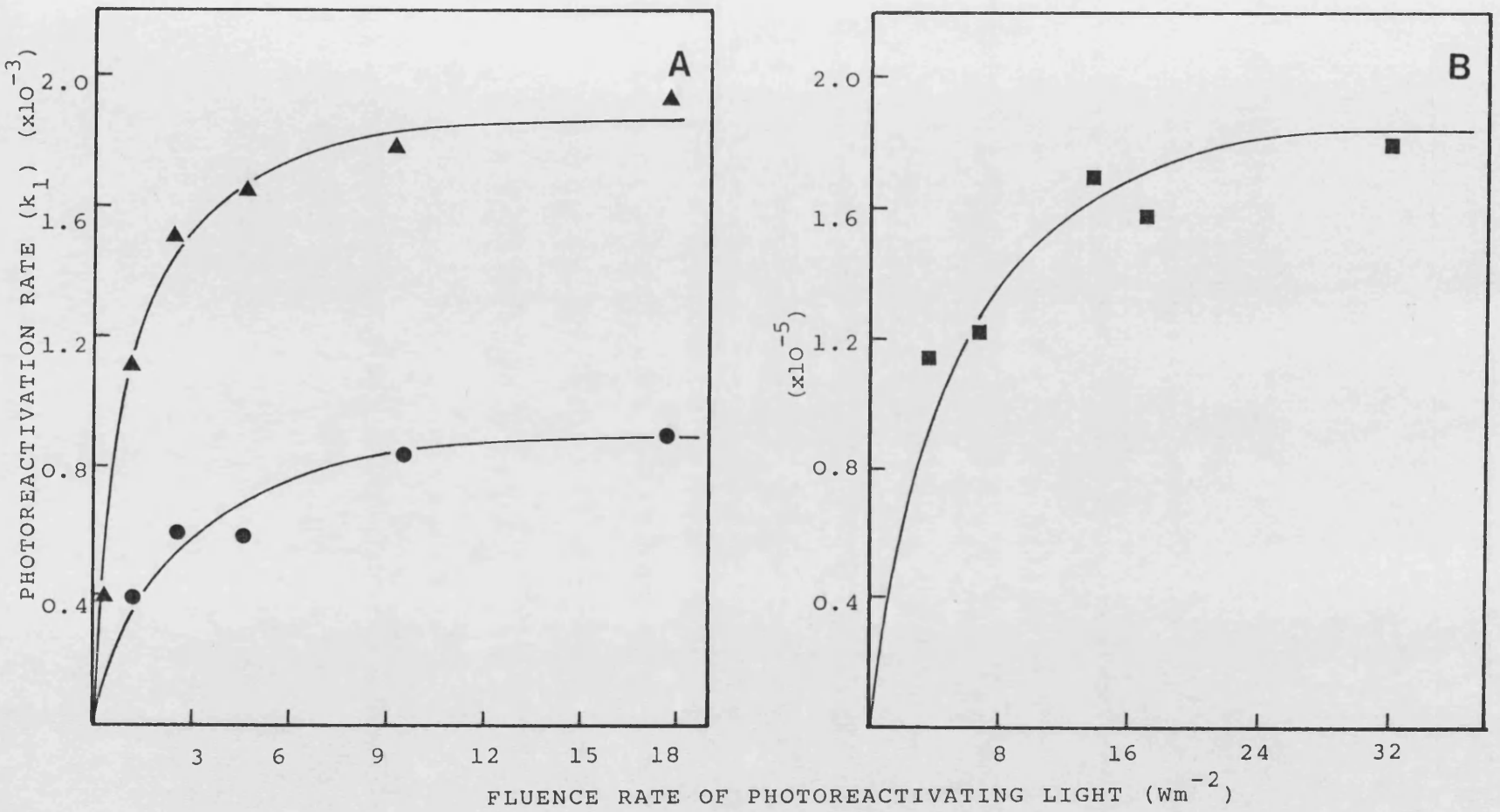

Fig. 3.9. The rate of photoreactivation as a function of the photoreactivating fluence rate at 25°C for AB2480 (▲), AS44 (●) and DY326 (■).

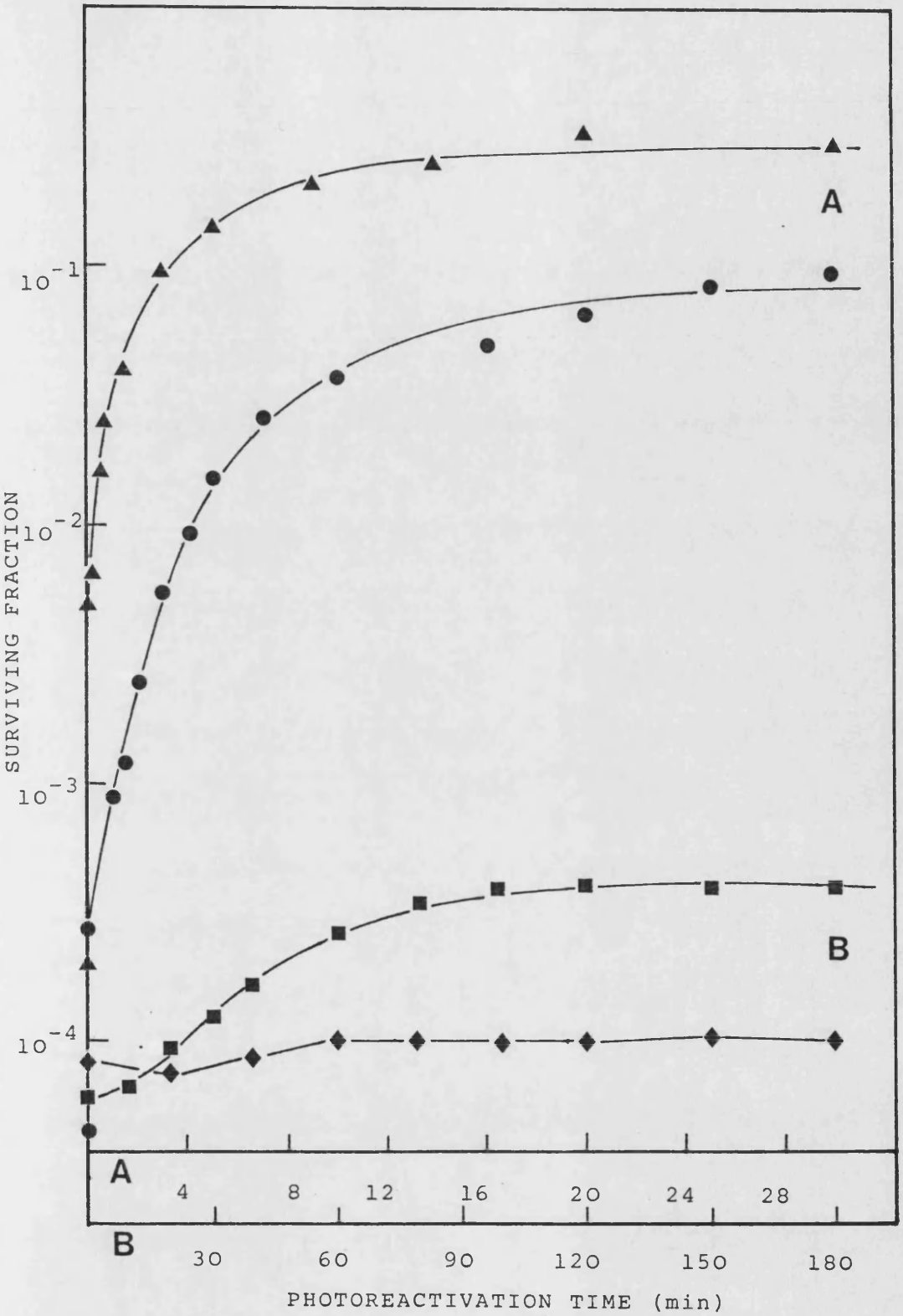

Fig. 3.10. Photoreactivation at 25°C of 254nm inactivated AB2480 (▲), AS44 (●), DY326(■) and AS46 (◆). (Fluence rate 17.6Wm^{-2})

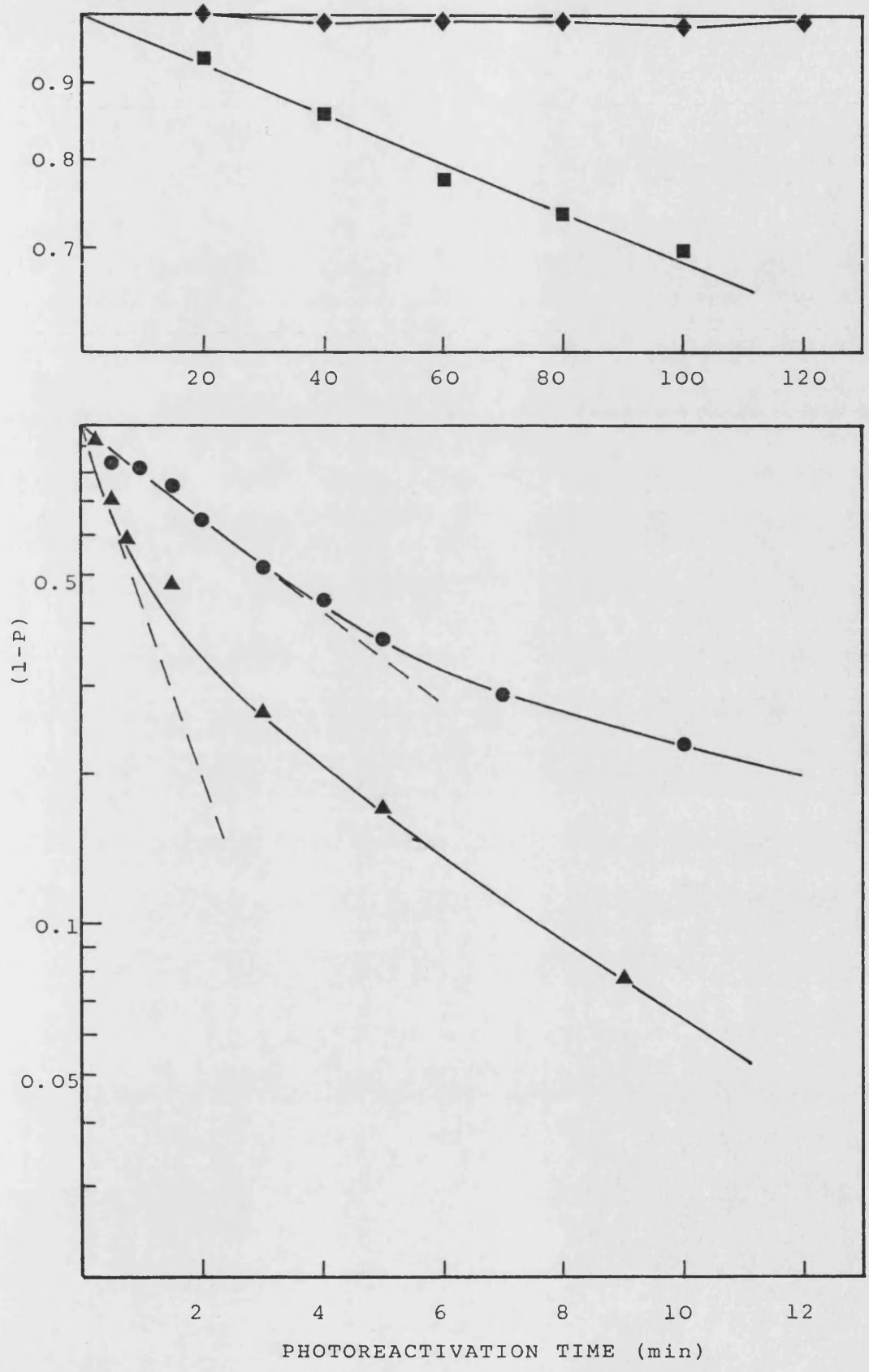

Fig. 3.11. 1-P analysis of the rate of photoreactivation of 254 nm inactivated AB2480 (▲), AS44 (●), DY326 (■) and AS46 (◆).

Table 3.4 Comparison of the mean initial rates of photoreactivation and estimates of the number of PRE molecules after 254 nm UV radiation at 25°C.

STRAIN	Rate ($x10^{-3}$) s^{-1}	Number of PRE Molecules
AB2480	11.5	6.4
AS44	3.5	1.95
DY326	0.062	0.034
AS46	-	-

Photoreactivation of 254 nm-UV-induced damage in AS44 proceeded at a rate of 30 per cent that of AB2480 (Table 3.4), in reasonable support of the data obtained by Sutherland and Hausrath (1979), using recombination-proficient strains. The photoreactivable-sector of both AB2480 and AS44 was calculated to be 0.82, again in agreement with the data of Tyrrell and Davies (1974) and Hodges et al. (1980) for AB2480. Of particular importance to this study was the evidence of PR in DY326 (Fig. 3.10), a strain which has the *phrB* mutation transduced from the photoreactivationless mutant *E. coli* B*phr*. This is in contrast to previous reports using *phrB* strains which have shown no PR of colony formation (Harm and Hillebrandt, 1962) or transforming DNA (Setlow, 1964). Both the rate and extent of repair of DY326 were markedly reduced compared with AB2480 and AS44 (Table 3.4). It has been assumed for the purpose of the (1-P) analysis that the

Table 3.5 EFFECT OF BUFFER HOLDING NON-IRRADIATED CELLS/ PHOTOREACTIVATING LIGHT AND IRRADIATED CELLS HELD IN THE DARK

STRAIN	NON-IRRADIATED CELLS EXPOSED TO PRL 25°C		IRRADIATED HELD CELLS IN THE DARK 25°C	
	TIME (Min)	SURVIVING FRACTION	TIME (Min)	SURVIVING FRACTION
AB2480	0	1.0	0	1.31×10^{-4}
	1	0.996	1	1.35×10^{-4}
	2	0.980	2	1.29×10^{-4}
	5	1.06	5	1.36×10^{-4}
	10	0.970	10	1.21×10^{-4}
	20	0.960	20	1.26×10^{-4}
	30	1.010	30	1.31×10^{-4}
	60	0.950	60	1.34×10^{-4}
AS44	0	1.0	0	9.61×10^{-5}
	1	0.962	1	9.42×10^{-5}
	5	1.05	5	1.13×10^{-4}
	10	1.11	10	1.01×10^{-4}
	20	0.97	20	9.36×10^{-5}
	30	0.94	30	9.81×10^{-5}
	45	0.996	45	9.60×10^{-5}
	60	0.96	60	9.58×10^{-5}
DY326	0	1.0	0	2.63×10^{-4}
	20	1.1	20	1.95×10^{-4}
	40	0.96	40	2.10×10^{-4}
	60	0.98	60	2.60×10^{-4}
	80	0.95	80	2.05×10^{-4}
	100	0.91	100	2.15×10^{-4}
	120	0.98	120	1.21×10^{-4}
	150	0.89	150	2.16×10^{-4}
	180	0.84	180	2.21×10^{-4}
AS46	0	1.0	0	8.05×10^{-5}
	20	1.08	20	8.12×10^{-5}
	40	1.006	40	7.52×10^{-5}
	60	0.961	60	7.29×10^{-5}
	80	0.920	80	8.95×10^{-5}
	100	0.914	100	5.34×10^{-5}
	120	0.842	120	6.17×10^{-5}
	150	0.804	150	7.00×10^{-5}

fraction of photoreactivable lesions was the same for all strains, that is, the reduced extent of PR seen with DY326 was not due to the presence of different, non-photoreactivable lesions. Because many workers have failed to show PRE activity in phrB mutants, it was necessary to consider whether the effect seen represented true enzymatic PR. As discussed in the Introduction to this work, Jagger et al.(1969) showed indirect PR in E. coli Bphr. This was not due to enzymatic dimer-splitting, but rather to the induced growth delay facilitating dark repair processes. Since DY326 is totally dark-repair-deficient, it was unlikely that the increase in survival could be attributed to this. It could also be argued that the increase in surviving fraction observed with UV-irradiated DY326 on exposure to photoreactivating light could be due to "leakiness" of the phrB mutation. However, there was no photoenzymatic repair of UV-induced damage with AS46 (Fig. 3.10) which is phrA phrB uvr^- rec^-, indicating that both the phrB and putative phrA loci may code for photoactive proteins. Sancar and Rupert (1979) have reported a residual PRE activity in a phr mutant of K-12 AB1886, which shows marked photoreactivation under the conditions used in this work (data not shown). When this mutation was transduced into the phrA background and subsequently made recombination-deficient, the photoreactivation effect was significantly reduced but not abolished, suggesting that the phrA mutant background does affect the photoreactivation state of the cell. It must be noted, however, that the apparent abolition of PRE activity in AS46 could be due to a fortuitous reduction in the activity of a slightly leaky phrB mutation to below measurable levels. These data do not absolutely rule out the possibility that the photoreactivation observed with DY326 was due to a partially

active phrB (50-kDa) photolyase or to an unknown photolyase from a third locus, but they do strongly indicate that a gene in the region of the proposed phrA locus does have a significant effect on PRE activity.

As a result of the data obtained with DY326 and AS46 being possibly indicative of the presence of two photoactive proteins in E. coli K-12, it was of interest to determine if there was any kinetic evidence supporting this hypothesis with strains AB2480 and AS44. The (1-P) analyses of both strains (Fig. 3.11) were biphasic; AB2480 being markedly more so. Thus for both strains, the rate of repair can be divided into an initial fast component and a slower component. With strain AB2480, approximately 50 per cent of the photoreversible lesions were repaired in the first minute of treatment at the fast rate, whereas with AS44, approximately 60 per cent of the lesions were repaired at the fast rate over a 5 minute period; albeit at a rate 30 per cent that of AB2480.

Johnson and Haynes (1986a) have developed a new method for analysing photoreactivation kinetics and have used this as evidence for multiple DNA photolyases in the yeast S. cerevisiae. As a comparison with the (1-P) analyses, all the photoreactivation data have been fitted to this model. It is appropriate to briefly discuss the theoretical basis for this treatment.

3.3.2.1 Lethal Hit Analysis

The central notion of the damage-repair hypothesis is that the observed experimental end-point is death (or mutation), rather than the initial physical 'hits', even though these are the causative agents. Biochemical modification of the damage-induced lesions by

repair processes abolishes any simple correlations between the excitations and the final observed biological end-points. Johnson and Haynes (1986a) state that it is these biological end-points or 'lethal hits', distributed randomly amongst the irradiated cell population, to which Poisson statistics should be applied. The important quantity in determining whether or not a cell survives a radiation insult is the number of lethal hits it has received. If it receives one or more lethal hits, by definition it is killed; if it receives zero hits, it survives. If the average number of lethal hits per cell, over the whole irradiated population, is H(x) for a radiation fluence x, then the probability of receiving zero hits is $e^{-H(x)}$. Therefore, for a fluence x the probability of survival(S(x)) is:

$$S(x) = e^{-H(x)} \qquad \ldots.1$$

The quantity H(x) will depend on: i) the number, F(x), of initial physical lesions per cell induced by the radiation fluence x, and ii) the efficiency r(x) with which the induced hits are repaired by whatever repair systems the cell possesses. Thus,

$$H(x) = F(x)\,[1-r(x)] \qquad \ldots.2$$

where [1-r(x)] is the probability that a hit escapes repair. If the initial survival is S(o) and the survival after maximum photorepair is $S(\infty)$, then $\ln [S\infty/So] = h(o)$ is the number of lethal hits repaired by photoreactivation. If photorepair has progressed only for a time t so that survival S(t) is less than $S(\infty)$, then $\ln [S\infty/St] = h(t)$ is the number of photorepairable hits

remaining. As t approaches infinity, S(t) approaches S(∞) and h(t) approaches ln (1) = 0.

CASE I

Johnson and Haynes (1986a) propose that if there is just one type of photolyase molecule present, and the probability of removal of a lethal hit per unit time is α, then

$$h(t) = h(o)e^{-\alpha t} \qquad \ldots.3$$

or

$$\ln[S\infty/St] = h(o)e^{-\alpha t} \qquad \ldots.4$$

Calculated values of ln[S∞/St] are made using an estimated value of S(∞) (i.e. survival after long periods of photo-reactivating treatment) and the experimental values of S(t). If a single photolyase is present, a plot of ln(ln[S∞/St]) against t will lie on a straight line with vertical intercept h(o) and slope = ($-\alpha$).

CASE II

If more than one type of photolyase is present, a plot of ln(ln[S∞/St]) against t will not give a straight line. If the number of photolyase types is 2, one with an associated constant repair probability per unit time α_1, the other α_2 (let $\alpha_1 > \alpha_2$), then,

$$h(t) = h_1(o)e^{-\alpha_1 t} + h_2(o)e^{-\alpha_2 t} \qquad \ldots. 3$$

In this instance, a plot of ln (h)t) against t will exhibit an

initial part with a steeper slope than the latter part, which should be linear. The initial part of the curve is,

$$h_1(o)e^{-\alpha_1 t} + h_2(o)e^{-\alpha_2 t}$$

but since α_1 is greater than α_2, $h_1(o)e^{-\alpha_1 t}$ approaches zero more rapidly than $h_2(o)e^{-\alpha_2 t}$, so the latter part just represents $h_2(o)e^{-\alpha_2 t}$. By regressing this latter linear portion, the constants $h_2(o)$ and α_2 can be estimated. Therefore, a new plot can be constructed from:

$$h_t - h_2(o)e^{-\alpha_2 t} = h_1(o)e^{-\alpha_1 t}$$

allowing determination of the constants $h_1(o)$ and α_1. If this plot does not give a straight line then there may be another component to be extracted. However, this method is unlikely to give satisfactory results for more than three componenets (R.G. Johnson, personal communication).

The photoreactivation data shown in Fig. 3.10 have been plotted in this form and are shown in Fig. 3.12. The data pertaining to these analyses are included in Tables A4.19-21. The calculated values for the slopes (α_1 and α_2), determined by linear regression analysis are included in Table 3.6 (marked *), together with similar values from replicate experiments. The intercept values (Ho) have not been included because their absolute value varies depending on the initial survival after 254 nm inactivation, thus producing a set of 'parallel' plots. In this series of experiments, the survival after 254 nm UV inactivation varied between 6×10^{-5} and 2×10^{-4}, due to the inherent variation in

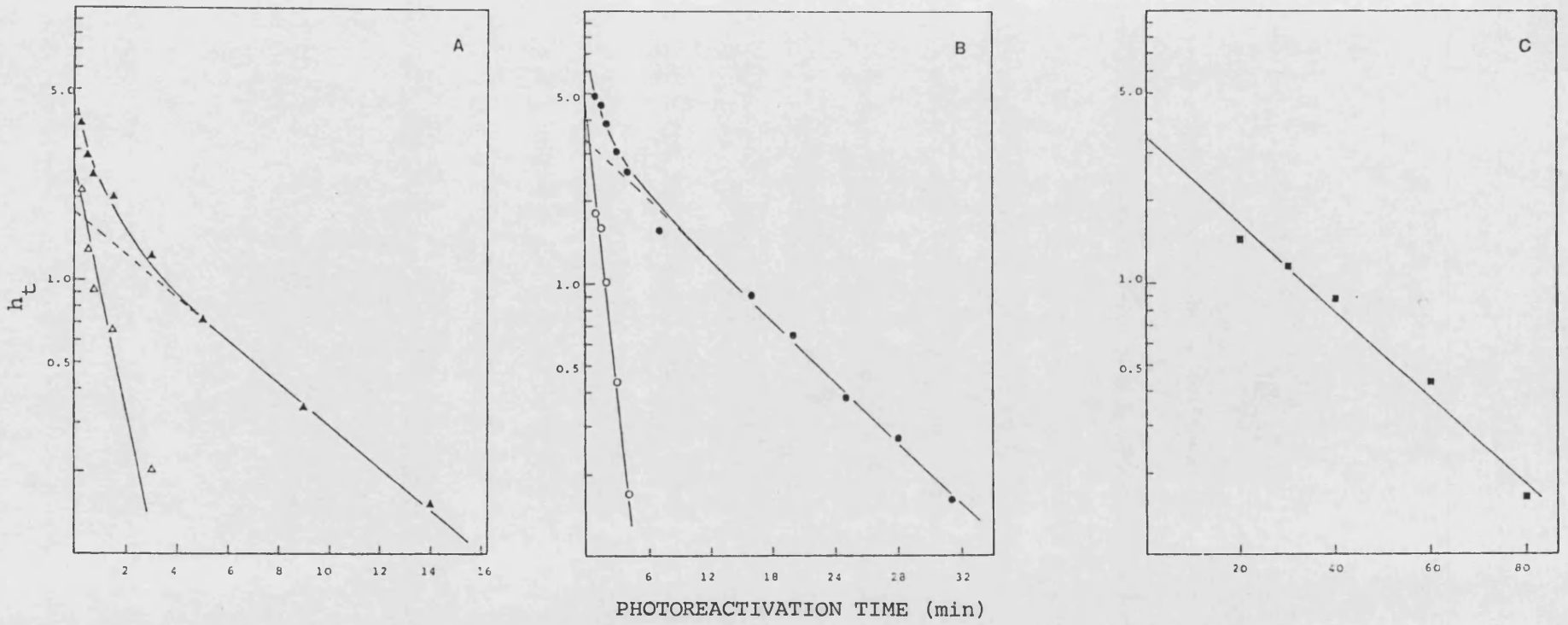

Fig. 3.12. Lethal hit analysis of photoreactivation at 25°C of AB2480 (Panel A), AS44 (Panel B) and DY326 (Panel C) (closed symbols) and after subtraction of slow component (open symbols)

Table 3.6 PHOTOREACTIVATION RATE ANALYSIS OF 254 nm IRRADIATED AB2480, AS44 AND DY326 AT 25°C AFTER AEROBIC GROWTH.

STRAIN	EXPT No.	α_1 (min^{-1})	α_2 (min^{-1})
AB2480	19a	-0.907*	-0.179*
	19b	-1.060	-0.129
	19c	-1.14	-0.198
	MEAN	-1.036±0.118	0.167±0.036
AS44	20a	-0.635*	-0.086*
	20b	-0.595	-0.086
	20c	-0.608	-0.088
	MEAN	-0.613±0.021	-0.0787±0.0104
DY362	21a	-	-0.0365*
	21b	-	-0.0406
	21c	-	-0.0463
	21d	-	-0.0370
	MEAN	-	-0.0401±0.045

fluence delivered from the electronic shutter assembly. It should be noted that Johnson and Haynes (1986b) have reported a decrease in the photorepair probability (α) with increasing 254 nm-UV fluence using a diploid strain of S. cerevisiae. The repair probability after 3-log-cycle inactivation was 78 per cent that after 1 log-cycle inactivation. The authors suggested that this may be attributable to i) greater competition for repair enzymes in cells which have greater numbers of lesions due to larger radiation fluences or ii) inactivation of the repair systems by the radiation. In this study, no such correlation was found, suggesting that there was either no significant variation in repair probability over the fluence range investigated, or that any differences were subsumed within experimental error. Therefore, it was justifiable to draw comparisons between the strains on the basis of the mean repair probabilities (α). Reference to Figs. 3.11 and 3.12 and Table 3.6 indicates that both strains AB2480 and AS44 exhibit biphasic kinetics, with the slower rate being reached after four to six minutes.

The rate constants α_1 and α_2 of AS44 were 60 and 47 per cent those of AB2480. These data may be taken as indicative of the action of two photolyase molecules present in both strains or that a single photolyase molecule has two repair capacities. A full consideration of these possibilities will be given after presentation of the growth temperature data (Section 3.6.2) and acetophenone-sensitized 313nm data (Section 3.7). However, it can be noted at this juncture that since AS44 is deleted at the proposed phrA locus, any model involving a second photolyase molecule in this strain would implicate the existence of a third unknown photoreactivation locus. Assuming that the phrA locus

codes for a photolyase molecule, it would then be necessary to raise the debate of a third photolyase molecule in AB2480. There is no evidence from the kinetic analysis presented in this report to support such a suggestion. It is not inconceivable that a single photolyase molecule could complex with different photoproducts such as T-T, C-T and C-C dimers, to form enzyme-substrate complexes which absorb photoreactivating light with different cross-sections, resulting in different rates of removal of these lesions. However, the ratio of dimer products (after approximately 400 Jm^{-2} of 254 nm UV radiation) published by Ellison and Childs (1981) of T-T:C-T:C-C being 1:0.8:0.3, does not provide a ready interpretation for this suggestion.

Strain DY326 exhibited one repair constant (Table 3.6), the magnitude of which was 51 per cent and 24 per cent of the slow rate constant α_2 of AS44 and AB2480, respectively. This should be contrasted with the approximately 100-fold lower rate derived from the (1-P) analysis (Table 3.4), however, attention should be drawn to the different assumptions associated with each analysis. As discussed previously, the (1-P) analysis for DY326 assumes that the UV-induced lesions are not mechanistically different from those induced in either AB2480 and AS44, and it thus shares the same theoretical photoreactivation sector (0.82), whereas the 'lethal hit' analysis measures the rate of repair of the experimentally determined photorepairable lethal hits. Taken alone, the data for DY326 suggest the action of one photolyase molecule, which may be attributable to either the phrA or phrB loci, or perhaps to a third unknown locus. However, when considering the data pertaining to all three strains it would seem most likely that the photolyase activity observed in DY326 is the result of partial

photoreactivating activity of the mutant phrB gene product or from a third locus. Furthermore, it can be argued that the product of the putative phrA gene functions as an activator of the phrB gene product, resulting in an approximately 2-fold increase in the two rate constants, α_1 and α_2, in agreement with the hypothesis proposed by Sutherland and Hausrath (1979).

3.4. The Dependence of Photoenzymatic Repair on Temperature

The effect of temperature on the velocity of enzyme reactions may be due to several different causes. It may be due to an effect on the stability of the enzyme; to an effect on the enzyme-substrate affinity (i.e. on k_1 and k_2 in the PR reaction scheme); to an effect on the affinity of the enzyme for activators or inhibitors; to a transfer of rate-limiting function from one enzyme to another, in a system involving two or more enzymes with different temperature coefficients; or even to such subsidiary causes as a change in concentration of dissolved O_2, perhaps resulting in alteration of the redox state of the cell.

Any one of these factors could have a significant effect on the rate of photoreactivation in E. coli, and so it was felt worthwhile to investigate the dependence of PR on temperature in AS44 and DY326 and compare the results with those published for AB2480.

Cells grown at 37°C were harvested in the usual manner and irradiated at 25°C to 1 x 10^{-4} surviving fraction with approximately 0.5 Jm^{-2} of 254 nm UV. The cells were held in the dark for 20 minutes to allow maximal complexation of the PRE with its dimer substrate, before being equilibrated to the experimental temperature for a further 5 minutes. The temperatures used were

15.0, 20.1, 25.3, 30.1, and 36.9°C. Consideration was given to the likely effect of [ES] complex dissociation during the temperature equilibration period, particularly at the lowest temperature used. However, published estimates of the dissociation rate constant *in vivo* range from 10^{-2} to 10^{-3} s^{-1} (Harm et al., 1971), suggesting that the complex is very stable in the dark, having a K_A of approximately 10^8. To further support this conclusion, the (1-P) values of the single flash recovery alone of AS44 at each temperature were not significantly different, having a mean of 0.769 ± 0.057.

As in previous experiments, a single flash was given at the commencement of exposure to continuous photoreactivating light. At each temperature, the survival of unirradiated cells exposed to photoreactivating light did not fall below 0.85, nor was there any change in the surviving fraction of irradiated cells held in the dark (data not shown). The photoreactivation data for AS44 at three temperatures are shown in Fig. 3.13 and the (1-P) analyses of the data obtained at the five temperatures for both AS44 and DY326 are included in Fig. 3.14. The data pertaining to these analyses are included in Tables A4.22-23. The slopes of these plots, determined by linear regression analysis, have been fitted to the Arrhenius relationship, and are shown in this form in Fig. 3.15. Where the (1-P) plots shown an initial fast rate of repair decreasing to a slower rate, the slope has been calculated on the basis of the time required for the fraction of photorepairable lesions to fall to 70 and 90 per cent for AS44 and DY326, respectively. The Arrhenius relationship between the rate constant (k_1) and temperature (T) is expressed by the equation:-

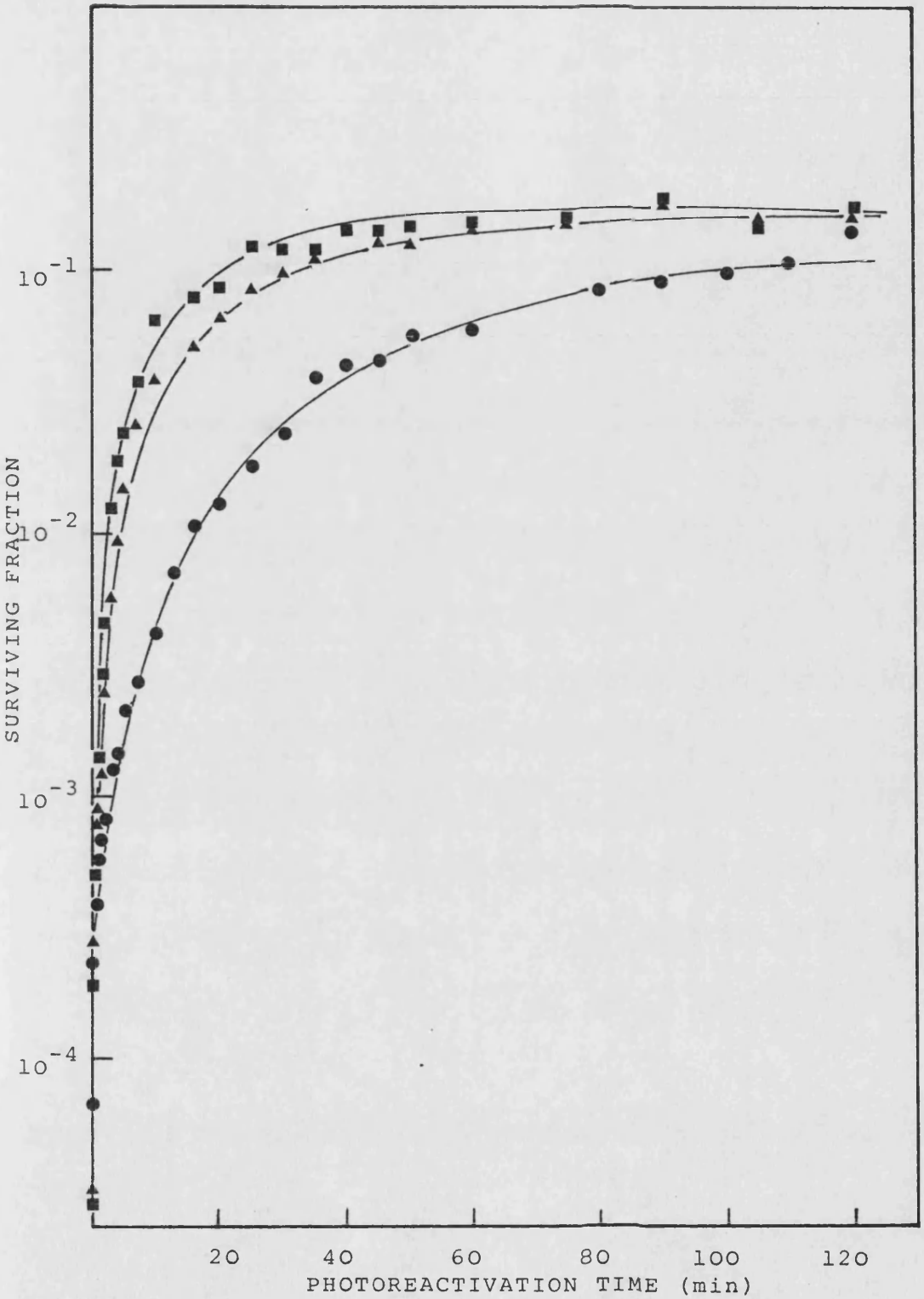

Fig. 3.13. Photoreactivation of 254 nm inactivated AS44 at 15.0 (●), 25.3 (▲) and 36.9°C (■). (Fluence rate 17.6 Wm^{-2})

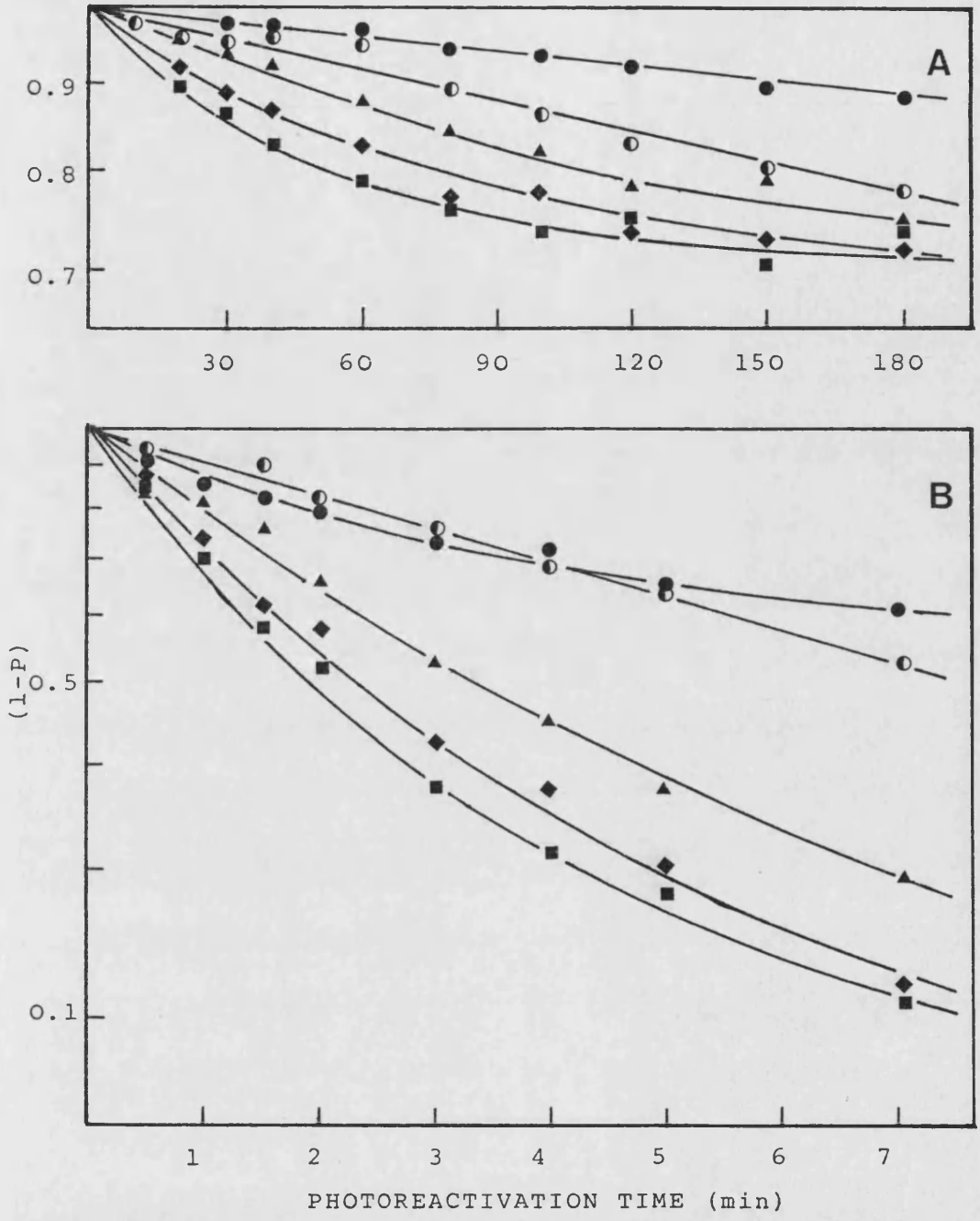

Fig. 3.14. 1-P analysis of the rate of photoreactivation of DY326 (Panel A) and AS44 (panel B) at 15.0 (●), 20.1 (◐), 25.3 (▲), 30.1 (◆) and 36.9°C (■).

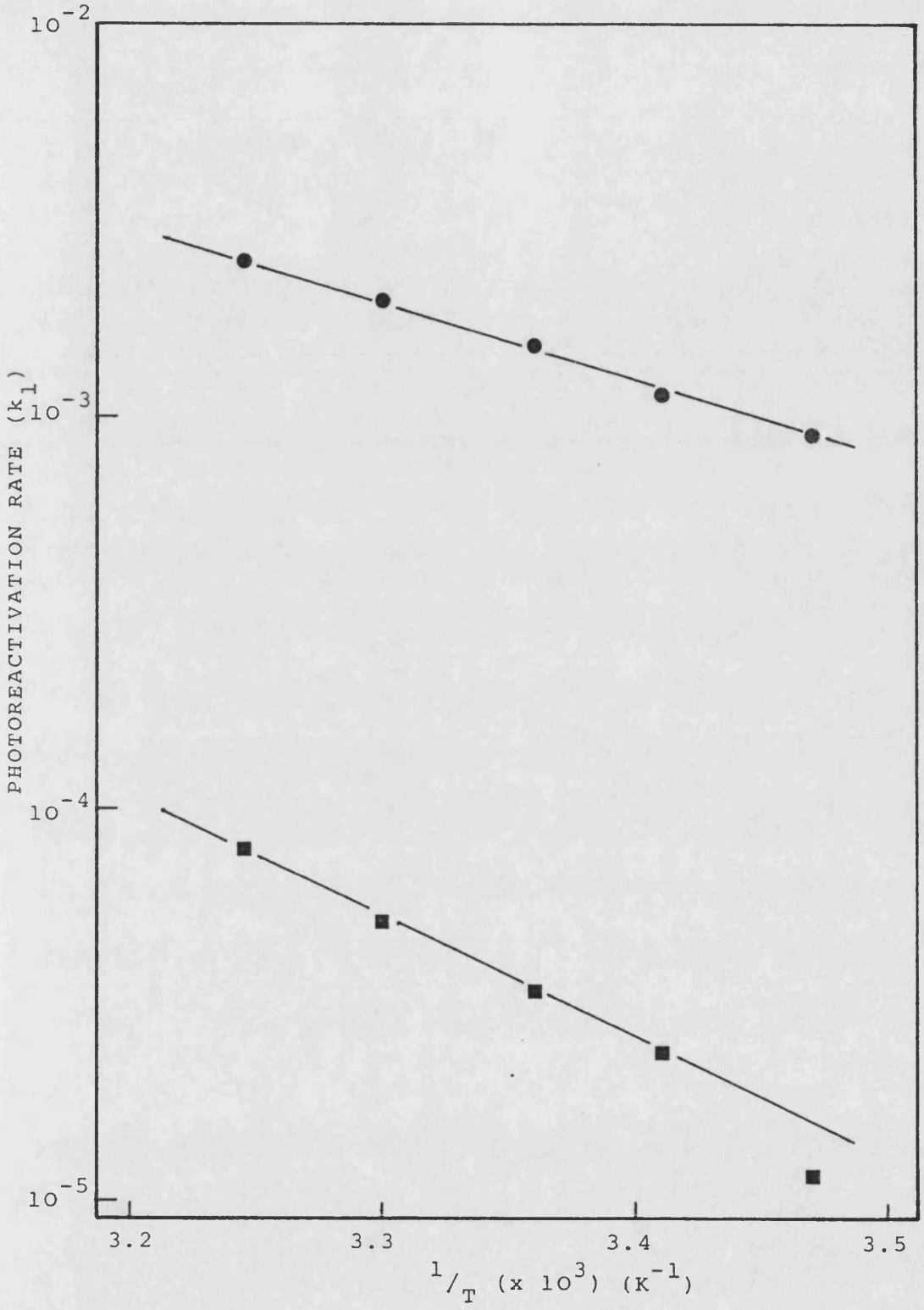

Fig. 3.15. Arrhenius plots illustrating the temperature-dependence of the photoreactivation rate (k_1) for AS44 (●) and DY326 (■).

$$k = A.e^{-Ea/RT}$$

where A = frequency factor (s^{-1})

R = gas constant (8.314 $kJ.K^{-1}.mole^{-1}$)

Ea = activation energy ($kJ.mole^{-1}$)

k = specific reaction rate

T = absolute temperature (K)

The activation energy, calculated from the gradient was found to be 38.4 and 55 $kJ.mol^{-1}$ for AS44 and DY326, respectively. The calculated frequency factors (A) for AS44 and DY326 were 8.0×10^3 and 1.7×10^5 sec^{-1}, respectively. The activation energies compare with 9.0 $kcal.mol^{-1}$ (35.5 $kJ.mole^{-1}$) for AB2480 (Tyrrell and Davies, 1974) and 11.0 $kcal.mol^{-1}$ (45.89 $kJ.mole^{-1}$) for E. coli B_{s-1} (Harm et al., 1971). It will be noted that AS44 does not differ significantly from AB2480 with respect to activation energy, and so the decreased rate of photorepair observed with AS44 cannot be attributed to a population of photolyase molecules from which only a small proportion have sufficient energy to undergo a fruitful collision. However the frequency factor (A) was only 27 per cent of the figure reported by Tyrrell (1971) for AB2480, suggesting that the rate of repair may be limited by collision frequency. It is interesting to note that the relative frequency factors paralleled the relative rate of repair in vivo.

The activation energy calculated for DY326 was significantly higher than other published values. This would suggest that the larger enthalpy associated with complex formation may reflect a greater degree of 'stretching and squeezing' of the PRE molecule in order to achieve the enzyme-substrate transition-state, rather than

to changes in the cellular milieu affecting the ability of the enzyme to move between substrate moieties; the latter would be presumed to be independent of the strains phr phenotype. The overall result of the greater energy of activation would be to decrease the proportion of PRE molecules which have sufficient energy to form the transition state. The frequency factor obtained for DY326 was approximately 50-100-fold greater than that obtained for either AS44 or AB2480. It has been suggested that the experimentally determined value for the frequency factor does not necessarily correspond with the calculated values based on theoretical collision frequecies. For example, in almost all chemical reactions, the molecules which collide must do so with the correct alignment or orientation to each other, with the result that many reactions are controlled by severe steric requirements. Thus it could be argued that the frequency factor measured with DY326 more closely approaches the theoretical maximum, but that the enzyme-substrate complex is in such a steric orientation that it has a low photoreactivation cross-section, whereas with AS44 and AB2480, the photolyase molecules have stricter steric requirements, but which never-the-less results in an enzyme-substrate complex having a high photoreactivation cross-section. The photo-reactivation data of AS44 have also been analysed by the 'lethal-hit' model of Johnson and Haynes (1986a), and the two repair probability constants α_1 and α_2 fitted to the Arrhenius relationship (Fig. 3.16). The data pertaining to these analyses are shown in Table A4.22. A regression analysis of all the data points for each plot resulted in activation energies of 53.2 and 41.0 kJ.mole^{-1} for α_1 and α_2, respectively. Visual inspection of these plots suggests that they may be biphasic in nature, with a

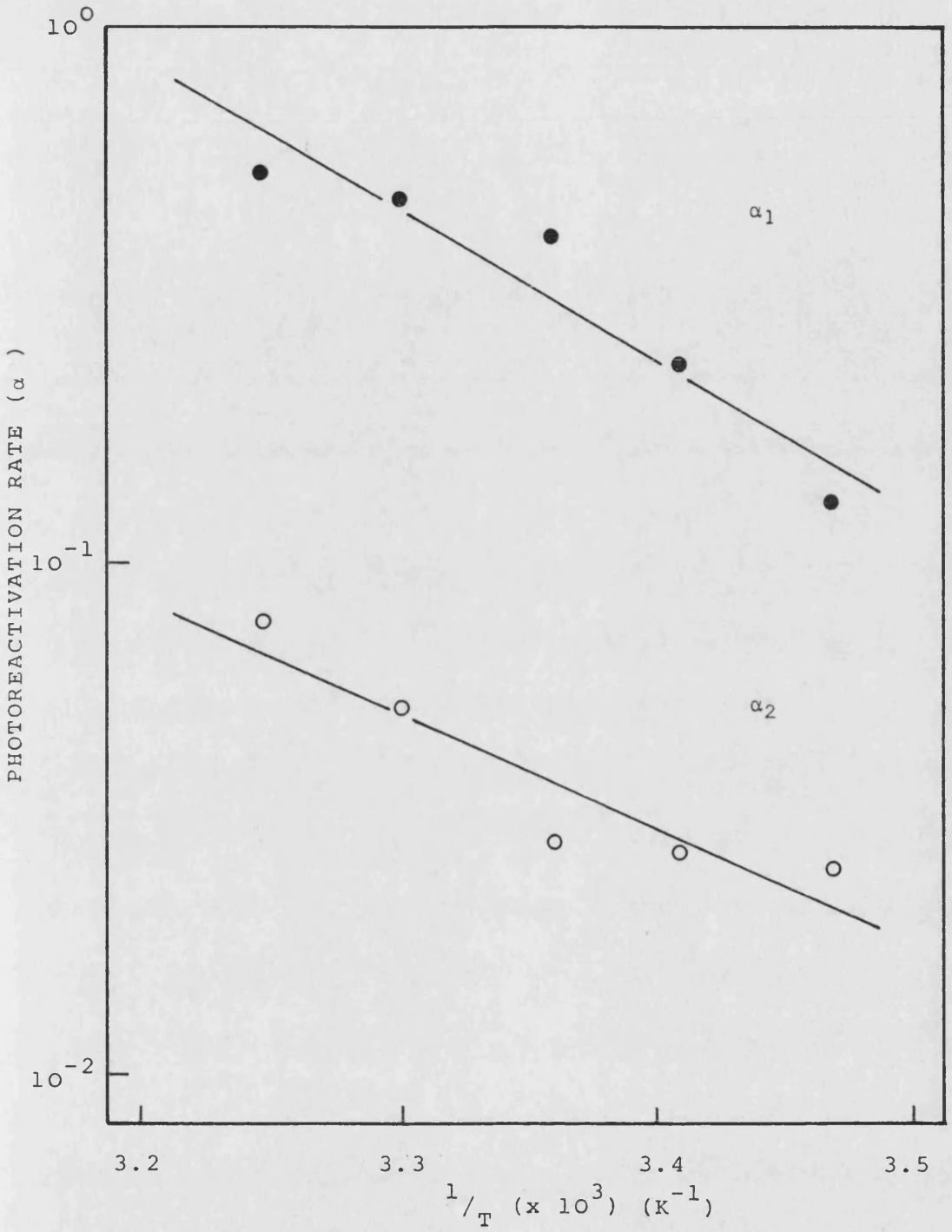

Fig. 3.16. Arrhenius plots illustrating the temperature-dependence of the photorepair probabilities derived from lethal hit analysis for AS44.

transition temperature at approximately 25°C. Several explanations have been put forward to account for biphasic Arrhenius plots, including the possibility that an enzyme may have two active centres with different temperature coefficients, such that the rate of the reaction with the higher coefficient increases more rapidly with temperature than the other, and therefore this reaction predominates at higher temperatures. The resulting Arrhenius plot should concave upwards. Similarly, if the enzyme exists in two forms in equilibrium with one another, both forms being active but having different activation energies, and if the effect of temperature on the change from one form to the other is large, then a sharp discontinuity in the Arrhenius plot will be observed. However, such explanations must remain highly speculative until more data points can be added to the Arrhenius plots. It should be noted that a t-test of the correlation coefficient r for each plot yielded values of 5.26 and 4.68 with 3 degrees of freedom for α_1 and α_2, respectively. The probability that t is equal to, or larger than 4.68 or 5.26 is between 0.005 and 0.01, indicating that there was a statistically significant linear relationship between the experimental data points.

3.5. The Dependence of Photoenzymatic Repair on the Wavelength of Photoreactivating Light

Having established a photoreactivable response in 254 nm UV-irradiated DY326, which was apparently enzymatic in nature (based on the temperature-dependence), it was considered worthwhile to determine the wavelength-dependence of the reaction for this strain and compare it with AB2480 and AS44.

Cell suspensions grown at 37°C were reduced to about 1×10^{-4}

surviving fraction with 0.5 Jm^{-2} of 254 nm UV radiation, held at 25°C for 20 minutes and then exposed to monochromatic light at 25°C. The fluence rate used at each wavelength was below saturating irradiance conditions and quantum corrected such that the number of quanta per unit time was the same. The actual quantum rate used was 2.885×10^{14} photons per second, equivalent to a fluence rate of 1.6 Wm^{-2} at 360 nm. Therefore, the rate of photolysis under conditions of limiting light at a given wavelength is a measure of the efficiency with which an absorbed photon causes photoreactivation.

Irradiated cell suspensions were given a single high-intensity flash at the commencement of exposure to monochromatic light. The wavelength was varied between 320 and 600 nm. Preliminary experiments indicated that exposure of AB2480, AS44 and DY326 for 2, 4 and 90 minutes, respectively, at each wavelength would give a reliable estimate of the rate of repair, using the calculated (1-P) value. Furthermore, complete photoreactivation experiments for AS44 using 350, 385 and 420 nm monochromatic photoreactivating light were carried out and are shown in Fig. 3.17. The (1-P) plots are included in Fig. 3.18. The gradient of the (1-P) plot, that is the rate of repair, was used as a measure of the 'efficiency' with which particular wavelengths of light brought about photolysis. The data for the three strains are shown in Fig. 3.19.

Strain DY326 exhibited a broad structureless peak over the range 360-400 nm, falling off sharply to no measurable repair beyond 430 nm. Below 350 nm the lethal effect outweighed repair. This was similar to enzymatic PR (reviewed by Harm, 1975) and is in contrast to known examples of non-enzyme-dependent photosensitized photoreversal of pyrimidine dimers, such as tryptophan-containing

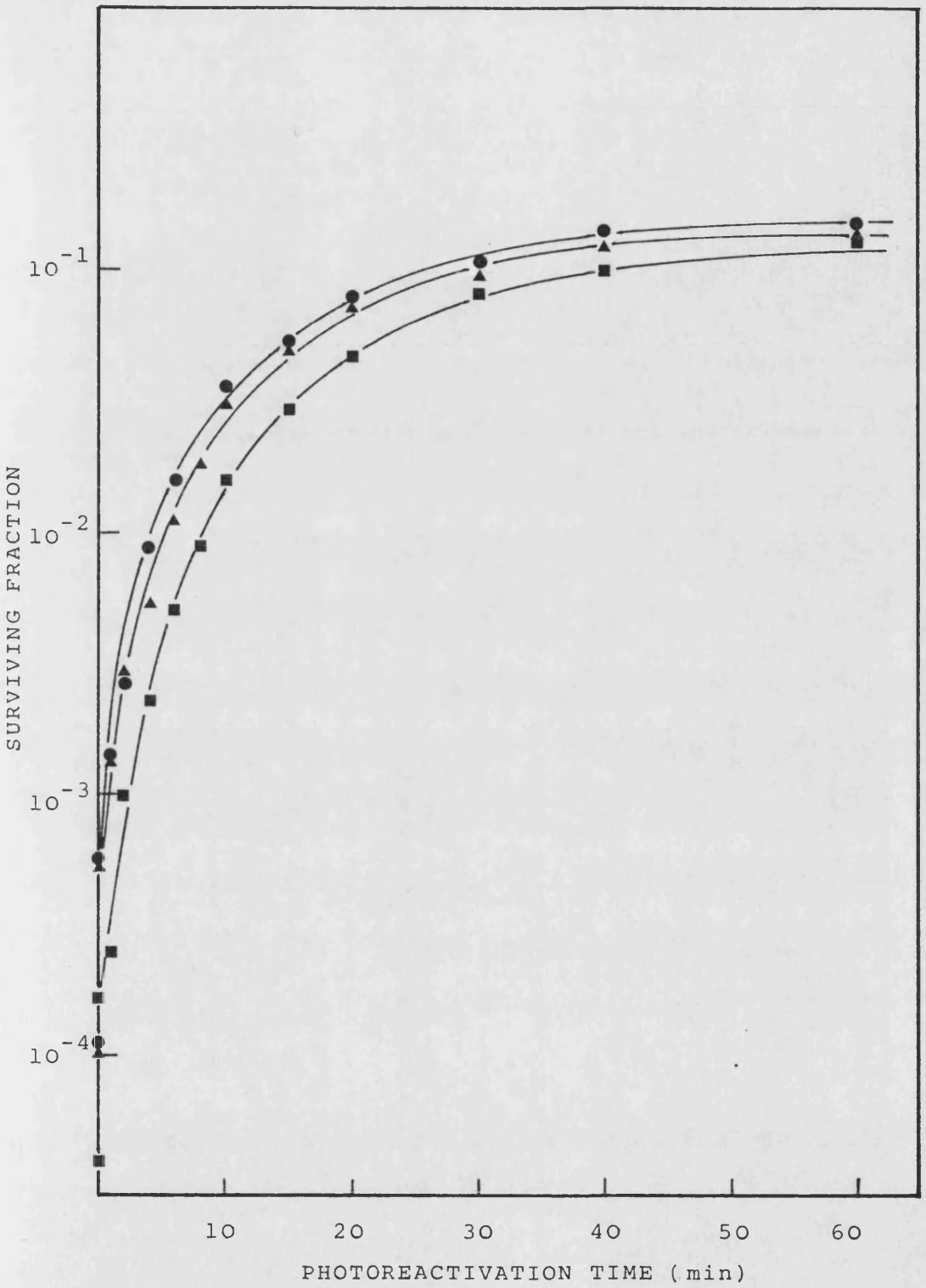

Fig. 3.17. Photoreactivation at 25°C of 254 nm inactivated AS44 with 350 (▲), 385 (●) and 420 nm (■) photoreactivating light.

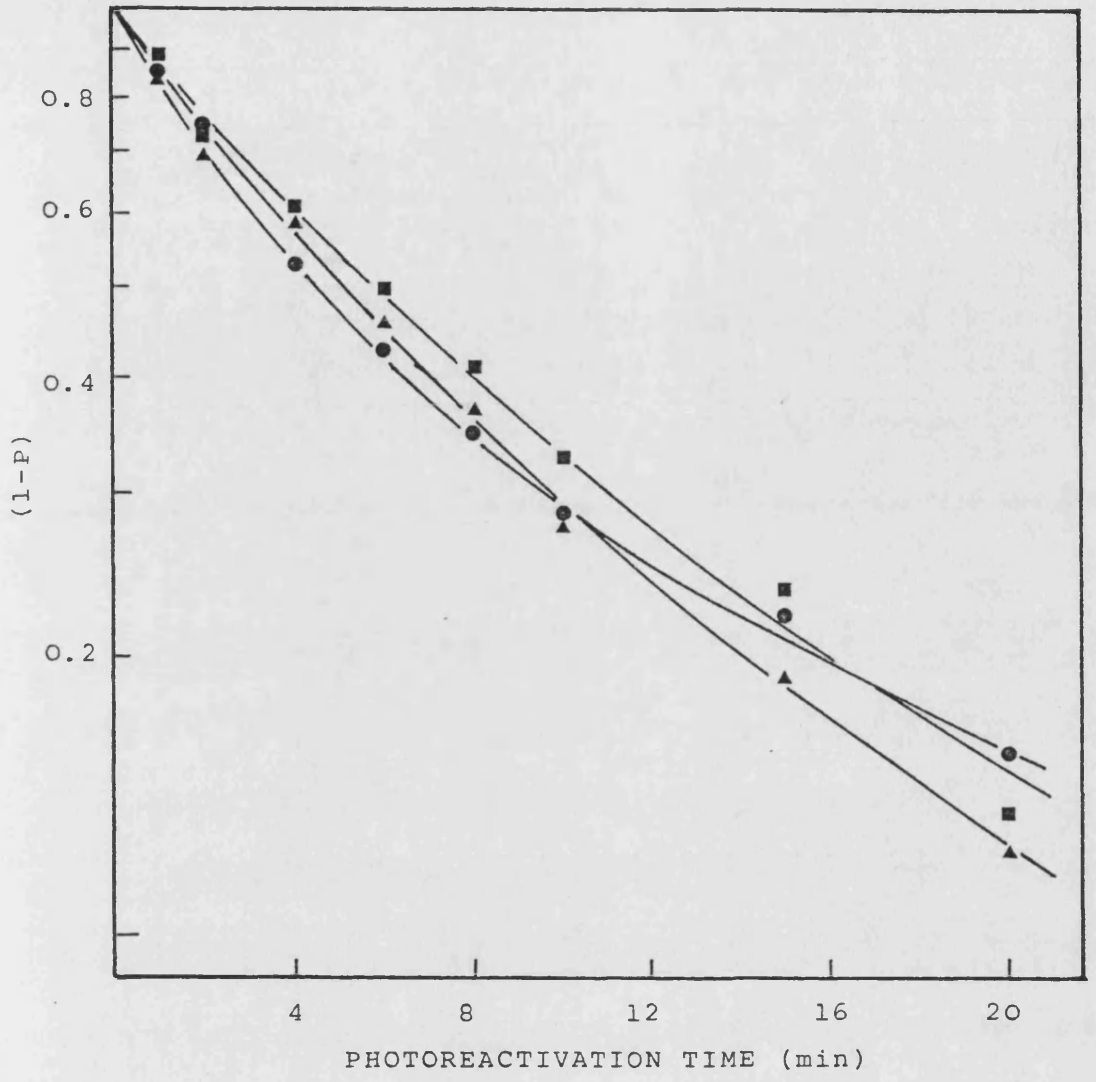

Fig. 3.18. 1-P analysis of the photoreactivation rate at 25°C of 254 nm inactivated AS44 with 350 (▲), 385 (●) and 420 nm (■) photoreactivating light.

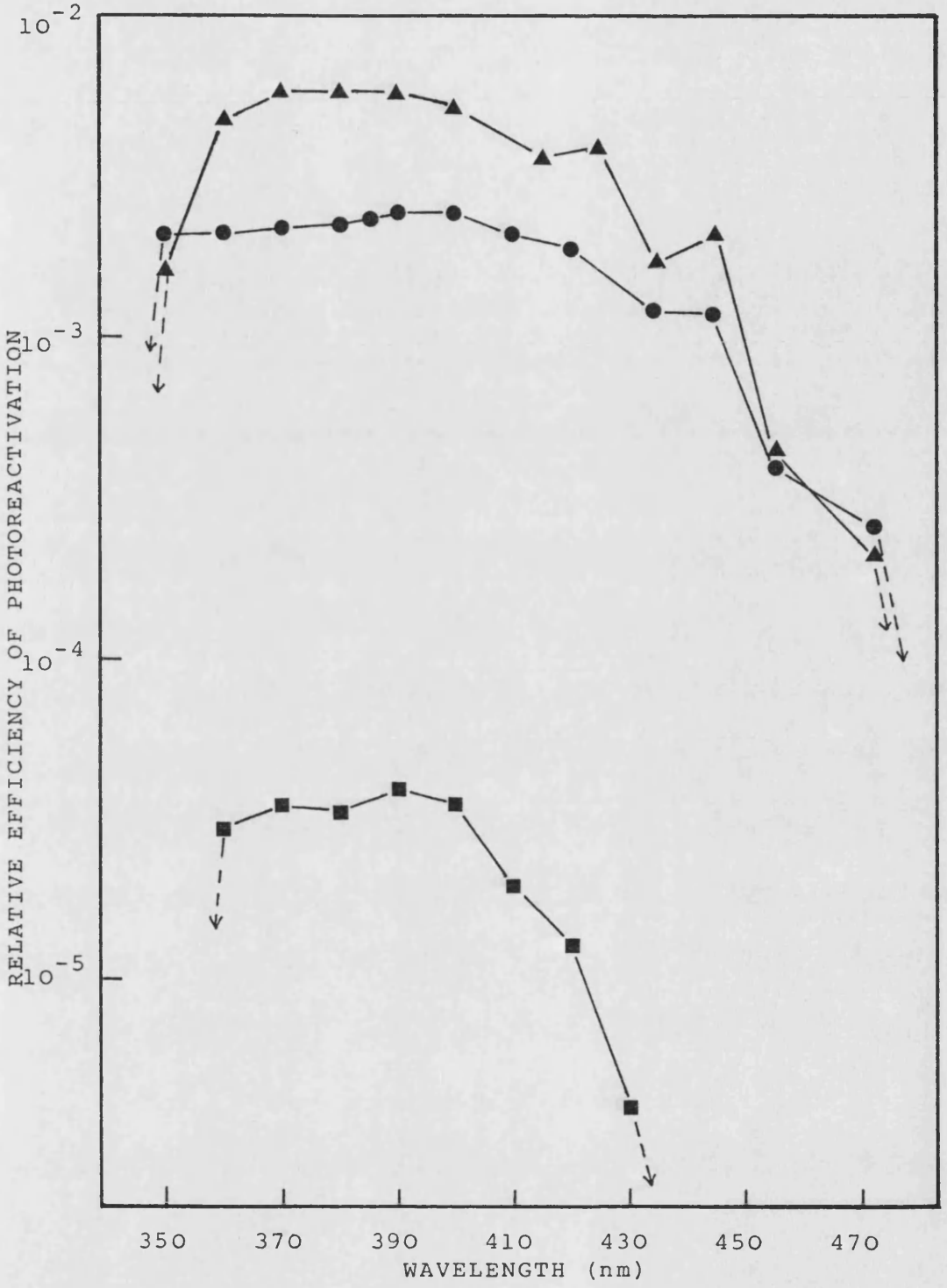

Fig. 3.19. The efficiency of photoreactivation of 254 nm induced damage as a function of the wavelength of photoreactivating light for AB2480 (▲), AS44 (●) and DY326 (■).

oligopeptides (Helene and Charlier, 1977) and the gene 32 protein of 'phage T4 (Helene et al., 1976), where no sensitized splitting was observed beyond 350 nm.

Strains AS44 and AB2480 showed approximately 50-100-fold greater 'efficiency' of repair, respectively, reflecting their higher first-order rate-constants. However, they exhibited a similar structureless peak over the range 360 to 400 nm, but had a small shoulder at 445 nm, with repair being measurable with photoreactivating light wavelengths up to 470 nm. The wavelength-dependence of PR observed with these strains was similar to the action spectra for PR in vivo published by Harm (1975) and Kondo and Kato (1966), which have a broad structureless peak at 385 nm. Harm (1970) calculated the photolytic rate constant for the photolysis of the PRE-substrate complex and found that PR was most efficient at 385 nm. In addition, these results are in agreement with the finding of Jorns et al. (1984), who showed that the cloned phrB gene product had an intense absorption band at 384 nm. This was attributed to a neutral flavin radical and a second chromophore associated with the enzyme. Sancar et al. (1987b) have determined the action spectrum of the blue photolyase enzyme in vitro which showed a peak at 385 nm, in good agreement both with the in vivo data presented in this report and the calculated absorption spectrum for the protein-bound second chromophore (Jorns et al., 1987), which had a maximum absorption at 390 nm. Whilst the similarity between the in vitro action spectrum and the absorption spectrum of the second chromophore has led Sancar et al. (1987a) to suggest that the latter makes a major contribution to the absorption of photolyase at 384 nm (approximately 65 per cent - Jorns et al., 1987) and must be the major sensitizer at this

wavelength, it cannot be the sole sensitizer because a small but significant level of activity was detected up to 625 nm. The second chromophore does not absorb beyond 450 nm, suggesting that the flavin chromophore may also be a photosensitizer. It is difficult to speculate on the role of the flavin chromophore *in vivo*, particularly since in this study, no repair was detected beyond 470 nm, suggesting that absorption by the flavin radical alone does not result in a detectable biological effect. However, Jorns et al. (1987) have shown that if the purified enzyme is treated with sodium dodecylsulphate at neutral pH (resulting in rapid oxidation of the FAD radical followed by a slower, irreversible decomposition of the second chromophore) and then treated with dithionite (to reduce the flavin radical), the decrease in second chromophore greatly exceeded the decrease in enzyme activity, suggesting that the enzyme can function in the absence of the second chromophore.

It is pertinent to discuss whether the decrease in 'efficiency' of photorepair of AS44 compared with AB2480, may be attributable to any photochemical explanations. It could be argued that the increase in repair rate observed in AB2480 was due to a larger photoreactivation cross-section. Sancar et al. (1987a) have tested this hypothesis using a Δ(*gal- uvrB*) strain and an otherwise isogenic strain. They obtained $\varepsilon\phi$ values of 3.3×10^4 and 4.4×10^4 M^{-1} cm^{-1}, which they found were not significantly different. However, such a difference, even if merely regarded as a gross trend, does hold out the possibility that a gene in the region of the proposed *phrA* locus may affect the quantum yield of DNA photolyase. The effect is apparently worthy of further investigation.

3.6. The Dependence of Photoenzymatic Repair on Pre-irradiation Growth Conditions

There have been several reports in the literature suggesting that pre-irradiation growth conditions can have a significant effect on photoenzymatic repair; namely aerobic versus anaerobic growth; growth temperature and the presence or absence of light.

3.6.1. Anaerobic Growth

Tyrrell (1973b) established suppression of photoreactivating enzyme production in E. coli K-12 strains grown under anaerobic conditions. It was considered worthwhile to determine what effect anaerobic growth would have on the four strains used in this study. The cultures were grown as described in Secion 3.2, but a mixture of 95% N_2 and 5% CO_2 was passed through the aeration apparatus (see General Methodology). Cell suspensions for irradiation and photoreactivation were prepared in the usual manner.

3.6.1.1 High-Intensity Flash Photolysis

Cell suspensions of anaerobically-grown AB2480, AS44, DY326 and AS46 were inactivated with graded fluences of 254 nm UV radiation, and 'flash-photoreactivated' to establish the 'fluence-decrement', as described in Section 3.2.1. Representative results from duplicate experiments for AB2480 and AS44 are shown in Fig. 3.20. The survival parameters are included in Table 3.7, together with those for DY326 and AS46. The data pertaining to these parameters are included in Tables A4.24-27. The analysis of covariance between the 254 nm UV inactivation data and the aerobic data (Table 3.1), derived from regression analysis of the pooled data, indicated there was no significant difference in either

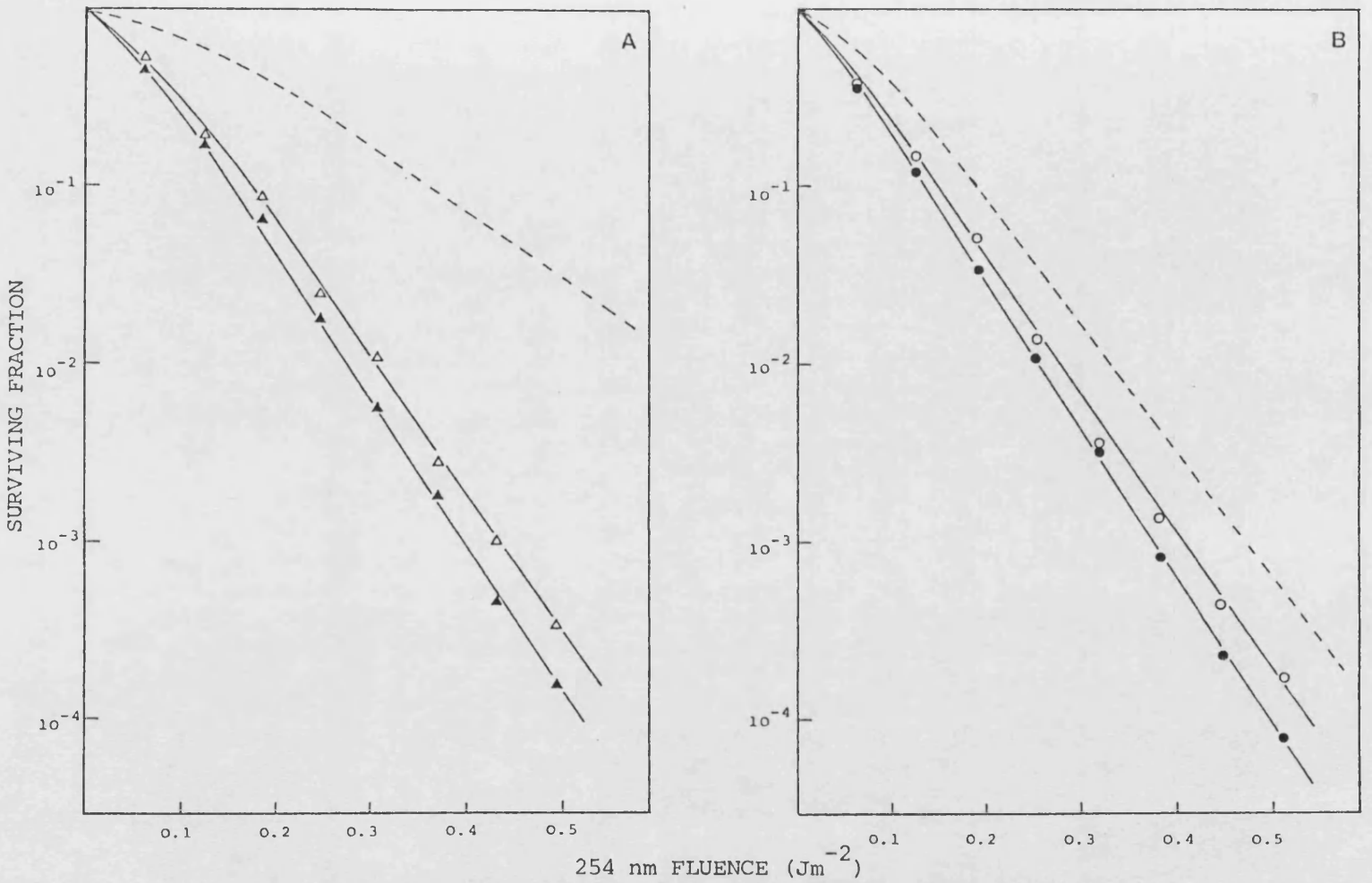

Fig. 3.20. Survival curves for anaerobically grown AB2480 (Panel A) and AS44 (Panel B) after 254 nm UV (closed symbols) and a single flash of light (open symbols). (- - - aerobic flash response)

Table 3.7 INACTIVATION PARAMETERS FOR ANAEROBICALLY GROWN AB2480, AS44, DY326 AND AS46 AFTER 254 nm UV IRRADIATION AND MAXIMUM FLASH PHOTOLYSIS AT 25°C

STRAIN	TREATMENT	INTERCEPT 'n'	INACTIVATION COEFFICIENT 'k' $(Jm^{-2})^{-1}$
AB2480	254 nm	1.93 ± 0.145	18.97 ± 0.193
(*phr*$^+$)	FLASH	2.34 ± 0.314	17.88 ± 0.186
AS44	254 nm	1.38 ± 0.112	19.23 ± 0.204
(*phrA*),	FLASH	1.24 ± 0.139	17.64 ± 0.192
DY326	254 nm	1.51 ± 0.146	19.20 ± 0.189
(*phrB*)	FLASH	1.48 ± 0.157	19.31 ± 0.196
AS46	254 nm	1.36 ± 0.142	19.16 ± 0.13
(*phrA*,*phrB*)	FLASH	1.40 ± 0.151	19.23 ± 0.162

intercept or slope location at the 5 per cent confidence interval ($p>0.05$). However, reference to Figs. 3.6 and 3.20 indicates a significant reduction in the fluence decrement for both AB2480 and AS44. The calculated values were 0.03 ± 0.0042 and 0.026 ± 0.0038 Jm^{-2} for AB2480 and AS44, respectively, which resulted in values of 1.6 ± 0.22 and 1.4 ± 0.20 for the estimates of the number of photo-reactivating enzyme-substrate complexes per cell present at the instant of the flash. Once again, no fluence decrement values were obtained with either DY326 or AS46. Whilst anaerobic culture has reduced the estimates of the number of PRE molecules per cell for both AB2480 and AS44 compared with aerobic growth (Section 3.2.1) it is noteworthy that the value for AB2480 was reduced to 10 per cent, whereas the value for AS44 was only reduced to 19 per cent, indicating that anaerobic culture had a proportionately greater effect in the *phr*$^+$ background of AB2480. Tyrrell (1973b) determined the fluence decrement from a single flash of 48 hour stationary-phase AB2480 grown in supplemented minimal medium under anaerobic conditions to be 0.15 $erg.mm^{-2}$; resulting in an estimate of one or two PRE molecules per cell. Two hypotheses can be put forward to explain these data. Firstly, the marked metabolic changes resulting from anaerobic respiration compared with aerobic respiration may cause a simple reduction in the production of PRE molecules. This alone would not account for the disproportionate reduction between AB2480 and AS44, necessitating the supposition of a direct effect on a component of the PRE molecule in AB2480 which is not present in AS44. This will be discussed in greater detail at the conclusion of this section. Secondly, there may be an inhibitor present in the anaerobically grown cells, perhaps allosteric in nature, which reduces the activity of the PRE, whilst

not abolishing it.

3.6.1.2. Photoreactivation With Continuous Illumination

The cultures were grown as described in Section 3.6.1.1, inactivated with 254 nm UV radiation and photoreactivated as described in Section 3.3.2. The photoreactivation data for the four strains are shown in Fig. 3.21 and the (1-P) analyses are included in Fig. 3.22. The rate constants, determined by least squares regression analysis of the initial linear portion of each (1-P) plot, have been used to estimate the average number of PRE molecules per cell; these values are included in Table 3.8 together with the aerobic values from Table 3.4.

Table 3.8 Comparison of the initial rate of photoreactivation and estimates of the number of PRE molecules after anaerobic culture. The aerobic values are included in parentheses.

Strain	Rate (k_1) ($\times 10^{-3}$) (s^{-1})	Number of PRE molecules
AB2480	4.18 (11.5)	2.32 (6.4)
AS44	2.3 (3.5)	1.28 (1.94)
DY326	0.02 (0.062)	0.01 (0.034)
AS46	- (-)	- (-)

The decrease in the rate of photoreactivation (Table 3.8)

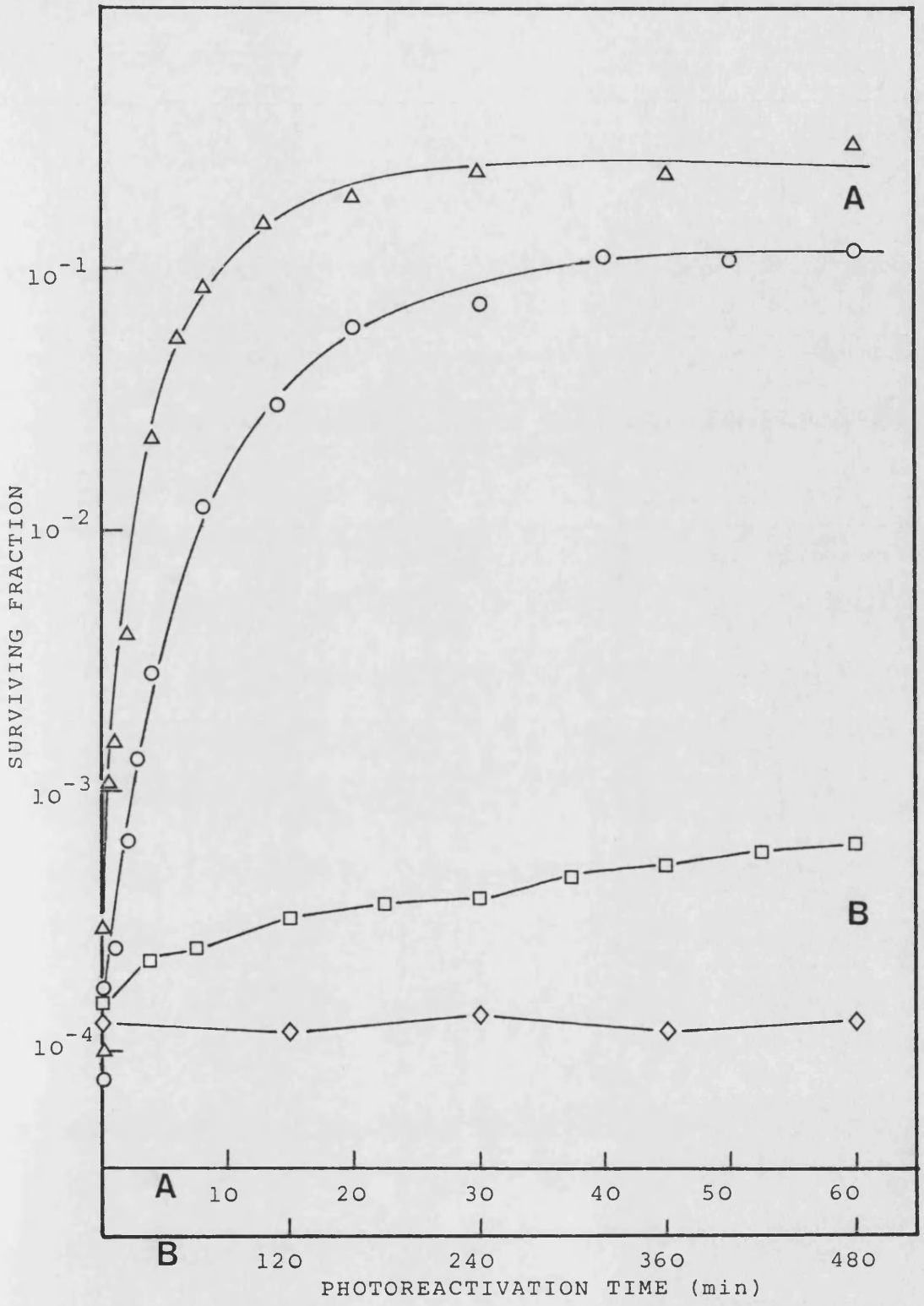

Fig. 3.21. Photoreactivation of anaerobically-grown, 254 nm UV inactivated AB2480 (△), AS44 (○), DY326 (□) and AS46 (◇) at 25°C. (Fluence rate 17.96 Wm^{-2}).

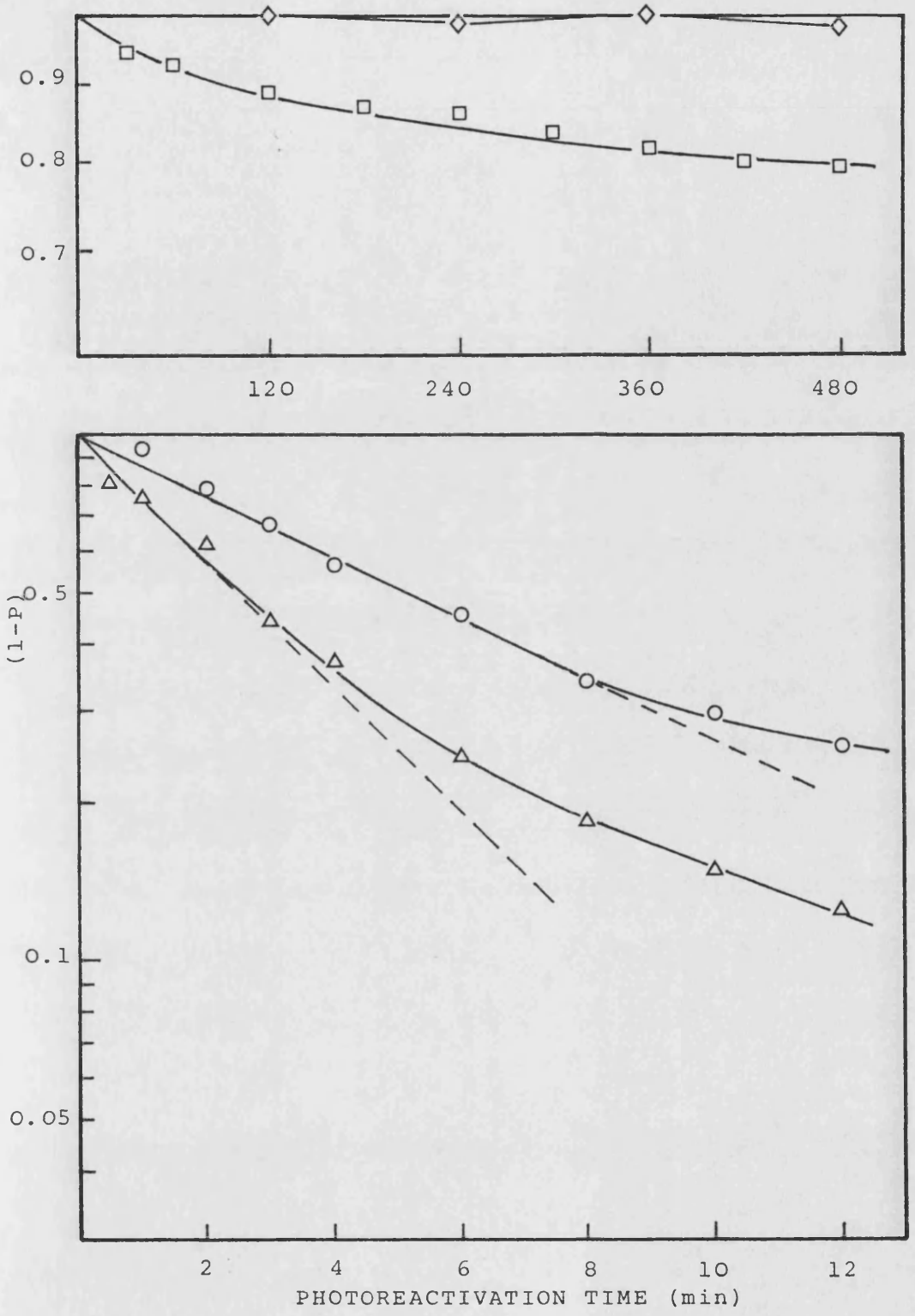

Fig. 3.22. 1-P analysis of the rate of photoreactivation at 25°C of 254 nm inactivated, anaerobically-grown AB2480 (△), AS44 (○), DY326 (□) and AS46 (◇).

paralleled the disproportionate reductions derived from the fluence decrements (Secion 3.6.1.1). The rates of photoreactivation for anaerobically grown AB2480, AS44 and DY326 were 36-, 66-, and 32 per cent, respectively, of the aerobic values. Once again, photoreactivation of AS44 was markedly less affected. It should be emphasised that the fluence decrement resulting from a single flash was more markedly affected than the initial rate of photo-reactivation after anaerobic growth. It could thus be argued that one of the effects of anaerobic culture is to decrease the affinity of the PRE for its substrate, perhaps by increasing the dark dissociation constant, k_2 (see Introduction). Therefore, the formation of the enzyme- substrate complex would be more transient, with the result that the number of complexes present at the instant of a single flash would be lower. However, during continuous illumination under saturating irradiance conditions, the complexes would be photolysed as soon as they were formed. Whilst the data presented in this report may suggest this explanation, they do not confirm it. This investigation could be pursued using the 'competing substrate' techniques described by Harm et al. (1971) to determine the dark dissociation constant, k_2.

The photoreactivation data have also been analysed by the 'lethal-hit' method developed by Johnson and Haynes (1986a), and are shown in this form in Fig. 3.23. The data pertaining to these figures are included in Tables A4.28-30. The mean photorepair constants α_1 and α_2 from two replicate experiments are included in Table 3.9, together with the corresponding values for aerobic growth conditions (from Table 3.6). Comparison of the repair probabilities α_1 and α_2 after anaerobic and aerobic growth indicated that with AS44, the slower rate constant α_2 was 4 per

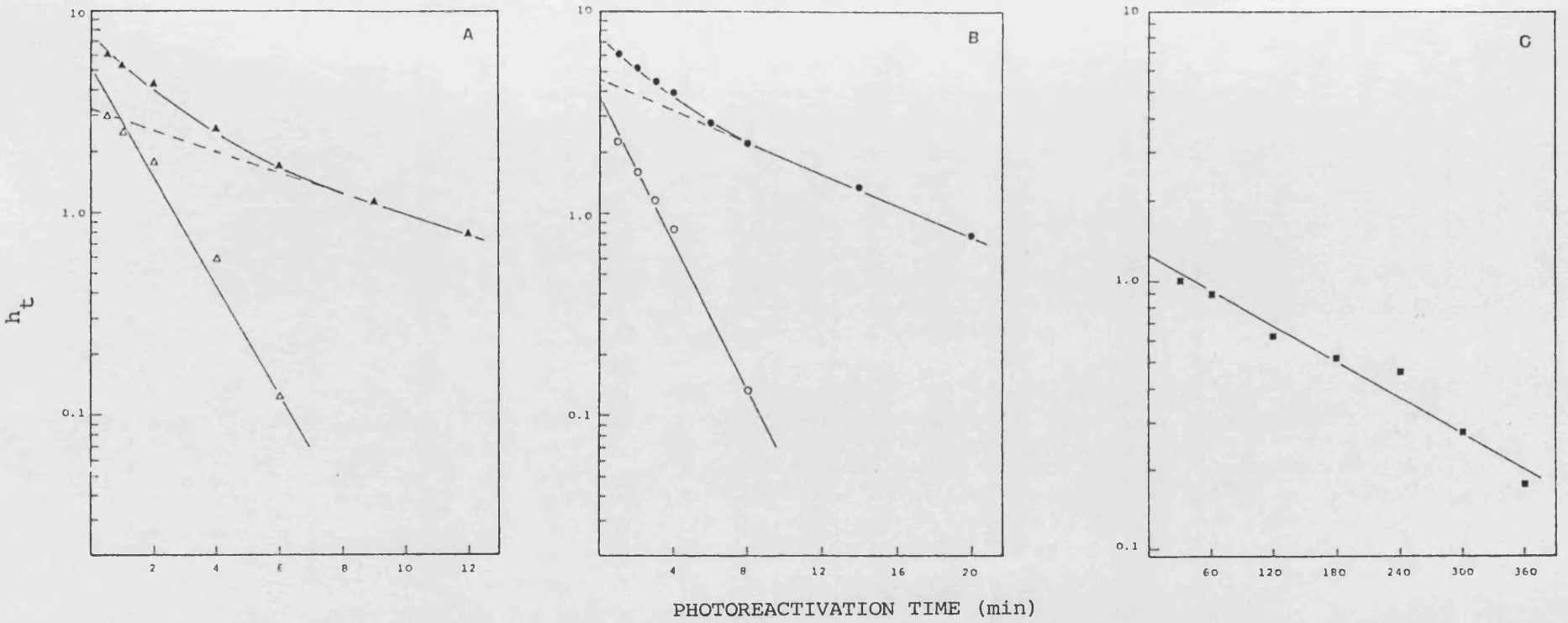

Fig. 3.23. Lethal hit analysis of the rate of photoreactivation at 25°C of anaerobically-grown, 254 nm UV inactivated AB2480 (Panel A), AS44 (Panel B) and DY326 (Panel C) (closed symbols) and after subtraction of the slow component (open symbols).

cent greater after anaerobic growth and so not significantly affected, whereas with AB2480 the rate constant was 30 per cent lower. The faster rate constant α_1 for AB2480 and AS44 were approximately 40 and 31 per cent lower, respectively. Indeed, the rate constant α_1 for AB2480 after anaerobic growth approached that of AS44 after aerobic growth. Taken together, these data suggest the disproportionate decrease in the rate of photoreactivation between AB2480 and AS44 is attributable to a greater effect on the slower rate constant α_2. This is reflected in the rate constant for DY326, which was approximately 12 per cent of the aerobic value.

Table 3.9 Photoreactivation rate analysis of 254 nm UV irradiated AB2480, AS44 and DY326 at 25°C after either aerobic or anaerobic growth at 37°C (Not measurable with AS46).

Strain	Growth Conditions	$\alpha_1(min^{-1})$	$\alpha_2(min^{-1})$
AB2480	Anaerobic	-0.616 ± 0.076	-0.115 ± 0.020
	Aerobic	-1.036 ± 0.118	-0.167 ± 0.036
AS44	Anaerobic	-0.43 ± 0.052	-0.082 ± 0.018
	Aerobic	-0.619 ± 0.021	-0.0787 ± 0.0096
DY326	Anaerobic	-	-0.005 ± 0.001
	Aerobic	-	-0.0401 ± 0.0045

These data could be taken as indicative of the presence of an

allosteric effector in AB2480 (and DY326), which in some way increases the repair constant α_2, but which is itself partially or completely repressed under anaerobic growth conditions. Whilst it is an attractive argument to attribute this allosteric effector to the proposed phrA locus in the gal- attλ interval, it could be argued that absence of a gene from the gal - chlA deletion of AS44 causes the strain to be partially respiratory-deficient, even under aerobic growth conditions. Within this region is the hemF locus, coding for an enzyme which catalyses the conversion of coproporphyrinogen III to protoprophyrin IX. Cox and Charles (1973) have isolated a hemF mutant, and demonstrated coproporphyrinogen accumulation, haem-deficiency and respiratory-deficiency. However, this was isolated as a secondary mutant of a strain which accumulated protoporphyrin IX. Neither the colony morphologies nor catalase activities of AB2480 and AS44 indicated that the latter was haem- or respiratory-deficient (data not shown). Recent work by Sancar et al. (1987b) has indicated that the redox state of the cell could be an important determinant of PRE activity. Using the cloned phrB gene product in vitro, these workers found that the quantum yield for photoreactivation only approached the in vivo value (approximately 1.0) when the enzyme was fully reduced with dithionite under anaerobic conditions; indicating that the enzyme contains a fully reduced flavin chromophore in vivo and not the partially oxidized flavin obtained as a result of the purification process. This could be interpreted to mean that E. coli grown under anaerobic conditions should possess higher photolyase activity than aerobically-grown cells, but it must be remembered that the irradiation and photoreactivation experiments reported in this work were carried out under aerobic conditions. A more

plausible explanation for the decrease in PRE activity of anaerobically-grown cells could be the "diversion" of FAD chromophore from the PRE molecule to components of the respiratory and electron transport chains (reviewed by Ingledew and Poole, 1984), such as lactate dehydrogenase and L-glycerol-3-phosphate dehydrogenase. Since lactate is a major product of the bacterial fermentation of glucose, the conversion of lactate to pyruvate, catalysed by NAD^+- independent lactate dehydrogenases (with the resultant coupling of lactate oxidation to energy transduction) is very significant during anaerobic growth. Sancar and Sancar (1984) used the membrane binding assay to determine the ratio of chromophore (a blue neutral flavin adenine dinucleotide radical) to apoenzyme, and found it to be 0.69, even though the apoenzyme had been amplified 15,000-fold. This suggested the chromophore was present in great abundance (or was induced by high levels of PRE apoenzyme). Therefore, it would be of interest to determine if anaerobic growth altered the production of apoenzyme, the ratio of apoenzyme to chromophore, or both.

3.6.2. Effect of Pre-Irradiation Growth Temperature

Fukui and Laskowski (1984a) studied the effect of pre-irradiation growth temperature on PRE activity in *S. cerevisiae*. They found that the number of PRE molecules (estimated by the fluence decrement method) after growth at 37°C was just 13 per cent of the value after growth at 23°C, even though the cellular protein concentration was the same. This suggested the existence of both active and inactive species of PRE molecules (see Introduction, Secion 2.6.1.1). It was thought that a similar investigation using *E. coli* would be of interest because there are no published

accounts of such a study, and it may also provide an explanation for the function of the proposed phrA gene.

3.6.2.1 254 nm UV Inactivation and Flash Photolysis

Cell suspensions of 24 hour stationary-phase cultures grown at 26°C were prepared in the usual manner, and 254 nm UV-irradiated and flash photoreactivated at 25°C as described in Section 3.2.1. Survival curves for the four strains after 254 nm UV-irradiation and one flash of photoreactivating light are shown in Figs. 3.24 and 3.25. The survival parameters from replicate experiments are included in Table 3.10. The data pertaining to these parameters are included in Tables A4.31-34. An analysis of covariance indicated there was no significant difference in intercept or slope location of these 254 nm UV-irradiated strains after growth at either 26° and 37°C. The changes in F-ratio for slope location of AS44, DY326 and AS46 were 2.8607 (1,232 d.f.), 1.069 (1,233 d.f.) and 0.068 (1,234 d.f.), respectively. The probability for the changes in F-ratio are 0.0952, 0.3057 and 0.8106, indicating no significant difference at the 5 per cent ($p>0.05$) confidence interval. The fluence decrements resulting from a single flash for A2480 and AS44 were 0.24 ± 0.046 and 0.172 ± 0.031, respectively. The calculated values for the average number of PRE molecules per cell based on these fluence decrements were 12.72 ± 2.44 and 9.12 ± 1.64, respectively. No fluence decrement was measurable with either DY326 or AS46. These data clearly indicate that decreasing the growth temperature results in an increase in the number of photolyase molecules, or, assuming the hypothesis of a pool of active and inactive molecules, an increase in the number of active PRE molecules.

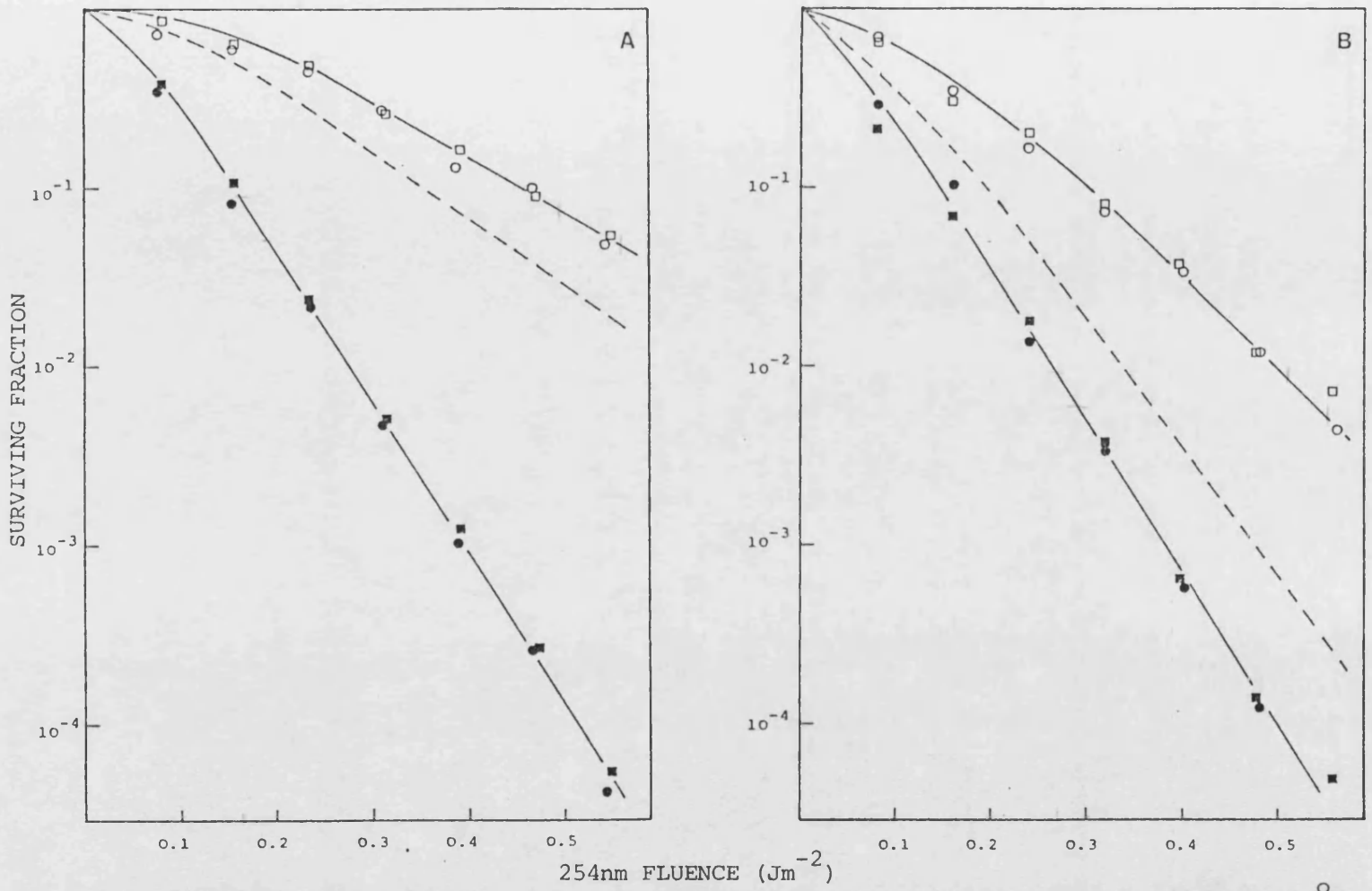

Fig. 3.24. Replicate survival curves for AB2480 (Panel A) and AS44 (Panel B) grown at 26°C after 254 nm UV (closed symbols) and a single light flash (open symbols) (- - - 37°C flash).

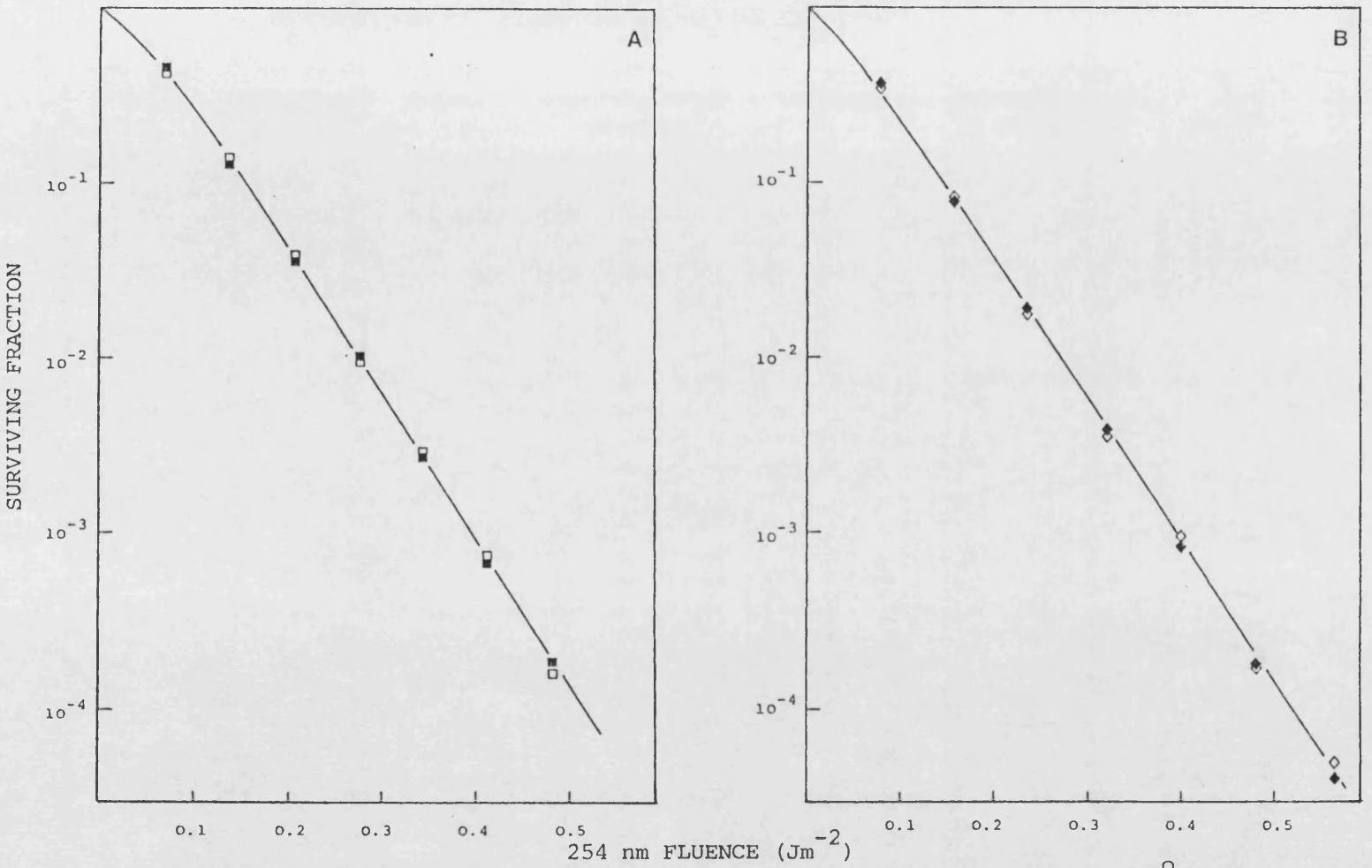

Fig. 3.25. Survival curves for DY326 (Panel A) and AS46 (Panel B) grown at 26°C after 254 nm UV (closed symbols) and a single light flash (open symbols).

Table 3.10 SURVIVAL PARAMETERS FOR AB2480, AS44, DY326 AND AS46 GROWN AT 26°C AFTER 254 nm UV INACTIVATION AND FLASH PHOTOLYSIS AT 25°C

STRAIN	EXPERIMENT NUMBER	SLOPE (log 10)	STANDARD ERROR OF SLOPE	INTERCEPT	STANDARD ERROR OF INTERCEPT	'k' $(Jm^{-2})^{-1}$	'n'
AB2480 (phr+)	254 nm 31a	-7.9683	0.0611	0.307	0.0238	18.347	2.00
	254 nm 31b	-8.200	0.1313	0.279	0.0561	18.888	1.90
	254 nm 31c	-8.477	0.1508	0.286	0.0563	19.519	1.934
	TOTAL	-8.2933	0.1151	0.291	0.0436	19.096	1.956
	FLASH 31a	-3.0406	0.064	0.394	0.0261	7.00	2.48
	31b	-3.0667	0.238	0.370	0.0962	7.06	2.35
	TOTAL	-3.054	0.018	0.382	0.0170	7.032	2.41
AS44 (phrA)	254 nm 32a	-8.3823	0.230	0.230	0.054	19.30	1.70
	254 nm 32b	-8.3124	0.1737	0.194	0.062	19.14	1.56
	254 nm 32c	-8.3724	0.1892	0.208	0.073	19.28	1.62
	TOTAL	-8.3372	0.L336	0.220	0.049	19.20	1.66
	FLASH 32a	-4.8933	0.1735	0.436	0.072	11.267	2.73
	32b	-4.6493	0.2792	0.398	0.115	10.705	2.50
	TOTAL	-4.7713	0.1725	0.417	0.027	10.99	2.61

Table 3.10 (Continued)

STRAIN	EXPERIMENT NUMBER	SLOPE (log 10)	STANDARD ERROR OF SLOPE	INTERCEPT	STANDARD ERROR OF INTERCEPT	'k' $(Jm^{-2})^{-1}$	'n'
DY326 (*phrB*)	254 nm 33a	-8.0461	0.084	0.200	0.032	18.53	1.60
	254 nm 33b	-8.3538	0.059	0.283	0.019	19.23	1.92
	254 nm 33c	-7.9336	0.218	0.152	0.085	18.27	1.42
	TOTAL	-8.111	0.217	0.212	0.066	18.68	1.63
	FLASH 33a	-7.9561	0.137	0.219	0.063	18.32	1.66
	33b	-8.1627	0.093	0.231	0.027	18.79	1.70
AS46 (*phrA*,*phrB*)	254 nm 34a	-8.2191	0.164	0.213	0.064	18.93	1.63
	34b	-8.4291	0.043	0.272	0.017	19.41	1.87
	34c	-8.0743	0.058	0.163	0.021	18.59	1.46
	TOTAL	-8.2408	0.178	0.216	0.055	18.97	1.64
	FLASH 34a	-7.9686	0.192	0.178	0.069	18.35	1.50
	34b	-7.9746	0.153	0.188	0.055	18.36	1.54
	TOTAL	-7.9716	0.004	0.183	0.007	18.36	1.524

3.6.2.2. Photoreactivation with Continuous Illumination

Cells suspensions for 254 nm UV inactivation and photoreactivation were prepared in the usual manner, and reduced to approximately 1×10^{-4} surviving fraction with an appropriate fluence of 254 nm UV radiation. After 20 minutes at 25°C, a single flash was given at the same instant as commencement of continuous photoreactivating light. The fluence rate used was 17 Wm^{-2}, above saturating irradiance conditions. The photoreactivation data for the four strains grown at 30° and 26°C are shown in Figs. 3.26 to 3.28. The (1-P) analyses are shown in Fig. 3.29 and the initial rates of photoreactivation and estimates of the number of PRE molecules per cell are included in Table 3.11. As in previous analyses, the (1-P) values for AB2480 and AS44 have been corrected to eliminate the lesions repaired by the single flash of photoreactivating light. Particularly after growth at 26°C, there was considerable variation in the flash response despite careful control of the culture and experimental conditions. The mean (1-P) values from a single flash for AB2480 and AS44 were 0.50 $\pm$ 0.18 and 0.67 $\pm$ 0.113, respectively, from four replicate experiments.

These data have also been analysed by the 'lethal hit' method developed by Johnson and Haynes (1986a) and are shown in this form in Figs. 3.30-3.33. The data pertaining to these figures are included in Tables A4.35-41. The calculated repair probabilities α_1 and α_2, are included in Table 3.12. It will be seen from Table 3.12 that alteration of the growth temperature produced a diverse set of effects depending on the strain. To summarise the principle effects, the faster rate constant α_1 was not observed with AB2480 grown at 26°, however, the slower rate constant α_2 was

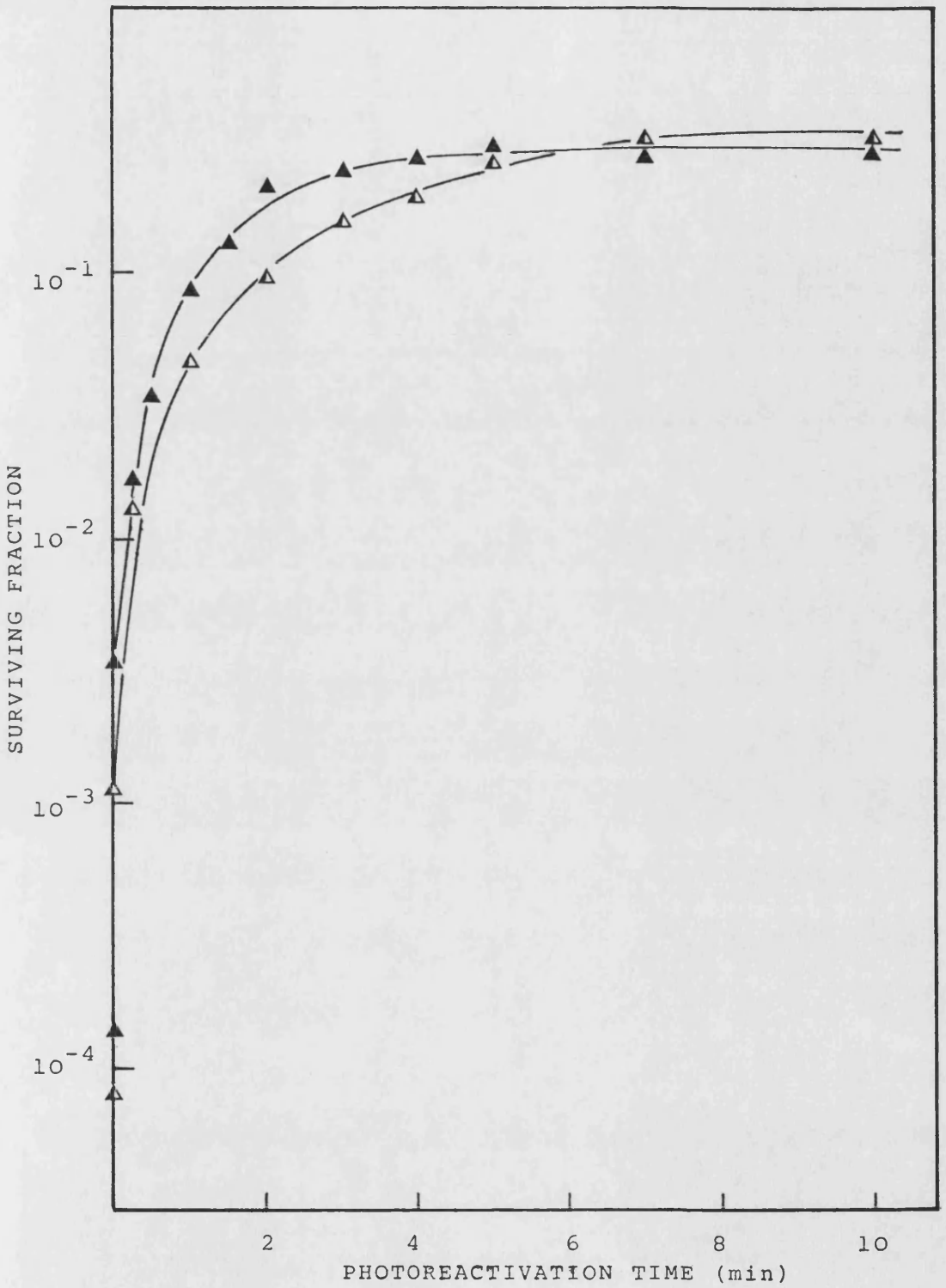

Fig. 3.26. Photoreactivation at 25°C of 254 nm inactivated AB2480 grown at 26° (▲) and 30°C (▲). (Fluence rate 17.6 Wm^{-2})

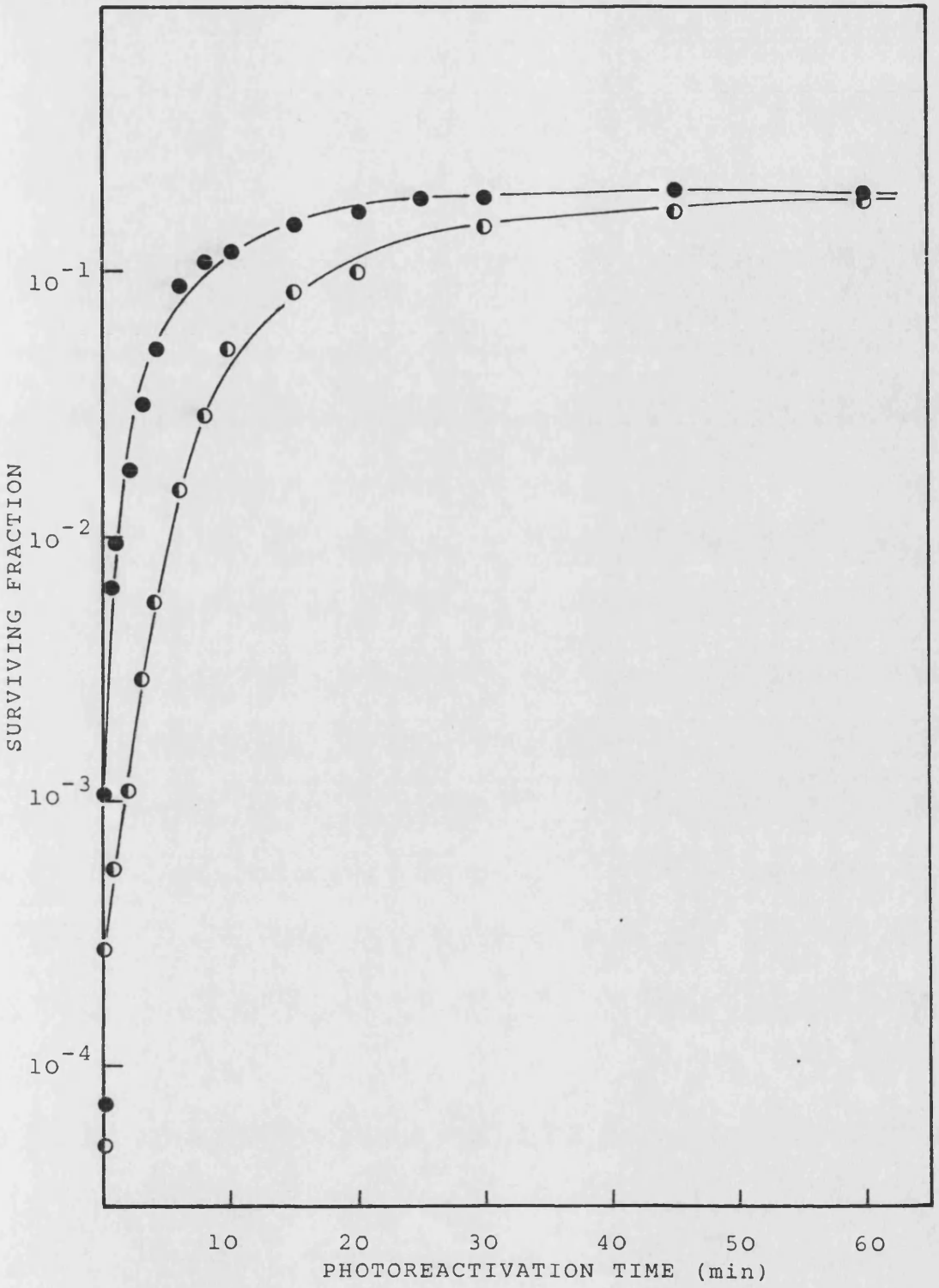

Fig. 3.27. Photoreactivation at 25°C of 254 nm inactivated AS44 grown at 26° (●) and 30°C (◐). (Fluence rate 17.6Wm^{-2})

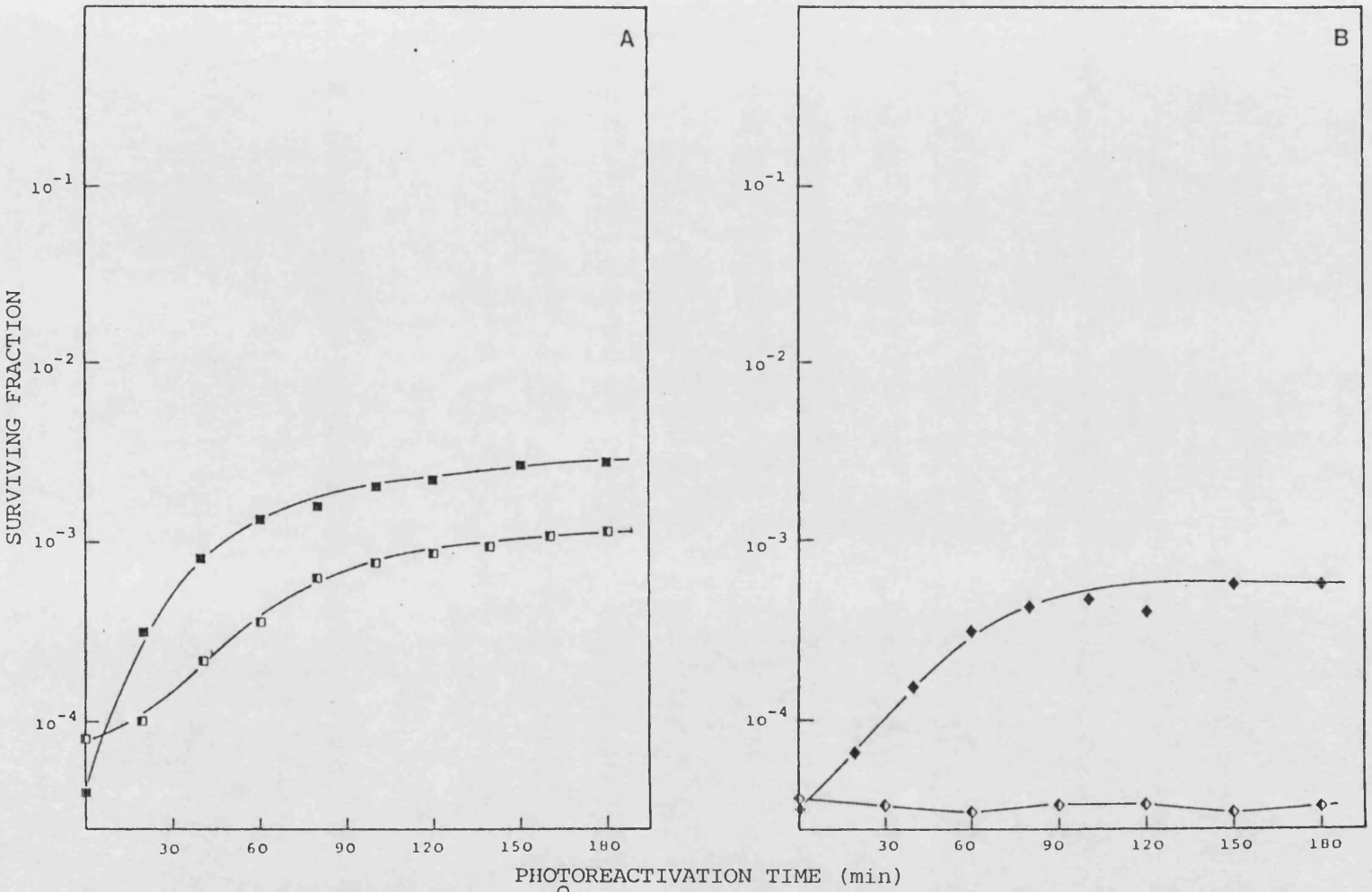

Fig. 3.28. Photoreactivation at 25°C of 254 nm inactivated DY326 (Panel A) and AS46 (Panel B) grown at 26° (■◆) and 30°C (◧◆). (Fluence rate 17.7 Wm^{-2})

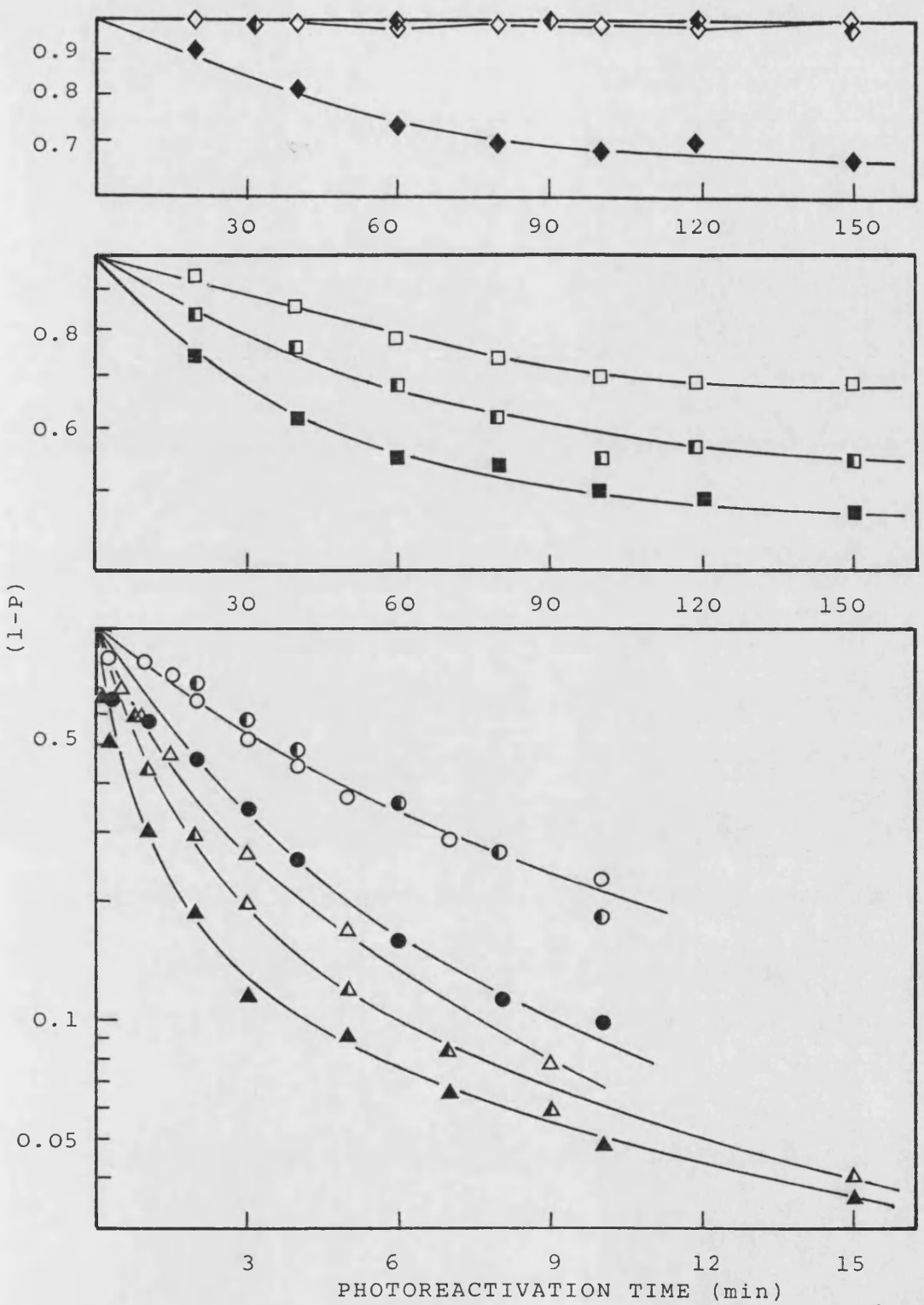

Fig. 3.29. 1-P analysis of the photoreactivation rate at 25°C of 254 nm inactivated AB2480 (▲,◮,△), AS44 (●,◐,○), DY326 (■,◧,□) and AS46 (◆,◈,◇) grown at 26° (▲,●,■,◆), 30° (◮,◐,◧,◈) and 37°C (△,○,□,◇)

Table 3.11 Comparison of the mean initial rates of photo-reactivation and estimates of the number of PRE molecules per cell at 25°C as a function of the growth temperature.

Strain	Growth Temperature(°C)	Rate ($\times 10^{-3}$)(s^{-1})	Number of PRE molecules per cell
AB2480	26	22.44	12.47
	30	13.60	7.56
	37	11.50	6.39
AS44	26	5.61	3.12
	30	2.85	1.58
	37	3.50	1.94
DY326	26	0.459	0.255
	30	0.114	0.063
	37	0.062	0.034
AS46	26	0.087	0.048
	30	-	-
	37	-	-

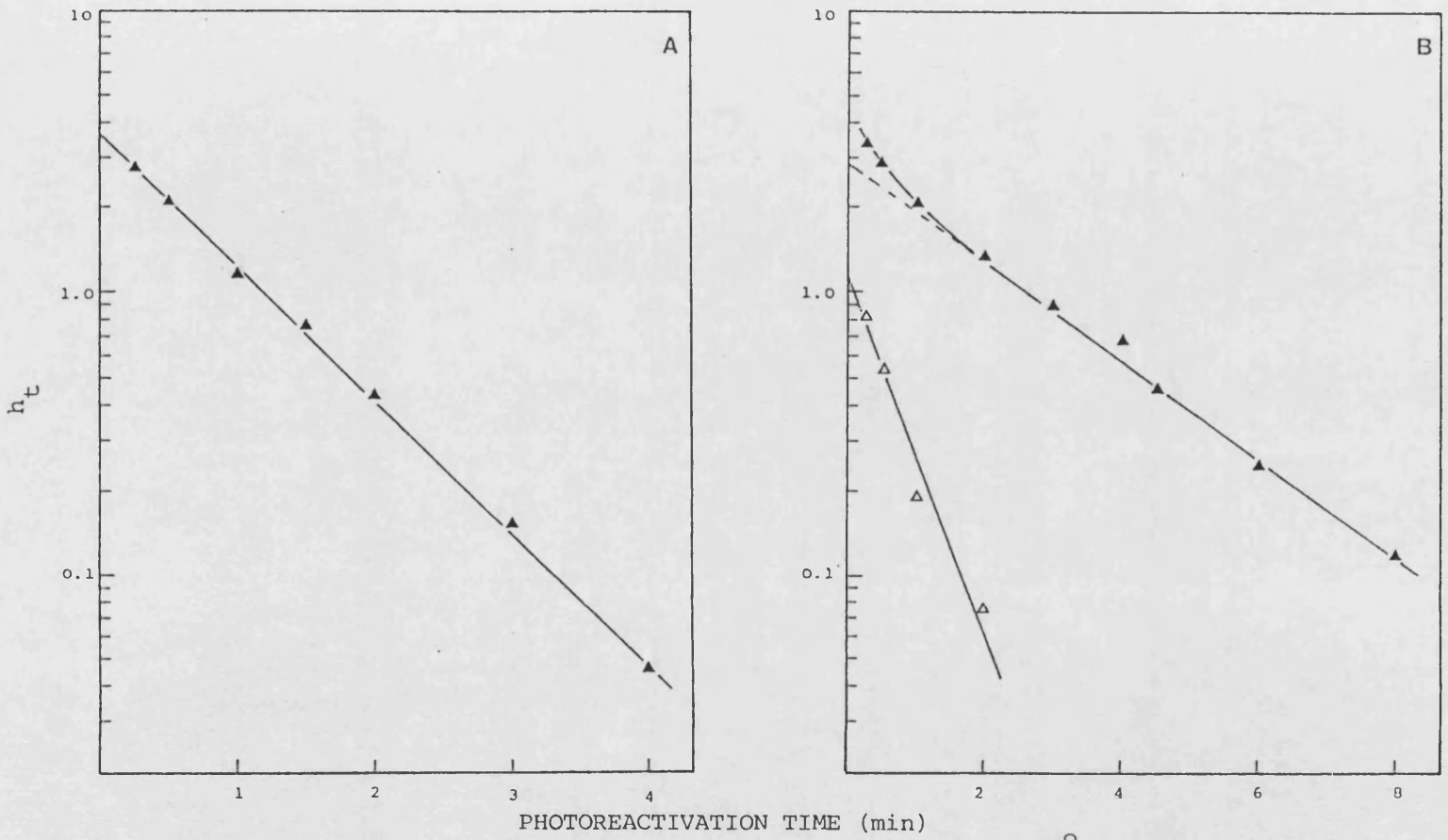

Fig. 3.30. Lethal hit analysis of the photoreactivation rate at 25°C of 254 nm inactivated AB2480 grown at 26° (Panel A) and 30°C (Panel B) (closed symbols) and after subtraction of the slow component (open symbols).

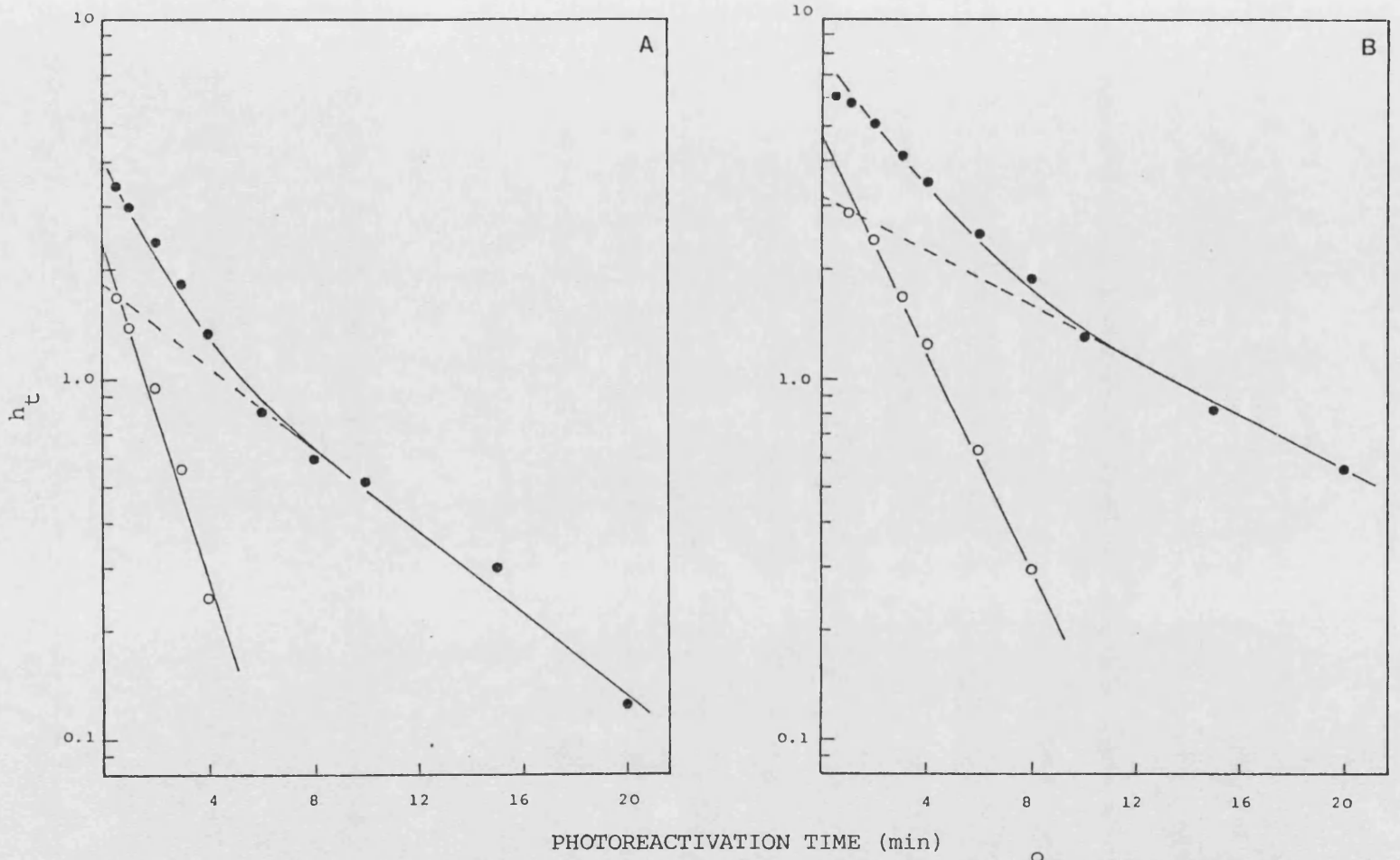

Fig. 3.31. Lethal hit analysis of the photoreactivation rate at 25°C of 254 nm inactivated AS44 grown at 26° (Panel A) and 30°C (Panel B) (closed symbols) and after subtraction of the slow component (open symbols)

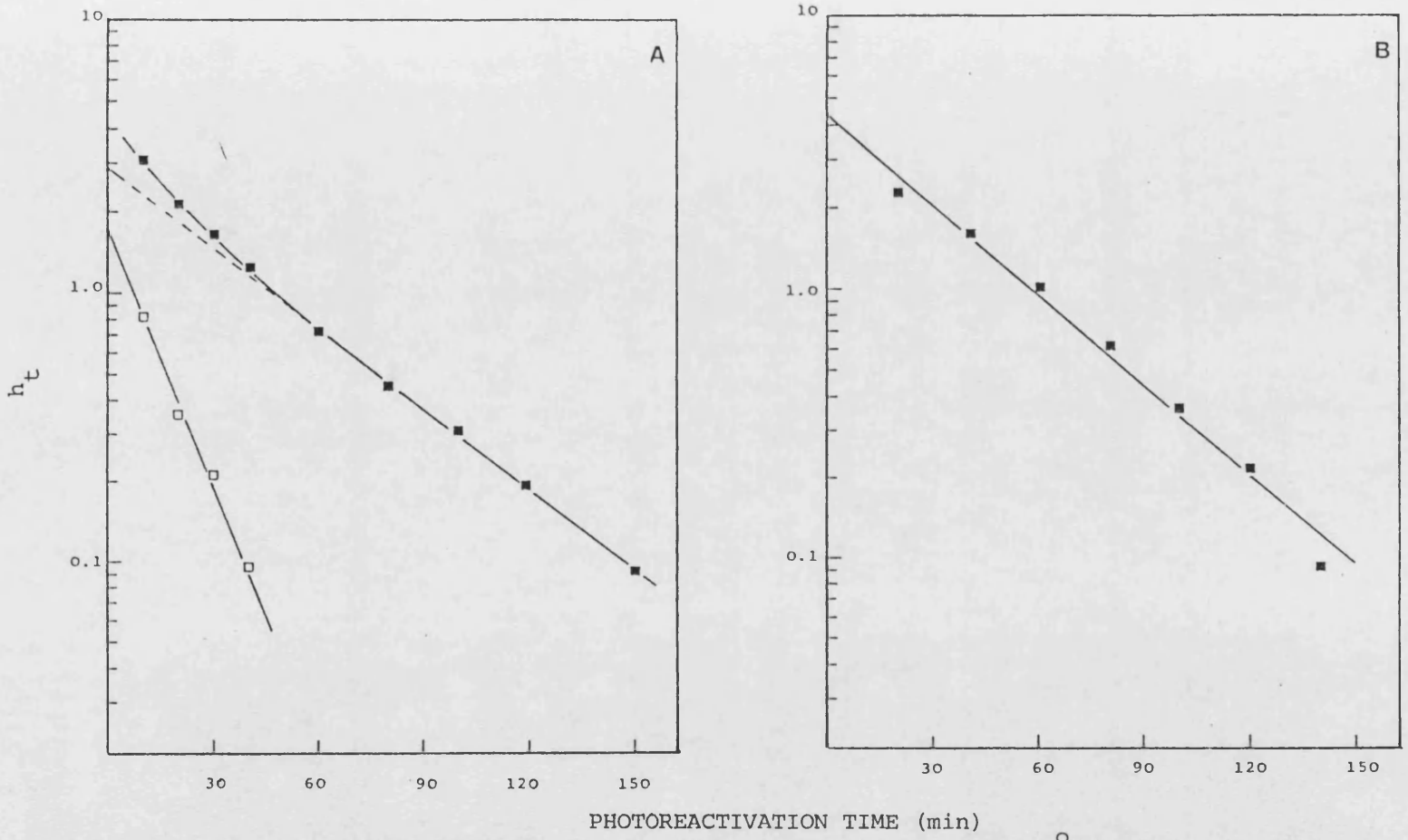

Fig. 3.32. Lethal hit ananlysis of the photoreactivation rate at 25°C of 254 nm inactivated DY326 grown at 26° (Panel A) and 30°C (Panel B) (closed symbols) and after subtraction of the slow component (open symbols).

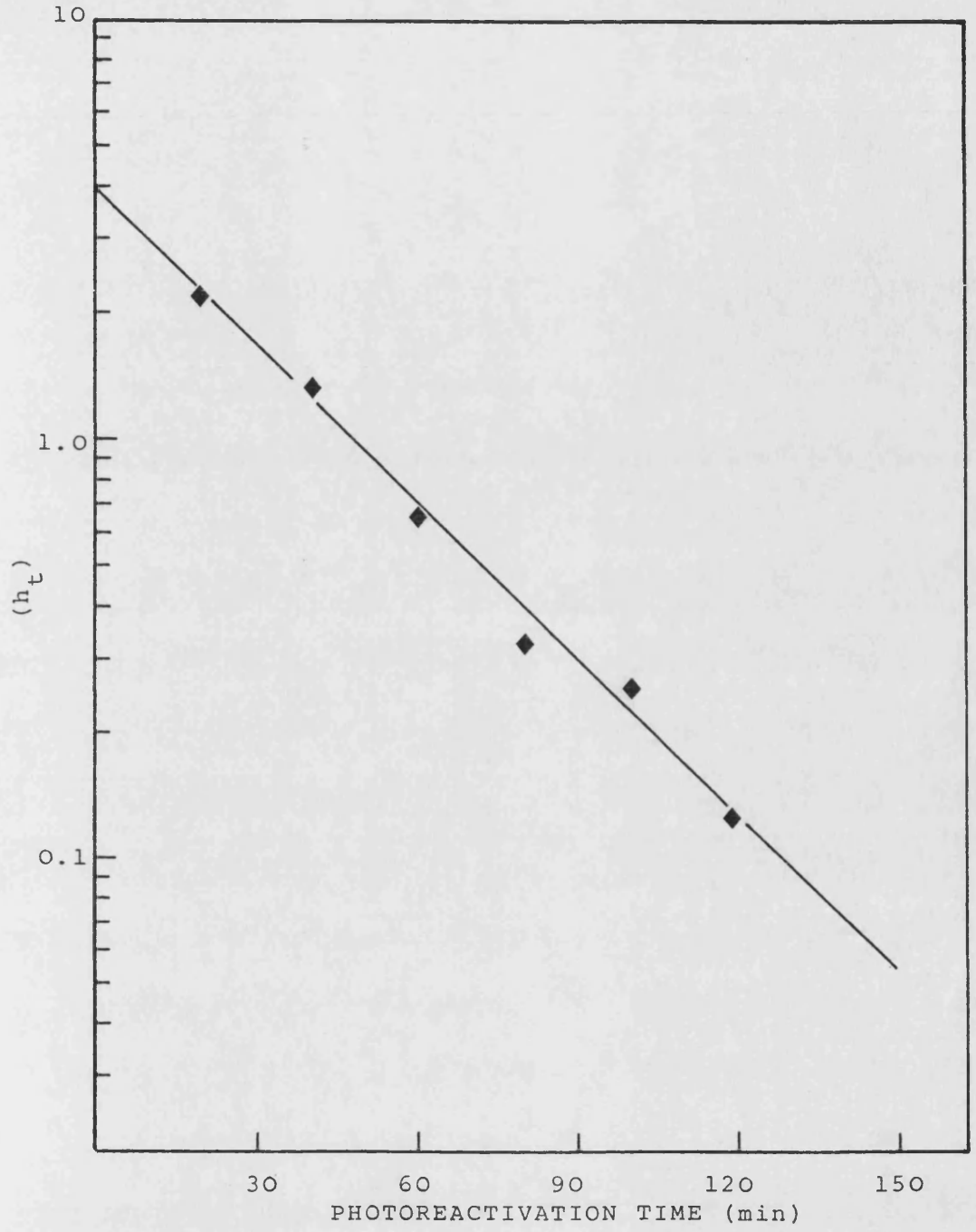

Fig. 3.33. Lethal hit analysis of the photoreactivation rate at 25°C of AS46 grown at 26°C after 254 nm inactivation.

Table 3.12 Photoreactivation rate analysis of 254 nm UV irradiated AB2480, AS44, DY326 and AS46 at 25°C after growth at 26°, 30° AND 37°C (from Table 3.5/6)

STRAIN	GROWTH TEMP	EXPT. No.	$\alpha_1(min)^{-1}$	$\alpha_2(min)^{-1}$
AB2480	26°	35a	-	-1.054
		35b	-	-1.113
	MEAN		-	-1.0835 ± 0.042
	30°	36a	-1.48	-0.392
		36b	-2.31	-0.388
	MEAN		-1.89 ± 0.58	-0.39 ± 0.028
	37°	MEAN	-1.036 ± 0.118	-0.167 ± 0.036
AS44	26°	37a	-0.534	-0.1327
		37b	-0.733	-0.142
		MEAN	-0.633 ± 0.141	-0.1373 ± 0.006
	30°	38a	-0.0354	-0.0858
		38b	-0.380	-0.1080
		MEAN	-0.367 ± 0.018	-0967 ± 0.016
	37°	MEAN	-0.613 ± 0.021	-0.080 ± 0.0096
DY326	26°	39a	-0.080	-0.022
		39b	-0.058	-0.0197
		39c	-0.074	-0.0260
		MEAN	-0.0707 ± 0.01	-0.0225 ± 0.003
	30°	40a	-	-0.051
		40b	-	-0.043
		MEAN	-	-0.047 ± 0.06
	37°C	MEAN	-	-0.040 ± 0.0045
AS46	26°	41a	-	-0.028
		41b	-	-0.031
		MEAN	-	-0.0295 ± 0.002
	30°		-	-
	37°		-	-

approximately 6.5-fold greater. However, after growth at 30°C, α_1 showed a 2-fold increase compared with 37°C growth. With strain AS44, after growth at 26°C there was no significant increase in α_1 but, α_2 was 1.4-fold greater compared with growth at 37°C. However, after growth at 30°C, where there was a slight decrease in the overall rate of repair, the rate constant α_1 was reduced to 60 per cent of the value obtained with 37°C growth, whilst the slower rate constant α_2 was approximately 20 per cent greater.

After growth at 26°C, DY326 exhibited biphasic repair kinetics which were not observed after growth at either 30° or 37°C. However, the slower rate constant α_2 was only 56 per cent of the value for cells grown at 37°C. The increase in the rate of repair observed after growth at 30°C was reflected in a 17 per cent increase in α_2. Of particular significance to this work was the appearance of a photoreactivable response with 254 nm UV-irradiated AS46 after growth at 26°C. Being a strain which is deleted at the proposed phrA locus and mutated at the phrB locus this raises the question as to whether there is a third phr locus in E. coli, or whether one of the 'known' loci and/or gene product(s) is temperature-dependent. As discussed earlier, there was no kinetic evidence in favour of the existence of either a third PRE molecule or one or two molecules having three repair activities in AB2480 and AS44.

A more plausible situation is one in which it must be recognised that either the mutant phrB gene product does retain some residual photoreactivating activity, as seen in DY326, (or there is a second photoactive protein from a third phr locus), which is not expressed in the phrA mutant background, or reduced to an undetectable level after growth at 37°C (Fig. 3.10). However,

as the growth temperature is decreased, the activity of the mutant phrB enzyme increases to such an extent that it can be detected even in the phrA mutant background. It could be argued that the photolyase molecules in phrB$^+$ and phrB strains exist in active and inactive forms, in equilibrium with each other, and that the function of the proposed phrA gene product is to displace the equilibrium in favour of the active form. Thus it could be seen as being purely fortuitous that in AS46 the equilibrium was displaced sufficiently in the reverse direction in favour of the mutant 'inactive' form, such that there was no phenotypic expression of photoenzymatic repair after growth at 37^{o}C. Whilst this model might go some way towards explaining the relationship between the photoreactivable responses of the four strains at any one growth temperature, it does assume that either the active form of the phrB$^+$ gene product has two repair capacities with different rate constants, whereas the mutant phrB gene product has only one repair activity, or there is a second photoactive protein from a third locus. One general trend arising from this growth temperature study was an increased effect on the slower rate constant α_2 with decreasing temperature, with the effect that the faster component was reduced in importance relative to the remaining slow component. This effect was similar to the conclusions reached by Johnson and Haynes (1986b) with a sensitive haploid strain of S. cerevisiae.

The finding that the photoreactivable responses of strains AS44 and AS46 were not significantly affected by growth at 30^{o} compared with growth at 37^{o}C, whereas there was difference in the PR response when grown at 26^{o}C, suggests that the postulated interactive effect of the proposed phrA gene product is temperature-dependent.

The demonstration of PR in AS46 suggests that the phrA locus does not code for a photolyase molecule, but that it may function to control the activity of the $phrB^+$ gene product and possibly a second photolyase molecule from an unknown locus, both of which appear to be temperature-dependent.

3.6.3. Effect of Pre-Illumination

There have been reports in the literature that pre-illumination of cells prior to irradiation can result in an increase in photoreactivating enzyme activity. Fukui and Laskowski (1984a) used the fluence-decrement method to show a 2.8-fold increase in the number of PRE molecules after growth in the light compared with growth in the dark in a sensitive haploid strain of S. cerevisiae. These workers also demonstrated an increase in the fluence decrement by pre-illuminating dark-grown cells with photo-reactivating light flashes prior to UV irradiation (Fukui and Laskowski, 1984b). There was an approximate 4-fold increase in cells in logarithmic growth compared with a 1.3-fold increase in stationary growth phase.

In an attempt to determine if these effects also occur in E. coli, cultures were grown and harvested in the dark, and the single flash and continuous photoreactivating light responses compared with cultures grown under continuous photoreactivating light. In addition, cultures grown and harvested in the dark were split into two aliquots, one of which was exposed to photoreactivating light for 20 minutes prior to irradiation whilst the other was maintained in the dark. In no case did any pre-illumination treatment affect either the rate or extent of photoenzymatic repair (data not

shown). Recently, Sancar et al. (1987b) have reported unpublished results that pre-illuminating the cloned phrB gene product in vitro under anaerobic conditions (and testing for activity immediately afterwards) results in a 5-fold increase in the quantum efficiency. Harm and Rupert (1976) have shown that PRE from yeast exhibits increased activity using the transforming DNA assay in vitro when it was pre-illuminated. The action spectrum for pre-illumination was similar to that for photoreactivation, however, light of wavelengths up to 546 nm was still effective. In addition, pre-illuminated enzyme was more stable to thermal inactivation.

3.7 Photoreactivation after Acetophenone-Sensitized 313 nm UV Irradiation

Having demonstrated that AB2480 and AS44 photoreactivate 254 nm UV-induced damage with biphasic kinetics, it was postulated that this may reflect different repair capacities towards the various dimer species, namely T-T, T-C and C-C. As discussed previously (see Introduction, Section 1.2.7), Lamola and Yamane (1967) demonstrated the efficient production of T-T dimers with 313 nm UV irradiation and acetophenone as a photosensitizer. They found the initial induction ratio of T-T:T-C:C-C to be approximately 1.0:0.01:0.005, respectively. This irradiation method was used to establish the photoreactivability of T-T dimers.

3.7.1. Acetophenone-Sensitized 313 nm UV Inactivation and Flash Photolysis

Cell suspensions of cultures grown at 37^{o}C were prepared in M9 salts solution with 0.1 per cent acetophenone. Dimethyl sulphoxide was added to 2 per cent v/v to ensure complete solubility of the

acetophenone at 0°C. Hodges et al. (1980) have shown that acetophenone at a concentration of 0.1 per cent v/v causes a high degree of sensitization. The cell suspension was transferred to the jacketed cuvette, and 5 minutes allowed to elapse for temperature equilibration to 0°C. Graded fluences of 313 nm UV radiation were given at a fluence rate in the range 1.0-2.0 Wm^{-2}, after which samples were taken to assay survival and flash recovery. For measurement of the high-intensity flash recovery, the cell samples were diluted 100-fold to reduce the possibility of any concomitant lethal effects. The survival curves and high intensity flash responses of the four strains are shown in Figs. 3.34-3.35, plotted against the corrected 313 nm fluence after application of the Morowitz factor (Morowitz, 1950). In calculating the correction factor it was assumed that there was efficient stirring of the bacterial suspension, in which case any one of the irradiated bacterial cells had an equal probability of being found in any one place in the cuvette. The correction factor was equal to the mean relative transmission of the suspension:

$$\text{Dose correction factor} = \int_0^1 10^{-Al}.dl$$

where A = absorbance

l = path length

$$= \frac{e^{-2.303.Al}}{2.303A}$$

$$= \frac{1 - e^{-2.303A}}{2.303}$$

The absorbance was obtained by placing the calibrated thermopile behind the irradiation cuvette and measuring the amount of radiation transmitted through a known concentration of acetophenone. The absorbance : concentration plot is shown in

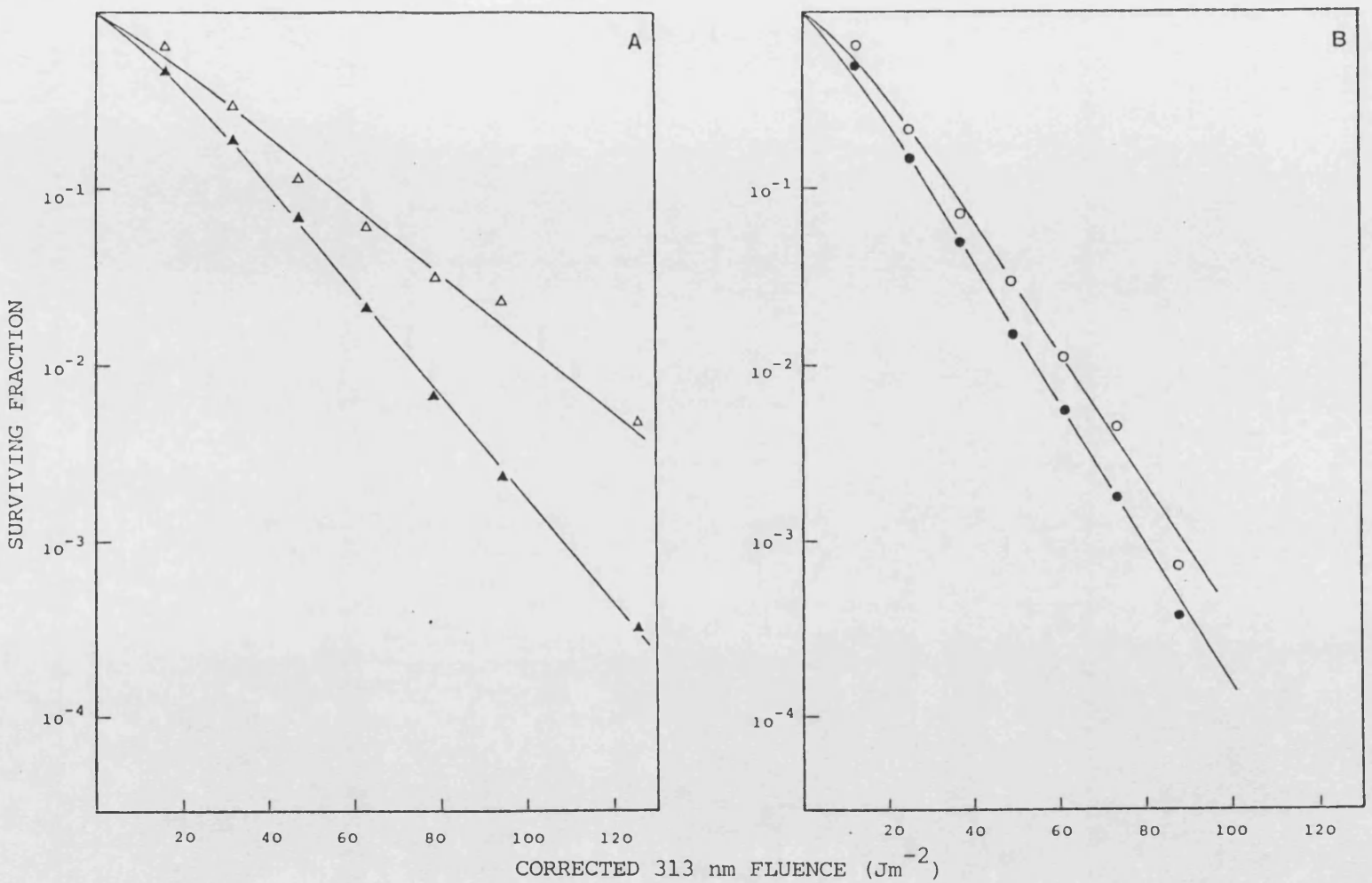

Fig. 3.34. Survival curves for AB2480 (Panel A) and AS44 (Panel B) after acetophenone-sensitised 313 nm UV (closed symbols) and a single light flash (open symbols).

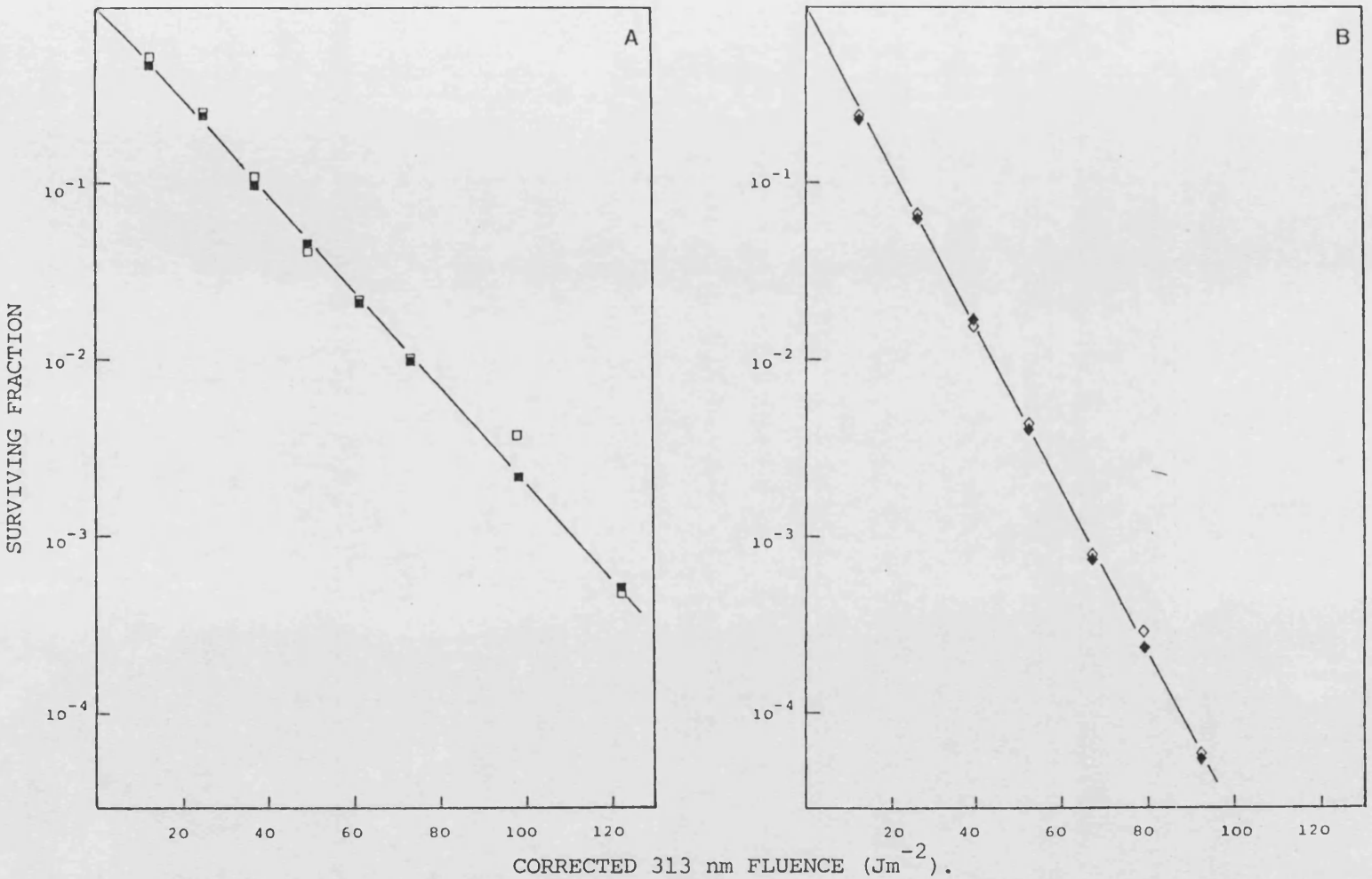

Fig. 3.35. Survival curves for DY326 (Panel A) and AS46 (Panel B) after acetophenone-sensitised 313 nm UV (closed symbols) and a single light flash (open symbols).

Appendix A3. The dose correction factor was calculated to be 0.6. The survival parameters from replicate experiments are shown in Table 3.13. The data pertaining to these parameters are included in Tables A4.42-45. These parameters have been compared by an analysis of covariance, measuring the change in F-ratio when the individual regression model for the pooled data for each strain was compared with the regression model for AB2480. The slope locations for AS44 and AS46 were significantly different giving changes in F-ratio of 102.82 and 53.5 with 1 and 83, and 1 and 85 degrees of freedom, respectively. The slope location for DY326 yielded a change in F-ratio of 0.503 with 1 and 84 degrees of freedom. The critical value on the F-distribution at the 5% confidence interval lies between 3.92 and 4.0, indicating that there was no significant difference in the inactivation coefficients between AB2480 and DY326 ($p>0.05$). A comparison of the slopes of AS44 and AS46 indicated that the slope of the latter was statistically significantly greater; the changes in F-ratio being 31.84 with 1 and 43 degrees of freedom. It would appear that there is an inherent difference in sensitivity between the strains which is not wholly attributable to their *phr* genotype. Strains AB2480 and DY326 are neither isogenic with each other nor with AS44 and AS46. However, AS44 and AS46 are isogenic with each other except for being *phrB*$^+$ and *phrB*, respectively. Thus it could be argued that the decrease in sensitivity of AS44 compared with AS46 could be due to concomitant photoreactivation during 313 nm irradiation. This does seem unlikely because the half-peak bandwidth at 313 nm was 7 nm and the Mylar-C filter cut off radiation below 310 nm, whilst the earlier investigation of the effect of wavelength of photo-reactivating light indicated no detectable photoreactivation below

Table 3.13 SURVIVAL PARAMETERS FOR ACETONPHENONE-SENSITIZED 313NM INACTIVATION AT 0°C FLASH PHOTOLYSIS AT 25°C FOR AB2480, AS44, DY326 AND AS46 GROWN AT 37°C

STRAIN	TREATMENT	EXPT. No.	SLOPE (log 10)	STANDARD ERROR OF SLOPE	INTERCEPT	STANDARD ERROR OF INTERCEPT	'k' $(Jm^{-2})^{-1}$	'n'
AB2480	313 nm + ACP	42a	-2.823×10^{-2}	4.954×10^{-4}	1.1964×10^{-1}	4.401×10^{-2}	6.5×10^{-2}	1.32
	313 nm + ACP	42b	-2.980×10^{-2}	4.56×10^{-3}	2.44×10^{-1}	3.68×10^{-2}	6.86×10^{-2}	1.75
	313 nm + ACP	42c	-2.86×10^{-4}	4.18×10^{-4}	1.326×10^{-2}	2.79×10^{-2}	6.58×10^{-2}	1.36
	313 nm + ACP	42d	-2.73×10^{-2}	1.43×10^{-3}	4.76×10^{-2}	1.267×10^{-2}	6.28×10^{-2}	1.16
	TOTAL		-2.81×10^{-2}	3.36×10^{-4}	1.09×10^{-1}	2.74×10^{-2}	6.47×10^{-2}	1.29
	FLASH	42a	-1.785×10^{-2}	1.11×10^{-3}	1.05×10^{-2}	4.11×10^{-2}	4.11×10^{-2}	1.17
	FLASH	42b	-1.812×10^{-2}	2.36×10^{-3}	7.21×10^{-2}	9.28×10^{-3}	4.17×10^{-2}	1.18
	TOTAL		-1.798×10^{-2}	1.91×10^{-4}	7.03×10^{-2}	2.51×10^{-3}	4.14×10^{-2}	1.176
AS44	313 nm + ACP	43a	-3.833×10^{-2}	1.68×10^{-3}	3.44×10^{-1}	1.22×10^{-1}	8.83×10^{-2}	2.21
	313 nm + ACP	43b	-3.682×10^{-2}	2.90×10^{-4}	3.42×10^{-4}	2.03×10^{-2}	8.43×10^{-2}	2.20
	313 nm + ACP	43c	-3.440×10^{-3}	1.17×10^{-3}	3.47×10^{-1}	8.58×10^{-2}	7.92×10^{-2}	2.22
	313 nm + ACP	43d	-3.751×10^{-2}	1.04×10^{-3}	3.47×10^{-1}	6.80×10^{-2}	8.64×10^{-2}	2.22
	TOTAL		-3.676×10^{-2}	1.69×10^{-3}	3.45×10^{-1}	2.45×10^{-3}	8.46×10^{-2}	2.21
	FLASH	43a	-3.310×10^{-2}	1.511×10^{-3}	1.07×10^{-1}	1.01×10^{-2}	7.62×10^{-2}	1.23
	FLASH	43b	-3.392×10^{-2}	2.51×10^{-3}	1.11×10^{-1}	3.68×10^{-2}	7.81×10^{-2}	1.29
	TOTAL		-3.351×10^{-2}	5.8×10^{-4}	1.09×10^{-1}	2.83×10^{-3}	7.72×10^{-2}	1.28

Table 3.13 (Continued)

STRAIN	TREATMENT	EXPT. No.	SLOPE (log 10)	STANDARD ERROR OF SLOPE	INTERCEPT	STANDARD ERROR OF INTERCEPT	'k' $(Jm^{-2})^{-1}$	'n'
DY326	313 nm + ACP	44a	-2.901×10^{-2}	7.52×10^{-4}	2.152×10^{-1}	6.8×10^{-2}	6.68×10^{-2}	1.64
	313 nm + ACP	44b	-3.09×10^{-2}	1.77×10^{-3}	1.70×10^{-2}	7.12×10^{-3}	7.12×10^{-2}	1.71
	313 nm + ACP	44c	-2.92×10^{-4}	3.15×10^{-4}	9.37×10^{-3}	2.32×10^{-2}	6.72×10^{-2}	1.02
	313 nm + ACP	44d	-3.149×10^{-4}	9.05×10^{-2}	4.60×10^{-2}	7.25×10^{-2}	7.25×10^{-2}	1.23
	TOTAL		-3.015×10^{-3}	1.23×10^{-3}	1.37×10^{-1}	1.06×10^{-1}	6.94×10^{-2}	1.37
	FLASH	44a	-2.88×10^{-2}	6.38×10^{-4}	9.22×10^{-2}	2.86×10^{-2}	6.65×10^{-2}	1.24
	FLASH	44b	-2.91×10^{-2}	5.23×10^{-4}	1.08×10^{-1}	6.34×10^{-2}	6.70×10^{-2}	1.28
	TOTAL		-2.895×10^{-2}	2.12×10^{-4}	1.001×10^{-1}	1.11×10^{-2}	6.67×10^{-2}	1.26
AS46	313 nm + ACP	45a	-4.442×10^{-2}	2.01×10^{-3}	1.969×10^{-1}	1.12×10^{-1}	1.023×10^{-1}	1.57
	313 nm + ACP	45b	-4.75×10^{-2}	1.44×10^{-3}	2.95×10^{-2}	6.76×10^{-3}	1.09×10^{-1}	1.07
	313 nm + ACP	45c	-4.67×10^{-2}	5.24×10^{-4}	1.94×10^{-2}	3.48×10^{-3}	1.07×10^{-1}	1.05
	TOTAL		-4.603×10^{-2}	1.69×10^{-3}	1.08×10^{-1}	9.67×10^{-1}	1.06×10^{-1}	1.28
	FLASH	45a	-4.08×10^{-2}	1.01×10^{-3}	1.08×10^{-1}	5.14×10^{-2}	9.4×10^{-2}	1.28
	FLASH	45b	-4.31×10^{-2}	3.18×10^{-3}	9.52×10^{-2}	1.09×10^{-2}	9.92×10^{-2}	1.25
	TOTAL		-4.20×10^{-2}	1.63×10^{-3}	1.02×10^{-1}	9.05×10^{-3}	9.67×10^{-2}	1.26

350 nm (Section 3.5). The fluence decrements resulting from one flash of photoreactivating light for AB2480 and AS44 were 38.0 ± 2.8 and 10 ± 1.2 Jm^{-2}, respectively. There is no published value for the induction of thymine dimers per Jm^{-2} of 0.1 per cent acetophenone-sensitized 313 nm UV radiation, so a quantitative comparison of the numbers of PRE molecules per cell was not possible. However, it is possible to say that the number of PRE-substrate complexes was 3.8 fold greater with AB2480 compared with AS44. A similar comparison after 254 nm UV inactivation yielded a value of 3.3, indicating no significant variation in flash response between a mixed population of dimer substrates and one consisting largely of T-T dimers. No fluence-decrement was obtained with either DY326 or AS46.

3.7.2 Photoreactivation with Continuous Illumination

Cell suspensions containing 0.1 per cent acetophenone were reduced to approximately 1×10^{-4} surviving fraction with an appropriate fluence of 313 nm UV radiation. The suspension was then diluted 100-fold with M9 salts solution, held at 25°C for 20 minutes and then exposed to continuous photoreactivating light at a fluence rate of 17 Wm^{-2} for time periods between 30 seconds and 3 hours. A single high intensity flash was given at the start of each photoreactivating light treatment. Concomitantly run control experiments using non-irradiated cells exposed to the PR light and irradiated cells held in the dark did not show any increased lethality. Hodges et al. (1980) have shown that pre-irradiation of acetophenone does not significantly affect its ability to sensitize inactivation.

The photoreactivation plots are shown in Fig. 3.36 and the

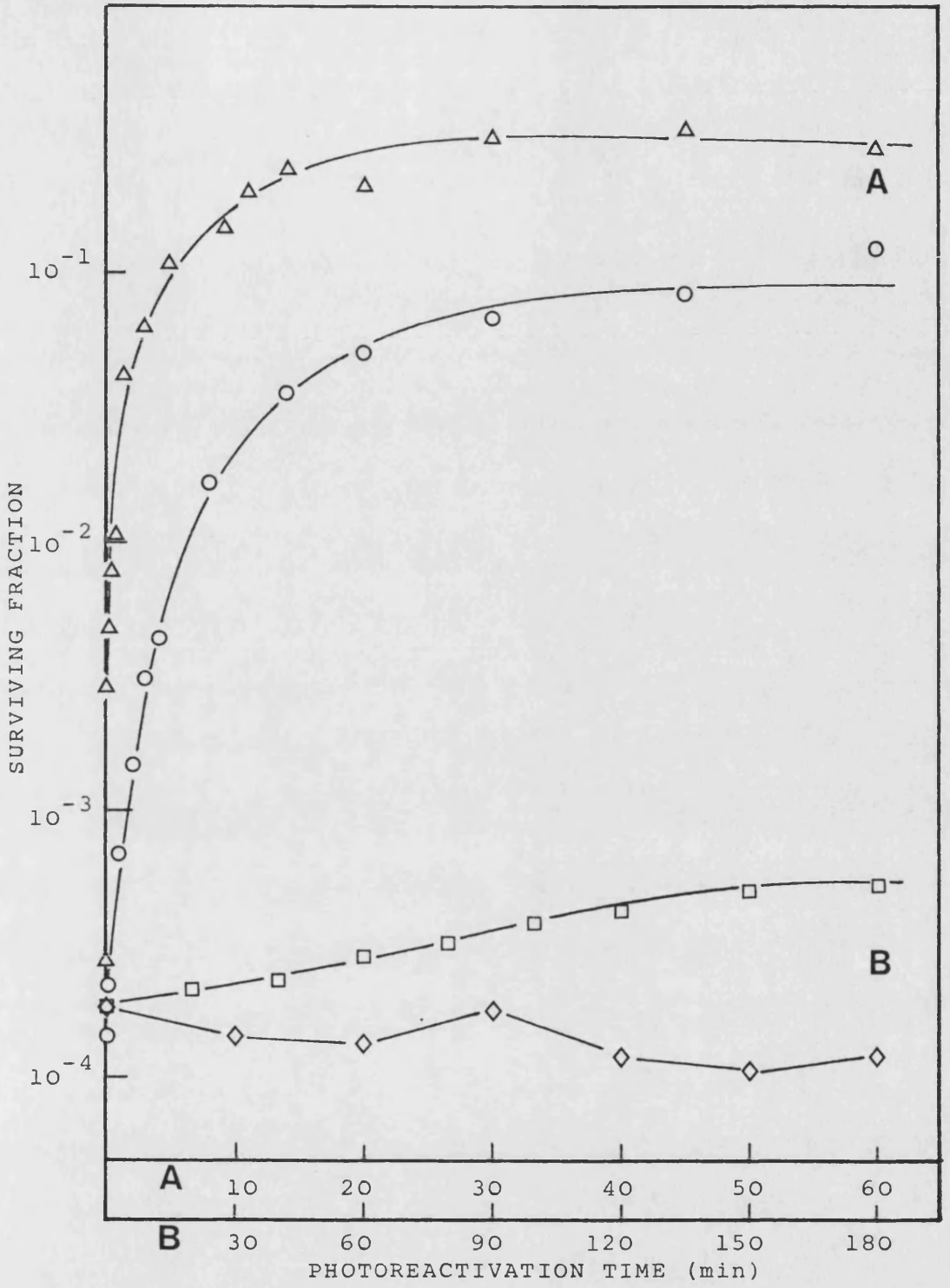

Fig. 3.36. Photoreactivation at 25°C of acetophenone-sensitised 313 nm inactivated AB2480 (△), AS44 (○), DY326 (□) and AS46 (◇). (Fluence rate 17.6 Wm^{-2})

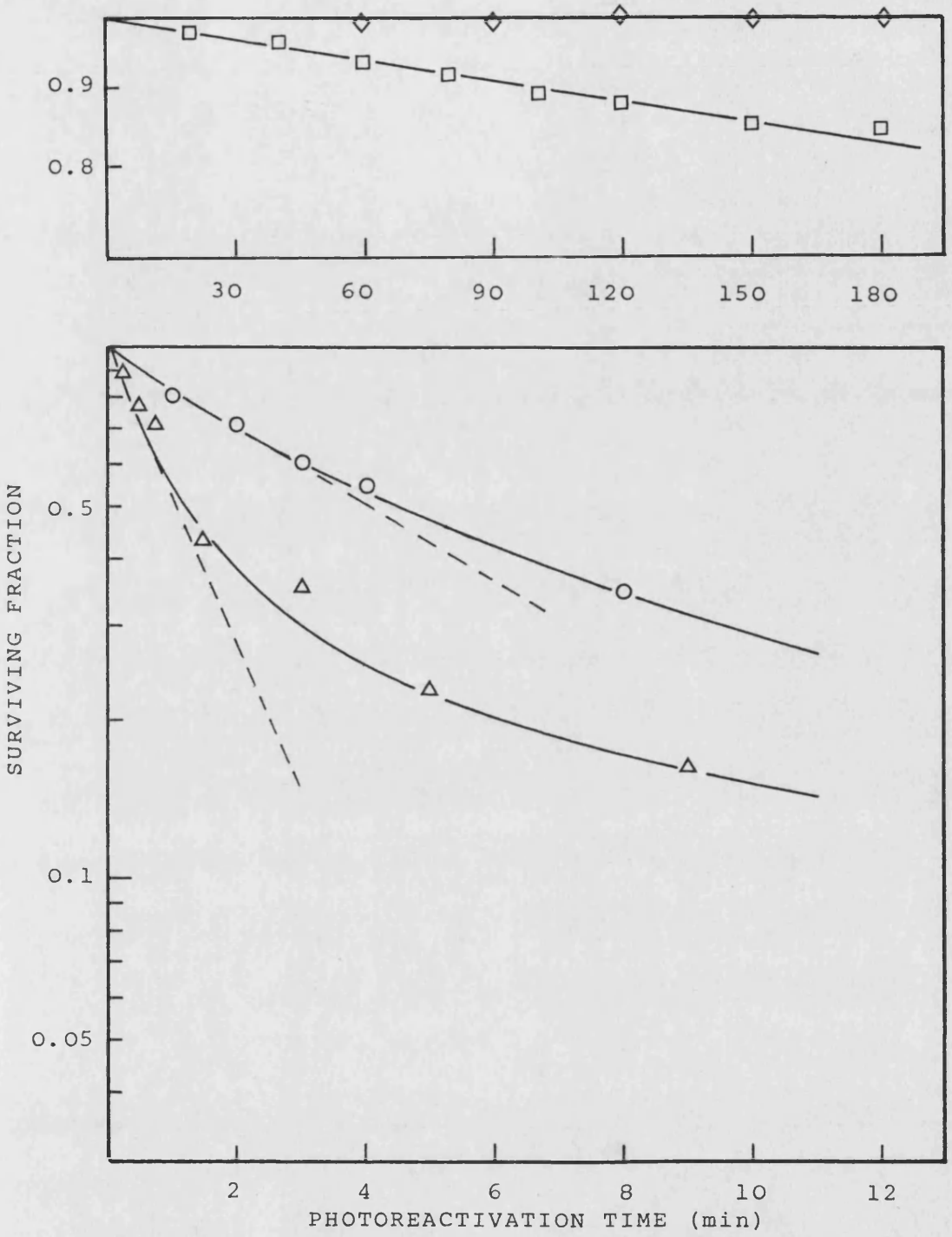

Fig. 3.37. 1-P analysis of the photoreactivation rate at 25°C of acetophenone-sensitised, 313 nm inactivated AB2480 (△), AS44 (○), DY326 (□) and AS46 (◇).

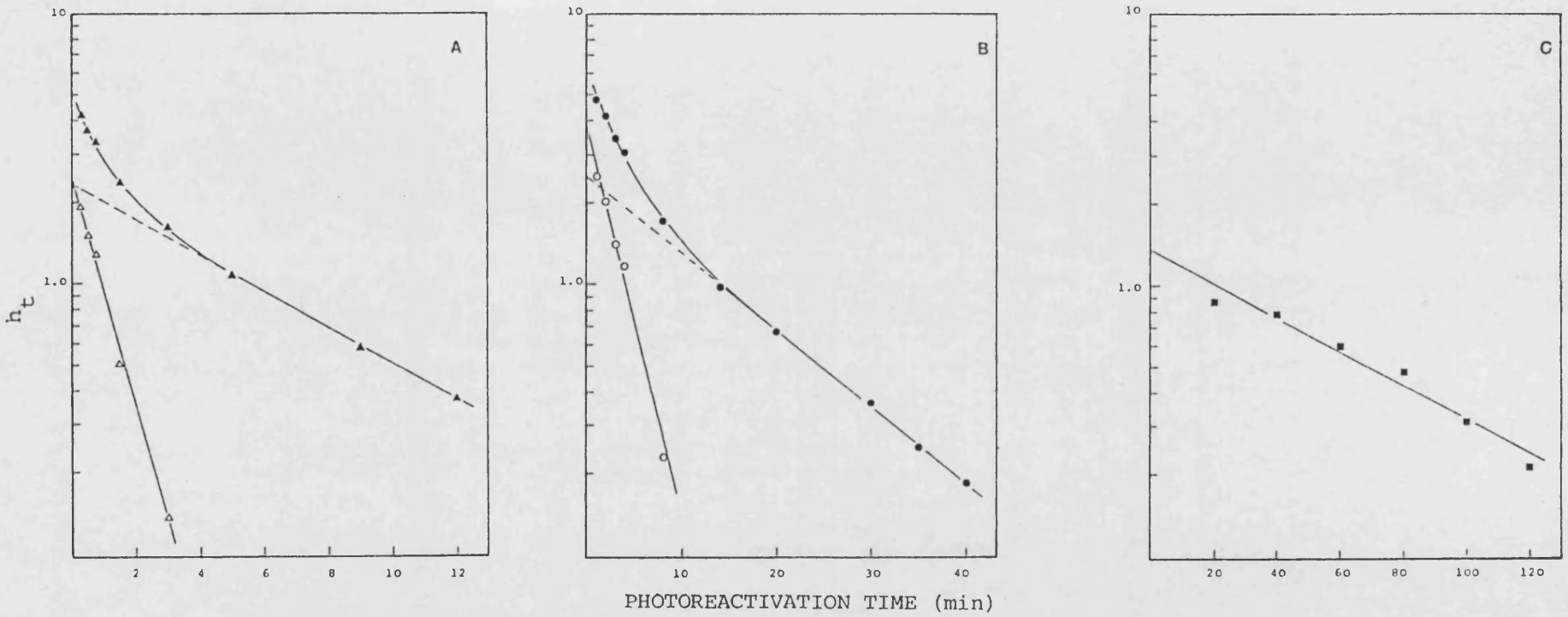

Fig. 3.38. Lethal hit analysis of the photoreactivation rate at 25°C of acetophenone-sensitised, 313 nm inactivated AB2480 (Panel A), AS44 (Panel B) and DY326 (Panel C) (closed symbols) and after subtraction of the slow component (open symbols).

data pertaining to them are included in Tables A4.46-48. These data have been analysed by the (1-P) method and the 'lethal hit' method and are shown in these forms in Figs. 3.37 and 3.38. The initial rates of photoreactivation from the (1-P) analyses and the repair probabilities for the 'lethal- hit' analyses are included in Tables 3.14 and 3.15, respectively.

Table 3.14 Comparison of the initial rates of photo-reactivation and estimates of the number of PRE molecules per cell at 25°C after 0.1% acetophenone-sensitized 313 nm irradiation. The 254 nm data from Table 3.4 is shown in the parentheses

STRAIN	RATE $(x10^{-3})(s^{-1})$	NUMBER OF PRE MOLECULES PER CELL
AB2480	12.04(11.50)	6.69(6.39)
AS44	2.76(3.50)	1.53(1.94)
DY326	0.017(0.062)	0.0094(0.034)
AS46	- (-)	- (-)

Table 3.15 Photoreactivation rate analysis of AB2480, AS44, DY326 and AS46 after acetophenone-sensitized 313 nm UV irradiation. the 254 nm data are included in parentheses

STRAIN	$\alpha_1(min^{-1})$	$\alpha_2(min^{-1})$
AB2480	-0.969(-1.036)	-0.152(-0.167)
AS44	-0.346(-0.619)	-0.065(0.0787)
DY326	- (-)	-0.0144(-0.0401)

When these data were analysed by either of the two methods, it was apparent that the rate of repair of AB2480 was not significantly affected irrespective of the relative ratio of thymine dimers. The estimate of the rate of repair from the (1-P) analysis was slightly greater after acetophenone-sensitized 313 nm irradiation compared with 254 nm UV irradiation, whereas the lethal-hit analysis indicated a marginally slower rate. This probably arose due to difficulty in measuring the initial rate of repair from the (1-P) analysis which was markedly curved even after short periods of photoreactivation. In contrast to AB2480, both AS44 and DY326 showed a significant decrease in the rate of repair; the values being 79 and 27 per cent of the values obtained after 254 nm UV irradiation. With AS44, this was reflected in a 45 per cent decrease in the faster repair constant α_1, whilst the slower rate constant α_2 was reduced by 17 per cent. Thus the faster rate constant α_1 made a relatively smaller contribution to the rate of

repair. The 73 per cent reduction in the rate of repair of DY326 was reflected in a 64 per cent decrease in the rate constant α_2.

Taken together these data suggest that the biphasic repair kinetics observed with both AB2480 and AS44 were not solely attributable to substrate heterogeneity, because the photorepair kinetics are similarly biphasic even when the substrate was essentially one species of dimer. Therefore, it must be concluded that the photolyase molecule(s) exhibit(s) two repair capacities even towards an essentially homogeneous substrate. It is axiomatic that Husain and Sancar (1987a) have found biphasic dark dissociation kinetics (k_2) with the purified phrB gene product on a synthetic 43-bp oligomer containing a single T-T dimer. Approximately 85-95 per cent of pre-existing enzyme-substrate complexes dissociated with a rate constant (k_2) 100-fold higher than the remaining complexes, as measured by the competing-substrate method in the gel retardation assay. The authors reported unpublished observations that this phenomenon was not attributable to the FAD or 'second' chromophore, and concluded that other factors such as "partially unfolded enzyme" or substrate in non-B form may contribute to the biphasic dissociation kinetics. Furthermore, Myles et al. (1987) have used the cloned phrB gene product and the UVR ABC excinuclease system *in vitro* to show that T-T dimers are good substrates for both binding and photolysis, whereas T-C, C-T and in particular C-C dimers are neither bound efficiently by the DNA photolyase (determined by lack of stimulation of ABC excinuclease activity) nor repaired efficiently (failure to remove *M. luteus* UV endonuclease sensitive sites). It was apparent from these findings that the biphasic repair kinetics reported in this study were not simply attributable to the action

of an homogeneous enzyme on an heterogeneous substrate nor to the effect of an enzyme with two repair capacities acting on a homogeneous substrate. The latter hypothesis of an enzyme having two (or more) repair capacities does seem more plausible and would support the data of Husain and Sancar (1987a), however, in this situation, we might reasonably expect to observe multiphasic (>2) repair kinetics with an heterogeneous substrate.

As discussed above, the rate of repair of acetophenone-sensitized 313 nm UV-induced damage observed with AS44 was proportionately slower than after 254 nm UV-induced damage compared with AB2480. Whilst it is problematic to suggest a specific reason for this effect because of the inherent differences in photosensitized 313 nm sensitivity (Table 3.13) it is potentially attributable to the deletion of the proposed phrA gene. These data suggest, but do not confirm, the hypothesis that the proposed phrA gene product enhances the ability of the phrB gene product to monomerize thymine-thymine dimers. It should be noted that despite the differences in sensitivity between AB2480 and AS44, the photo-reactivable sector after acetophenone-sensitized 313 nm UV irradiation for both strains was 0.86; estimated from the photo-reactivation plots of Fig. 3.36. This was lower than the value of 0.98 reported by Hodges et al. (1980) for AB2480, for which there is no satisfactory explanation. However, these workers did extend the fluence range studied to 4500 Jm^{-2}, and noted a biphasic response in the survival curve after maximal photoreactivation. The gradient of the slope after high UV fluences was less than that after low UV fluences.

Both the low rate and extent of repair observed with DY326 (Fig. 3.36) suggest that the photoactive protein presumed to be

present was less able to monomerize the T-T dimer than a mixed population of dimer substrates; possibly inferring a slightly higher affinity towards the C-T or T-C dimer. Furthermore, the data indicated that the limit of photoreactivability was not attributable to a unique specificity for one species of pyrimidine dimer.

Summary

The data in this Section may be summarised as follows:

1. A totally dark-repair-deficient strain deleted at the proposed phrA locus (AS44) photorepaired 254 nm UV-induced damage at a rate 30 per cent that of a similarly dark-repair-deficient, but non-isogenic photoreactivation-proficient strain. This was also reflected in a 68 per cent decrease in the fluence decrement resulting from a single high-intensity flash. Both strains repaired the damage with biphasic kinetics.

2. There was measurable photoreactivation in a dark-repair-deficient strain mutated at the phrB locus, in contrast to the consensus that these strains are completely photoreactivation-deficient. However, no photorepair was observed when this mutation was transduced into a strain deleted at the proposed phrA locus, after growth at 37^{o}C.

3. The phr^{+}, phrA and phrB strains all exhibited a positive relationship between the rate of repair and temperature of the

reaction.

4. The three strains showed a similar wavelength-dependence of photoreactivating light. They exhibited a broad structureless peak over the range 360 to 400 nm, with repair being measured to 470 nm with AS44 and AB2480.

5. In agreement with published results, anaerobic growth reduced the photoreactivable responses of the *phr*$^+$, *phrA*, and *phrB* strains. However, AS44 was markedly less effected. Consideration of the rate constants associated with the biphasic repair kinetics revealed that the slower rate constant α_2 was significantly reduced with AB2480 and DY326, but not with AS44. However, the faster rate constant α_1 for both AB2480 and AS44 was similarly depressed, suggesting that the disproportionate decrease in the rate of photorepair of AB2480 was attributable to the effect on the slower rate constant.

6. Decreasing the pre-irradiation growth temperature from 37° to 26°C resulted in an increase in the rate of repair of AB2480 and AS44, and an increase in both the rate and extent of repair of DY326 after 254 nm UV irradiation. Significantly, a photoreactivable response was measured with the 'double' *phr* mutant AS46. As with the anaerobic growth study, it was the slower rate constant α_2 which was more markedly affected. Since AS46 is deleted at the proposed *phrA* locus, the observed photoreactivable response raises the debate of whether there is a third PRE molecule in *E. coli* which becomes 'active' at

26°C. However, there was no evidence for the existence of a third photolyase molecule in any of the other strains, although DY326 (phrB) did exhibit biphasic repair kinetics after growth at 26°C. Thus it seems most likely that the photorepair measured in DY326 was the result of either the mutant phrB gene product retaining some residual photolyase activity, or that there is a second photoactive protein from an unknown phr locus, both of which are temperature-dependent in the phrA mutant background. It does, however, seem likely that the absence of a gene from the region of the proposed phrA locus does significantly reduce the rate of repair in the phrB$^+$ and phrB backgrounds. In the latter case, the reduction is so severe as to abolish any measurable response after growth at 37°C.

8. Pre-illumination of dark-grown cells, or growth of cells either in the dark or in the presence of photoreactivating light, did not result in any significant variation in the photoreactivability of any of the four strains.

9. When the cells were irradiated at 313 nm in the presence of acetophenone, the rate of repair of AB2480 was not significantly different when compared with repair of 254 nm UV induced damage. However, the rate of repair of AS44 (Δ phrA) was reduced by 20 per cent, which was reflected in a 45 per cent decrease in the faster rate constant, α_1. It was noted that both AB2480 and AS44 repaired acetophenone-sensitized 313 nm damage with biphasic kinetics. Hence, the data reported in this section can neither be solely attributed to the action of

two enzymes on an homogeneous substrate nor to the action of a single molecule with different repair affinities towards an heterogeneous substrate population. The latter hypothesis seems more likely, although it would have to assume two repair capacities/affinities towards the thymine-thymine dimer to satisfactorily explain the photosensitized data. However, since only biphasic repair kinetics have been encountered, such a model for photorepair does not explain the different affinities measured towards the various dimer species *in vitro*. The rate of photorepair of the *phrB* mutant, DY326, was markedly reduced after acetophenone-sensitized 313 nm UV irradiation. These data indicated that the reduced rate and extent of repair compared with either AB2480 or AS44 was not the result of a unique affinity towards one dimer species.

The implications of these data for the interactive role postulated for the proposed *phrA* gene product will be analysed in the concluding discussion.

RESULTS AND DISCUSSION - PART IV

The three previous sections have been concerned with the construction and characterisation of dark-repair-deficient strains mutated at one or both of the proposed *phr* loci. Although it is difficult to make quantitative comparisons between the strains because of their non-isogenicity, it was apparent that a gene in the *gal*-*attλ* interval did have a marked effect on the photoreactivability of 254 nm UV-induced damage. The work described in this section centres on an attempt to isolate plasmids having restriction fragment insertions from the *gal*-*attλ* chromosomal region, and determining if the decrease in photoreactivability observed in Δ(*gal*-*chlA*) strains could be reversed by transformation with these plasmids.

4.1 Isolation and Selection Protocol

From the onset of this work, two interdependent problems were envisaged. Firstly, what would be the source of 'donor' DNA, and secondly, how would the the proposed *phrA*$^+$ plasmid be picked from a pool of recombinant DNA-containing molecules? Sancar and Rupert (1978b) have described a protocol for cloning the *phrB* gene in *E. coli*, using chromosomal DNA as the source of 'donor' DNA. The DNA was restricted, UV-irradiated and mixed with purified yeast photolyase, with the result that the photolyase would bind to the UV-damaged DNA. The DNA was ligated with an appropriately restricted plasmid vector and passed through a nitrocellulose filter. The attached protein caused retention of the recombinant molecules, whilst molecules not having 'donor' DNA passed through. The bound DNA was repaired of its UV damage and released for insertion into cells by exposure to photoreactivating light. The

authors estimated that this resulted in an approximately 350-fold enrichment of the *phrB* gene. The transformed cells were grown up, and subjected to three cycles of UV inactivation and photoreactivation. Approximately 50 per cent of the final clones had the PHR^+ phenotype (Sancar and Rupert, 1978b). Although this protocol would be applicable to isolating the $phrA^+$ gene, several problems mitigated against it. Principally, the data presented in Part III indicated that the activity attributable to the proposed *phrA* locus is orders of magnitude less than the *phrB* gene product. Therefore, it was considered unlikely that the selection protocol would be successful if chromosomal DNA was used as the source of 'donor' DNA. Using strain AS46 as the the recipient strain, transformed derivatives would be expected to have similar photoreactivability to DY326, that is, 1 log-cycle photorecovery after 4 log-cycle UV inactivation. Thus it was considered appropriate to construct a λ*dgal* specialised transducing 'phage, which would carry the *gal*-*attλ* region, and use this as the source of DNA in the cloning experiments. Therefore, we would be cloning with restriction fragments from an approximately 50-kbp piece of DNA specifically carrying the region of the proposed gene of interest. The recombinant DNA enrichment technique using purified yeast DNA photolyase developed by Sancar and Rupert (1978b) has largely been superseded by the availability of calf intestinal alkaline phosphatase, which removes 5' phosphate groups, and so prevents self-ligation of a restricted plasmid vector. The cloning protocol which will be described in detail was as follows:-

1). Selection of a strain lysogenic for a λ*dgal*λ transducing 'phage.

2). Induction/production of a λ*dgal*λ high-frequency transducing

(HFT) lysate and preparation of DNA. Restriction enzyme analysis to determine the size of the DNA fragments.

3). Large-scale preparation of pBR322 plasmid DNA.

4). In vitro restriction of λdgalλ DNA (partial digest) and pBR322 DNA (total digest) with restriction enzyme SphI.

5). Treatment of SphI restricted pBR322 DNA with alkaline phosphatase.

6). Ligation of SphI restricted λdgalλ DNA with SphI/alkaline phosphatase-treated pBR322, using bacteriophage T4 DNA ligase.

7). Transformation of competent cells of strain AS46 with recombinant DNA mixture.

8). Repeated cycles of UV irradiation and photoreactivation treatments, first in liquid culture and finally using individual colonies replicated on solid media.

4.2 Preparation of Stock Solutions

1M Tris. 121.1 g of Tris base (Sigma, St. Louis) was dissolved in 800 ml of glass distilled water on a magnetic stirrer at 20°C. Appropriate quantities of concentrated HCl (BDH, Poole) were added to achieve the desired pH. After making up the volume to 1 litre, 100 ml aliquots were dispensed and sterilized by autoclaving.

0.5M EDTA (pH 8.0). 186.1 g of disodium ethylene diamine tetraacetate.$2H_2O$ (EDTA, Sigma) was added to 800ml of water. The pH was adjusted to 8.0 by the addition of approximately 20 g of NaOH pellets (BDH, Poole) and the solution stirred vigorously on a magnetic stirrer (the disodium salt of EDTA will not dissolve until the solution is adjusted to pH 8.0). The solution was made

up to 1 litre, dispensed in 50 ml aliquots and sterilized by autoclaving.

0.1M EGTA. 380.4 mg of ethylene glycol bis- (β-aminoethyl ether) N,N,N',N'-tetraacetic acid (EGTA, Sigma) was dissolved in 8 ml of water. The solution was made up to 10 ml, sterilized through a 0.2 μm membrane filter, and stored in a sterile plastic universal container (Sterilin, Feltham).

5M NaCl. 292.2 g of NaCl (BDH, Poole) was dissolved in 800 ml of water. The volume was adjusted to 1 litre, dispensed into 100 ml aliquots and sterilized by autoclaving.

1M $MgCl_2$. 203.3 g of $MgCl_2.6H_2O$ (BDH, Poole) was dissolved in 800 ml of water. The volume was adjusted to 1 litre, dispensed into 100 ml aliquots and sterilized by autoclaving.

3M Sodium acetate (pH 5.2). 40.81 g of sodium acetate.$3H_2O$ (BDH, Poole) was dissolved in 80 ml of water. The pH was adjusted to 5.2 with glacial acetic acid (Fisons, Loughborough), and the volume adjusted to 100 ml. The solution was dispensed into 20 ml aliquots and sterilized by autoclaving.

1M Dithiothreitol (DTT). 3.09 g of DTT (Boehringer, Lewes) was dissolved in 20 ml of 0.01M sodium acetate (pH 5.2). The solution was filtered through a 0.2 μm membrane, and 1 ml aliquots dispensed into sterile microfuge tubes (Boehringer, Lewes - 1.5 ml capacity) and stored at -20°C. Once thawed, these were not refrozen.

2-Mercaptoethanol (BME). 2-Mercaptoethanol (14.4M) was purchased from Sigma and stored in the dark at 4°C.

Sodium dodecylsulphate (SDS) 10%. 10 g of 'Analar' grade sodium dodecylsulphate (BDH, Poole) was dissolved in 90 ml of water at 68°C. The pH was adjusted to 7.2 with concentrated HCl. The volume was adjusted to 100 ml and dispensed into 20 ml aliquots.

5M Ammonium acetate. 7.7 g of ammonium acetate (BDH, Poole) was dissolved in 16 ml of water. The solution was made up to 20 ml, filtered through a 0.2 µm membrane and stored in a sterile, screw-topped plastic universal container.

5M Potassium acetate. 11.5 ml of glacial acetic acid and 28.5 ml of water was added to 60 ml of 5M potassium acetate. The resulting solution was 3M with respect to potassium and 5M with respect to acetate.

Ethidium bromide 10 mg/ml. 100 mg of ethidium bromide (EtBr, Sigma) was dissolved in 10 ml of water by stirring on a magnetic stirrer for several hours. The container was wrapped in aluminium foil and stored at 4°C.

6mM ATP. 36 mg of adenosine-5'-triphosphate (ATP, crystallized disodium salt, special quality - Boehringer, Lewes) was dissolved in 8 ml of water and adjusted to pH 7.0 with 0.1M NaOH. The solution was made up to 10 ml, sterilized through a 0.2 µm membrane filter, dispensed into small aliquots and stored at -20°C

for up to one week. Once thawed, these were not refrozen.

4.3 Preparation of Organic Reagents

Tris-equilibrated phenol. Liquefied phenol (phenol 80% in water) was purchased from Thornton and Ross (Huddersfield). 8-hydroxyquinoline (Sigma) was added to a final concentration of 0.1%. The phenol was then extracted several times with an equal volume of buffer (1.0M Tris.Cl [pH 8.0], followed by 0.1M Tris.Cl [pH 8.0] and 0.2% BME), until the pH of the aqueous phase was greater than 7.6. The phenol was stored under equilibration buffer in aluminium-wrapped, screw-topped glass bottles at -20^{o}C for up to one month.

Chloroform:Isoamyl alcohol (24:1). A mixture of chloroform (Fisons, Loughborough) and isoamyl alcohol (Fisons) was used to remove proteins from nucleic acid preparations. Neither reagent required treatment before use and the mixture was stored in aluminium-wrapped, screw-topped glass bottles at room temperature.

4.4 Preparation of Dialysis Tubing

Dialysis tubing (14 mm diameter, Fisons) was cut into 10 cm lengths, boiled for ten minutes in a large volume of 2 per cent sodium bicarbonate and 1mM EDTA, rinsed thoroughly with distilled water, and boiled for further 10 minutes in distilled water. After cooling, the tubing was stored at 4^{o}C, submersed in water.

4.5 Enzymes

Lysozyme. Lysozyme (from egg white) was purchased from Sigma and stored in a desiccator at -20°C.

RNase (DNase-free) 1 mg/ml. 20 mg of pancreatic RNase A (Sigma) was dissolved in 20 ml of 10mM Tris.Cl [pH 7.5] and 15mM NaCl. The solution was heated at 100°C for 15 minutes, and allowed to cool slowly to room temperature. After sterilizing through a 0.2 µm membrane filter, the solution was dispensed into 50 µl aliquots and stored at -20°C.

Deoxyribonuclease I (DNase I) 5 mg/ml. Bovine pancreas DNase I (type II), containing 1890 Kunitz units per mg, was purchased from Sigma. One ml of membrane-sterilized 0.15M NaCl and 50% glycerol was added to each 5 mg vial, at 0°C. The solution was dispensed into 0.1 ml aliquots and stored at -20°C. The protocols used in this work did not require the preparation to be RNase-free.

Alkaline phosphatase. Special quality calf intestinal alkaline phosphatase, containing 19,000 units/ml (2600 units/mg) was purchased from Boehringer, and stored at 4°C. The enzyme was used in accordance with the manufacturers instructions. The incubation buffer used was Tris.Cl, 50mM; EDTA, 0.1mM; pH 8.0 (25°C).

T4 DNA ligase. T4 DNA ligase from E. coli NM989, containing 1000 units/ml (3000 units/mg protein), was purchased from Boehringer and stored at -20°C. The incubation buffer used was Tris.Cl, 50mM; $MgCl_2$, 10mM; DTT, 10mM; ATP, 0.6mM; pH 7.6 (37°C), in

accordance with the manufacturers instructions.

Restriction Endonuclease EcoRI. EcoRI from E. coli BS5, containing 5 units/µl, was purchased from Boehringer, and stored at -20°C. The incubation buffer used was Tris.Cl, 100mM; NaCl, 50mM; $MgCl_2$, 10mM; pH 7.5 (37°C). The endonuclease recognizes the sequence G/AATTC, generating fragments with 5'-cohesive termini. There are five recognition sites in Lambda DNA and one site in pBR322 DNA.

Restriction Endonuclease SphI. SphI from Streptomyces phaeochromogenes, containing 4 units/µl, was purchased from Boehringer, and stored at -20°C. The incubation buffer used was Tris.Cl, 6mM; NaCl, 125mM; $MgCl_2$, 6mM; BME, 7mM; Triton X-100 (Sigma), 0.01%; pH 7.7 (37°C), in accordance with the manufacturers instructions. The endonuclease recognizes the sequence GCATG/C, generating fragments with 3'-cohesive termini. There are six recognition sites in Lambda DNA, and one site in pBR322 DNA.

Test of Restriction Endonuclease Activity

The specific example given will be to test EcoRI activity, although the methodology is applicable to other restriction endonucleases. One unit is defined as the enzyme activity which completely cleaves 1 µg of lambda DNA in 1 hour at 37°C in 50 µl of incubation buffer. To test the activity of the enzyme, dilutions were made in incubation buffer ranging from 0.1 to 10 units/µg, and incubated with 1 µg of lambda DNA at 37°C for 1 to 2 hours.

Restriction endonuclease EcoRI 5 units/µl (claimed)

Dilution A

1 µl enzyme + 9 µl buffer = 0.5 units/µl

Dilution B

1 µl (A) + 49 µl buffer = 0.01 units/µl

$\lambda cI_{857}S_{am7}$ DNA (Boehringer) 100 ng/µl.

Enzyme concentration	5x Buffer	DNA (µl)	Enzyme (µl)	H_2O (µl)	Total (µl)
0	10	1	-	39	50
0.1	10	1	1B	38	50
1.0	10	1	10B	29	50
5.0	10	1	1A	38	50
10.0	10	1	2A	37	50

After incubation at 37°C for 2 hours, 10 µl of 'Stop mix' was added to each sample (see Agarose Gel Electrophoresis), and stored at 4°C, prior to electrophoresis. A photograph of an agarose electrophoretic gel of an EcoRI restriction endonuclease test is shown in Fig. 4.1.

4.6 Agarose Gel Electrophoresis

Horizontal agarose electrophoresis in a Bio-Rad mini-gel apparatus was used to separate restriction fragments, and analyse

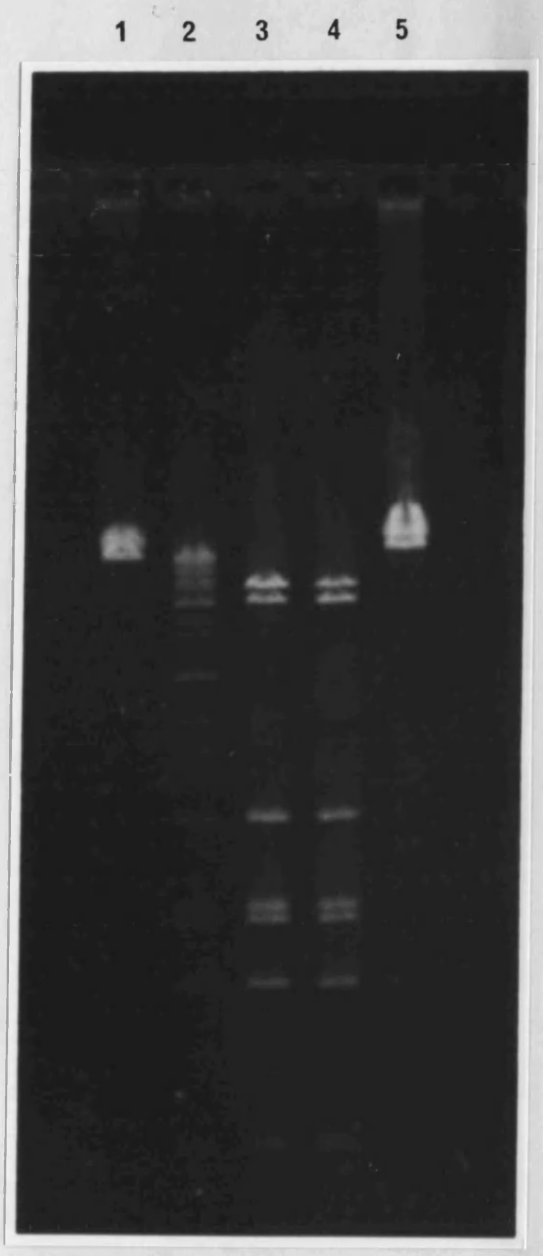

Fig. 4.1. Restriction endonuclease EcoRI test on λ DNA.
Lane 1, 0.1 u/µg; lane 2, 1.0 u/µg; lane 3, 5.0 u/µg
lane 4, 10.0 u/µg; lane 5, Control.

plasmid molecules.

Gel electrophoresis tank and power supply. A Bio-Rad Mini-sub DNA cell of 250 ml nominal capacity was used in conjunction with a Bio-Rad 250/2.5 power supply.

Running Buffer. 250 ml of Tris.acetate buffer (Tris.acetate, 40mM; EDTA, 1mM) was prepared from a 10x stock solution and recirculated around the electrophoresis tank by a flow-inducer (Watson-Marlow, Falmouth). The 10x stock solution was prepared by dissolving 24.2 g of Tris base in 400 ml of water, and adding 5.7 ml of glacial acetic acid and 10 ml of 0.5M EDTA (pH 8.0). The volume was adjusted to 500 ml, and the solution stored at room temperature.

Gel preparation. An agarose concentration of 0.8% was chosen to afford separation of linear DNA molecules in the range 0.6 to 9 kbp (Maniatis et al., 1982). 0.24 g of electrophoresis-grade agarose (BDH, Poole) was dissolved in 30 ml of Tris.acetate buffer by heating at 100^{o}C for 3 minutes on a magnetic stirrer. The well-forming comb was adjusted to approximately 2 mm above the gel tray, whilst the ends of the tray were sealed with adhesive tape. After cooling to approximately 50^{o}C, the molten agarose was cast, and allowed to solidify for a minimum of 30 minutes.

Loading buffer (Stop mix) and Gel loading. Stop mix was prepared by dissolving 50 mg of SDS and 2.5 mg of bromophenol blue (Sigma) in 4 ml of water. Five ml of glycerol was added, and the volume made up to 10 ml. Stop mix was added to approximately 10 per cent of the reaction volume to be electrophoresed. Once the

well-forming comb had been removed, the wells were flooded with running buffer. Depending on the well size, either 7 µl or 12 µl reaction volumes were loaded using a micropipette (Jencons, Hemel Hempstead). The gel was submerged in the electrophoresis tank, and electrophoresed at 3-6 V per cm for 2-8 hours according to the molecular weight of the sample.

Gel staining, visualization and photography. Electrophoresed gels were immersed in 250 ml of a solution containing 0.05 µg/ml ethidium bromide in water for 20 minutes. DNA fragments were visualized on a UV Products transilluminator and photographed with a CU-5 Fotodyne camera and Type 55 Polaroid film.

4.7 Preparation of pBR322 Plasmid DNA

(Adapted from Maniatis et al., 1982)

1) Large-scale preparation.

a) Amplification. Ten ml of pre-warmed LB broth (Appendix 2), containing 50 µg/ml ampicillin, was inoculated with a single colony of *E. coli* DH1/pBR322 and grown overnight at 37°C with vigorous shaking. 50 ml of LB broth, supplemented with 50 µg/ml ampicillin, in a 250 ml flask, was inoculated with 0.5 ml of the overnight culture, and shaken at 37°C until the OD_{600} reached approximately 0.6 (late log-phase). Five ml of this late log-phase culture was used to inoculate each of ten 250 ml flasks containing 100 ml of pre-warmed LB broth supplemented with 50 µg/ml ampicillin. The culture was shaken at 37°C for exactly 2 hours, after which 0.5 ml of a solution of chloramphenicol (34 mg/ml in ethanol) was added. The final concentration of chloramphenicol in the culture was 170 µg/ml. The culture was

shaken at 37°C overnight.

b) Harvesting. The bacterial cells were harvested by centrifugation in the 6x250 ml rotor of the MSE Superspeed 18 centrifuge at 4,000 rpm (2500 g) for 20 minutes at 4°C. The pellets were stored at -20°C until required.

c) Lysis by boiling. The bacterial pellet (from 1 litre of culture) was resuspended in 10 ml of STE (NaCl, 100mM; Tris.Cl[pH 8.0], 10mM; and EDTA, 0.1mM) and transferred to a 50 ml capacity, round-bottomed flask. One ml of a freshly prepared lysozyme solution (20 mg/ml in 10mM Tris.Cl[pH 8.0]) was added. The flask was held over the open flame of a Bunsen burner and shaken vigorously until the liquid just started to boil, before being immersed in a large beaker of boiling water for 40 seconds. The flask was cooled by immersion in ice-cold water for 5 minutes. The viscous contents were transferred to Beckman polyallomer ultracentrifuge tubes (13.5 ml nominal capacity) and centrifuged at 32,000 rpm for 30 minutes at 4°C in a Beckman Type-70.1Ti rotor in a Beckman L8-70M ultracentrifuge.

d) Purification. The plasmid DNA was purified by centrifugation to equilibrium in caesium chloride-ethidium bromide gradients. The volume of the supernatant from the last ultracentrifugation step was measured in a sterile 50 ml measure. One g of finely ground caesium chloride (BDH, Poole) was added for every 1 ml of solution. This was gently mixed until all the salt had dissolved. For every 10 ml of caesium chloride/DNA solution, 0.8 ml of ethidium bromide solution (10 mg/ml in water) was added. The solution was transferred to Beckman 'Quickseal' 13x51 mm tubes (filled and balanced with light paraffin oil as necessary) and centrifuged in a Beckman VTi 65 rotor at 45,000 rpm for 36 hours

at 20°C. The bands of DNA were visualized with broad-band ultraviolet light (UV Products transilluminator), the lower band being the supercoiled plasmid DNA. The shoulder of the centrifuge tube was punctured to create an airway, and the plasmid band removed through a Type 21 hypodermic needle inserted into the side of the tube just below the band. The solution was dispensed into 0.1 ml aliquots in sterile microfuge tubes.

e) Removal of ethidium bromide. The EtBr was removed by repeated extraction with isoamyl alcohol until all the pink colour had disappeared from the aqueous layer. An equal volume of isoamyl alcohol was mixed with the EtBr/DNA solution and centrifuged at 1500g for 3 minutes (MSE MicroCentaur, Fisons). The lower aqueous phase was transferred to a fresh microfuge tube and the extraction repeated.

f) Dialysis. The final solution (approximately 0.5 ml) was transferred to prepared dialysis tubing and dialysed against 5 x 1 litre volumes of TE (Tris.Cl [pH 8.0], 10mM; EDTA, 1mM) at 4°C. The absorbance at 260 nm of the dialysed solution was measured in a Perkin Elmer 550S spectrophotometer. A value of 0.2 was obtained routinely, equivalent to 1 µg of DNA per µl.

2) Mini plasmid preparation

1.5 ml of an overnight culture of the required plasmid strain (grown at 37°C in LB broth supplemented with 50 µg/ml ampicillin) was centrifuged for 1 minute in an Eppendorf microfuge (MSE MicroCentaur, Fisons). The medium was removed by aspiration and the pellet resuspended in 100 µl of a freshly-prepared, ice-cold solution of glucose, 50mM; EDTA, 10mM and Tris.Cl[pH 8.0], 25mM,

containing lysozyme 4 mg/ml. After 5 minutes at room temperature, 200 µl of a freshly-prepared, ice-cold solution of 0.2N NaOH and 1% SDS was added; mixing being by gentle inversion three times. This was stored on ice for 5 minutes. 150 µl of an ice-cold solution of 5M potassium acetate (see 'Preparation of Stock Solutions') was added, and the tube vortexed in an inverted position for 10 seconds. After storing on ice for 5 minutes, the contents were centrifuged in a microfuge for 5 minutes at 4°C. The supernatant was transferred to a fresh tube, and an equal volume of phenol/chloroform (phenol:chloroform:isoamyl alcohol 50:48:2) added. The two phases were mixed by gentle vortexing. After centrifuging for 2 minutes in a microfuge, the aqueous supernatant was transferred to a fresh tube. Two volumes of ethanol (>95%) were added, vortexed and left to stand for 2 minutes at room temperature. The precipitated DNA was centrifuged for 5 minutes at room temperature in a microfuge. The supernatant was removed, and the tubes left to drain in an inverted position. The pellet was washed with 70% ethanol, re-centrifuged, and dried briefly in a vacuum desiccator. Approximately 50 µl of TE (pH 8.0), containing DNase-free pancreatic RNase (20 µg/ml) was added. The samples were stored at 4°C until required for electrophoresis.

The large-scale plasmid preparation was routinely used for batch purposes for cloning experiments, whilst the 'mini-prep' was used for rapid screening of individual clones.

4.8 Construction of a λdgalλ specialised transducing 'phage

a) Induction of a λ lysogen. Strain GY247, which is lysogenic for λcI_{857} carrying the temperature-sensitive cI repressor protein, was a gift from Dr. A. Wheals (University of Bath). The strain was shaken at 30°C overnight in 10 ml of LB broth containing 10mM $MgSO_4$. 0.5 ml of this overnight culture was used to inoculate 50 ml of supplemented LB broth, and the culture shaken at 30°C until early log phase was reached, after which it was shaken at 42°C for 90 minutes (until lysis was complete). The cell debris was centrifuged at 4000 rpm (3600 g) in the 4x25 ml rotor of the MSE Chilspin for 20 minutes at 4°C. The lysate (referred to as a low frequency transducing [LFT] lysate) was stored in screw-topped glass containers with a few drops of chloroform at 4°C.

b) Lysate titer. E. coli W3350 (Appendix 1) was chosen as the recipient strain in all the lambda 'phage experiments, because its galKT genotype would be an appropriate indicator for λdgal transducing activity. An overnight culture of W3350 was prepared by inoculating 100 ml of TB broth (Appendix 2) supplemented with 0.2% maltose and 10mM $MgSO_4$, and shaking at 30°C. The overnight culture was centrifuged at 4,000 rpm (3,600 g) in the 4x250 ml rotor of the MSE Chilspin for 20 minutes at 4°C, and resuspended in 10mM $MgSO_4$, pre-warmed to 37°C. Dilutions of the 'phage lysate were prepared in λ -dil buffer (Appendix 2) in the range 10^{-2} to 10^{-10}. The bacterial cells and 'phage lysate were pre-adsorbed by mixing 0.1 ml of cells with 0.1 ml of lysate at room temperature for 5 minutes. The pre-adsorption mixture was added to 3.5 ml of molten TB top agar (Appendix 2) at 42°C and poured over TB plates

(Appendix 2). The plates were incubated overnight at 37°C, resulting in clear plaques, since no lysogens could be formed at this restrictive temperature. The results from four experiments are shown in Table 4.1.

Table 4.1. Lysate titers of λ 'phage after lysogen induction.

Experiment Number	Plaque counts	Mean	Plaque forming units per ml
1	111, 120, 105	$x10^7$	1.12×10^{10}
2	49, 39, 55	$x10^7$	4.76×10^9
3	63, 71, 65	$x10^7$	6.63×10^9
4	316, 285, 291	$x10^7$	2.97×10^{10}

c) Selection of a Lambda lysogen of strain C600. E. coli C600 was used as the gal$^+$ donor in the construction of the λgal specialised transducing 'phage, because this strain was used by Sutherland et al. (1972) for their phr amplification studies. This strain was grown overnight at 30°C in LB broth supplemented with 10mM $MgSO_4$ and 0.2% maltose. The suspension was centrifuged at 2500 g for 20 minutes and resuspended in half the original volume of 10mM $MgSO_4$. 0.1 ml of cells was mixed with 3.5 ml of molten TB soft agar at 42°C and poured over TB plates. Once the agar had solidified, the surface was spotted with 0.05 ml of the LFT lysate obtained from

induction of GY247. The plates were incubated overnight at 30°C. An inoculating loopful was picked from the turbid centre of the plaque and streaked onto the surface of a fresh TB plate. After incubation overnight at 30°C, colonies were replicated onto TB plates and incubated at 30° and 42°C. Cells unable to grow at 42°C (due to cell lysis) were identified as Lambda lysogens.

d) Selection of a λdgalλ double lysogen. The Lambda lysogen of C600 was induced as described previously, and the titer of the LFT lysate (low galactose transducing activity) determined. E. coli W3350 (galKT) was used as the GAL^- marker for galactose transducing activity. W3350 was grown overnight in LB broth supplemented with 10mM $MgSO_4$ and 0.2% maltose, and resuspended in half the original volume of 10mM $MgSO_4$. 0.1 ml of cells was mixed with 3.5 ml of molten TB soft agar at 42°C and poured over eosin-methylene blue-galactose (EMB-gal) plates (Appendix 2). Strains which can utilise galactose appear as purple colonies on this medium, whereas gal^- colonies appear white. After the agar had solidified, 0.05 ml aliquots of the LFT lysate grown on C600 were spotted onto the surface. The plates were incubated at 30°C for 48 hours. Fifty one purple colonies were picked from the centre of the turbid plaques, and replicated onto EMB-gal plates and incubated at 30° and 42°C. Eight of the colonies exhibited growth at the higher temperature, and 10 colonies showed no spontaneous segregation of GAL^- mutants. These were probably Lambda lysogens, but GAL^+ by recombination. Of the remaining λdgalλ 'double lysogens', one was picked for further analysis.

e) Induction of W3350 λdgalλ lysogen and lysate titer. The lysogen

was grown and induced as described previously. The resulting lysate is termed a high-frequency transducing (HFT) lysate, having high galactose transducing activity. The W3350 λdgalλ lysogen was a double-lysogen of both λdgal and λ'phage because it must have gained λdgal to become GAL^+, but in addition, it will also have been infected with λ'phage due to the very small proportion of λ dgal 'phage particles in the LFT lysate. It was therefore possible to determine the titer of the λ'helper' 'phage, and the λ dgal transducing 'phage. The λ'phage titer was determined as described previously, and a value of 2.8×10^9 plaque forming units (pfu) per ml was obtained. The transducing activity was assayed using both a 'spot' assay, and a full assay. For the 'spot' assay, W3350 was grown overnight and overlaid in TB soft agar over EMB-galactose plates as described previously. 0.05 ml aliquots of the HFT lysate were spotted onto the plate. After incubation at 30°C for 48 hours, an intense purple colour was noted in the centre of each plaque. This indicated that the majority of lysogens formed had acquired the GAL^+ phenotype. For the full assay, W3350 was grown overnight at 30°C in LB medium, supplemented with 10mM $MgSO_4$ and 0.2% maltose, and resuspended in half the original volume of 10mM $MgSO_4$. 0.1 ml aliquots of the cells were incubated with 10^0 to 10^{-6} dilutions of the HFT lysate (prepared in λ-dil buffer), at room temperature for 30 minutes. This pre-adsorption mixture was plated in molten F-top agar (Appendix 2) over galactose minimal-medium plates (Appendix 2). The colonies were counted after 72 hours incubation at 30°C. A value of 1.19×10^5 per ml was obtained. This was 10^4 lower than the titer of the lambda 'helper' 'phage. However, it should be noted that λdgal cannot form lysogens very readily. This does not appear to be

related to deletion of genes responsible for integration and recombination, since these are present in λdgal 'phages. It is thought that the normal Lambda 'helper' 'phage integrates at the E. coli attλ chromosomal attachment site and provides a site at which λdgal λ'phage can integrate. Therefore, as the lambda 'phage titer is decreased by dilution, the λdgal becomes relatively less able to form lysogens. However, despite these considerations, the data did indicate that the proposed W3350 λdgalλ 'double lysogen' did produce λ'phage particles which carried the chromosomal region between gal and attλ.

f) Isolation of λdgalλ DNA (after Silhavy et al., 1984). W3350 λdgalλ was grown overnight in LB broth supplemented with 10mM $MgSO_4$ and 0.2% maltose at 30°C. This culture was subcultured 1 in 100 into 1 litre of fresh supplemented LB broth and shaken at 30° for 60 minutes, before being induced at 42°C for 30 minutes. The culture was then shaken at 37°C for 90 minutes, until lysis was complete. One ml of chloroform was added, and the suspension shaken for a further 30 minutes. The lysate was chilled to room temperature and DNase I and RNase A added to a final concentration of 1 µg/ml. This was incubated at room temperature for 30 minutes. Solid NaCl was added to a final concentration of 1M (58.4 g per litre of lysate) and dissolved by gentle mixing. After holding on ice for 60 minutes, the lysate was centrifuged at 11,000 g (8300 rpm in the 6x250 ml rotor of the MSE Superspeed 18) for 10 minutes at 4°C. The volume of the supernatant was measured, and polyethylene glycol 6000 (PEG, BDH, Poole) added to 10% final concentration. The PEG 6000 was dissolved by stirring on a magnetic stirrer at room temperature. After complete dissolution, the

lysate was held on ice-water for exactly 60 minutes, to allow the 'phage particles to co-precipitate with the PEG. The pellet was collected by centrifugation at 11,000 g (8300 rpm in the 6x250 ml rotor of the MSE Superspeed 18) for 10 minutes at 4°C, and resuspended in TM buffer (Tris.Cl [pH 7.5], 50mM $MgSO_4$, 10mM). The PEG-'phage suspension was extracted with an equal volume of chloroform in a sealed Beckman 13.5 ml polyallomer ultracentrifuge tube, by gentle inversion for 1 minute. This was centrifuged at 2,000 g for 10 minutes to separate the layers. The upper aqueous layer was transferred to a sterile tube, and the PEG-chloroform interface re-extracted with 5 ml of TM. A glycerol step-gradient was prepared in a Beckman 13.5 ml polyallomer tube, comprising 3 ml of 40 per cent glycerol, 3 ml of 5 per cent glycerol and approximately 7 ml of lysate, added in that order. This was centrifuged at 34400 rpm in the Beckman Type-70.1Ti rotor for 60 minutes at 4°C. The supernatant was discarded, and the 'phage pellet resuspended in 1 ml of TM buffer. RNase A and DNase I were added to a final concentration of 10 µg/ml and 1 µg/ml, respectively. This was incubated at 37°C for 30 minutes, after which 0.2 final volume of STEP buffer (0.5% SDS, Tris.Cl [pH 7.5], 50mM; EDTA, 0.4M; proteinase K powder added to a final concentration of 1 mg/ml immediately before use) was added. This was heated to 50°C for 15 minutes, and then extracted with an equal volume of Tris-equilibrated phenol. The lower phenolic phase was removed, leaving the interface and the aqueous phase,which were re-extracted with phenol/chloroform. The phases were separated by centrifugation at 1,000g (Beckman Type-70.1Ti rotor) for 5 minutes. The top aqueous layer was transferred to a sterile polypropylene centrifuge tube and extracted with an equal volume of chloroform.

Once again the phases were separated by centrifugation. The upper aqueous layer was transferred to prepared dialysis tubing, and dialysed against 5 x 1 litre changes of TE buffer (pH 8.0) at room temperature. A 1 in 10 dilution of the dialysed preparation was made, and the absorbance determined at 260 and 280 nm. The values obtained were 0.08 and 0.04, respectively. The value of 0.08 for the OD_{260} resulted in an estimate of 78 µg/µl of DNA, assuming the molar extinction coefficient to be 6.7×10^{-3} and 660 to be the molecular weight of a base-pair. The yield of Lambda DNA from this protocol was approximately 1 mg per litre of lysate.

g) SphI restriction of λdgalλ DNA. The lambda DNA, prepared from the procedure described above, was restricted with 20 units/µg of restriction endonuclease SphI, according to the protocol shown below. In addition, Lambda DNA, purchased from Boehringer (Lewes) was similarly restricted with SphI and also with 25 units/µg of EcoRI.

SphI restriction endonuclease 4 µnits/ul

Dilution A

1 µl SphI + 9 µl buffer = 0.4 units/µl

Enzyme Concentration	10x Buffer	DNA (µl)	Enzyme (µl)	H_2O (µl)	Total (µl)	Lane
0	1.2	1	-	9.8	12	1
20	1.2	1	5A	4.8	12	2
0	1.2	1	-	9.8	12	3
20	1.2	1	5A	4.8	12	4

EcoRI restriction endonuclease 5 units/µl

Dilution B

1µl EcoRI + 9 µl buffer = 0.5 units/µl

Enzyme Concentration	10x Buffer	DNA (µl)	Enzyme (µl)	H_2O (µl)	Total (µl)	Lane
0	2.4	1	-	8.6	12	5
25	2.4	1	5B	3.6	12	6

Lanes 3 and 4 λdgalλ DNA

Lanes 1,2,5 and 6 λ DNA (Boehringer)

The samples were incubated at 37°C for 8 hours.

The restricted samples were electrophoresed in a 0.8 per cent agarose gel at 40 V for 6 hours. A photograph of a typical gel is shown in Fig. 4.2. The photographic negative was scanned with a Joyce-Loebl microdensitometer. The resulting trace (Fig. 4.3) was used to compare the electrophoretic mobilities of restriction fragments, by measuring the distance from the peak representing the loading well to each peak corresponding to a DNA fragment. The SphI and EcoRI digests of the Lambda DNA purchased from Boehringer served as a control which permitted the construction of a standard curve, by plotting the distance migrated by each fragment as a function of its size. Novel bands, identified as being present in the λdgalλ SphI restriction, but absent from the λ control SphI restriction, were also plotted on this curve, from which their size could be determined. The plot of the relative distances migrated by the bands as a function of their molecular weights is shown in Fig. 4.4, and the data pertaining to this figure are given

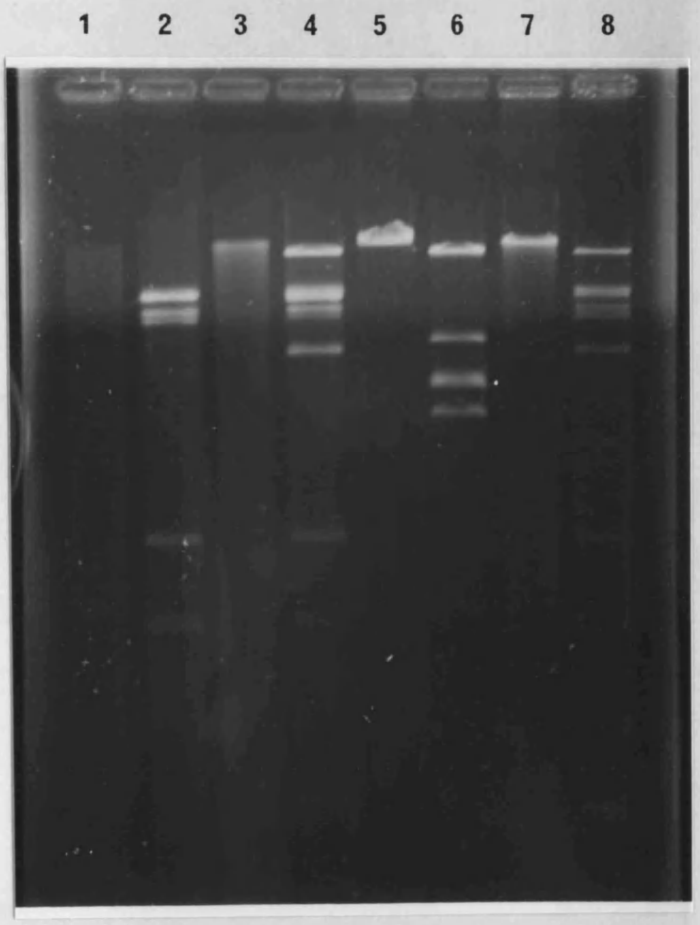

Fig. 4.2. Electrophoretic separation of unrestricted λDNA (Lanes 1 and 5), SphI restricted λDNA (Lane 2), unrestricted λ*dgal*λ DNA (Lanes 3 and 7), SphI restricted λ*dgal*λ DNA (lanes 4 and 8) and EcoRI restricted λ DNA (Lane 6).

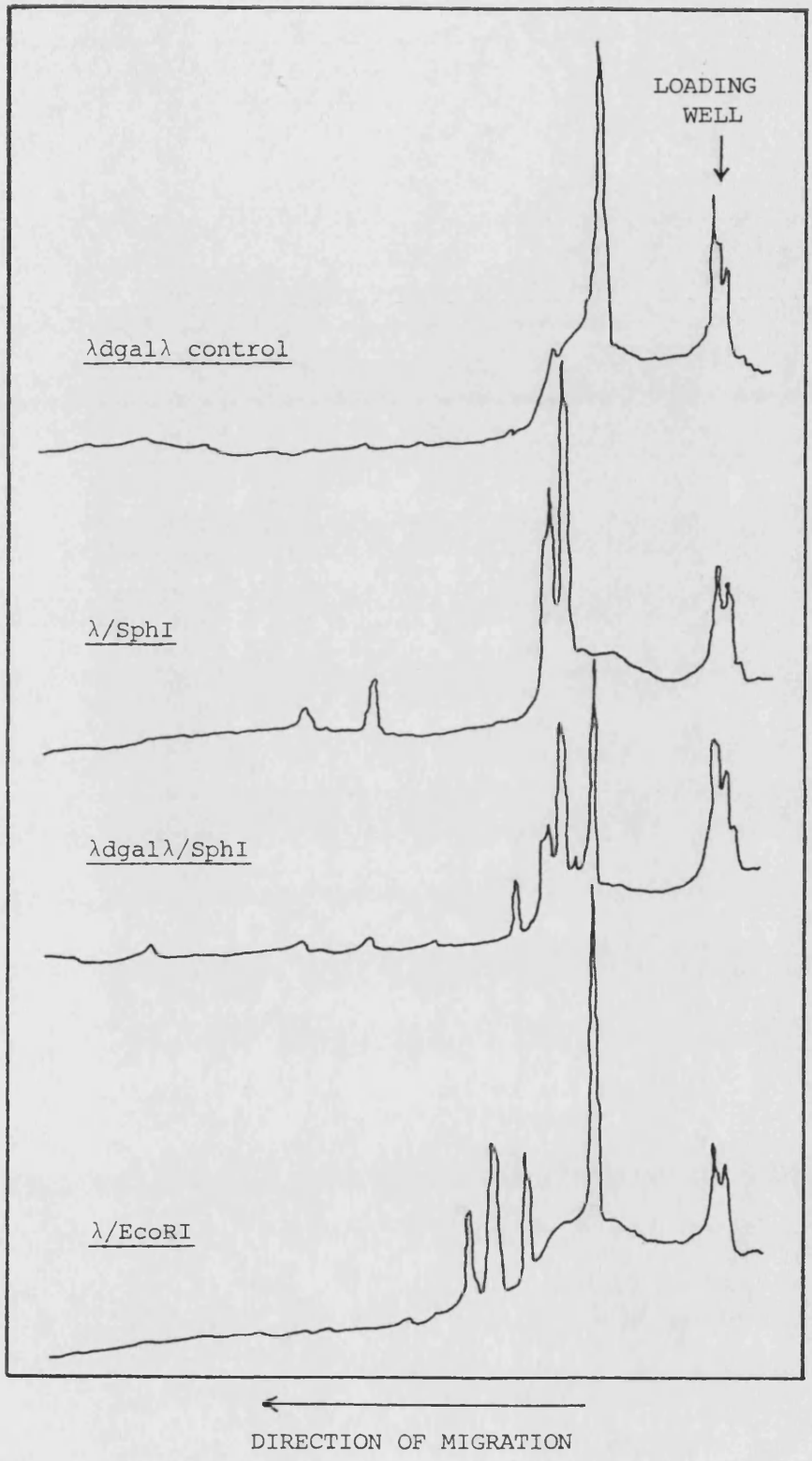

Fig. 4.3. Microdensitometer traces of the photographic negative shown in Fig. 4.2.

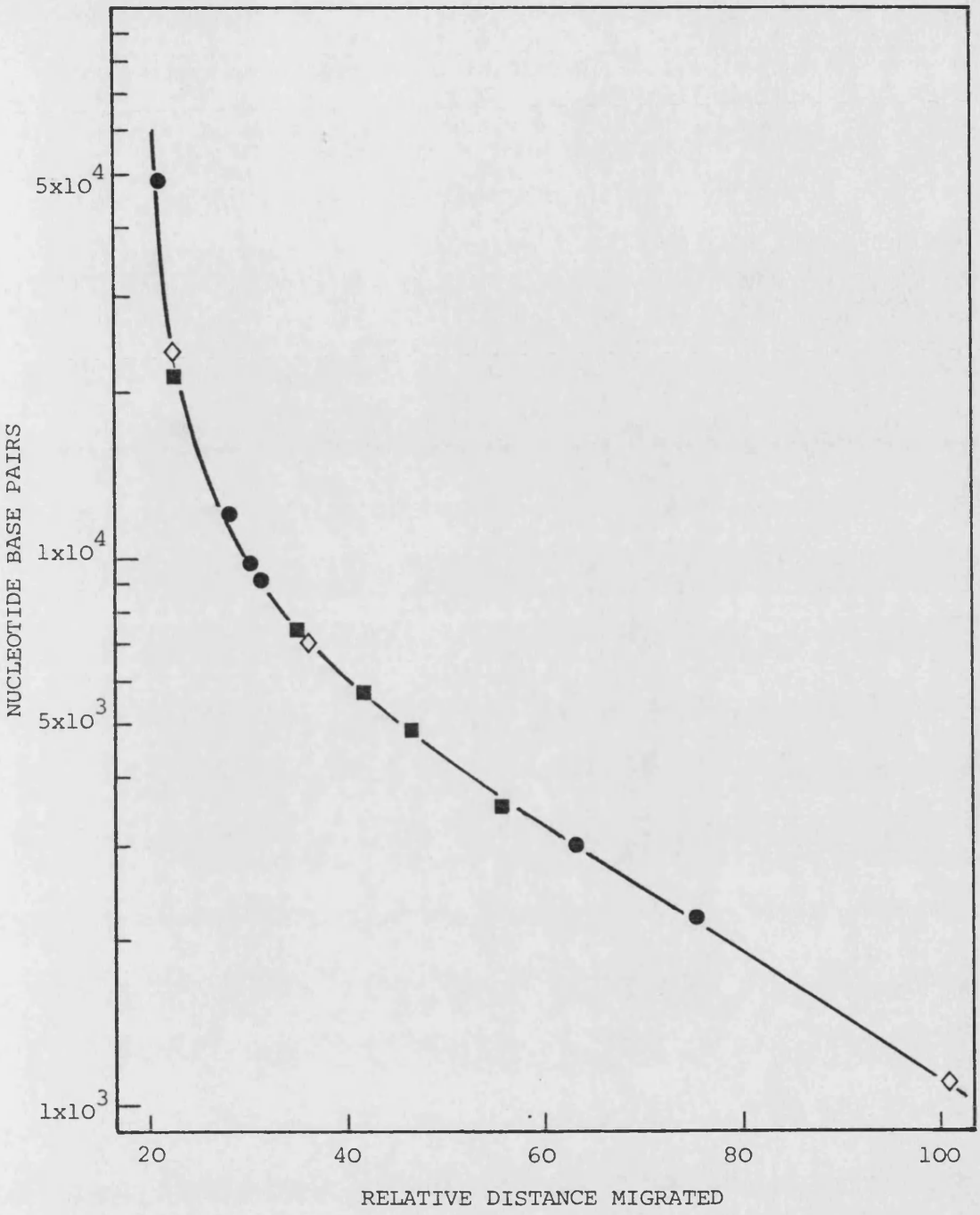

Fig. 4.4. Determination of base-pair lengths of novel fragments produced by SphI restriction of λdgalλ DNA (◇). The standard curve represents EcoRI (■) and SphI (●) restriction of λcontrol DNA

Table 4.2. Relative distance migrated by EcoRI and SphI restriction fragments of λdgal λ and λ DNA as a function of their molecular weight.

Molecular Weight	Distance Migrated	
	SphI	EcoRI
48502	21.0	21.0
Novel	22.4	-
21226	-	22.5
12044/11940	28.5	-
9791	30.2	-
9083	31.2	-
7421	-	34.7
Novel	36.0	-
5804/5643	-	41.5
4878	-	46.3
3530	-	55.9
3003	62.7	-
2212	74.5	-
Novel	100.5	-

in Table 4.2. It will be seen that SphI restriction of the λdgal preparation resulted in the appearance of 3 novel bands in addition to the expected λ restriction pattern (◇ in Fig 4.4). The migration of the 3 bands corresponded to molecular weights of approximately 23.5-, 7- and 1-kbp, respectively. These data, and the demonstration of galactose transducing activity in vivo, strongly indicated that the λdgalλ preparation carried the chromosomal region up to and including the galKT operon. Therefore, it was appropriate to attempt to clone the phrA locus using this preparation as the source of 'donor' DNA.

4.9 Cloning of the phrA Gene Product.

1)Preparation of an SphI partial digest of λdgalλ DNA. It was important to achieve a partial digest of the donor DNA in case the gene of interest had an SphI restriction endonuclease cleavage site within it. The following reaction mixture was prepared and incubated at 37°C for 2 hours.

λdgalλ DNA (5 μg)	10 μl
10x SphI buffer	2 μl
SphI (4 units/μl)	1 μl
H_2O	7 μl

The restriction endonuclease was inactivated by the addition of 0.1 volume of 100mM EDTA and heating to 75°C for 5 minutes. The restricted DNA was precipitated by the addition of 0.4 volume of 5M ammonium acetate and 2 volumes of iso-propanol. The reaction mixture was centrifuged for 10 minutes in a microfuge at room

temperature. The supernatant was aspirated off, and the pellet resuspended in 10 µl of TE (pH 8.0). This was stored at 4°C until required.

2) Preparation of SphI restricted pBR322 DNA. The following reaction mixture was prepared, and incubated at 37°C for 16 hours:-

pBR322 DNA (10 µg)	30 µl
10x SphI buffer	5 µl
SphI (4 units/µl)	2 µl
H_2O	13 µl

A 5 µl aliquot was electrophoresed to determine if the restriction was complete. Reference to Fig. 4.5 (Lane 1) indicated there was no supercoiled or open circle DNA present, compared with the un-restricted sample shown in Lane 8. The restriction endonuclease was inactivated, and the plasmid DNA precipitated, as described above. The pellet was resuspended in 20 µl of TE (pH 8.0).

3) Alkaline phosphatase treatment of SphI restricted pBR322 DNA. The following reaction mixture was prepared, and incubated at 37°C for 1 hour:-

SphI restricted pBR322 DNA	20 µl
10x AP buffer	2.5 µl
Alkaline phosphatase (19 units/µl)	1 µl
H_2O	1.5 µl

The alkaline phosphatase was inactivated by adding 0.1 volume of 100mM EGTA and heating to 65°C for 45 minutes. The DNA was precipitated by adding 0.4 volume of 5M ammonium acetate and 2 volumes of iso-propanol. After centrifugation, the DNA pellet was resuspended in 20 µl of TE (pH 8.0).

The activities of the alkaline phosphatase and T4 DNA ligase were tested in the following way:-

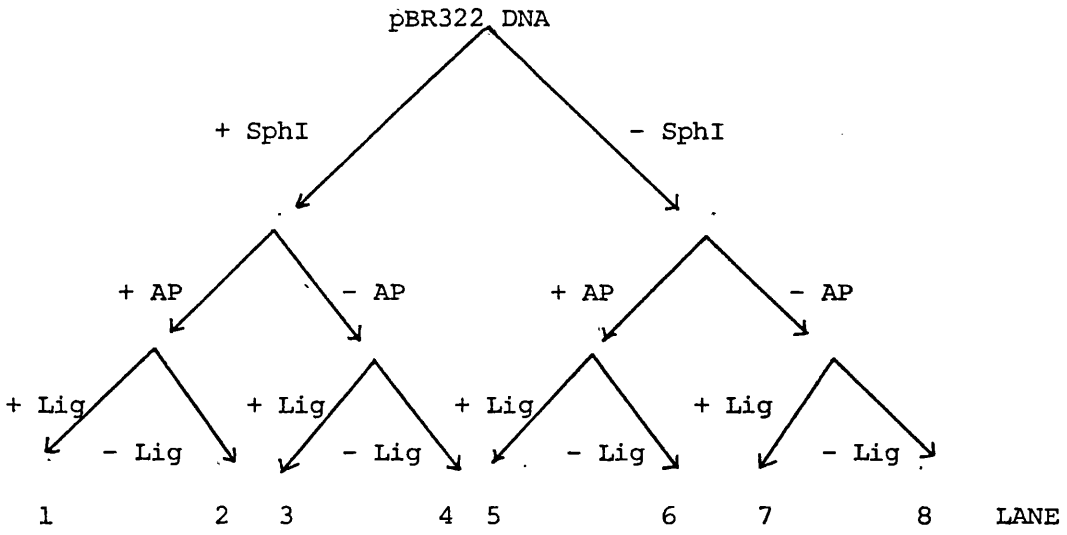

Each reaction mixture was analysed by agarose gel electrophoresis, and the photograph is shown in Fig. 4.5. There was evidence of ligation in Lane 3, which used restricted pBR322 DNA as the substrate, but this was not apparent in Lane 1, where the DNA had also been treated with alkaline phosphatase. These data indicated that both the alkaline phosphatase and T4 DNA ligase gave satisfactory results under the experimental conditions used in the work.

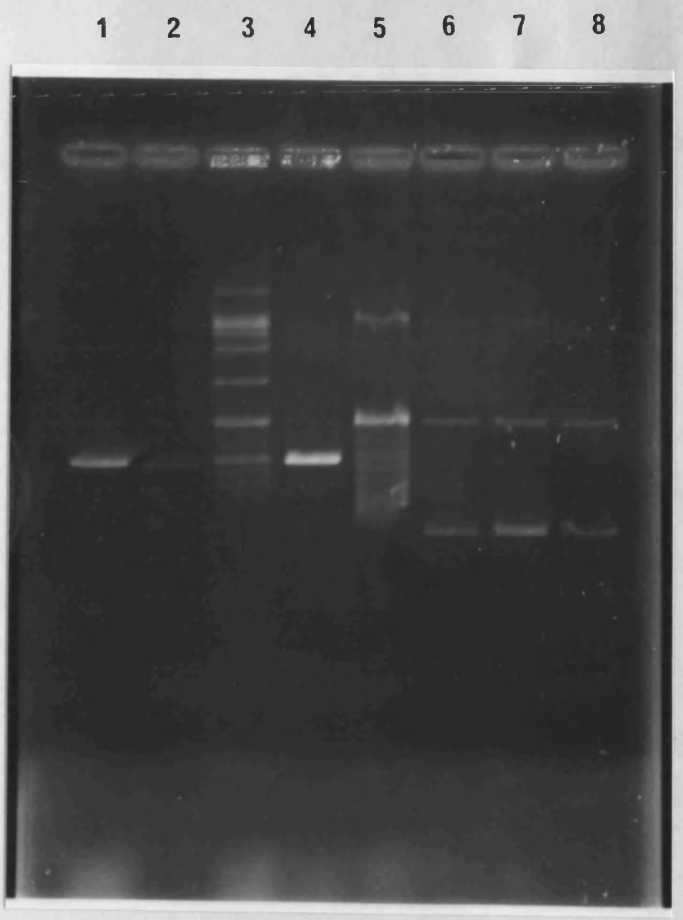

Fig. 4.5. Electrophoretic separation of SphI restricted, alkaline phosphatase-treated pBR322 DNA, + DNA Ligase (Lane 1) - DNA Ligase (Lane 2), SphI restricted pBR322 DNA + DNA Ligase (Lane 3), - DNA Ligase (lane 4). Lanes 5 - 8 as 1 - 4 but without SphI restriction.

4) Ligation of λdgal λ /SphI with pBR322/SphI/AP. The following reaction mixture was prepared, and incubated at 14°C for 20 hours:-

pBR322/SphI/AP	5 µl
λdgal λ /SphI	5 µl
10x ligation buffer	3 µl
100mM DTT	3 µl
6mM ATP	3 µl
T4 DNA ligase (1 unit/µl)	2 µl
H_2O	9 µl

5) Preparation of AS46 cells competent for transformation (adapted from Maniatis et al., 1982). Strain AS46 was grown overnight in LB broth supplemented with 5mM $CaCl_2$ at 37°C. 100 ml of pre-warmed, supplemented LB broth, in a 250 ml flask, was inoculated with 1 ml of the overnight culture. The cells were grown with vigorous shaking until an OD_{470} of 0.5 was reached (approximately 5 x 10^7 cells/ml). The culture was chilled on ice for 10 minutes, and then centrifuged at 2,500 g for 20 minutes at 4°C. The supernatant was discarded, and the cells resuspended in half the original culture volume of an ice-cold, sterile solution of 50mM $CaCl_2$ and 10mM Tris.Cl [pH 8.0]. The cell suspension was placed in an ice-bath for 15 minutes, before being centrifuged and resuspended in $^1/_{15}$ of the original culture volume of ice-cold 50mM $CaCl_2$ and 10mM Tris.Cl [pH 8.0]. 0.2 ml aliquots were dispensed into pre- chilled tubes, and stored at 4°C for 18 hours.

6) Transformation of competent AS46 cells (adapted from Maniatis et al., 1982). The ligation reaction mixture was diluted 10-fold with

ligation buffer, and 30 ul aliquots of this mixture dispensed into each tube containing 0.2 ml of competent AS46 cells. These were stored on ice for 30 minutes, before being transferred to a 42°C water-bath for 2 minutes. One ml of pre-warmed LB broth was added to each tube, which were then incubated at 37°C for 1 hour. After this time, which allowed for expression of plasmid-encoded ampicillin resistance, 3 ml of LB broth, supplemented with 67 µg/ml ampicillin, was added to each tube (resulting in a final ampicillin concentration of 50 µg/ml). The tubes were incubated at 37°C for a further 24 hours. Eight out of 10 tubes were turbid, indicating the presence of ampicillin-resistant E. coli. There was no growth in the tube containing competent cells only, indicating that the resistant cells had probably not arisen from selection of a spontaneous Ap^R mutant.

7) Selection and isolation. One ml of the 24 hour transformation mixture was centrifuged and resuspended in M9 salts solution to approximately 1 x 10^8 cells per ml. Ten ml of the suspension was exposed to 0.5 Jm^{-2} of 254 nm UV radiation and 2 hours of broad-band photoreactivating light. This treated suspension was diluted into 100 ml of pre-warmed nutrient broth (Oxoid), supplemented with 50 µg/ml ampicillin and 15 µg/ml tetracycline HCl, and shaken at 37°C for 24 hours. The UV radiation/ photoreactivation treatments were repeated twice, after which appropriate dilutions were plated onto the surface of antibiotic-supplemented, nutrient agar plates (Oxoid). Sixty three colonies were replicated onto the surface of three supplemented nutrient agar plates. Plate 1 was exposed to 45 Jm^{-2} of 254 nm UV radiation, Plate 2 was UV-irradiated and photoreactivated for 2

hours, and Plate 3 was the control. Of these colonies, 8 appeared to have some photoreactivating enzyme activity. One clone, numbered AS46/pAS01, was chosen for further investigation. This plasmid was extracted from AS46/pAS01 by the 'mini-prep' technique, and used to transform competent cells of DY326 and AS44. In addition, strains AS46, DY326 and AS44 were transformed with the host plasmid, pBR322. These three strains were used as controls in the *in vivo* photoreactivation experiments described below.

Agarose gel electrophoresis of the supercoiled plasmid, pAS01, indicated a molecular weight of approximately 12.4-kbp, suggesting that the gene was possibly within a partial digest of the 7- and 1-kbp novel *SphI* fragments.

4.10 Photoreactivation of AS46/pAS01 and DY326/pAS01 in vivo.

Strains AS46/pAS01, AS46/pBR322, DY326/pAS01 and DY326/pBR322 were grown in the dark at 37^{o}C in the usual manner. Twenty four hour secondary cultures were harvested and resuspended in M9 salts solution to approximately 1 x 10^{7} colony forming units/ml. The cell suspensions were exposed to graded fluences of 254 nm UV radiation; the surviving fraction being reduced to approximately 1 x 10^{-4}. The inactivation parameters are included in Table 4.3, and the data pertaining to these survivor curves are shown in Tables A4.49-54. Cell suspensions which had been reduced to 1 x 10^{-4} were held in the dark at 25^{o}C for 20 minutes, before being exposed to continuous photoreactivating light at a fluence rate of 17.6 Wm^{-2} for up to 3 hours. The cell survival was assayed in the usual manner on Oxoid nutrient agar plates. The photoreactivation plots

Table 4.3. 254 nm UV inactivation parameters for transformed AS46 and DY326 at 25°C

STRAIN/ GROWTH TEMP.	Expt. No.	SLOPE (log 10)	Std. ERROR of SLOPE	INTERCEPT (log 10)	Std. ERROR of INTERCEPT	'k' (Jm^{-2})	'n'
AS46/pBR322 37°C	49a	-8.471	0.209	0.211	0.071	19.50	1.62
	49b	-8.116	0.450	0.145	0.017	18.69	1.40
	Mean	-8.294	0.251	0.178	0.047	19.10	1.51
AS46/pBR322 26°C	50a	-8.626	0.127	0.186	0.042	19.86	1.53
	50b	-8.583	0.104	0.219	0.034	19.71	1.66
	Mean	-8.605	0.030	0.202	0.023	19.81	1.59
AS46/pAS01 37°C	51a	-8.349	0.244	0.242	0.020	19.22	1.74
	51b	-8.430	0.392	0.157	0.015	19.41	1.44
	Mean	-8.390	0.057	0.200	0.060	19.31	1.58
AS46/pAS01 26°C	52a	-8.374	0.110	0.147	0.042	19.28	1.40
	52b	-8.034	0.310	0.184	0.117	18.50	1.53
	Mean	-8.204	0.240	0.166	0.026	18.89	1.46
DY326/pBR322 37°C	53a	-8.073	0.107	0.050	0.036	18.59	1.12
	53b	-7.949	0.161	0.084	0.047	18.30	1.21
	Mean	-8.011	0.087	0.067	0.024	18.44	1.17
DY326/pAS01 37°C	54a	-8.054	0.124	0.120	0.042	18.54	1.32
	54b	-8.282	0.307	0.142	0.068	19.07	1.39
	Mean	-8.168	0.161	0.131	0.016	18.80	1.39

for AS46/pAS01 and AS46/pBR322 are shown in Fig. 4.6. These data have been analysed by the (1-P) and 'lethal hit' methods, and are shown in these forms in Fig. 4.7. The rate constants from these analyses, and those associated with DY326/pAS01 and DY326/pBR322 are included in Tables 4.4-5. In addition, the UV inactivation and photoreactivation experiments were repeated with AS46/pAS01 and AS46/pBR322 after growth at 26^{o}C. The survival parameters are included in Table 4.3, and the photoreactivation rate parameters are included in Tables 4.4-5. The data pertaining to these experiments are included in Tables A4.55-60, respectively.

There was no significant difference in either the intercept or inactivation constants between the pairs of strains transformed with pBR322 and pAS01, respectively (Table 4.3). An analysis of covariance of the slope and intercept values for AS46/pBR322 and AS46/pAS01 gave values for the change in F-ratio of 3.911 with 1 and 27 degrees of freedom, and 3.468 (1,26 d.f.) for the slope and intercept, respectively. The critical values are 4.21 and 4.23, respectively, at the 5 per cent confidence interval. Therefore, it may be concluded that the presence of plasmid pAS01 did not result in a significant variation in the sensitivity of either AS46 or DY326 after 254 nm UV inactivation. It will be seen from Fig. 4.6 that transformation of AS46 with plasmid pBR322 did not result in any photoreactivation of 254 nm UV-induced damage after growth at 37^{o}C. However, transformation with plasmid pAS01 resulted in a marked photoreactivable response, having a value of approximately 2 x 10^{-5} s^{-1} for the rate constant k_1 (Table 4.4), and 1.3 x 10^{-2} min^{-1} for the repair probability α_2, determined by 'lethal hit' analysis. This indicated that a gene present on plasmid pAS01 either coded for a protein having photolyase activity, or in some

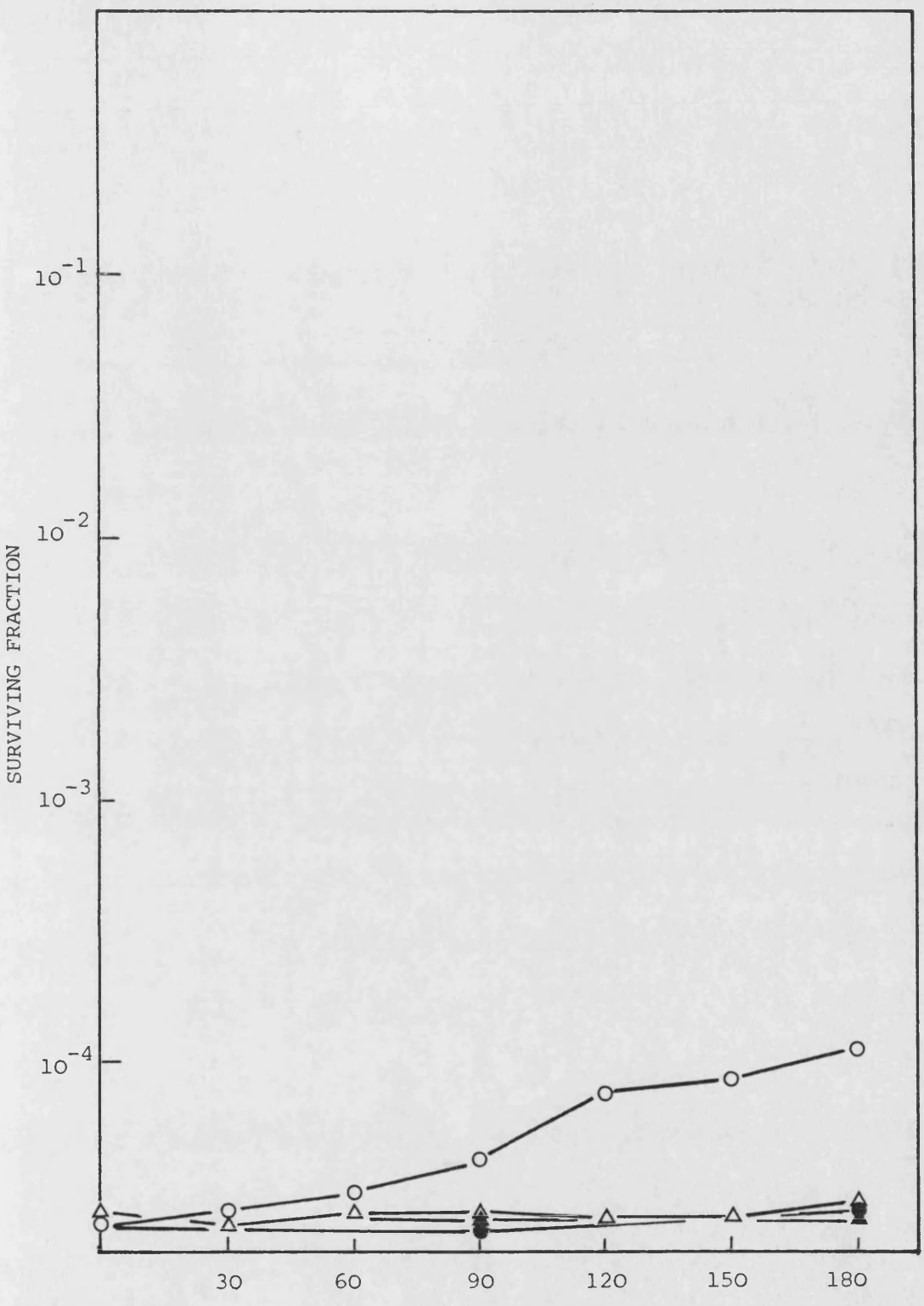

Fig.4.6. Photoreactivation at 25°C of 254 nm inactivated AS46/pBR322 (△,▲dark control) and AS46/pASOl (○,●dark control) at a photoreactivating light fluence rate of 17.6 Wm^{-2}.

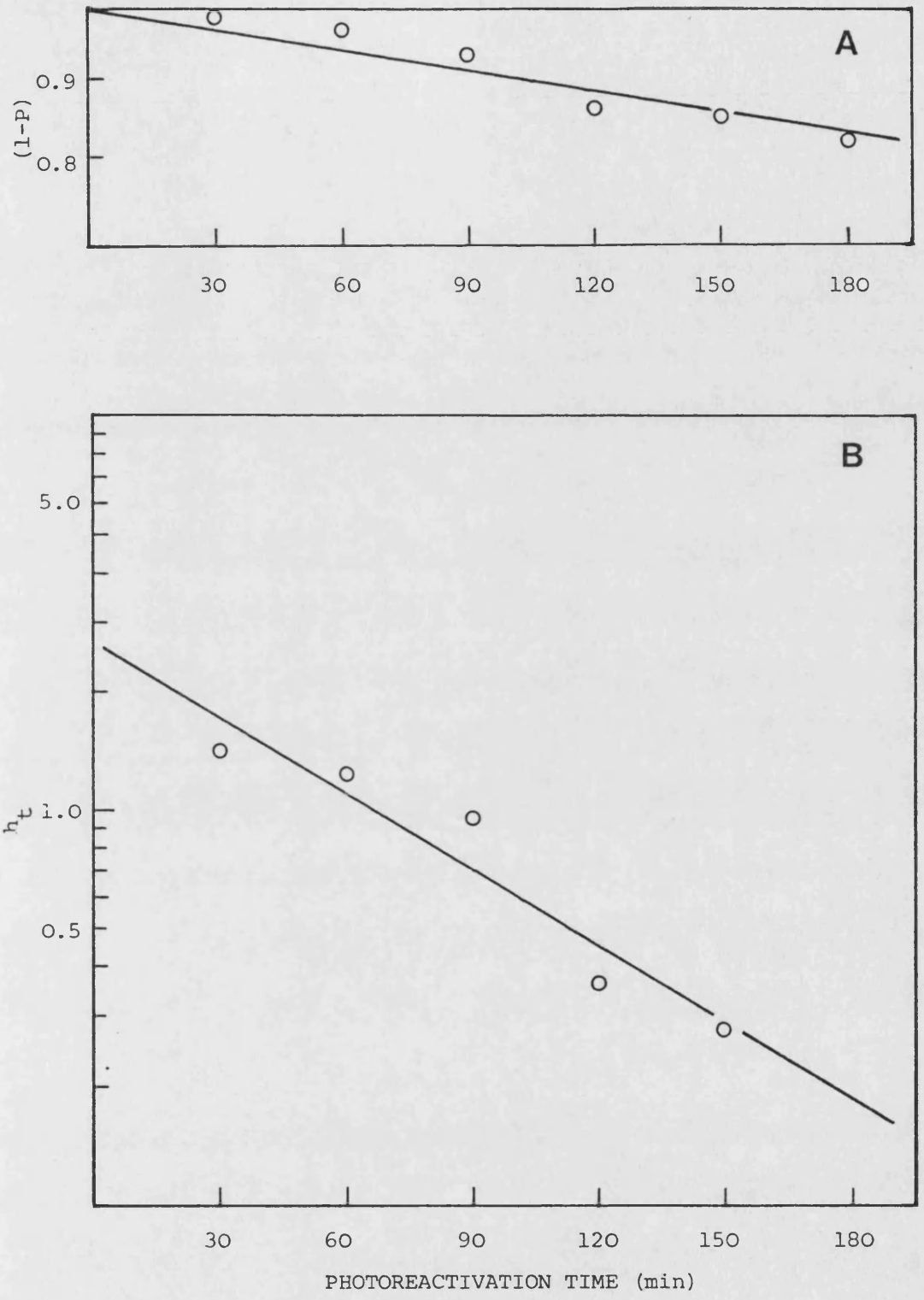

Fig. 4.7. 1-P analysis (Panel A) and 'lethal hit' analysis (Panel B) of the photoreactivation rate at 25°C of 254 nm inactivated AS46/pASO1.

Table 4.4. Photoreactivation rate constants and estimates of the number of photoreactivating enzyme-substrate complexes after 254 nm UV inactivation at 25°C.

Strain/ Growth Temp.	Expt. No.	Rate Constant k_1 ($\times 10^{-5}$) (s^{-1})	Number of PRE Molecules ($\times 10^{-2}$)
AS46/pBR322	55a	~0*	~0*
37°C	55b	~0*	~0*
AS46/pBR322	56a	3.96	2.2
26°C	56b	3.42	1.9
AS46/pAS01	57a	2.03	1.13
37°C	57b	1.95	1.08
AS46/pAS01	58a	6.10	3.39
26°C	58b	6.02	3.38
DY326/pBR322	59a	3.62	2.01
37°C	59b	3.14	1.74
DY326/pAS01	60a	1.88	1.04
37°C	60b	1.92	1.07

* - not measurable.

Table 4.5 Repair probability α derived from 'lethal hit' analysis of photoreactivation of 254 nm UV-induced damage at 25°C.

Strain/Growth Temp.	Expt. No.	Repair Probability ($\times 10^{-2}$) (min^{-1})
AS46/pBR322/37°C	55a	~0*
	55b	~0*
AS46/pBR322/26°C	56a	2.1
	56b	2.3
AS46/pAS01/37°C	57a	1.5
	57b	1.1
AS46/pAS01/26°C	58a	4.0
	58b	3.8
DY326/pBR322/37°C	59a	1.9
	59b	1.9
DY326/pAS01/37°C	60a	1.5
	60b	1.8

* - not measurable.

way stimulated the cellular photolyase activity of AS46, perhaps by completing an interrupted biochemical pathway. To test this hypothesis, DY326/pBR322 and DY326/pAS01 were UV-inactivated and photoreactivated. The presence of pAS01 did not increase the photoreactivable response beyond that measured with DY326/pBR322; indeed, the rate constant k_1, and repair probability values were slightly decreased (Tables 4.4-5). These data strongly suggested that the gene presumed to be present on pAS01 did not code for a protein with photolyase activity, since we would expect to see a similar increase in the photoreactivable response of both AS46 and DY326. However, we cannot rule out the possibility that the gene is the subject of feedback control, and so not expressed in DY326. These data do indicate that the plasmid may complement a cellular defect in photolyase activity of AS46, which results in the cell having a similar photoreactivability to DY326. Thus, a gene present on pAS01 may code for the 'effector' molecule postulated in Part III to increase the activity of the *phrB* gene product. Therefore, we have partially reversed the defect in photolyase activity of AS46 by cloning restriction fragments from the *gal-attλ* region, and so it seems likely that the proposed *phrA* gene product does have an effect on cellular photolyase activity. To further test this hypothesis, the photoreactivable responses of AS46/pBR322 and AS46/pAS01 were measured after growth at 26°C. Transformation with plasmid pAS01 resulted in a 64 per cent increase in the rate constant k_1 (Table 4.4) and a 77 per cent increase in the repair probability α (Table 4.5), compared with AS46/pBR322. Unfortunately, it was not

possible to make quantitative comparisons between these data and those presented in Part III, because the Anscomatic/ Sylvania FFX light source and housing had to be replaced with a Leitz Pradovit projector fitted with a 250W quartz-iodine lamp. However, it should be noted that the biphasic repair kinetics based on the 'lethal hit' analysis of the photo-repair of DY326 after growth at 26°C (Section 3.6.2 Part III) were not observed with AS46/pAS01 grown under similar conditions.

4.11 Photoreactivation of AS44/pAS01 and AS44/pBR322 in vivo

Having established that a gene presumed to be present on pAS01 caused a photoreactivable response in AS46 to a level similar to that of DY326 after 254 nm UV inactivation, but does not affect the response of the latter, it was of interest to determine if the plasmid would have any effect in the *phrB*$^+$ Δ(*gal-chlA*) *recA56* background of AS44.

Flash Photolysis

Twenty four hour secondary cultures of AS44/pBR322 and AS44/pAS01 were harvested and resuspended in M9 salts solution in the usual manner. The cell suspensions were given graded fluences of 254 nm UV radiation and assayed for cell survival and flash photoreactivation, as described in Section 3.2, Part III. The survival curves are shown in Figs. 4.8 to 4.9. The 254 nm UV inactivation and flash photo-reactivation curves were analysed by least squares linear regression analysis, beyond a fluence of 0.1 and 0.16 Jm^{-2},

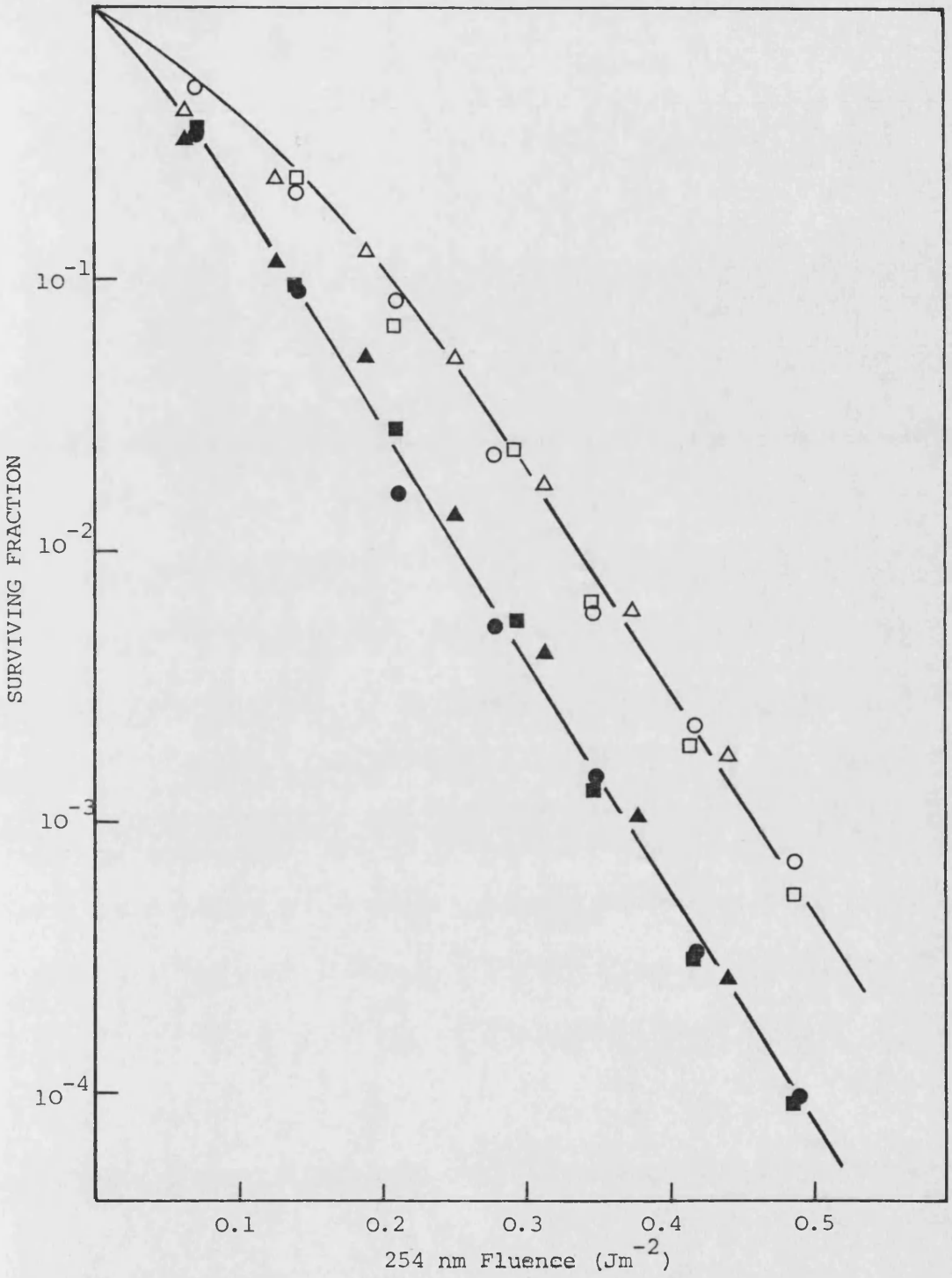

Fig. 4.8. Replicate survival curves for AS44/pBR322 grown at 37°C after 254 nm inactivation (closed symbols) and a single light flash (open symbols) at 25°C.

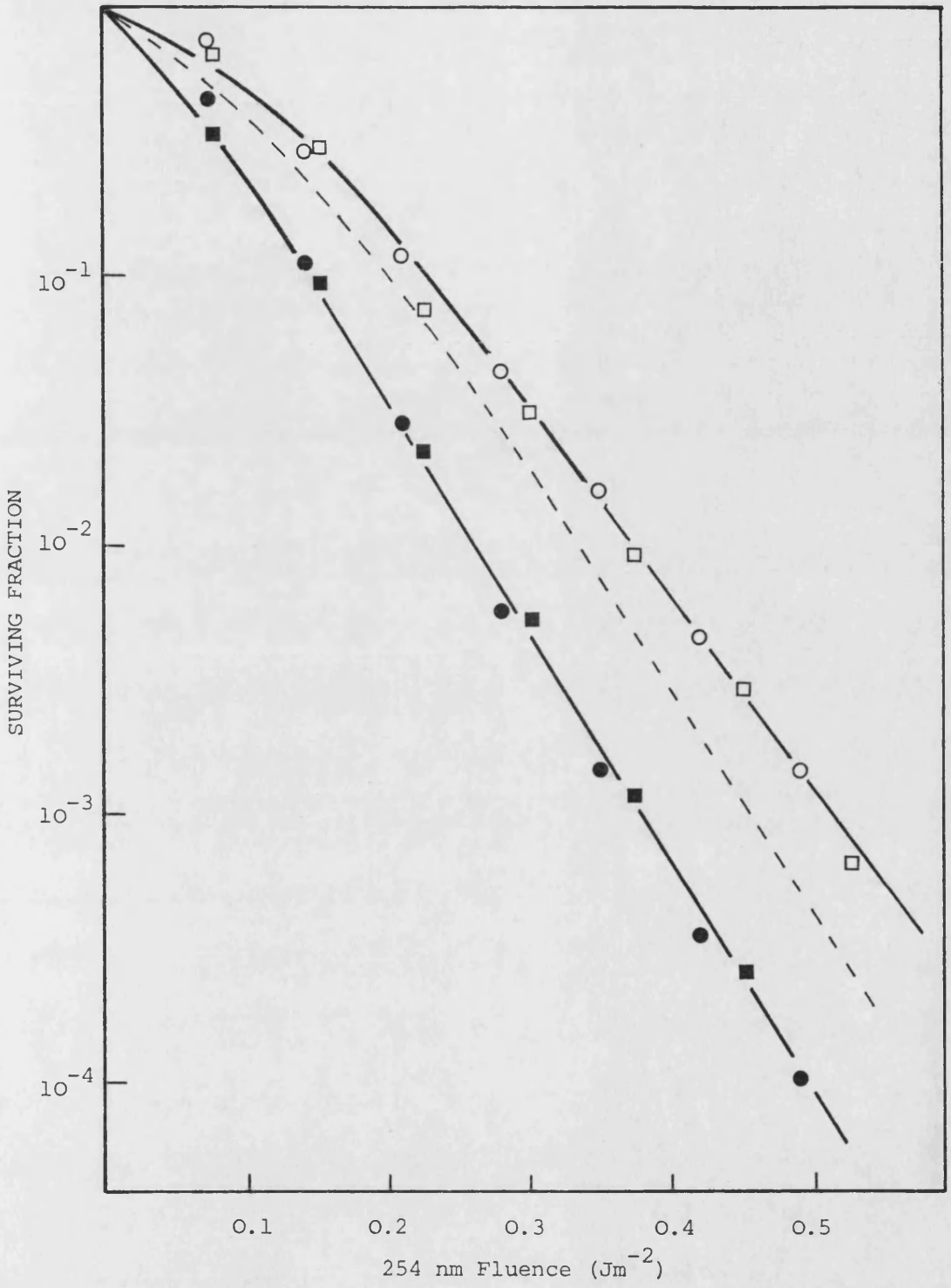

Fig. 4.9. Replicate survival curves for AS44/pASO1 grown at 37°C after 254 nm inactivation (closed symbols) and a single light flash (open symbols) at 25°C. The dashed line represents the flash response of AS44/pBR322.

respectively. The survival parameters are included in Table 4.6, and the data pertaining to them are included in Tables A4.61-62. The survival parameters after 254 nm UV inactivation were compared by an analysis of covariance. The change in F-ratio was found to be 2.244 (1,27 d.f.) and 0.011 (1,26 d.f.) for the intercept and slope location, respectively. The critical values at the 5 per cent confidence interval are 4.21 and 4.23, respectively, indicating no significant difference between the strains. However, when comparing the linear portion of the flash photoreactivation survival curves, by an analysis of covariance, the change in F-ratio was 46.722 (1,23 d.f.) and 65.565 (1,22 d.f.) for the intercept and slope location, respectively. These values were highly significant, even at the 0.5 per cent confidence interval, where the critical values are 9.63 and 9.73, respectively. Therefore, it may be concluded that the presence of plasmid pAS01 resulted in a statistically significant increase in the fluence decrement caused by a single flash of photoreactivating light. The mean values for the fluence decrement for AS44/pBR322 and AS44/pAS01 were 0.088 and 0.141 Jm^{-2}, respectively. These fluence decrements resulted in values of 4.66 and 7.47 for the estimates of the average number of PRE-substrate complexes per cell. Thus, the presence of pAS01 resulted in a 1.6-fold increase in the number of PRE-substrate complexes per cell. It should be noted that the flash response of AS44/pBR322 was consistently lower than that measured for AS44, for which there was no available explanation (compare fluence decrements of 0.088 and 0.143 Jm^{-2}, respectively).

Table 4.6. 254 nm UV inactivation parameters for transformed AS44 at 25°C

STRAIN/ TREATMENT	Expt. No.	SLOPE (log 10)	Std. Error of SLOPE	INTERCEPT (log 10)	Std. Error of INTERCEPT	'k' $(Jm^{-2})^{-1}$	'n'
AS44/pBR322 254 nm	61a	-8.533	0.213	0.102	0.071	19.65	1.26
	61b	-8.950	0.268	0.272	0.090	20.61	1.87
	61c	-8.498	0.322	0.242	0.098	19.57	1.75
	Mean	-8.706	0.141	0.218	0.047	20.04	1.65
Flash	61a	-7.438	0.251	0.449	0.091	17.13	2.81
	61b	-7.809	0.430	0.545	0.156	17.98	3.51
	61c	-7.306	0.216	0.525	0.070	16.82	3.35
	Mean	-7.634	0.242	0.543	0.085	17.58	3.49
AS44/pAS01 254 nm	62a	-8.752	0.169	0.258	0.057	20.15	1.81
	62b	-8.664	0.082	0.308	0.03	19.95	2.03
	Mean	-8.708	0.062	0.283	0.035	20.05	1.92
Flash	62a	-6.858	0.198	0.542	0.072	15.79	3.48
	62b	-6.780	0.343	0.470	0.133	15.61	2.95
	Mean	-6.844	0.188	0.515	0.071	15.75	3.27

The presence of the plasmid may divert the protein synthetic machinery away from cellular protein synthesis, but there did not seem to be any evidence of specific inhibition of photolyase activity. However, the relative increase in 'flash-fluence decrement' of AS44/pAS01 compared with AS44/pBR322 approached the 2-fold difference in flash response between AB2480 and AS44, noted in Section 3.2, Part III.

Continuous photoreactivation.

Twenty four hour secondary cultures of AS44/pBR322 and AS44/pAS01 were harvested in the usual manner, and reduced to approximately 1×10^{-4} surviving fraction with an appropriate fluence of 254 nm UV radiation. After a holding period at 25°C in the dark for 20 minutes, the cells suspensions were exposed to continuous photoreactivating light. A single high-intensity light flash was given at the commencement of each photoreactivating light treatment, as described in Section 3.3, Part III. The photoreactivation plots from one of two replicate experiments are shown in Fig. 4.10. These data have been analysed by the (1-P) and 'lethal hit' methods, and are shown in these forms in Figs. 4.11-12. The photoreactivation rate parameters derived from least squares linear regression analysis of the linear portion of each curve (the time required to reduce the fraction of photoreactivable lesions to 0.4 for the (1-P) analysis), are included in Tables 4.7-8. The data pertaining to these parameters are included in Tables A4.63-64.

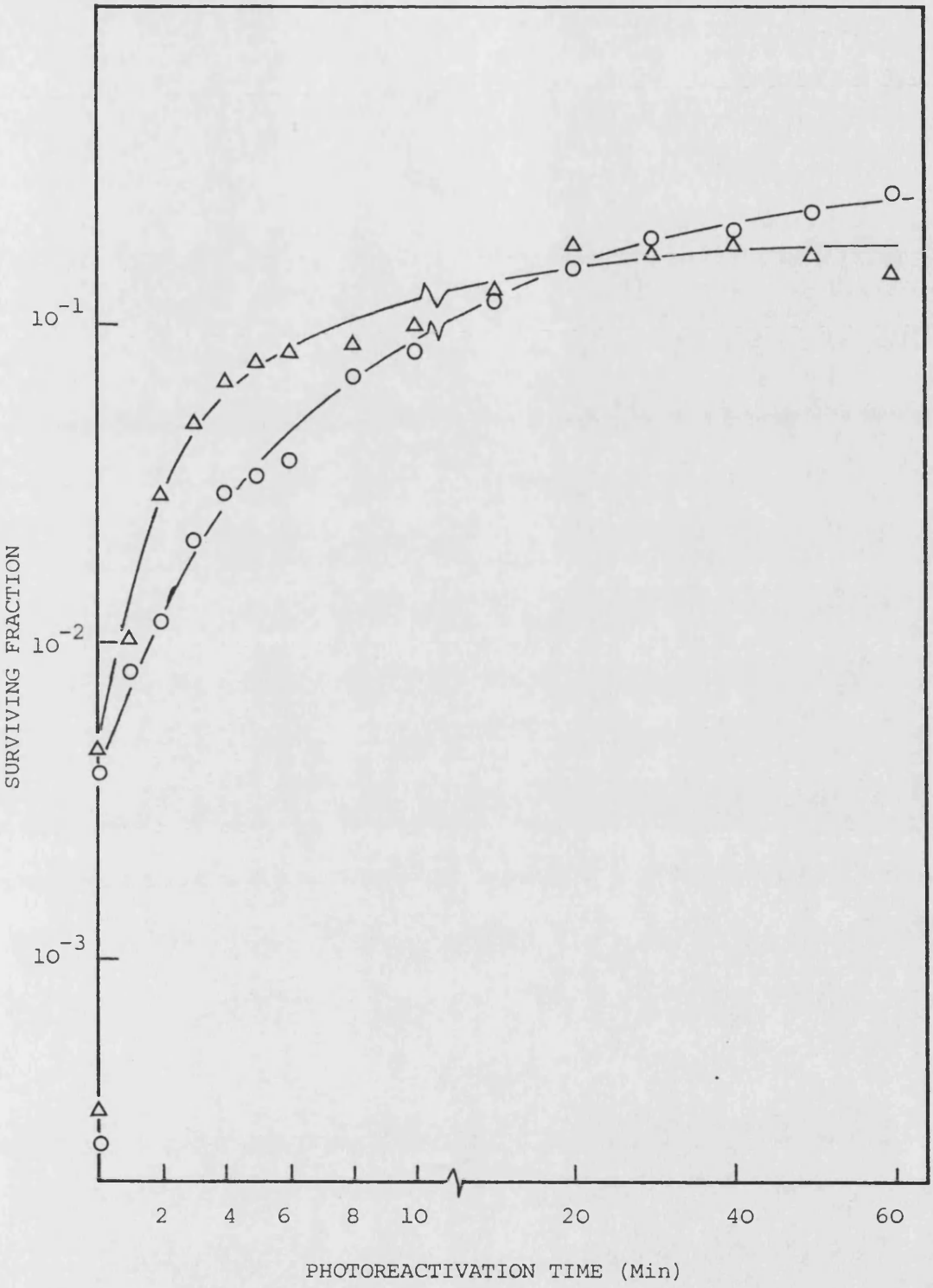

Fig. 4.10. Photoreactivation at 25°C of 254 nm inactivated AS44/pBR322 (O) and AS44/pASO1 (Δ) at a photoreactivating light fluence rate of 17.6 Wm^{-2}.

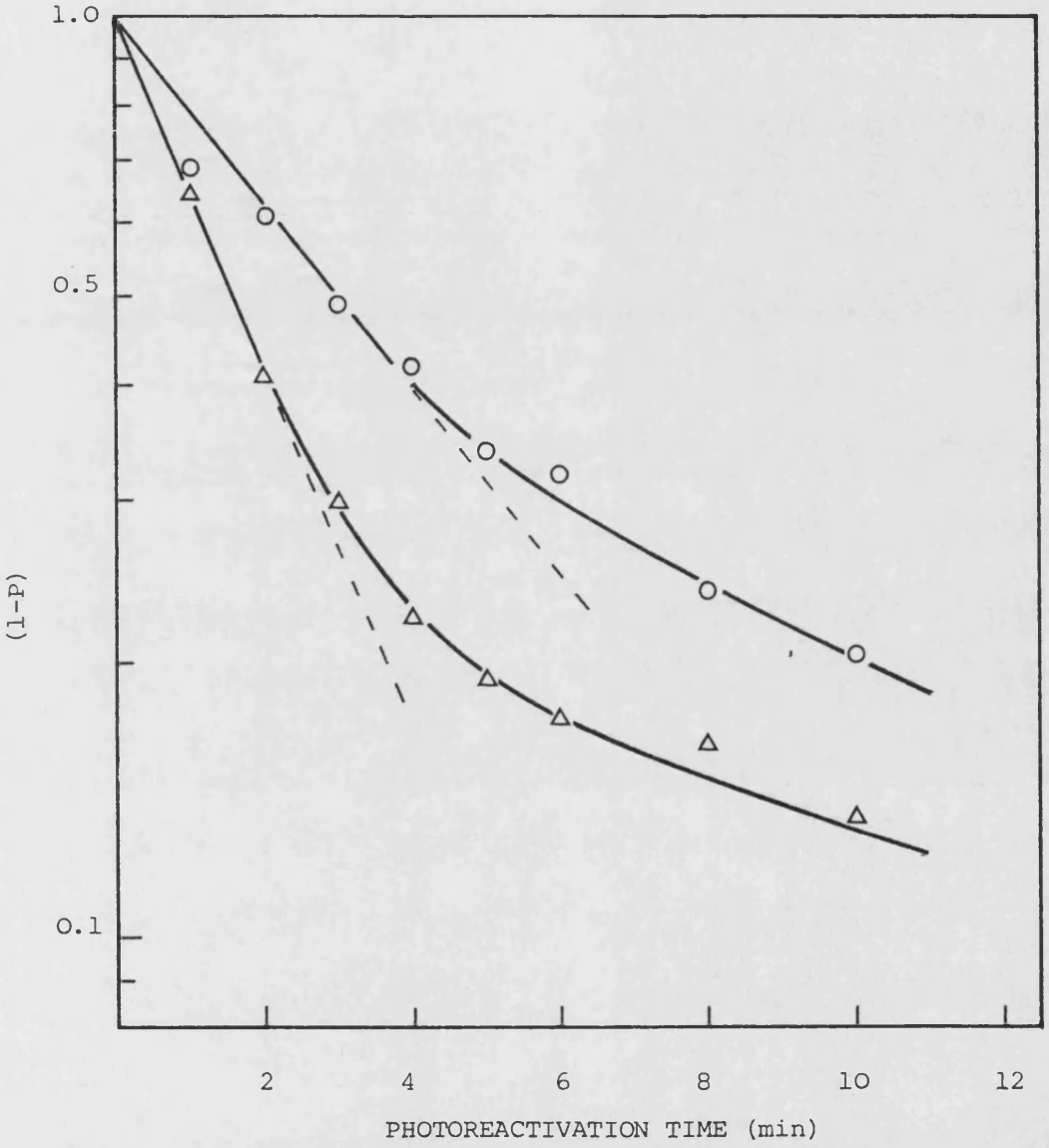

Fig. 4.11. 1-P analysis of the rate of photoreactivation at 25°C of 254 nm inactivated AS44/pBR322 (O) and AS44/pASO1 (Δ).

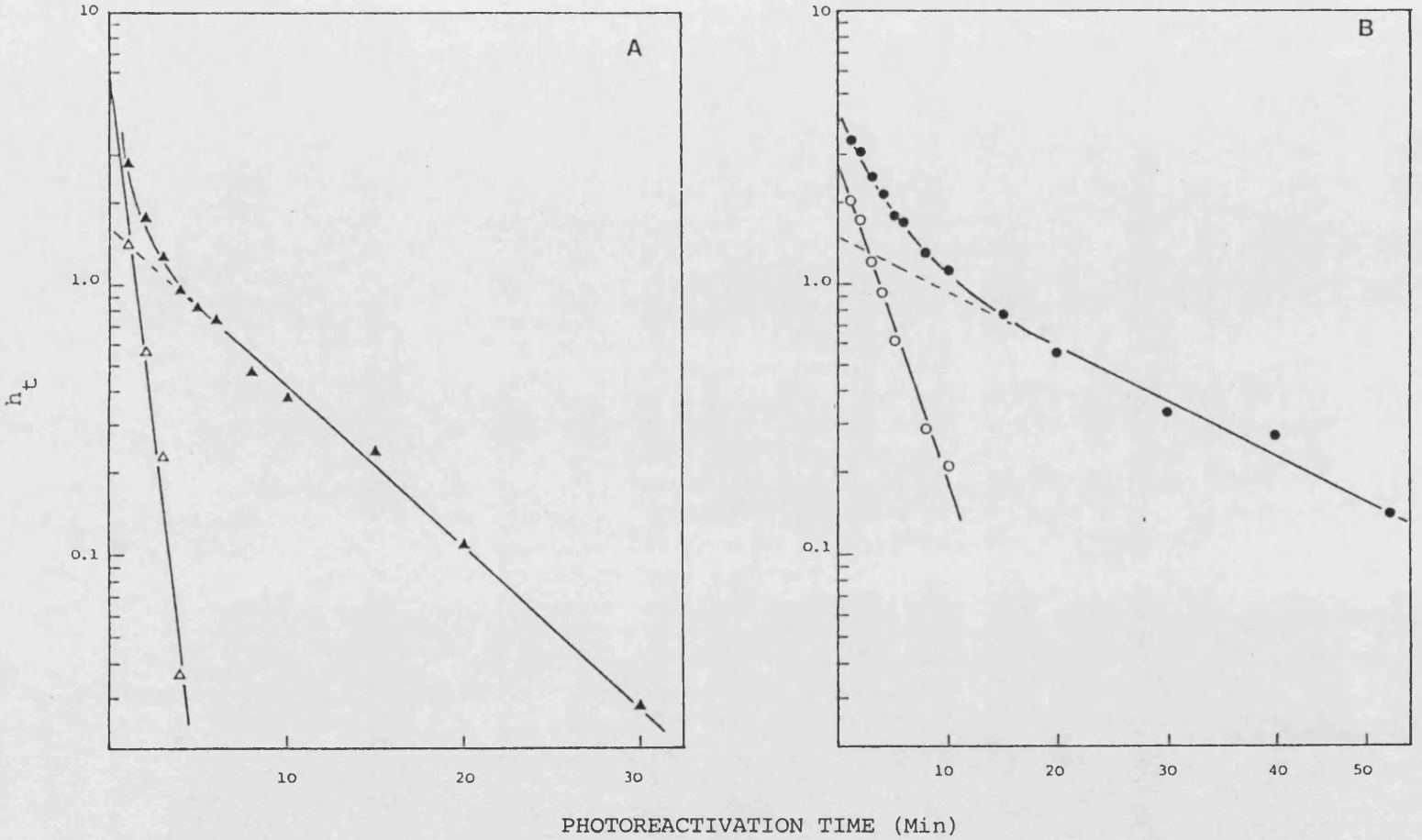

Fig. 4.12. Lethal hit analysis of the rate of photoreactivation at 25°C (closed symbols) of AS44/pASO1 (Panel A) and AS44/pBR322 (Panel B) and after subtraction of the slow component (open symbols).

Table 4.7. Photoreactivation rate constants and estimates of the number of photoreactivating enzyme-substrate complexes after 254 nm UV inactivation at 25°C.

Strain	Expt. No.	Rate constant ($\times 10^{-3}$) (s^{-1})	Number of PRE Molecules
AS44/pBR322	63a	3.68	2.04
	63b	3.08	1.71
AS44/pAS01	64a	7.37	4.09
	64b	7.02	3.90

Table 4.8. The repair probabilities derived from 'lethal hit' analysis of photoreactivation of 254 nm UV-induced damage at 25°C.

Strain	Expt. No.	α_1 (min^{-1})	α_2 (min^{-1})
AS44/pBR322	63a	-0.267	-0.047
	63b	-0.198	-0.052
AS44/pAS01	64a	-1.185	-0.133
	64b	-1.140	-0.112

Transformation of AS44 with plasmid pAS01 resulted in a 2-fold increase in the photoreactivation rate constant k_1 compared with AS44/pBR322. Comparing the repair probabilities α_1 and α_2, the presence of pAS01 increased each by 5- and 2-fold, respectively. Although quantitative comparisons with the data for AS44 and AB2480 presented in Part III were not strictly permissible because of the different photoreactivating light systems, it should be noted that the repair probabilities, α_1 and α_2, were 1.7- and 2.5-fold greater in AB2480 compared with AS44. Therefore, it may be concluded that pAS01 increased the photoreactivable response of AS44 to a level comparable with AB2480, by a disproportionate increase in the two repair probabilities.

As with the work described using AS46, it has been shown that transformation of AS44 with a plasmid containing recombinant DNA from the gal-attλ region partially complements the photoreactivation defect attributed to the Δ(gal-attλ) deletion.

In summary, the data presented in this section demonstrated the construction of a Lambda specialised transducing 'phage carrying the galactose operon, and its use in cloning experiments to isolate a plasmid carrying the proposed phrA gene. The specialised λdgalλ transducing 'phage exhibited galactose transducing activity in vivo, and the isolated DNA had three novel SphI restriction fragments. After three cycles of UV inactivation, photoreactivation, and replica plating, a clone numbered AS46/pAS01 was isolated. The plasmid had an approximate molecular weight of 12.4-kbp, suggesting that the cloned gene was possibly within a partial

digest of the 7- and 1-kbp novel restriction fragments. Strain AS46/pAS01 exhibited a photoreactivable response after 254 nm UV inactivation, which was not observed with AS46/pBR322. However, there was no significant difference between the photoreactivable responses of either DY326/pAS01 or DY326/pBR322, suggesting that the plasmid does not code for a photolyase protein, but functions to increase the activity of the *phrB* gene product (or partially active *phrB*/unknown gene product in DY326). Strain AS44/pAS01 exhibited an increase in both the single flash response and rate of photoreactivation compared with AS44/pBR322, once again indicating that a gene cloned from the *gal-attλ* region was capable of increasing the photoreactivable response of a Δ (*gal-chlA*) strain. These data may be taken as further evidence for the presence of a locus within the *gal-attλ* region which markedly influences the photoreactivable response of 254 nm UV-inactivated *E. coli* K-12. It does, however, seem unlikely that the gene product has any marked photolyase activity; rather it functions to either increase the pool of active photolyase molecules, or to increase the affinity of the photolyase molecule for its substrate, perhaps by completing an interrupted biochemical pathway. It is not readily apparent why the photoreactivable responses of strains transformed with pAS01 did not reach those of *phrA*$^+$ strains. However, it should be noted that the *phrA*$^+$ strains were not isogenic, and so quantitative comparisons were not strictly permissible. Until pAS01 has been further analyzed, any reasons must remain speculative.

These data suggest a number of additional experiments,

which are listed below:-

1). Restriction endonuclease mapping and isolation of the gene on the plasmid by transposon insertional inactivation.

2). Sequence analysis of pAS01 to identify the open reading frame and presence of the promoter (if present in the restriction fragment), and comparison of the degree of homology with the *phrB* gene, and the consensus sequence for the *E. coli* promoter.

3). Identification of the plasmid-coded proteins, and molecular weight analysis on SDS-polyacrylamide gels.

4). Subclone the gene into an inducible, high-expression vector. Determine if the gene product has inherent photolyase activity, or if it increases the activity of the *phrB* gene product *in vitro*.

5). Isolation of a transposon insertion in the cloned *phrA* gene, and its use to construct an isogenic series of strains having point mutations in *phrA* and/or *phrB*.

CONCLUDING DISCUSSION

The work reported in this thesis is centred on the debate of whether there are multiple photolyase molecules present in E. coli K-12. As discussed previously, two loci, phrA and phrB, have been proposed for the genetic control of photoreactivation by Sutherland and Hausrath (1979). They suggested that the phrA gene or gene product contained information affecting the functional properties of the phrB gene product. However, the phrA gene also had apparent photoreactivating enzyme activity in vitro, when isolated from a strain lysogenic for a λdgal specialised transducing 'phage (Snapka and Sutherland, 1980). The turnover number of this preparation (pyrimidine dimers per minute) was approximately 1000-fold lower than that of the cloned phrB gene product, leading Sancar et al. (1984b) to speculate that the PRE activity measured by Snapka and Sutherland (1980) may be due to low-level contamination with the phrB gene product. In addition to this speculation, both Youngs and Smith (1978), and Sancar and Rupert (1978a), failed to show any difference in photoreactivation between phrA$^+$ and phrA deletion mutants, although no kinetic analyses have been published. Therefore, it was of interest to determine if there was any in vivo evidence in favour of the existence of multiple photolyase molecules. The experiments of Sutherland and Hausrath (1979) were repeated using strains AB1886, SA206, DY314 and AS45 (Appendix 1), with broad-band photoreactivating light in the range 350 - 420 nm. The kinetic analyses revealed a reaction rate 70 per cent slower for SA206 Δ(gal-chlA) compared with the phr$^+$ strain A1886. Whilst quantitative comparisons between these strains must be uncertain because of their non-isogenicity, it was apparent that the rate of photorepair was significantly reduced in

a strain deleted at the proposed phrA locus. However, consideration must be given to the functions of other genes within the gal to attλ region, which may affect the rate of photoreactivation. Of particular interest is the hemF locus, coding for an enzyme which catalyses the conversion of coproporphyrinogen III to protoporphyrin IX in the haem biosynthetic pathway. Cox and Charles (1973) isolated a hemF mutant, and demonstrated coproporphyrinogen accumulation, haem deficiency and respiratory deficiency. However, this was isolated as a secondary mutant of a strain which accumulated protoporphyrin IX. That the Δ(gal-chlA) strains may be partially respiratory-deficient is of particular importance because Tyrrell (1973b) has shown that anaerobic growth conditions suppresses the production of PRE molecules. However, comparison of colony morphologies and catalase activities of the strains did not show any significant differences (data not shown).

A small photoreactivable response was noted in strain DY314 (phrB) after 254 nm UV irradiation, which was absent in strain AS45 (Δ(gal-chlA),phrB), suggesting a second locus coded for photoactive protein in addition to the phrB locus. To further characterise these responses, and to rule out any effects due to recombination repair, recA derivatives of the four strains were used; isolation being by bacteriophage P1-mediated transduction where necessary. The photoreactivable responses of these strains were characterised by high-intensity flash-photolysis and continuous broad-band photoreactivating light treatment after 254 nm UV and acetophenone-sensitized 313 nm UV irradiation.

After 254 nm UV irradiation, the inactivation parameters of AB2480, (uvrA recA); AS44, (Δ(gal-chlA) recA); DY326, (uvrA uvrB phrB recA) and AS46 (Δ(gal-chlA) phrB recA) were not significantly

different, indicating that in the totally dark-repair-deficient background, the presence of a *phr* mutation does not affect survival when assessed in the absence of photoreactivating light. The rate of photoreactivation of AS44 was 30 per cent that of AB2480 after 254 nm UV irradiation, suggesting that a gene in the *gal* to *attλ* region may have an affect on the rate of photoreactivation *in vivo*. There was also evidence of photoreactivation in DY326, a strain which has the *phrB* mutation transduced from the photoreactivationless mutant *E. coli* B*phr*. This was in contrast to previous reports using *phrB* strains which have shown no photoreactivation of colony formation (Harm and Hillbrandt, 1962) or transforming DNA (Setlow, 1964). However, Setlow (1964) demonstrated that pre-incubation of *H. influenzae* transforming DNA with an extract of *E. coli* B*phr* in the light showed an increase in the initial rate of photoreactivation of transforming ability with yeast extract PRE, as compared with pre-incubation in the dark. Both the rate and extent of photorepair of DY326 were markedly reduced compared with AB2480 and AS44. Since DY326 is totally dark-repair-deficient, it is unlikely that the observed response could be attributed to indirect photoreactivation. Furthermore, no photorepair was observed with 254 nm UV-irradiated AS46, a *recA* derivative of SA206, but which has had the *phrB* of DY314 transduced into it. Thus, there was no light-dependent repair in a strain mutated at both the *phrB* and putative *phrA* loci. It could therefore be argued that this was strong evidence in favour of two photolyase molecules, coded by the *phrA* and *phrB* loci, respectively. However, a photoreactivable response was observed with 254 nm UV-irradiated AS46 after growth at 26°C, indicating that the strain was capable of producing a photoactive protein and

therefore not totally photoreactivation-deficient. This result raises the question whether there is a third phr locus in E. coli, or if the mutant phrB gene product has some temperature-dependent activity. It should be emphasised that decreasing the growth temperature resulted in an increase in the rate of photoreactivation of 254 nm UV-induced damage in all four strains. However, the rate of repair of AS46 ('phrA' phrB) did not approach that of DY326 (phrB), even after growth at 26°C (Table 3.11), indicating that if the mutant phrB gene product does have some photolyase activity, then it is markedly reduced in the putative phrA mutant background. This conclusion is further supported by the slower rate of repair observed with 254 nm UV-irradiated AS44 compared with AB2480. Whilst it could be argued that the small photoreactivable response observed with 254 nm UV-irradiated DY326 (and AS46 after growth at 26°C) could be attributed to a direct photosensitized monomerization reaction, such as those observed with tryptophan-containing oligopeptide (Helene et al., 1978) or the substance SF420 from Streptomyces griseus (Eker et al., 1981), it should be noted that there was no measurable repair below 350 nm. This suggested that the reaction was not mediated by a tryptophan-containing oligopeptide, since in these cases the reaction does not occur above 350 nm. Whilst the chromophoric moiety SF420 from S. griseus cells did bring about photochemical splitting of thymine dimers in the actinic wavelength region for enzymatic photoreactivation (Eker et al., 1981), we would not expect it to exhibit enzymatic properties, such as temperature-dependence. However, the kinetics of photorepair of 254 nm UV-inactivated DY326 did show temperature-dependence over the range 15 to 37°C, resulting in an activation energy term (derived from the Arrhenius

relationship) approximately 25 per cent greater than the values obtained with AB2480 and AS44. The overwhelming conclusion from these data is that the observed photorepair has all the characteristics of photoenzymatic repair, and therefore most likely mediated by a photolyase-like molecule. However, since there were no obvious differences in the measured characterisation of wavelength- and temperature-dependence, it was not possible to conclude whether the response was mediated by a photolyase molecule which is different from the major *phrB*$^+$ gene product or whether the response is a manifestation of a mutant form of the latter. If the former hypothesis is correct, that is, the response is mediated by a photolyase molecule coded by the *phrA*$^+$ gene, then we might reasonably expect to see the effects of both molecules in AB2480, but only that of the *phrB*$^+$ gene product in AS44. The kinetic analyses of the photoreactivation data for 254 nm UV-irradiated AB2480 and AS44 resulted in biphasic reactions when analysed by either the (1-P) (Tyrrell and Davies, 1974) or 'lethal hit' methods (Johnson and Haynes, 1986a). Furthermore, two specific rate constants were derived from the lethal hit analyses; circumstances which Johnson and Haynes (1986a) claim are indicative of the action of two photolyase molecules. The values for AS44 were 35 and 58 per cent of those of AB2480, suggesting that the rate of photo- repair of AS44 is probably not attributable to a simple decrease in the number of PRE molecules. When the growth temperature was decreased to 26^{o}C, the slower rate constant for AB2480 was increased 10-fold, and indeed masked any contribution to the reaction by the faster rate process, whilst the same rate constant for AS44 was only increased 1.7-fold. These data suggest that the repair constants, and hence repair activities of the PRE

molecule(s) present in AB2480 are relatively more able to respond to adverse culture conditions than those in AS44. The most simplistic interpretation of the biphasic kinetic data is that the reaction is either mediated by a single photolyase molecule which has different repair capacities, perhaps towards one or more substrates, or that the reaction is mediated by two photolyase molecules. The suggestion that the biphasic reaction kinetics may be attributable to the different species of cyclobutane-type pyrimidine dimer is particularly attractive since Myles et al. (1987) have shown that the purified 50-kDa photolyase (phrB gene product) binds well to T-T dimers and photolyses them efficiently, whilst T-C, C-T and in particular C-C dimers are neither bound nor repaired efficiently by the enzyme. However, biphasic photoreactivation kinetics were obtained after acetophenone- sensitized 313 nm UV-irradiation of both AB2480 and AS44, indicating that if there is just one type of PRE molecule present, then it must have two repair activities towards an essentially homogeneous population of T-T dimers. It is interesting to note that Husain and Sancar (1987a) found that the purified 50-kDa photolyase (phrB$^+$ gene product) dissociated from a 43 bp oligonucleotide having a single T-T dimer with biphasic kinetics. Approximately 10 per cent of the PRE molecules dissociated with a rate constant 50-fold slower than the other 90 per cent, suggesting that two apparently homogeneous components seem to make at least two different classes of complexes, or the two components make a homogeneous complex which can dissociate by two separate pathways. Although no photolysis data have been published using this defined substrate technique, it is not unreasonable to expect that two different classes of enzyme-substrate complexes would have different photoreactivation cross-

sections. Therefore, it is not possible to conclude from these kinetic studies whether the reaction is mediated by one or two photolyase molecules.

In a recent study, Husain and Sancar (1987b) reported no difference in the rate of photoreactivation between 254 nm UV-irradiated 18 hour cells of SA206 (Δ(gal-chlA)) and SA205 (Δ(attλ -chlA), although they did note a 2-fold difference in near-UV sensitivity. In contrast to this study, wherein a marked difference in photoreactivation rate was noted between SA206 and AB1884, AB1885, AB1886 and SA446 (Δ(attλ-chlA) (see Fig. 2.10, Results and Discussion Part II) using broad-band photoreactivating light having a peak at 380 nm (see Fig. 7, General Methodology), the authors used two Sylvania F15T8/BLB lamps as the light source and two layers of window glass to cut out wavelengths below 300 nm. These light sources have a peak at 350 nm, a wavelength at which we would not expect to see any differences in the rate of photorepair, since in the wavelength-dependence study reported in Section 3.5 (Results and Discussion Part III), the photorepair rate constant (k_1) for AB2480 (phr$^+$) was slightly lower compared with AS44 (ΔphrA). The difference in the rate of photorepair was only noted with wavelengths between 360 and 420 nm. Whilst this is a plausible explanation for the observed differences between these two studies, it should be emphasised that the photoreactivation procedure used by Husain and Sancar (1987b) was identical to that reported by Sutherland and Hausrath (1979). There is no obvious reason why these workers should obtain apparently conflicting results. Sancar et al. (1987a) measured the photoreactivation cross-section at 384 nm in a Δ(gal-uvrB) strain, and obtained a value of $\varepsilon\phi = 3.3 \times 10^4\ M^{-1}.cm^{-1}$, compared with $\varepsilon\phi = 4.4 \times 10^4\ M^{-1}.cm^{-1}$

for an otherwise isogenic strain. Although the authors found this to be not statistically different within the limits of the accuracy of *in vivo* measurements, the difference in quantum yield may contribute to the difference in the rate of photoreactivation which we observed with 380 nm broad-band photoreactivating light. Husain and Sancar (1987b) found that *uvrA phrB* strains inactivated to 1 x 10^{-4} surviving fraction with 254 nm UV radiation, exhibited a 10 to 30-fold increase in survival after 5 hours of black-light photoreactivation treatment and correction for PR light-induced lethality. They tested the hypothesis that this may be attributable to the 40-kDa protein encoded by the *phrA* gene by comparing the photoreactivation kinetics of a *uvrA* Δ*phrB* strain with a *uvrA* Δ*phrB*, Δ(*gal*-*attλ*) strain. After correction for the PR light-induced lethality, both strains showed a 10-fold increase in survival after 254 nm UV inactivation to 1 x 10^{-4} surviving fraction. The kinetics of repair were similar for both strains. These results have important implications for the interpretation of the data presented in this thesis. Firstly, they suggest that the repair observed in the *phrB* mutant strains may be attributable to an unknown photolyase molecule, rather than the *phrB* mutant gene product having some partial photolyase activity. This latter suggestion could be easily tested by cloning the mutant *phrB* gene and testing for PRE activity, in a manner similar to that described for the *uvrB5* mutation by Backendorf et al. (1986). The mutation could be conveniently isolated using the cloned *phrB*$^{+}$ gene as a probe in hybridization experiments. Secondly, the data reported by Husain and Sancar (1987b), indicating that a Δ*phrB* Δ*phrA* mutant exhibits the same photoreactivable response as a Δ*phrB* strain, suggests that the photolyase activity cannot be attributed to the

40-kDA photolyase coded by the putative *phrA* gene. Whilst their observation that *uvrA* Δ*phrA* Δ*phrB* strains are not totally photoreactivation-deficient agrees with the conclusion that AS46 (Δ*phrA* *phrB* Δ*uvrB* *recA*) has some photolyase activity (when the growth temperature is lowered), it does not explain why we consistently find a reduced rate of photoreactivation in strains deleted at the putative *phrA* locus. Although this could be attributed to the non-isogenicity of the strains, we have shown that cloning an approximately 8-kbp *SphI* restriction fragment from the *gal* to *attλ* region (carried on a Lambda specialised transducing 'phage) resulted in a photoreactivable response in strain AS46 when grown at 37°C, compared with the same strain transformed with the host vector pBR322. Furthermore, this same plasmid, named pAS01, resulted in an increase in the single photoreactivating flash response and rate of photorepair using continuous broad-band photoreactivating light in strain AS44 compared with AS44/pBR322. Therefore, it must be concluded that a gene from the *gal* to *attλ* interval is capable of increasing the rate of photorepair in Δ(*gal*-*attλ*) strains, implying that there is a gene present capable of affecting the rate of photoenzymatic repair in *E. coli* K-12. However, available evidence from this study and other published work would seem to argue against the gene coding for a protein with photolyase activity, particularly since the '*phrA* plasmid', pAS01, did not affect the rate of photorepair in the *phrA*$^{+}$ *phrB* *uvrAB* *recA* strain, DY326. This would seem to cast doubt on the existence of the 40-kDa glycoribonucleoprotein isolated from the *gal*-*attλ* interval by Sutherland et al. (1973). Husain and Sancar (1987b) note the observation of Silhavy et al. (1983), that generally *E. coli* does not have glycoproteins. Furthermore, the 40-kDA

photolyase (and the highly controversial photoreactivating enzyme from human cells) is the only photolyase isolated to-date which lacks an intrinsic chromophore and does not exhibit any absorbance in the actinic wavelength region. It is interesting to note that Husain and Sancar (1987b) reported a significant increase in near-UV sensitivity of SA206 (Δ(gal-chlA)) compared with SA205 (Δ(attλ-chlA)). Whilst there are several explanations for this difference, including sensitization due to a build-up of porphyrin precursors, it is tempting to suggest that the phrA gene product may have a role in near-UV-induced lethality. This would suggest a reason why the gene has been retained during evolution, since over the last half a billion years the wavelengths which are most likely to induce photoreactivable pyrimidine dimers have been filtered by the ozone layer. However, in defence of photoreactivation as a DNA repair mechanism, it should be noted that pyrimidine dimers have been detected in bacterial DNA after 365 nm UV irradiation (Tyrrell, 1973a), as has photoreactivation of 365 nm UV-induced inactivation (Brown and Webb, 1972).

It is hoped that the preliminary investigations with plasmid pAS01 will be carried further to characterise the gene product and isolate an isogenic series of phr mutants. At present, its proposed 'interaction' with the phrB gene/product can only be the subject of speculation. There are several possibilities for this interaction including a simple increase in the number of photolyase molecules, a shift in the equilibrium from an inactive- to an active state, or perhaps a change in the higher-order structure of the photolyase molecule to either increase its ability to complex with the substrate or to increase the photoreactivation cross-section of the enzyme-substrate complex.

Finally, if the photorepair measured in the *phrB* mutant DY326 is due to an unknown photolyase molecule, then the characterisation reported in this thesis suggests that the molecule has many of the classic properties of a photoreactivating enzyme. This argues against such suggestions as direct photoreversal of pyrimidine dimers by photoreactivating light or sensitized dimer-cleavage by flavin adenine dinucleotide, as mechanisms for the observed response.

In conclusion, it is hoped this work makes a positive contribution towards the current debate on the genetic control of photoenzymatic repair in *E. coli*. The data confirm the notion that the *phrB*$^{+}$ gene product is the major photolyase, but also indicate that a gene within the *gal*-*attλ* interval has a significant effect on the kinetics of photorepair, but probably does not code for a photoactive protein. However, the data do support the intriguing possibility that there is a second photolyase molecule in *E. coli*, the genetic locus of which is not known.

APPENDIX 1

TABLE A1 BACTERIAL STRAINS : DERIVATION AND SOURCES

STRAIN DESIGNATION	GENOTYPE AND DERIVATION	SOURCE OR REFERENCE
AB1157	*thr-1 leu-6 thi-1 lacY1 galK2 ara-14 xyl-5 mtl-1 Δ(gpt-proA)62 his-4 argE3 rpsL31 tsx-33 supE44*	DeWitt and Adelberg, 1962.
AB1886	AB1157*uvrA6* - nitrous acid treatment	Howard-Flanders and Theriot, 1966.
AB1885	AB1157*uvrB5* - nitrous acid treatment	Howard-Flanders and Theriot, 1966.
AB1884	AB1157*uvrC34* - nitrous acid treatment	Howard-Flanders and Theriot, 1966.
AB2480	*F^- uvrA6 recA13 Δ(gpt-proA)62 thi-1 lacY1 galK2 rpsL31*	Howard-Flanders and Theriot, 1966.
*SA206	*Δ(gal-chlA)* mutant of C400 (wild-type) by selection on chlorate agar.	Adhya et al., 1968.
SA446	*Δ(attλ-chlA)* mutant of C400 (wild-type) by selection on chlorate agar.	Adhya et al., 1968.
Hs30	*E. coli Bphr uvrB* - *uvrB* derivative of *E. coli Bphr*	Kondo and Kato, 1966. (Harm and Hillebrandt, 1962).
W3110	*F^- bio rha lacZ str^R thyA thyR metE malB*	(D. Youngs)
JC5080	*HfrKL-16 recA56 thr ilv spec*	J. Gross (D. Youngs)
DY292	*F^- leuB bio rha lacZ str^R thyA thyR $metE^+$ uvrA6* (P1.AB1886 x W3110 - select mal^+)	D. Youngs

TABLE A1 BACTERIAL STRAINS : DERIVATION AND SOURCES

STRAIN DESIGNATION	GENOTYPE AND DERIVATION	SOURCE OR REFERENCE
*DY314	*F⁻ leuB rha lacZ str^R thyA thyR metE uvrA6 uvrB phr* (P1.Hs30 x DY292 - select *bio*$^+$)	Youngs and Smith, 1978.
*DY326	*F⁻ leuB rha LacZ str^R thyA thyR*$^+$ *metE uvrA6 uvrB phr recA56* (DY314 x JC5080 - select *thy*$^+$)	D. Youngs
*JC10240	*Hfr(P045) thi-300 ilv-318 spc-300 srlA300::Tn10 recA56*	Csonka and Clarke, 1980.
AS44	*Δ(gal-chlA) srlA300::Tn10 recA56* (P1.JC10240 x SA206 - select Tc^R)	This work.
AS45	*Δ(gal-chlA) phr* (P1.DY314 x SA206 - select *gal*$^+$)	This work.
AS46	*Δ(gal-chlA) phr srlA300::Tn10 recA56* (P1.DY314 x AS45 - select Tc^R)	This work.
C600	*F⁻ thr-1 leuB6 tonA21 lacY1 supE44 thi-1* λ^-	Appleyard, 1954.
W3350	*F⁻ galT22 galK2 IN(rrnD-rrnE)1* λ^-	Campbell, 1961.
*X9170	*F⁻ kdp gltA gal*	W. Epstein (D. Youngs)

*obtained from Professor K. C. Smith, Stanford University

APPENDIX 2

GROWTH MEDIA

Galactose Minimal Medium

Oxoid Agar No. 3	1.2 g
Water	88.5 ml
after autoclaving:-	
M9A	2 ml
M9B	8 ml
Galactose 20%	1 ml
Thiamine 1 mg/ml	0.5 ml

Chlorate Agar

Bacto Nutrient broth	8 g
Oxoid Agar No. 3	12 g
after autoclaving:-	
Glucose 20%	10 ml
$NaClO_3$ 20%	10 ml

Eosin-Methylene Blue-Galactose Agar

Bacto-Tryptone	10 g
Bacto-Yeast Extract	1 g
NaCl	5 g
KH_2PO_4	2 g
Water	930 ml
after autoclaving:-	
Eosin Yellow 4%	10 ml
Methylene Blue 0.65%	10 ml
Galactose 20%	50 ml

TB Broth

Bacto-Tryptone	10 g
NaCl	5 g
Water	990 ml
after autoclaving:-	
1M $MgSO_4$	10 ml

for TB 'top' agar add 0.8% Agar No. 3
for TB 'plate' agar add 1.2% Agar No. 3

λ -Dil

1M Tris.Cl [pH 7.5]	5 ml
NaCl	580 mg
$MgSO_4.7H_2O$	200 mg
Gelatin 2%	0.5 ml
Water to	100 ml

LB Broth

Bacto-Tryptone	10 g
Bacto-Yeast Extract	5 g
NaCl	10 g
Water to	1 litre

for plates, add 1.2% Agar No. 3

YENB Medium

Bacto-Nutrient Agar	23 g
Bacto-Yeast Extract	7.5 g
Water to	1 l

L-CAP Medium

Bacto-Tryptone	10 g
Bacto-Yeast Extract	5 g
NaCl	500 mg
Water	975 ml
after autoclaving:-	
Glucose 40%	5 ml
Chloramphenicol 2 mg/ml	10 ml

Lysogen Broth

Bacto-Tryptone	10 g
Bacto-Yeast Extract	5 g
NaCl	500 mg
Water	980 ml
after autoclaving:-	
1M $MgSO_4$	10 ml

R Medium

Bacto-Tryptone	10 g
Bacto-Yeast Extract	1 g
NaCl	8 g
Oxoid Agar No. 3	8 g 'top'
	12 g 'plate'
Water to	1 litre
after autoclaving:-	
1M $CaCl_2$	2 ml
Galactose 20%	5 ml

F-Top Agar

NaCl	8 g
Oxoid Agar No. 3	8 g
Water to	1 litre

APPENDIX 3

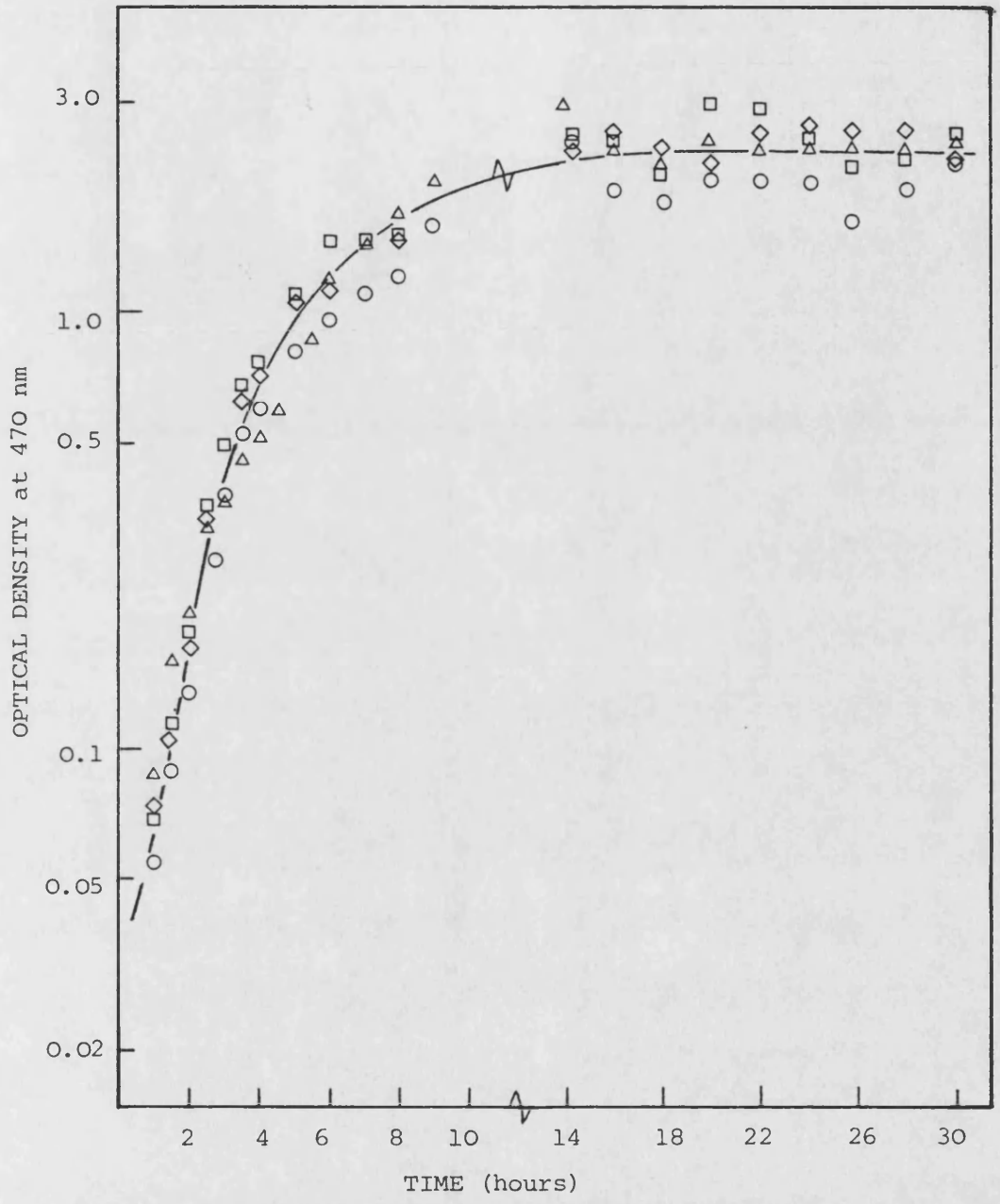

Fig. A3.1. Growth curves for AB2480 (△), AS44 (○), DY326 (□) and AS46 (◇) shaken at 100 cycles/minute at 37°C.

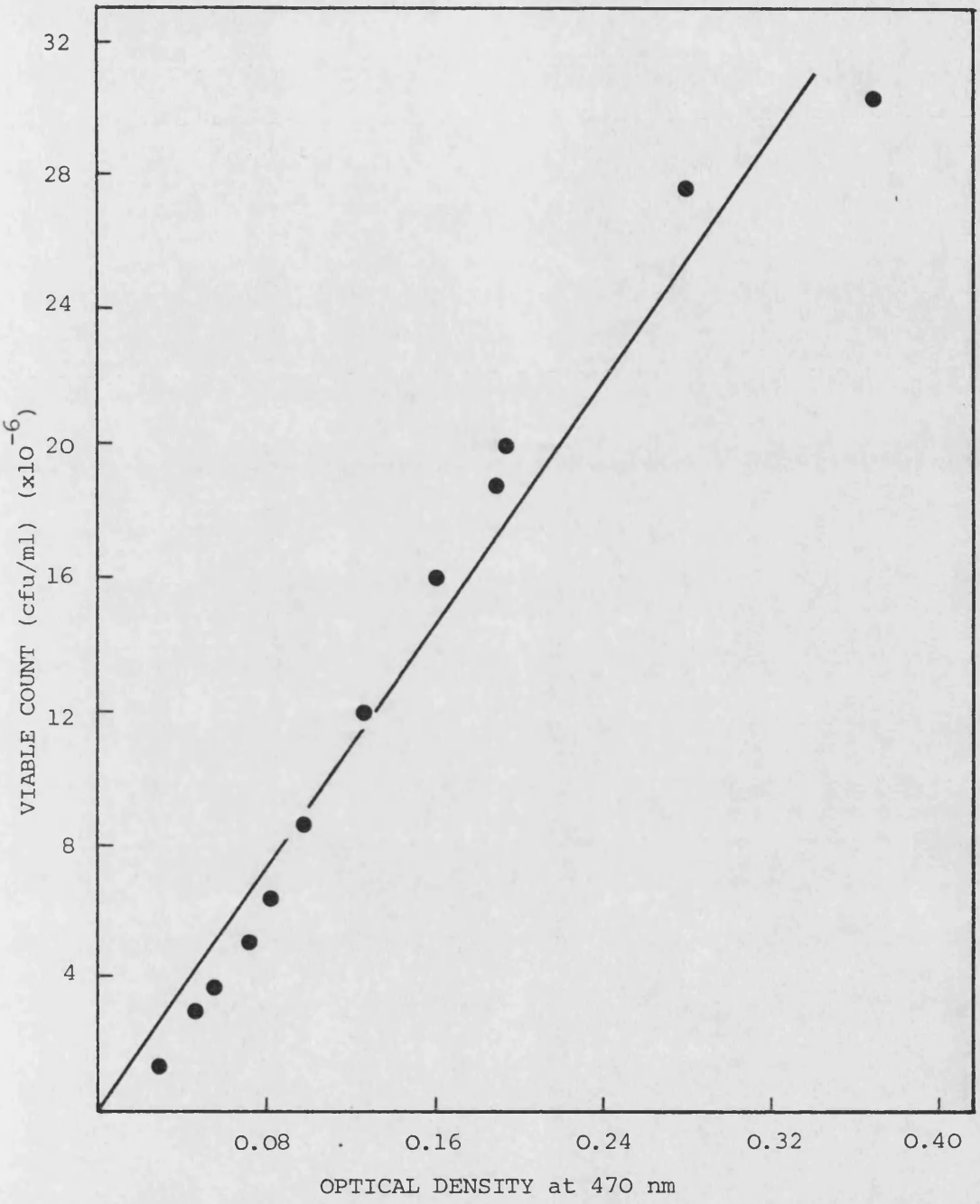

Fig. A3.2. Calibration plot of viable count versus OD_{470} for 24 hour stationary phase AS44, grown at 37°C.

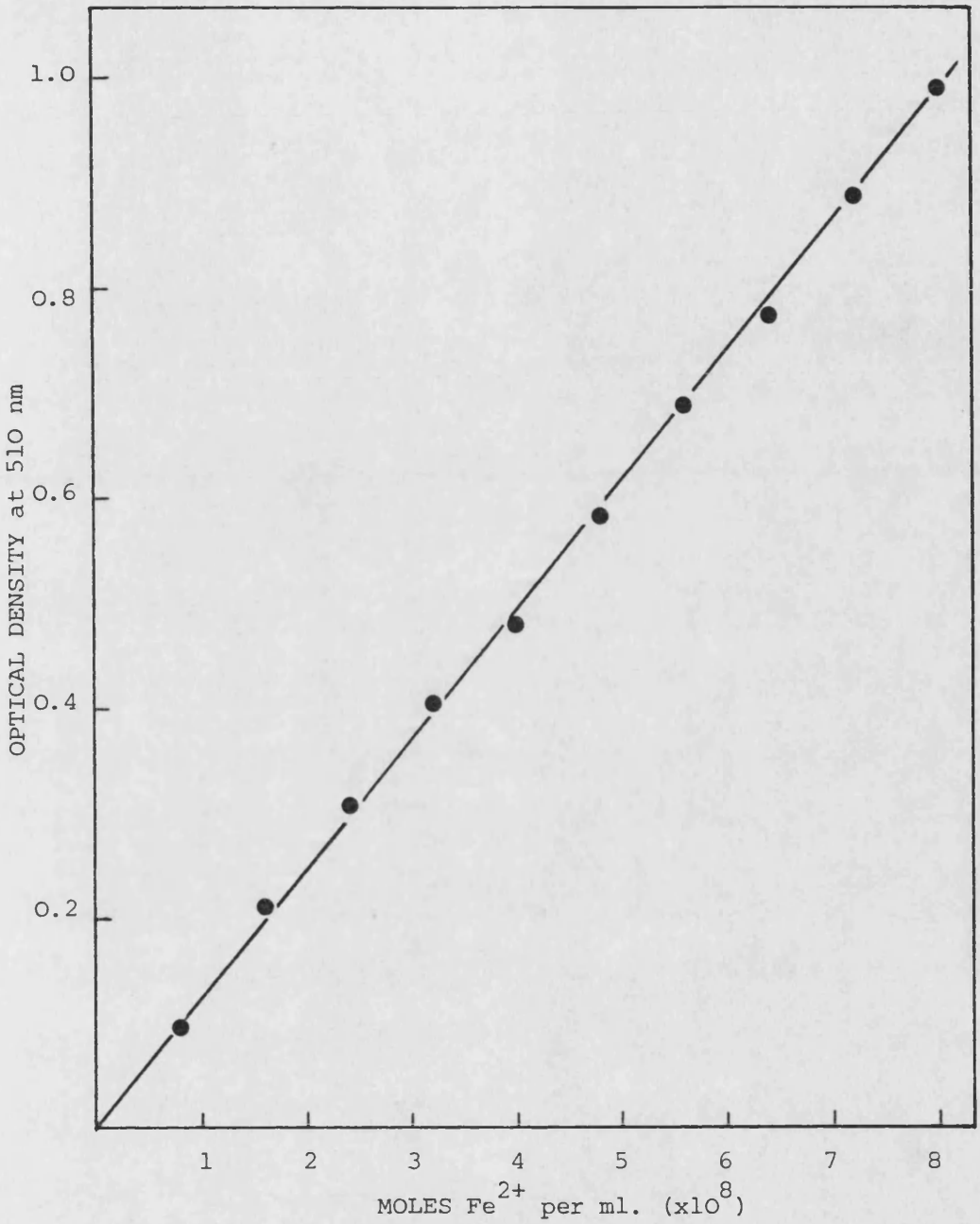

Fig. A3.3. Calibration plot of OD_{510} versus number of moles Fe^{2+} ion for potassium ferrioxalate actinometry.

(a = 7.6×10^{-3}, b = 1.214×10^{7}, r = 0.9994)

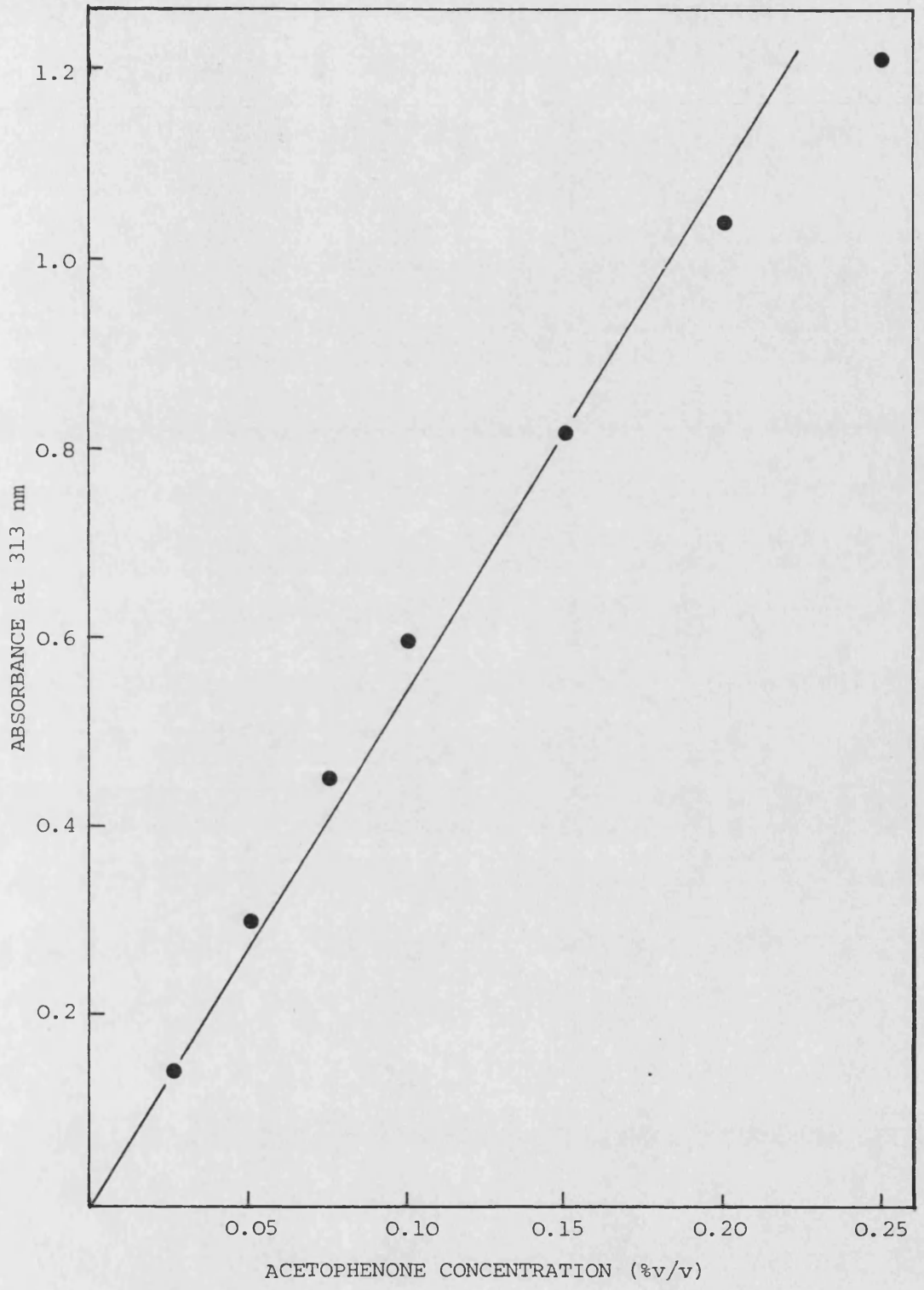

Fig. A3.4. Calibration curve to determine Morowitz correction factor for acetophenone at 313 nm (after Morowitz, 1950). (a = 0.017, b = 5.556, r = 0.997)

APPENDIX 4

Table A4.1 DATA PERTAINING TO THE SURVIVAL CURVES OBTAINED WHEN AB1886 WAS IRRADIATED AT 254 nm (FIG. 2.1, TABLE 2.1)

EXPT No.	INITIAL VIABLE COUNT (ml^{-1})	FLUENCE RATE Wm^{-2}	FLUENCE Jm^{-2}	SURVIVING FRACTION
1a	2.32×10^{7}	0.068	3.06	$\underline{6.47 \times 10^{-1}}$
			6.11	1.85×10^{-1}
			9.17	4.32×10^{-2}
			12.22	8.28×10^{-3}
			15.28	2.34×10^{-3}
			18.33	5.20×10^{-4}
			21.39	2.21×10^{-4}
			24.44	6.18×10^{-5}
1b	2.62×10^{7}	0.068	3.06	$\underline{6.06 \times 10^{-1}}$
			6.11	1.63×10^{-1}
			9.17	4.30×10^{-2}
			12.22	9.05×10^{-3}
			15.28	3.00×10^{-3}
			18.33	6.05×10^{-4}
			21.39	2.13×10^{-4}
			24.44	5.58×10^{-5}
1c	2.40×10^{7}	0.068	3.06	$\underline{6.86 \times 10^{-1}}$
			6.11	2.11×10^{-1}
			9.17	5.76×10^{-2}
			12.22	1.02×10^{-2}
			15.28	3.08×10^{-3}
			18.33	7.52×10^{-4}
			21.39	3.01×10^{-4}
			24.44	7.23×10^{-5}

Table A4.2 DATA PERTAINING TO THE SURVIVOR CURVES OBTAINED WHEN SA206 WAS INACTIVATED AT 254 nm (FIG. 2.1, TABLE 2.1)

EXPT No.	INITIAL VIABLE COUNT (ml^{-1})	FLUENCE RATE Wm^{-2}	FLUENCE Jm^{-2}	SURVIVING FRACTION
2a	1.81×10^{7}	0.053	3.20	5.85×10^{-1}
			6.40	1.29×10^{-2}
			9.61	3.91×10^{-2}
			12.81	8.15×10^{-3}
			16.00	1.87×10^{-3}
			19.21	6.00×10^{-4}
			22.41	1.27×10^{-4}
2b	1.64×10^{7}	0.053	3.20	6.14×10^{-1}
			6.40	1.41×10^{-1}
			9.61	4.19×10^{-2}
			12.81	8.66×10^{-3}
			16.00	1.94×10^{-3}
			19.21	5.73×10^{-4}
			22.41	1.49×10^{-4}
2c	1.39×10^{7}	0.053	3.20	7.41×10^{-1}
			6.40	2.00×10^{-1}
			9.61	4.67×10^{-2}
			12.81	1.30×10^{-2}
			16.00	2.61×10^{-3}
			19.21	7.77×10^{-4}
			22.41	1.99×10^{-4}

Table A4.3 DATA PERTAINING TO THE SURVIVOR CURVES OBTAINED WHEN DY314 WAS INACTIVATED AT 254 nm (FIG. 2.2, TABLE 2.1)

EXPT No.	INITIAL VIABLE COUNT (ml^{-1})	FLUENCE RATE Wm^{-2}	FLUENCE Jm^{-2}	SURVIVING FRACTION
3a	8.2×10^{6}	0.053	3.20	8.65×10^{-1}
			6.40	1.44×10^{-1}
			9.61	2.32×10^{-2}
			12.81	4.57×10^{-3}
			16.00	1.43×10^{-3}
			19.21	3.47×10^{-4}
			22.41	1.11×10^{-4}
3b	8.9×10^{6}	0.053	3.20	7.70×10^{-1}
			6.40	7.56×10^{-2}
			9.61	1.98×10^{-2}
			12.81	5.13×10^{-3}
			16.00	1.34×10^{-3}
			19.21	5.24×10^{-4}
			22.41	1.92×10^{-4}
3c	7.8×10^{6}	0.053	3.20	8.68×10^{-1}
			6.40	1.65×10^{-1}
			9.61	2.00×10^{-2}
			12.81	5.79×10^{-3}
			16.00	2.43×10^{-3}
			19.21	6.30×10^{-4}
			22.41	1.95×10^{-4}

Table A4.4 DATA PERTAINING TO THE SURVIVOR CURVES OBTAINED WHEN AS45 WAS INACTIVATED AT 254 nm (FIG. 2.2, TABLE 2.1)

EXPT No.	INITIAL VIABLE COUNT (ml^{-1})	FLUENCE RATE Wm^{-2}	FLUENCE Jm^{-2}	SURVIVING FRACTION
4a	1.64×10^{7}	0.053	3.20	7.97×10^{-1}
			6.40	1.99×10^{-1}
			9.61	4.12×10^{-2}
			12.81	8.56×10^{-3}
			16.00	2.54×10^{-3}
			19.21	6.28×10^{-4}
			22.41	1.45×10^{-4}
4b	1.73×10^{7}	0.053	3.20	7.25×10^{-1}
			6.40	1.99×10^{-1}
			9.61	3.82×10^{-2}
			12.81	8.52×10^{-3}
			16.00	2.90×10^{-3}
			19.21	6.88×10^{-4}
			22.41	1.57×10^{-4}
4c	1.89×10^{7}	0.053	3.20	6.10×10^{-1}
			6.40	1.91×10^{-1}
			9.61	4.31×10^{-2}
			12.81	9.40×10^{-3}
			16.00	2.47×10^{-3}
			19.21	6.32×10^{-4}
			22.41	1.51×10^{-4}

Table A4.5 DATA PERTAINING TO THE SURVIVAL CURVES OBTAINED WHEN AB1885 WAS IRRADIATED AT 254 nm (FIG. 2.3. TABLE 2.1)

EXPT No.	INITIAL VIABLE COUNT (ml^{-1})	FLUENCE RATE Wm^{-2}	FLUENCE Jm^{-2}	SURVIVING FRACTION
5a	2.46×10^{7}	0.068	3.06	5.95×10^{-1}
			6.11	2.03×10^{-1}
			9.17	4.34×10^{-2}
			12.22	8.94×10^{-3}
			15.28	2.84×10^{-3}
			18.33	7.35×10^{-4}
			21.39	2.45×10^{-4}
			24.44	7.36×10^{-5}
5b	2.31×10^{7}	0.068	3.06	6.74×10^{-1}
			6.11	2.03×10^{-1}
			9.17	5.67×10^{-2}
			12.22	9.55×10^{-3}
			15.28	3.33×10^{-3}
			18.33	7.91×10^{-4}
			21.39	3.06×10^{-4}
			24.44	8.77×10^{-5}
5c	2.60×10^{7}	0.068	3.06	6.65×10^{-1}
			6.11	1.99×10^{-1}
			9.17	4.76×10^{-2}
			12.22	9.59×10^{-3}
			15.28	2.88×10^{-3}
			18.33	6.57×10^{-4}
			21.39	3.46×10^{-4}
			24.44	8.09×10^{-5}

Table A4.6 DATA PERTAINING TO THE SURVIVOR CURVES OBTAINED WHEN AB1884 WAS IRRADIATED AT 254 nm (FIG. 2.3, TABLE 2.1)

EXPT No.	INITIAL VIABLE COUNT (ml^{-1})	FLUENCE RATE Wm^{-2}	FLUENCE Jm^{-2}	SURVIVING FRACTION
6a	1.08×10^{7}	0.063	3.85	7.05×10^{-1}
			5.70	2.22×10^{-1}
			8.55	8.25×10^{-2}
			11.39	1.49×10^{-2}
			14.24	5.02×10^{-3}
			17.09	8.80×10^{-4}
			19.94	2.71×10^{-4}
			22.79	8.09×10^{-5}
			25.64	2.59×10^{-5}
6b	1.20×10^{7}	0.063	2.85	6.87×10^{-1}
			5.70	2.74×10^{-1}
			8.55	8.45×10^{-2}
			11.39	1.63×10^{-2}
			14.24	5.21×10^{-3}
			17.09	1.30×10^{-3}
			19.94	3.49×10^{-4}
			22.79	1.04×10^{-4}
			25.64	2.99×10^{-5}

Table A4.7 DATA PERTAINING TO THE PHOTOREACTIVATION OF AB1886, AB1885 AND AB1884 (FIGS. 2.4,6-7)

PR TIME (min)	AB1886		AB1885		AB1884	
	S/So	(1-P)	S/So	(1-P)	S/So	(1-P)
0	2.22×10^{-4}		2.70×10^{-4}		4×10^{-4}	
2.5	9.50×10^{-4}	0.79	1.10×10^{-3}	0.76	2.39×10^{-3}	0.73
5	2.63×10^{-3}	0.64	4.69×10^{-3}	0.55	2.87×10^{-3}	0.71
7.5	3.60×10^{-3}	0.59	9.58×10^{-3}	0.43	5.74×10^{-3}	0.60
10	6.98×10^{-3}	0.50	1.38×10^{-2}	0.32	8.60×10^{-3}	0.54
15	1.65×10^{-2}	0.29	1.91×10^{-2}	0.18	1.95×10^{-2}	0.42
17	-	-	-	-	3.96×10^{-2}	0.32
20	2.93×10^{-2}	0.25	4.54×10^{-2}	0.17	6.74×10^{-2}	0.24
25	3.80×10^{-2}	0.22	4.90×10^{-2}	0.13	9.64×10^{-2}	0.18
30	4.94×10^{-2}	0.18	6.50×10^{-2}	0.09	1.25×10^{-1}	0.14
40	6.42×10^{-2}	0.14	8.32×10^{-2}	0.06	1.52×10^{-1}	0.12
50	8.49×10^{-2}	0.10	9.81×10^{-2}	0.05	2.31×10^{-1}	0.05
60	1.10×10^{-1}	0.07	9.9×10^{-2}	0.05	2.72×10^{-1}	0.03
80	1.32×10^{-1}	0.03	1.28×10^{-1}	0.02	3.2×10^{-1}	-
100	1.80×10^{-1}	-	1.45×10^{-1}		3.4×10^{-1}	-
120	2.17×10^{-1}	-	1.44×10^{-1}		3.3×10^{-1}	-

TABLE A4.8 DATA PERTAINING TO THE PHOTOREACTIVATION OF SA206 AND SA446 (FIGS. 2.5 AND 2.8)

PR TIME (min)	SA206		SA446	
	S/So	(1-P)	S/So	(1-P)
0	2.19×10^{-4}	-	6.92×10^{-5}	-
2	-	-	9.23×10^{-4}	0.66
4	3.05×10^{-4}	0.94	4.34×10^{-3}	0.46
6	4.40×10^{-4}	0.88	9.02×10^{-3}	0.37
8	-	-	1.57×10^{-2}	0.29
10	6.20×10^{-4}	0.82	-	-
15	1.10×10^{-3}	0.73	5.51×10^{-2}	0.13
20	2.26×10^{-3}	0.61	6.70×10^{-2}	0.10
30	4.08×10^{-3}	0.51	1.10×10^{-1}	0.04
40	7.43×10^{-3}	0.41	1.04×10^{-1}	0.05
50	1.56×10^{-2}	0.28	1.26×10^{-1}	0.02
60	-	-	1.30×10^{-1}	0.02
75	5.10×10^{-2}	0.08	-	-
80	-	-	1.42×10^{-1}	-
100	6.50×10^{-2}	0.04	1.49×10^{-1}	-
120	8.00×10^{-2}	-	1.40×10^{-1}	-

TABLE A4.9 DATA PERTAINING TO PHOTOREACTIVATION OF DY314 AND AS45 (FIG. 2.9)

PR TIME (min)	DY314		AS45	
	S/So	(1-P)	S/So	(1-P)
0	1.33×10^{-4}	-	4.60×10^{-4}	-
30	1.65×10^{-4}	0.970	3.40×10^{-4}	-
60	1.63×10^{-4}	0.970	4.71×10^{-4}	0.98
90	1.80×10^{-4}	0.955	4.69×10^{-4}	0.99
120	1.80×10^{-4}	0.955	5.01×10^{-4}	0.97
150	1.90×10^{-4}	0.97	4.63×10^{-4}	1.00
180	2.49×10^{-4}	0.907	4.41×10^{-4}	-

Table A4.10 DATA PERTAINING TO THE SURVIVOR CURVES OBTAINED WHEN AB2480 WAS IRRADIATED AT 254 nm, THE INACTIVATION PARAMETERS OF WHICH ARE GIVEN IN TABLE 3.1

EXPT No.	INITIAL VIABLE COUNT (ml^{-1})	254 nm FLUENCE RATE Wm^{-2}	FLUENCE Jm^{-2}	SURVIVING FRACTION
10a	1.61×10^{7}	0.0756	0.059	5.45×10^{-1}
			0.119	1.93×10^{-1}
			0.179	4.58×10^{-2}
			0.238	1.50×10^{-2}
			0.298	4.60×10^{-3}
			0.358	1.52×10^{-3}
			0.417	4.90×10^{-4}
			0.478	1.45×10^{-4}
10b	1.51×10^{7}	0.0966	0.067	4.92×10^{-1}
			0.135	1.52×10^{-1}
			0.202	4.62×10^{-2}
			0.269	1.09×10^{-2}
			0.336	4.13×10^{-3}
			0.403	1.09×10^{-3}
			0.471	2.77×10^{-4}
			0.537	1.00×10^{-4}
10c	1.71×10^{7}	0.0756	0.060	4.88×10^{-1}
			0.119	1.68×10^{-1}
			0.180	5.94×10^{-2}
			0.239	1.73×10^{-2}
			0.300	5.57×10^{-3}
			0.360	1.59×10^{-3}
			0.420	4.10×10^{-4}
			0.479	1.42×10^{-4}
10d	1.32×10^{7}	0.0969	0.136	1.32×10^{-1}
			0.273	9.59×10^{-3}
			0.408	6.63×10^{-4}
			0.539	6.65×10^{-5}
10e	1.86×10^{7}	0.0970	0.129	1.90×10^{-1}
			0.258	1.90×10^{-2}
			0.387	2.00×10^{-3}
10f	1.56×10^{7}	0.0971	0.131	1.59×10^{-1}
			0.262	1.71×10^{-2}
			0.392	1.55×10^{-3}
10g	1.26×10^{7}	0.0971	0.132	1.66×10^{-1}
			0.263	1.84×10^{-2}
			0.396	1.99×10^{-3}
10h	7.57×10^{-6}	0.0630	0.078	2.95×10^{-1}
			0.234	2.60×10^{-2}
			0.389	1.45×10^{-3}
			0.545	7.84×10^{-5}

Table A4.11 DATA PERTAINING TO THE SURVIVOR CURVES OBTAINED WHEN AS44 WAS IRRADIATED AT 254 nm, THE INACTIVATION PARAMETERS OF WHICH ARE GIVEN IN TABLE 3.1

EXPT No.	INITIAL VIABLE COUNT (ml^{-1})	254 nm FLUENCE RATE (Wm^{-2})	FLUENCE (Jm^{-2})	SURVIVING FRACTION
11a	7.8×10^{6}	0.0969	0.066	3.34×10^{-1}
			0.133	1.05×10^{-1}
			0.197	3.04×10^{-1}
			0.265	3.04×10^{-1}
			0.332	6.67×10^{-3}
			0.399	5.85×10^{-4}
			0.466	1.53×10^{-4}
			0.533	4.32×10^{-5}
11b	8.2×10^{6}	0.054	0.071	2.99×10^{-1}
			0.143	8.66×10^{-2}
			0.216	2.40×10^{-2}
			0.288	6.71×10^{-3}
			0.360	1.25×10^{-3}
			0.431	3.41×10^{-4}
			0.502	1.04×10^{-4}
11c	5.7×10^{6}	0.054	0.073	2.1×10^{-1}
			0.145	7.72×10^{-2}
			0.219	1.84×10^{-2}
			0.290	3.60×10^{-3}
			0.362	9.30×10^{-4}
			0.434	2.67×10^{-4}
			0.506	7.9×10^{-5}
11d	6.7×10^{6}	0.0646	0.079	2.39×10^{-1}
			0.239	1.52×10^{-2}
			0.400	7.06×10^{-4}
			0.480	1.65×10^{-4}
11e	8.5×10^{6}	0.0760	0.067	3.18×10^{-1}
			0.200	2.27×10^{-2}
			0.334	1.89×10^{-3}
			0.468	1.33×10^{-4}
11f	8.6×10^{6}	0.0972	0.135	8.80×10^{-2}
			0.271	7.40×10^{-3}
			0.406	4.90×10^{-4}
11g	8.7×10^{6}	0.056	0.130	1.21×10^{-1}
			0.260	8.08×10^{-3}
			0.388	7.51×10^{-4}
11h	6.7×10^{6}	0.056	0.131	1.05×10^{-1}
			0.263	6.62×10^{-4}
			0.394	4.03×10^{-4}

Table A4.12 DATA PERTAINING TO THE SURVIVOR CURVES OBTAINED WHEN DY326 WAS IRRADIATED AT 254 nm, THE INACTIVATION PARAMETERS OF WHICH ARE GIVEN IN TABLE 3.1

EXPT No.	INITIAL VIABLE COUNT (ml^{-1})	254 nm FLUENCE RATE (Wm^{-2})	FLUENCE (Jm^{-2})	SURVIVING FRACTION
12a	1.62×10^{7}	0.0760	0.072	3.94×10^{-1}
			0.143	1.01×10^{-1}
			0.214	2.70×10^{-2}
			0.286	6.68×10^{-3}
			0.357	1.56×10^{-3}
			0.429	4.49×10^{-4}
			0.500	9.83×10^{-5}
12b	1.50×10^{7}	0.0760	0.071	4.61×10^{-1}
			0.142	1.32×10^{-1}
			0.213	4.54×10^{-2}
			0.284	7.06×10^{-3}
			0.354	1.78×10^{-3}
			0.425	5.52×10^{-4}
			0.425	5.52×10^{-4}
			0.496	1.31×10^{-4}
12c	1.49×10^{7}	0.0760	0.068	3.90×10^{-1}
			0.137	1.40×10^{-1}
			0.206	8.86×10^{-2}
			0.274	1.11×10^{-2}
			0.343	2.10×10^{-3}
			0.411	7.45×10^{-4}
			0.480	2.07×10^{-4}
12d	5.4×10^{6}	0.076	0.073	3.02×10^{-1}
			0.145	9.01×10^{-2}
			0.218	1.79×10^{-2}
			0.290	5.49×10^{-3}
			0.363	1.41×10^{-3}
			0.436	4.32×10^{-4}
			0.509	9.26×10^{-5}

cont'd....

Table A4.12 (cont'd)

EXPT No.	INITIAL VIABLE COUNT (ml^{-1})	254 nm FLUENCE RATE (Wm^{-2})	FLUENCE (Jm^{-2})	SURVIVING FRACTION
12e	1.30×10^{7}	0.075	0.068	3.66×10^{-1}
			0.136	8.49×10^{-2}
			0.205	2.17×10^{-2}
			0.272	5.60×10^{-3}
			0.340	1.81×10^{-3}
			0.408	4.50×10^{-4}
			0.476	8.95×10^{-5}
12f	2.05×10^{7}	0.082	0.147	9.96×10^{-2}
			0.293	6.35×10^{-3}
			0.437	4.10×10^{-4}
			0.583	3.06×10^{-5}
12g	7.33×10^{6}	0.067	0.064	4.68×10^{-1}
			0.127	1.61×10^{-1}
			0.190	4.09×10^{-2}
			0.252	1.10×10^{-2}
			0.315	2.91×10^{-3}
			0.377	1.01×10^{-3}
			0.440	3.00×10^{-4}
12h	1.73×10^{7}	0.076	0.675	3.93×10^{-1}
			0.136	1.20×10^{-1}
			0.203	3.04×10^{-2}
			0.272	7.40×10^{-3}
			0.339	2.30×10^{-3}
			0.408	5.10×10^{-4}
			0.476	1.08×10^{-4}

Table A4.13 DATA PERTAINING TO THE SURVIVOR CURVES OBTAINED WHEN AS46 WAS IRRADIATED AT 254 nm, THE INACTIVATION PARAMETERS OF WHICH ARE GIVEN IN TABLE 3.1

EXPT No.	INITIAL VIABLE COUNT (ml^{-1})	254 nm FLUENCE RATE (Wm^{-2})	FLUENCE (Jm^{-2})	SURVIVING FRACTION
13a	2.95×10^{6}	0.061	0.080	1.90×10^{-1}
			0.162	5.86×10^{-2}
			0.242	1.07×10^{-2}
			0.324	2.24×10^{-3}
			0.404	2.93×10^{-4}
			0.485	1.08×10^{-4}
			0.565	3.62×10^{-5}
13b	6.23×10^{6}	0.0603	0.074	4.33×10^{-1}
			0.153	8.98×10^{-2}
			0.228	2.29×10^{-2}
			0.303	5.88×10^{-3}
			0.376	1.64×10^{-3}
			0.450	4.60×10^{-4}
			0.525	8.66×10^{-5}
13c	8.83×10^{6}	0.0570	0.134	9.7×10^{-2}
			0.267	9.10×10^{-3}
			0.402	6.87×10^{-4}
			0.535	5.74×10^{-5}
13d	8.77×10^{6}	0.065	0.140	1.01×10^{-1}
			0.281	7.2×10^{-3}
			0.423	4.41×10^{-4}
			0.565	4.03×10^{-5}
13e	6.57×10^{6}	0.065	0.142	1.01×10^{-1}
			0.284	7.56×10^{-3}
			0.427	5.23×10^{-4}
			0.568	4.26×10^{-5}
13f	8.57×10^{6}	0.060	0.129	1.23×10^{-1}
			0.261	1.00×10^{-2}
			0.394	8.52×10^{-4}
			0.527	8.72×10^{-5}
13g	9.10×10^{6}	0.0646	0.141	1.09×10^{-1}
			0.284	8.32×10^{-3}
			0.426	6.96×10^{-4}
			0.569	4.69×10^{-5}
13h	3.13×10^{6}	0.060	0.130	1.29×10^{-1}
			0.262	1.15×10^{-2}
			0.393	9.36×10^{-4}
			0.528	8.08×10^{-5}

Table A4.14 DATA PERTAINING TO THE SURVIVOR CURVES OBTAINED WHEN AB2480 WAS IRRADIATED WITH 254 nm AND AFTER A SINGLE PHOTOREACTIVATING FLASH, THE DATA ARE SHOWN IN FIG. 3.6 (PANEL A)

EXPT No.	INITIAL VIABLE COUNT (ml^{-1})	FLUENCE (Jm^{-2})	SURVIVING FRACTION 254nm	FLASH
14a	8.6×10^{6}	0.079	$\underline{4.53 \times 10^{-1}}$	9.49×10^{-1}
		0.159	1.13×10^{-1}	$\underline{6.86 \times 10^{-1}}$
		0.237	2.87×10^{-2}	3.06×10^{-1}
		0.315	7.05×10^{-3}	2.03×10^{-1}
		0.394	1.57×10^{-3}	8.02×10^{-2}
		0.473	3.49×10^{-4}	4.96×10^{-2}
		0.552	8.60×10^{-5}	2.19×10^{-2}
14b	7.57×10^{6}	0.078	$\underline{2.95 \times 10^{-1}}$	6.04×10^{-1}
		0.156	0.05×10^{-1}	$\underline{4.45 \times 10^{-1}}$
		0.234	2.60×10^{-2}	2.50×10^{-1}
		0.310	4.45×10^{-3}	1.30×10^{-1}
		0.389	1.45×10^{-3}	7.30×10^{-2}
		0.468	3.48×10^{-4}	3.79×10^{-2}
		0.545	7.84×10^{-5}	1.70×10^{-2}

Table A4.15 DATA PERTAINING TO THE SURVIVOR CURVES WHEN AS44 WAS IRRADIATED WITH 254 nm UV AND AFTER A SINGLE PHOTOREACTIVATING FLASH, THE DATA ARE SHOWN IN FIG. 3.6 (PANEL B)

EXPT No.	INITIAL VIABLE COUNT (ml^{-1})	FLUENCE (Jm^{-2})	SURVIVING FRACTION 254nm	FLASH
15a	6.7×10^{6}	0.079	$\underline{2.39 \times 10^{-1}}$	4.13×10^{-1}
		0.160	7.16×10^{-2}	$\underline{1.42 \times 10^{-1}}$
		0.239	1.52×10^{-2}	5.17×10^{-2}
		0.320	3.38×10^{-3}	1.19×10^{-2}
		0.400	7.06×10^{-4}	3.83×10^{-3}
		0.480	1.65×10^{-4}	1.15×10^{-3}
		0.559	3.83×10^{-5}	3.63×10^{-4}
15b	1.58×10^{7}	0.069	$\underline{3.56 \times 10^{-1}}$	-
		0.139	9.59×10^{-2}	$\underline{2.1 \times 10^{-1}}$
		0.210	1.65×10^{-2}	8.52×10^{-2}
		0.278	5.36×10^{-3}	2.33×10^{-2}
		0.347	1.49×10^{-3}	6.19×10^{-3}
		0.417	3.27×10^{-4}	2.35×10^{-3}
		0.486	9.49×10^{-5}	7.21×10^{-4}

Table A4.16 DATA PERTAINING TO PHOTOREACTIVATING FLUENCE RATE PLOTS FOR AB2480 SHOWN IN FIG. 3.7A

PR TIME	16a 0.28 Wm^{-2}		16b 1.1 Wm^{-2}		16c 2.19 Wm^{-2}		16d 4.55 Wm^{-2}		16e 9.16 Wm^{-2}		16f 17.76 Wm^{-2}	
(min)	S/So	1-P	S/So	1-P	S/So	1-P	S/So	1-P	S/So	1-P	S/So	1-P
0	2.01×10^{-4}	-	1.44×10^{-4}	-	1.87×10^{-4}	-	1.97×10^{-4}	-	2.82×10^{-4}	-	2.0×10^{-4}	-
FLASH	2.5×10^{-3}	1.0	1.40×10^{-3}	1.0	3.5×10^{-3}	1.0	3.0×10^{-3}	1.0	4×10^{-3}	1.0	4.9×10^{-4}	1.0
0.25	-	-	-	-	1.41×10^{-2}	0.70	1.32×10^{-3}	0.85	5.02×10^{-2}	0.41	6.5×10^{-3}	0.93
0.5	-	-	-	-	1.97×10^{-2}	0.63	9.66×10^{-3}	0.74	-	-	1.6×10^{-2}	0.7
0.75	-	-	-	-	2.28×10^{-2}	0.59	2.74×10^{-2}	0.51	9.59×10^{-2}	0.26	2.4×10^{-2}	0.6
1.0	-	-	1.87×10^{-2}	0.51	-	-	-	-	-	-	-	-
1.5	-	-	-	-	3.12×10^{-2}	0.52	8.65×10^{-2}	0.26	1.29×10^{-1}	0.19	4.0×10^{-2}	0.48
2.0	5.33×10^{-3}	0.84	2.55×10^{-2}	0.45	-	-	-	-	-	-	-	-
3	-	-	5.44×10^{-2}	0.30	9.24×10^{-2}	0.26	1.28×10^{-1}	0.17	1.82×10^{-1}	0.11	9.2×10^{-2}	0.27
4	1.26×10^{-2}	0.66	5.61×10^{-2}	0.29	-	-	-	-	-	-	-	-
5	-	-	-	-	1.28×10^{-1}	0.18	1.82×10^{-1}	0.095	2.27×10^{-1}	0.061	1.4×10^{-1}	0.17
6	2.2×10^{-2}	0.49	1.17×10^{-1}	0.16	-	-	-	-	-	-	-	-
9	-	-	-	-	2.04×10^{-1}	0.074	2.29×10^{-1}	0.044	3.34×10^{-1}	-	2.0×10^{-1}	0.078
10	5.58×10^{-2}	0.32	1.62×10^{-1}	0.097	-	-	-	-	-	-	-	-
14	-	-	-	-	2.51×10^{-1}	0.026	2.67×10^{-1}	0.010	3.21×10^{-1}	-	2.4×10^{-1}	0.021
15	1.26×10^{-1}	0.17	1.91×10^{-1}	0.066	-	-	-	-	-	-	-	-
20	1.18×10^{-1}	0.18	2.98×10^{-1}	-	3.41×10^{-1}	-	2.56×10^{-1}	-	3.2×10^{-1}	-	3.2×10^{-1}	-
25	1.63×10^{-1}	0.10	-	-	-	-	-	-	-	-	-	-
30	1.63×10^{-1}	0.11	2.91×10^{-1}	-	3.2×10^{-1}	-	3.14×10^{-1}	-	3.77×10^{-1}	-	2.85×10^{-1}	-

S/So - Surviving Fraction

Table A4.17 DATA PERTAINING TO PHOTOREACTIVATING FLUENCE RATE PLOTS FOR AS44 SHOWN IN FIG 3.7B

PR TIME (min)	17a 1.12 Wm^{-2}		17b 2.23 Wm^{-2}		17c 4.45 Wm^{-2}		17d 9.16 Wm^{-2}		17e 17.62 Wm^{-2}	
	S/So	1-P	S/So	1-P	S/So	1-P	S/So	1-P	S/So	1-P
0	1.3×10^{-4}	-	1.16×10^{-4}	-	1.71×10^{-4}	-	1.26×10^{-4}	-	2.26×10^{-4}	-
FLASH	6.35×10^{-4}	1.0	7.65×10^{-4}	1.0	4.82×10^{-4}	1.0	3.60×10^{-4}	1.0	6.21×10^{-4}	1.0
0.5	-	-	-	-	-	-	-	-	-	-
1	-	-	1.59×10^{-3}	0.86	7.97×10^{-4}	0.91	1.12×10^{-3}	0.81	9.47×10^{-4}	0.83
2	1.77×10^{-3}	0.81	4.87×10^{-3}	0.64	1.66×10^{-3}	0.78	3.33×10^{-3}	0.63	2.96×10^{-3}	0.66
3	-	-	-	-	-	-	-	-	7.35×10^{-3}	0.55
4	4.82×10^{-3}	0.62	1.18×10^{-2}	0.47	8.12×10^{-3}	0.51	6.1×10^{-3}	0.53	1.45×10^{-2}	0.43
7	1.03×10^{-2}	0.48	-	-	-	-	-	-	-	-
8	-	-	3.26×10^{-2}	0.28	2.03×10^{-2}	0.35	1.12×10^{-2}	0.43	4.29×10^{-2}	0.24
10	1.90×10^{-2}	0.37	-	-	-	-	-	-	-	-
12	-	-	-	-	-	-	3.44×10^{-2}	0.24	-	-
14	-	-	-	-	-	-	6.38×10^{-2}	0.13	8.1×10^{-2}	0.12
15	4.4×10^{-2}	0.22	7.14×10^{-2}	0.13	6.55×10^{-2}	0.14	-	-	-	-
20	6.95×10^{-2}	0.13	9.61×10^{-2}	0.07	9.35×10^{-2}	0.08	9.53×10^{-2}	0.06	1.01×10^{-1}	0.08
30	9.42×10^{-2}	0.073	1.28×10^{-2}	0.015	1.34×10^{-1}	0.02	1.25×10^{-1}	0.02	1.60×10^{-1}	-
45	1.11×10^{-1}	0.043	1.42×10^{-1}	-	1.73×10^{-1}	-	2.28×10^{-1}	-	1.59×10^{-1}	-
60	1.58×10^{-1}	-	2.27×10^{-1}	-	1.86×10^{-1}	-	2.1×10^{-1}	-	2.0×10^{-1}	-

S/So - Surviving Fraction

Table A4.18 DATA PERTAINING TO PHOTOREACTIVATING FLUENCE RATE PLOTS FOR DY326 SHOWN IN FIG 3.7C

PR TIME (min)	18a 1.36 Wm^{-2}		18b 3.41 Wm^{-2}		18c 6.82 Wm^{-2}		18d 13.64 Wm^{-2}		18e 20.46 Wm^{-2}	
	S/So	1-P	S/So	1-P	S/So	1-P	S/So	1-P	S/So	1-P
0	6.49×10^{-5}	1.0	3.16×10^{-5}	1.0	5.38×10^{-5}	1.0	5.75×10^{-5}	1.0	5.64×10^{-5}	1.0
20	6.70×10^{-5}	0.996	-	-	-	-	-	-	-	-
30	-	-	3.08×10^{-5}	1.0	7.39×10^{-5}	0.962	1.02×10^{-4}	0.951	6.4×10^{-5}	0.984
40	7.10×10^{-5}	0.989	-	-	-	-	-	-	6.8×10^{-5}	0.976
60	6.18×10^{-5}	1.01	4.38×10^{-5}	0.962	1.22×10^{-4}	0.901	1.92×10^{-4}	0.889	9.5×10^{-5}	0.932
80	6.07×10^{-5}	1.01	6.74×10^{-5}	0.921	-	-	2.11×10^{-4}	0.853	1.09×10^{-4}	0.915
100	5.56×10^{-5}	1.02	8.26×10^{-5}	0.889	2.49×10^{-4}	0.810	2.93×10^{-4}	0.842	1.34×10^{-4}	0.888
120	5.89×10^{-5}	1.01	1.19×10^{-4}	0.848	2.90×10^{-4}	0.796	3.81×10^{-4}	0.77	1.85×10^{-4}	0.846
150	6.53×10^{-5}	0.999	1.48×10^{-4}	0.823	4.38×10^{-4}	0.746	-	-	2.07×10^{-4}	0.832
180	7.50×10^{-5}	0.982	1.97×10^{-4}	0.789	3.58×10^{-4}	0.770	-	-	2.58×10^{-4}	0.803

Table A4.19a DATA PERTAINING TO AB2480 PHOTOREACTIVATION PARAMETERS IN TABLE 3.6 (Expt. 19a)

PR TIME (min)	SURVIVING FRACTION	h_t	$h_2 e^{-\alpha_2 t}$	$h_t - h_2 e^{-\alpha_2 t}$
0	2.02×10^{-4}			
FLASH	4.99×10^{-3}	-	-	-
0.25	6.47×10^{-3}	3.80	1.664	2.136
0.50	1.61×10^{-2}	2.88	1.590	1.290
0.75	2.50×10^{-2}	2.44	1.520	0.920
1.50	3.94×10^{-2}	1.99	1.33	0.660
3.0	9.32×10^{-2}	1.22	1.02	0.200
5.0	1.4×10^{-1}	0.721	-	-
9.0	2.04×10^{-1}	0.345	-	-
14.0	2.5×10^{-1}	0.142	-	-
20	3.2×10^{-1}	-	-	-
30	2.88×10^{-1}	-	-	-

Table A4.19b DATA PERTAINING TO AB2480 PHOTOREACTIVATION PARAMETERS IN TABLE 3.6 (Expt. 19b)

PR TIME (min)	SURVIVING FRACTION	h_t	$h_2e^{-\alpha_2 t}$	$h_t-h_2e^{-\alpha_2 t}$
0	5.5×10^{-5}	-	-	-
FLASH	6.0×10^{-4}	-	-	-
0.25	1.32×10^{-3}	5.47	0.975	4.5
0.50	9.55×10^{-3}	3.48	0.934	2.55
0.75	2.74×10^{-2}	2.44	0.905	1.54
1.50	8.65×10^{-2}	1.29	0.821	0.47
3.0	1.23×10^{-1}	0.897	0.676	0.221
5.0	1.82×10^{-1}	0.518	-	-
9.0	2.29×10^{-1}	0.316	-	-
14.0	2.67×10^{-1}	0.162	-	-
20.0	2.75×10^{-1}	0.132	-	-
30.0	3.14×10^{-1}	-	-	-

Table A4.19c DATA PERTAINING TO AB2480 PHOTOREACTIVATION PARAMETERS IN TABLE 3.6 (Expt. 19c)

PR TIME (min)	SURVIVING FRACTION	h_t	$h_2e^{-\alpha_2 t}$	$h_t-h_2e^{-\alpha_2 t}$
0	2.82×10^{-4}	-	-	-
FLASH	4.00×10^{-3}	-	-	-
0.25	5.02×10^{-2}	1.94	1.102	0.838
0.50	6.50×10^{-2}	1.68	1.05	0.63
0.75	9.59×10^{-2}	1.29	0.998	0.292
1.50	1.29×10^{-1}	0.998	0.950	0.048
3.0	1.82×10^{-1}	0.648	-	-
5.0	2.27×10^{-1}	0.433	-	-
9.0	2.90×10^{-1}	0.188	-	-
14.0	3.25×10^{-1}	0.074	-	-
20.0	3.25×10^{-1}	0.074	-	-
30.0	3.50×10^{-1}	-	-	-

Table A4.20a DATA PERTAINING TO AS44 PHOTOREACTIVATION PARAMETERS IN TABLE 3.6 (Expt. 20a)

PR TIME (min)	SURVIVING FRACTION	h_t	$h_2 e^{-\alpha_2 t}$	$h_t - h_2 e^{-\alpha_2 t}$
0	3.22×10^{-5}	-	-	-
FLASH	2.77×10^{-4}	-	-	-
1	8.94×10^{-4}	4.94	3.133	1.81
1.5	1.23×10^{-3}	4.62	3.003	1.62
2	2.51×10^{-3}	3.91	2.88	1.03
3	5.71×10^{-3}	3.09	2.645	0.44
4	9.32×10^{-3}	2.60	3.43	0.17
7	2.58×10^{-2}	1.58	-	-
12	3.78×10^{-2}	1.20	-	-
16	5.00×10^{-2}	0.916	-	-
20	6.52×10^{-2}	0.65	-	-
25	8.5×10^{-2}	0.386	-	-
30	9.49×10^{-2}	0.275	-	-
35	1.07×10^{-1}	0.155	-	-
40	1.23×10^{-1}	0.016	-	-
50	1.25×10^{-1}	-	-	-

Table A4.20b DATA PERTAINING TO AS44 PHOTOREACTIVATION PARAMETERS IN TABLE 3.6 (Expt. 20b)

PR TIME (min)	SURVIVING FRACTION	h_t	$h_2 e^{-\alpha_2 t}$	$h_t - h_2 e^{-\alpha_2 t}$
0	1.26×10^{-4}	-	-	-
FLASH	7.80×10^{-4}	-	-	-
1	1.12×10^{-3}	5.23	3.56	1.67
2	3.33×10^{-3}	4.15	2.75	1.41
3	6.10×10^{-3}	3.54	2.56	0.98
4	1.12×10^{-2}	2.93	2.39	0.54
8	3.44×10^{-2}	1.81	-	-
14	6.38×10^{-2}	1.20	-	-
20	9.45×10^{-2}	0.79	-	-
30	1.11×10^{-1}	0.64	-	-
40	1.58×10^{-1}	0.285	-	-
50	1.78×10^{-1}	0.165	-	-
60	2.10×10^{-1}	-	-	-

Table A4.20c DATA PERTAINING TO AS44 PHOTOREACTIVATION PARAMETERS IN TABLE 3.6 (Expt. 20c)

PR TIME (min)	SURVIVING FRACTION	h_t	$h_2 e^{-\alpha_2 t}$	$h_t - h_2 e^{-\alpha_2 t}$
0	2.26×10^{-4}	-	-	-
FLASH	6.21×10^{-4}	-	-	-
1	9.47×10^{-4}	5.35	2.90	2.45
3	7.35×10^{-3}	3.30	2.46	0.84
4	1.45×10^{-2}	2.62	2.26	0.36
8	4.29×10^{-2}	1.54	-	-
14	8.1×10^{-2}	0.90	-	-
20	1.01×10^{-1}	0.683	-	-
30	1.60×10^{-1}	0.223	-	-
45	1.85×10^{-1}	0.078	-	-
60	2.0×10^{-1}	-	-	-

Table A4.21 DATA PERTAINING TO DY326 PHOTOREACTIVATION PARAMETERS IN TABLE 3.6

PR TIME	Expt 21a		Expt 21b		Expt 21c		Expt 21d	
(min)	S/So	h_t	S/So	h_t	S/So	h_t	S/So	h_t
0	6×10^{-5}		4.22×10^{-5}	-	3.5×10^{-5}	-	6.18×10^{-5}	-
20	9.5×10^{-5}	1.44	4.12×10^{-5}	2.14	4.15×10^{-5}	2.14	9.4×10^{-5}	1.40
40	1.65×10^{-4}	0.855	8.61×10^{-5}	1.40	8.70×10^{-5}	1.60	2.3×10^{-4}	0.502
60	2.6×10^{-4}	0.430	1.84×10^{-4}	0.67	1.58×10^{-4}	0.46	2.6×10^{-4}	0.38
80	3.4×10^{-4}	0.163	2.22×10^{-4}	0.46	1.93×10^{-4}	0.46	3.27×10^{-4}	0.15
100	3.9×10^{-4}	0.025	3.19×10^{-4}	0.092	1.61×10^{-4}	0.46	3.80×10^{-4}	-
120	4.0×10^{-4}	-	2.55×10^{-4}	0.32	2.15×10^{-4}	0.15	-	-
150	3.90×10^{-4}	-	3.5×10^{-4}	-	$2.5 \times 10_{-4}$	-	-	-
180	3.95×10^{-5}	-	2.92×10^{-4}	-	2.15×10^{-4}	-	-	-

Table A4.22a DATA PERTAINING TO THE PHOTOREACTIVATION OF AS44 AT 15°C

PR TIME (min)	SURVIVING FRACTION	(CORRECTED) 1-P	h_t	$h_2e^{-\alpha_2 t}$	$h_t - h_2e^{-\alpha_2 t}$
0	6.82×10^{-5}	-	-	-	-
FLASH	2.29×10^{-4}	0.84/1.0	-	-	-
0.5	3.83×10^{-4}	0.92	5.68	3.33	2.35
1	5.63×10^{-4}	0.86	5.29	3.29	2.00
1.5	6.78×10^{-4}	0.83	5.11	3.24	1.87
2	8.08×10^{-4}	0.80	4.93	3.20	1.73
3	1.26×10^{-3}	0.734	4.49	3.11	1.381
4	1.36×10^{-3}	0.722	4.41	3.03	1.38
5	2.11×10^{-3}	0.654	3.97	2.95	1.02
7	2.75×10^{-3}	0.613	3.71	2.71	0.92
10	4.21×10^{-3}	0.546	3.28	2.57	0.71
13	7.20×10^{-3}	0.462	2.74	2.36	0.38
16	1.09×10^{-2}	0.400	2.33	-	-
20	1.29×10^{-2}	0.372	2.16	-	-
25	1.8×10^{-2}	0.230	1.83	-	-
30	2.37×10^{-2}	0.277	1.55	-	-
35	4.02×10^{-2}	0.194	1.02	-	-
40	4.44×10^{-2}	0.178	0.916	-	-
45	4.48×10^{-2}	0.178	0.196	-	-
50	5.67×10^{-2}	0.141	0.681	-	-
60	5.94×10^{-2}	0.134	0.634	-	-
80	8.35×10^{-2}	0.081	0.294	-	-
100	9.77×10^{-2}	0.056	0.137	-	-
120	1.42×10^{-1}	-	-	-	-

Table A4.22b DATA PERTAINING TO THE PHOTOREACTIVATION OF AS44 AT 20.1°C

PR TIME (min)	SURVIVING FRACTION	(CORRECTED) 1-P	h_t	$h_2e^{-\alpha_2 t}$	$h_t-h_2e^{-\alpha_2 t}$
0	3.68×10^{-5}	-	-	-	-
FLASH	2.13×10^{-4}	0.794/1.00	-	-	-
0.5	2.98×10^{-4}	0.95	6.5	3.81	2.69
1.0	2.88×10^{-4}	0.96	6.54	3.75	2.79
1.5	3.98×10^{-4}	0.91	6.22	3.70	3.52
2	6.82×10^{-4}	0.83	5.68	3.64	2.04
3	1.05×10^{-3}	0.76	5.25	3.54	1.71
4	1.78×10^{-3}	0.69	4.44	3.44	1.0
5	2.37×10^{-3}	0.64	3.86	3.34	0.52
7	5.07×10^{-3}	0.53	3.07	-	-
10	7.21×10^{-3}	0.48	3.32	-	-
13	1.23×10^{-2}	0.40	2.79	-	-
16	1.71×10^{-2}	0.35	2.46	-	-
20	2.35×10^{-2}	0.31	2.14	-	-
25	3.48×10^{-2}	0.25	1.75	-	-
30	3.85×10^{-2}	0.23	1.65	-	-
35	5.6×10^{-2}	0.18	1.27	-	-
40	6.02×10^{-2}	0.166	1.20	-	-
45	5.7×10^{-2}	0.174	1.25	-	-
50	7.11×10^{-2}	0.141	1.30	-	-
60	9.85×10^{-2}	0.093	0.71	-	-
90	1.45×10^{-1}	0.036	0.32	-	-
120	1.85×10^{-1}	-	-	-	-

Table A4.22c DATA PERTAINING TO THE PHOTOREACTIVATION OF AS44 AT 25.3°C

PR TIME (min)	SURVIVING FRACTION	(CORRECTED) 1-P	h_t	$h_2e^{-\alpha_2 t}$	$h_t-h_2e^{-\alpha_2 t}$
0	3.22×10^{-5}	-	-	-	-
FLASH	2.77×10^{-4}	0.794/1.0	-	-	-
0.5	7.71×10^{-4}	0.841	5.37	1.18	4.19
1.0	8.94×10^{-4}	0.820	5.22	1.16	4.06
1.5	1.23×10^{-3}	0.768	4.90	1.15	3.75
2	2.51×10^{-3}	0.657	4.19	1.13	3.06
3	5.71×10^{-3}	0.529	3.36	1.09	2.27
4	9.32×10^{-3}	0.452	2.88	1.06	1.82
5	1.52×10^{-2}	0.376	2.38	1.03	1.35
7	2.58×10^{-2}	0.294	1.85	0.97	0.88
10	3.78×10^{-2}	0.234	1.47	0.88	0.59
13	3.61×10^{-2}	0.241	1.52	-	-
16	5.0×10^{-2}	0.191	1.19	-	-
20	6.52×10^{-2}	0.150	0.928	-	-
25	8.50×10^{-2}	0.108	0.663	-	-
30	9.49×10^{-2}	0.091	0.553	-	-
35	1.07×10^{-2}	0.072	0.433	-	-
40	1.23×10^{-1}	0.050	0.294	-	-
45	1.25×10^{-1}	0.048	0.278	-	-
50	1.25×10^{-1}	0.048	0.278	-	-
60	1.43×10^{-1}	0.027	0.143	-	-
90	1.78×10^{-1}	-	-	-	-
120	1.61×10^{-1}	-	-	-	-

Table A4.22d DATA PERTAINING TO THE PHOTOREACTIVATION OF AS44 AT 30.1°C

PR TIME (min)	SURVIVING FRACTION	(CORRECTED) 1-P	h_t	$h_2e^{-\alpha_2 t}$	$h_t - h_2e^{-\alpha_2 t}$
0	2.98×10^{-5}	-	-	-	-
FLASH	4.44×10^{-4}	0.685/1.0	-	-	-
0.5	9.24×10^{-4}	0.875	5.07	1.80	3.27
1	2.02×10^{-3}	0.74	4.31	1.75	2.56
1.5	4.05×10^{-3}	0.624	3.61	1.70	1.891
2	5.11×10^{-3}	0.584	3.38	1.66	1.72
3	1.28×10^{-2}	0.428	2.46	1.57	0.89
4	1.71×10^{-2}	0.378	2.17	1.49	0.71
5	2.61×10^{-2}	0.306	1.75	1.41	0.34
7	4.35×10^{-2}	0.220	1.24	-	-
10	6.07×10^{-2}	0.163	0.91	-	-
13	5.76×10^{-2}	0.172	0.957	-	-
16	6.18×10^{-2}	0.160	0.886	-	-
20	7.41×10^{-2}	0.129	0.705	-	-
25	1.03×10^{-1}	0.073	0.376	-	-
30	1.11×10^{-1}	0.060	0.310	-	-
35	1.02×10^{-1}	0.075	0.386	-	-
40	1.16×10^{-1}	0.053	0.257	-	-
45	1.33×10^{-1}	0.029	0.120	-	-
50	1.27×10^{-1}	0.037	-	-	-
60	1.58×10^{-1}	0.037	-	-	-
90	1.48×10^{-1}	-	-	-	-
120	1.58×10^{-1}	-	-	-	-

Table A4.22e DATA PERTAINING TO THE PHOTOREACTIVATION OF AS44 AT 36.9°C

PR TIME (min)	SURVIVING FRACTION	(CORRECTED) 1-P	h_t	$h_2e^{-\alpha_2 t}$	$h_t-h_2e^{-\alpha_2 t}$
0	2.8×10^{-5}	-	-	-	-
FLASH	1.89×10^{-4}	0.779/1.0	-	-	-
0.5	5.06×10^{-4}	0.854	5.76	2.19	3.57
1.0	1.39×10^{-3}	0.704	4.75	2.11	2.64
1.5	3.07×10^{-3}	0.586	3.95	2.03	1.92
2	4.63×10^{-3}	0.526	3.54	1.95	1.59
3	1.25×10^{-2}	0.378	2.55	1.80	0.75
4	1.90×10^{-2}	0.316	2.13	1.66	0.47
5	2.38×10^{-2}	0.283	1.90	1.54	0.36
7	3.85×10^{-2}	0.210	1.42	1.32	0.10
10	6.30×10^{-2}	0.138	0.932	-	-
13	6.84×10^{-2}	0.126	0.85	-	-
16	7.67×10^{-2}	0.109	0.735	-	-
20	1.00×10^{-1}	0.094	0.47	-	-
25	1.23×10^{-1}	0.039	0.262	-	-
30	1.30×10^{-1}	0.036	0.208	-	-
35	1.38×10^{-1}	0.026	0.148	-	-
40	1.43×10^{-1}	0.017	0.112	-	-
45	1.43×10^{-1}	0.0165	-	-	-
50	1.45×10^{-1}	0.0114	-	-	-
60	1.40×10^{-1}	-	-	-	-
90	1.77×10^{-1}	-	-	-	-
120	1.76×10^{-1}	-	-	-	-

Table A4.23 DATA PERTAINING TO THE ARRHENIUS PLOT FOR DY326 (FIG. 3.15).

PR TIME	23a 15°		23b 20°		23c 25°		23d 30°		23e 37°	
(min)	S/S_0	1-P	S/S_0	1-P	S/S_0	1-P	S/S_0	1-P	S/S_0	1-P
0	5.75×10^{-5}	-	6.7×10^{-6}	-	5.75×10^{-5}	-	5.27×10^{-5}	-	9.05×10^{-5}	-
10	7.6×10^{-5}	0.980	6.98×10^{-5}	0.974	6.29×10^{-5}	0.998	6.49×10^{-5}	0.988	1.18×10^{-4}	0.963
20	7.3×10^{-5}	0.984	6.98×10^{-5}	0.962	5.99×10^{-5}	0.969	7.05×10^{-5}	0.977	1.89×10^{-4}	0.898
30	7.6×10^{-5}	0.981	7.05×10^{-5}	0.960	6.05×10^{-5}	0.952	7.16×10^{-5}	0.972	2.39×10^{-4}	0.866
40	8.2×10^{-5}	0.976	7.78×10^{-5}	0.959	1.02×10^{-4}	0.924	7.54×10^{-5}	0.922	3.11×10^{-4}	0.829
60	8.64×10^{-5}	0.973	7.98×10^{-5}	0.953	1.43×10^{-4}	0.879	7.65×10^{-5}	0.901	4.11×10^{-4}	0.791
80	1.30×10^{-4}	0.946	1.13×10^{-4}	0.894	1.92×10^{-4}	0.840	1.46×10^{-4}	0.830	4.59×10^{-4}	0.775
100	1.50×10^{-4}	0.936	1.50×10^{-4}	0.866	2.11×10^{-4}	0.827	0.02×10^{-4}	0.814	4.67×10^{-4}	0.773
120	1.82×10^{-4}	0.923	1.93×10^{-4}	0.828	2.93×10^{-4}	0.784	2.09×10^{-4}	0.789	3.55×10^{-4}	0.811
150	2.83×10^{-4}	0.894	2.02×10^{-4}	0.806	2.72×10^{-4}	0.794	2.35×10^{-4}	0.778	-	-
180	3.14×10^{-4}	0.887	2.93×10^{-4}	0.782	3.81×10^{-4}	0.749	3.53×10^{-4}	0.744	-	-

Table A4.24 DATA PERTAINING TO THE SURVIVOR CURVES OBTAINED WHEN ANAEROBICALLY-GROWN AB2480 WAS IRRADIATED WITH 254 nm UV AND AFTER A SINGLE PHOTOREACTIVATING FLASH, THE MEAN PARAMETERS ARE INCLUDED IN TABLE 3.7

EXPT No.	INITIAL VIABLE COUNT (ml^{-1})	FLUENCE (Jm^{-2})	SURVIVING FRACTION 254 nm	FLASH
24a	1.29×10^{7}	0.061	$\underline{4.54 \times 10^{-1}}$	5.28×10^{-1}
		0.123	1.78×10^{-1}	$\underline{1.91 \times 10^{-1}}$
		0.185	6.65×10^{-2}	8.76×10^{-2}
		0.247	1.82×10^{-2}	2.55×10^{-2}
		0.308	5.75×10^{-3}	1.12×10^{-2}
		0.370	1.85×10^{-3}	2.8×10^{-2}
		0.432	4.56×10^{-4}	1.03×10^{-3}
		0.494	1.61×10^{-4}	3.48×10^{-4}
24b	1.69×10^{-7}	0.063	$\underline{4.50 \times 10^{-1}}$	6.10×10^{-1}
		0.124	1.61×10^{-1}	$\underline{2.00 \times 10^{-1}}$
		0.187	7.50×10^{-2}	9.03×10^{-2}
		0.242	1.96×10^{-2}	2.78×10^{-2}
		0.301	6.50×10^{-3}	1.20×10^{-2}
		0.368	2.26×10^{-3}	4.20×10^{-3}
		0.429	6.01×10^{-4}	1.30×10^{-3}
		0.501	1.92×10^{-4}	4.60×10^{-4}

Table A4.25 DATA PERTAINING TO THE SURVIVOR CURVES OBTAINED WHEN ANAEROBICALLY-GROWN AS44 WAS IRRADIATED WITH 254 nm UV AND AFTER A SINGLE PHOTOREACTIVATING FLASH, THE MEAN PARAMETERS ARE INCLUDED IN TABLE 3.7

EXPT No.	INITIAL VIABLE COUNT (ml^{-1})	FLUENCE (Jm^{-2})	SURVIVING FRACTION 254 nm	FLASH
25a	1.14×10^{7}	0.063	$\underline{3.59 \times 10^{-1}}$	3.62×10^{-1}
		0.126	1.21×10^{-1}	$\underline{1.49 \times 10^{-1}}$
		0.190	3.44×10^{-2}	5.16×10^{-2}
		0.254	1.09×10^{-2}	1.38×10^{-2}
		0.319	3.34×10^{-3}	3.34×10^{-3}
		0.383	8.33×10^{-4}	1.40×10^{-3}
		0.447	2.32×10^{-4}	4.50×10^{-3}
		0.511	7.9×10^{-1}	1.75×10^{-4}
25b	9.73×10^{6}	0.061	$\underline{3.97 \times 10^{-1}}$	8.97×10^{-1}
		0.122	1.81×10^{-1}	$\underline{2.41 \times 10^{-1}}$
		0.183	3.50×10^{-2}	5.10×10^{-2}
		0.245	1.31×10^{-2}	2.08×10^{-2}
		0.306	5.10×10^{-3}	8.03×10^{-3}
		0.368	1.59×10^{-3}	2.61×10^{-3}
		0.430	3.49×10^{-4}	6.75×10^{-4}
		0.491	1.10×10^{-4}	2.20×10^{-4}

Table A4.26 DATA PERTAINING TO THE SURVIVOR CURVES OBTAINED WHEN ANAEROBICALLY-GROWN DY326 WAS IRRADIATED WITH 254 nm UV AND AFTER ONE PHOTOREACTIVATING FLASH, THE MEAN PARAMETERS ARE INCLUDED IN TABLE 3.7

EXPT No.	INITIAL VIABLE COUNT (ml^{-1})	FLUENCE (Jm^{-2})	SURVIVING FRACTION 254 nm	FLASH
26a	1.51×10^{7}	0.069	3.2×10^{-1}	3.27×10^{-1}
		0.138	1.12×10^{-1}	1.02×10^{-1}
		0.206	2.83×10^{-2}	3.21×10^{-2}
		0.276	7.65×10^{-3}	2.04×10^{-3}
		0.415	4.50×10^{-4}	4.87×10^{-4}
		0.484	1.27×10^{-4}	1.37×10^{-4}
		0.554	4.16×10^{-5}	3.05×10^{-5}
26b	1.27×10^{7}	0.070	3.11×10^{-1}	3.18×10^{-1}
		0.139	1.06×10^{-1}	1.04×10^{-1}
		0.206	3.08×10^{-2}	3.20×10^{-2}
		0.274	6.92×10^{-3}	7.21×10^{-3}
		0.345	2.21×10^{-3}	2.25×10^{-3}
		0.419	4.41×10^{-4}	4.67×10^{-4}
		0.490	1.18×10^{-4}	1.21×10^{-4}
		0.560	3.96×10^{-5}	3.63×10^{-5}

Table A4.27 DATA PERTAINING TO THE SURVIVOR CURVES OBTAINED WHEN ANAEROBICALLY-GROWN AS46 WAS IRRADIATED WITH 254 nm UV AND AFTER ONE PHOTOREACTIVATING FLASH, THE MEAN PARAMETERS ARE INCLUDED IN TABLE 3.7

EXPT No.	INITIAL VIABLE COUNT (ml^{-1})	FLUENCE (Jm^{-2})	SURVIVING FRACTION 254 nm	FLASH
27a	6.23×10^{6}	0.074	$\underline{4.33 \times 10^{-1}}$	$\underline{2.78 \times 10^{-1}}$
		0.153	8.98×10^{-1}	8.98×10^{-2}
		0.228	2.29×10^{-2}	2.47×10^{-2}
		0.303	5.88×10^{-3}	5.13×10^{-3}
		0.376	1.64×10^{-3}	1.54×10^{-3}
		0.450	4.60×10^{-4}	4.50×10^{-4}
		0.525	8.66×10^{-5}	8.56×10^{-5}
27b	1.07×10^{7}	0.069	$\underline{4.12 \times 10^{-1}}$	5.03×10^{-1}
		0.149	9.28×10^{-2}	$\underline{9.01 \times 10^{-2}}$
		0.224	2.36×10^{-2}	2.26×10^{-2}
		0.295	6.50×10^{-3}	6.34×10^{-3}
		0.374	1.71×10^{-3}	1.68×10^{-3}
		0.446	4.92×10^{-4}	4.61×10^{-4}
		0.514	8.12×10^{-5}	8.78×10^{-5}

Table A4.28 DATA PERTAINING TO PHOTOREACTIVATION OF ANAEROBICALLY-GROWN AB2480 (FIG. 3.23a)

PR TIME (min)	SURVIVING FRACTION	CORRECTED (1-P)	h_t	$h_2 e^{-\alpha_2 t}$	$h_t - h_2 e^{-\alpha_2 t}$
0	1.03×10^{-4}	-	-	-	-
FLASH	3.02×10^{-4}	0.866/1.00	-	-	-
0.5	7.5×10^{-4}	0.814	6.02	3.00	3.02
1	1.46×10^{-3}	0.773	5.53	2.83	2.53
2	4.06×10^{-3}	0.625	4.34	2.52	1.82
4	2.28×10^{-2}	0.376	2.61	2.01	0.60
6	5.56×10^{-2}	0.248	1.72	1.595	0.125
8	8.50×10^{-2}	0.187	1.29	1.26	0.03
12	1.32×10^{-1}	0.105	0.853	-	-
20	1.88×10^{-1}	0.072	0.500	-	-
30	2.38×10^{-1}	-	-	-	-
45	2.32×10^{-1}	-	-	-	-
60	3.10×10^{-1}	-	-	-	-

Table A4.29 DATA PERTAINING TO PHOTOREACTIVATION OF ANAEROBICALLY-GROWN AS44 (FIG. 3.23b)

PR TIME (min)	SURVIVING FRACTION	CORRECTED (1-P)	h_t	$h_2e^{-\alpha_2 t}$	$h_t-h_2e^{-\alpha_2 t}$
0	7.9×10^{-5}	-	-	-	-
FLASH	1.75×10^{-4}	0.891/1.0	-	-	-
1	2.52×10^{-4}	0.945	6.14	3.88	2.26
2	6.48×10^{-4}	0.800	5.196	3.58	1.62
3	1.35×10^{-3}	0.686	4.46	3.29	1.17
4	2.84×10^{-3}	0.572	3.72	2.87	0.85
8	1.26×10^{-2}	0.343	2.23	2.095	0.135
14	3.05×10^{-2}	0.207	1.34	-	-
20	5.30×10^{-2}	0.100	0.792	-	-
30	8.2×10^{-2}	0.071	0.355	-	-
40	1.14×10^{-1}	0.004	0.157	-	-
50	9.96×10^{-2}	0.025	0.161	-	-
70	1.17×10^{-1}	-	-	-	-

Table A4.30 DATE PERTAINING TO PHOTOREACTIVATION OF ANAEROBICALLY-GROWN DY326 (FIG 3.23c)

PR TIME (min)	SURVIVING FRACTION	(1-P)	h_t
0	1.55×10^{-4}	-	-
30	2.25×10^{-4}	0.945	1.014
60	2.5×10^{-4}	0.930	0.908
120	3.3×10^{-4}	0.889	0.630
180	3.7×10^{-4}	0.872	0.520
240	3.9×10^{-4}	0.865	0.463
300	4.7×10^{-4}	0.837	0.277
360	5.2×10^{-4}	0.823	0.176
420	5.9×10^{-4}	0.804	0.049
480	6.2×10^{-4}	0.797	-

Table A4.31 DATA PERTAINING TO THE SURVIVOR CURVES OBTAINED WHEN AB2480 WAS GROWN AT 26°C AND IRRADIATED WITH 254 nm AND ONE PHOTOREACTIVATING FLASH (FIG. 3.25a).

EXPT No.	INITIAL VIABLE COUNT (ml^{-1})	FLUENCE (Jm^{-2})	SURVIVING FRACTION 254 nm	SURVIVING FRACTION FLASH
31a	2.22×10^{7}	0.079	$\underline{3.89 \times 10^{-1}}$	8.63×10^{-1}
		0.157	1.09×10^{-1}	$\underline{6.42 \times 10^{-1}}$
		0.235	2.42×10^{-2}	4.87×10^{-1}
		0.314	5.14×10^{-3}	2.64×10^{-1}
		0.392	1.25×10^{-3}	1.65×10^{-1}
		0.470	2.69×10^{-4}	9.00×10^{-2}
		0.548	6.72×10^{-5}	5.40×10^{-2}
31b	1.02×10^{7}	0.077	$\underline{3.46 \times 10^{-1}}$	7.16×10^{-1}
		0.155	8.26×10^{-2}	$\underline{6.0 \times 10^{-1}}$
		0.232	2.19×10^{-2}	4.50×10^{-1}
		0.310	4.77×10^{-3}	2.80×10^{-1}
		0.388	1.02×10^{-3}	1.30×10^{-1}
		0.466	2.34×10^{-4}	1.02×10^{-1}
		0.543	4.25×10^{-5}	4.80×10^{-2}

Table A4.32 DATA PERTAINING TO THE SURVIVOR CURVES OBTAINED WHEN AS44 WAS GROWN AT 26°C AND IRRADIATED WITH 254 nm AND ONE PHOTOREACTIVATING FLASH (FIG. 3.25b).

EXPT No.	INITIAL VIABLE COUNT (ml^{-1})	FLUENCE (Jm^{-2})	SURVIVING FRACTION 254 nm	FLASH
32a	7.23×10^{6}	0.079	$\underline{2.95 \times 10^{-1}}$	6.91×10^{-1}
		0.159	1.07×10^{-1}	$\underline{3.50 \times 10^{-1}}$
		0.239	1.4×10^{-2}	1.71×10^{-1}
		0.319	3.46×10^{-3}	7.60×10^{-2}
		0.400	5.67×10^{-4}	3.46×10^{-2}
		0.481	1.24×10^{-4}	1.22×10^{-2}
		0.561	2.03×10^{-5}	4.55×10^{-3}
32b	5.13×10^{6}	0.079	$\underline{2.14 \times 10^{-1}}$	6.36×10^{-1}
		0.159	6.95×10^{-2}	$\underline{4.12 \times 10^{-1}}$
		0.239	1.77×10^{-2}	2.03×10^{-1}
		0.318	3.64×10^{-3}	8.05×10^{-2}
		0.397	6.5×10^{-4}	3.82×10^{-2}
		0.477	1.40×10^{-4}	1.21×10^{-2}
		0.558	5.00×10^{-5}	7.34×10^{-3}

Table A4.33 DATA PERTAINING TO THE SURVIVOR CURVES OBTAINED WHEN DY326 WAS GROWN AT 26°C AND IRRADIATED WITH 254 nm AND ONE PHOTOREACTIVATING FLASH (FIG. 3.26a).

EXPT No.	INITIAL VIABLE COUNT (ml^{-1})	FLUENCE (Jm^{-2})	SURVIVING FRACTION 254 nm	FLASH
33a	2.92×10^{7}	0.069	$\underline{4.7 \times 10^{-1}}$	$\underline{4.56 \times 10^{-1}}$
		0.137	1.32×10^{-1}	1.41×10^{-1}
		0.206	3.74×10^{-2}	3.81×10^{-2}
		0.274	1.00×10^{-2}	9.69×10^{-3}
		0.343	2.78×10^{-3}	2.82×10^{-3}
		0.411	6.92×10^{-4}	7.12×10^{-4}
		0.480	1.83×10^{-4}	1.62×10^{-4}
33b	1.17×10^{7}	0.068	$\underline{4.41 \times 10^{-1}}$	$\underline{4.37 \times 10^{-1}}$
		0.136	1.20×10^{-1}	1.25×10^{-1}
		0.204	3.22×10^{-2}	3.60×10^{-2}
		0.273	8.54×10^{-3}	9.51×10^{-3}
		0.346	2.10×10^{-3}	2.65×10^{-3}
		0.414	6.57×10^{-4}	7.61×10^{-4}
		0.491	1.29×10^{-4}	1.21×10^{-4}

Table A4.34 DATA PERTAINING TO THE SURVIVOR CURVES OBTAINED WHEN AS46 WAS GROWN AT 26 °C AND IRRADIATED WITH 254 nm AND ONE PHOTOREACTIVATING FLASH (FIG. 3.26b).

EXPT No.	INITIAL VIABLE COUNT (ml^{-1})	FLUENCE (Jm^{-2})	SURVIVING FRACTION 254 nm	FLASH
34a	7.87×10^{6}	0.078	3.76×10^{-1}	3.60×10^{-1}
		0.158	8.27×10^{-2}	8.30×10^{-2}
		0.237	1.85×10^{-2}	1.94×10^{-2}
		0.320	3.85×10^{-3}	3.75×10^{-3}
		0.400	8.48×10^{-4}	9.78×10^{-4}
		0.480	1.87×10^{-4}	1.71×10^{-4}
		0.562	3.95×10^{-5}	5.00×10^{-5}
34b	6.53×10^{6}	0.069	4.90×10^{-1}	1.51×10^{-1}
		0.136	1.34×10^{-1}	1.26×10^{-1}
		0.206	3.43×10^{-2}	3.59×10^{-2}
		0.273	9.35×10^{-3}	9.91×10^{-3}
		0.343	2.40×10^{-3}	2.36×10^{-3}
		0.414	6.06×10^{-4}	6.04×10^{-4}
		0.480	1.68×10^{-4}	1.62×10^{-4}

Table A4.35a DATA PERTAINING TO PHOTOREACTIVATION OF AB2480 GROWN AT 26°C (Expt. 35a)

PR TIME (min)	SURVIVING FRACTION	CORRECTED (1-P)	h_t	$h_2e^{-\alpha_2 t}$	$h_t-h_2e^{-\alpha_2 t}$
0	1.4×10^{-4}	-	-	-	-
FLASH	3.5×10^{-3}	0.50/1.00	-	-	-
0.25	1.68×10^{-2}	0.661	2.81	-	-
0.50	3.39×10^{-2}	0.510	2.11	-	-
1.0	8.71×10^{-2}	0.310	1.645	-	-
2.0	1.8×10^{-1}	0.189	0.442	-	-
3.0	2.4×10^{-1}	0.116	0.154	-	-
4.0	2.7×10^{-1}	0.112	0.036	-	-
5.0	2.8×10^{-1}	0.107	-	-	-
7.0	2.75×10^{-1}	0.067	-	-	-
10.0	2.87×10^{-1}	0.049	-	-	-
15	3.6×10^{-1}	0.036	-	-	-
20	3.02×10^{-1}	-	-	-	-
25	3.37×10^{-1}	-	-	-	-
30	3.28×10^{-1}	-	-	-	-

Table A4.35b DATA PERTAINING TO PHOTOREACTIVATION OF AB2480 GROWN AT 26°C (Expt. 35b)

PR TIME (min)	SURVIVING FRACTION	CORRECTED (1-P)	h_t	$h_2e^{-\alpha_2 t}$	$h_t-h_2e^{-\alpha_2 t}$
0	1.8×10^{-4}	-	-	-	-
FLASH	4.6×10^{-3}	0.56/1.00	2.27	-	-
0.25	3.05×10^{-2}	0.55	1.72	-	-
0.50	5.30×10^{-2}	0.41	1.30	-	-
1.0	1.1×10^{-1}	0.240	0.99	-	-
2.0	2.15×10^{-1}	0.077	0.32	-	-
3.0	2.66×10^{-1}	0.026	0.107	-	-
4.0	2.86×10^{-1}	0.008	0.035	-	-
5.0	2.90×10^{-1}	0.005	0.020	-	-
7.0	2.96×10^{-1}	-	-	-	-
10	2.95×10^{-1}	-	-	-	-
15	3.16×10^{-1}	-	-	-	-
20	3.08×10^{-1}	-	-	-	-
25	2.90×10^{-1}	-	-	-	-
30	2.95×10^{-1}	-	-	-	-

Table A4.36a DATA PERTAINING TO PHOTOREACTIVATION OF AB2480 GROWN AT 30°C (Expt. 36a)

PR TIME (min)	SURVIVING FRACTION	CORRECTED (1-P)	h_t	$h_2e^{-\alpha_2 t}$	$h_t-h_2e^{-\alpha_2 t}$
0	2.97×10^{-4}	-	-	-	-
FLASH	1.14×10^{-3}	0.81/1.0	-	-	-
0.25	1.29×10^{-2}	0.474	3.396	2.558	0.838
0.50	2.20×10^{-2}	0.422	2.860	2.319	0.541
1	4.71×10^{-2}	0.361	2.100	1.906	0.194
2	9.83×10^{-2}	0.234	1.365	1.288	0.077
3	1.57×10^{-1}	0.125	0.897	-	-
4	1.94×10^{-1}	0.118	0.685	-	-
5	2.60×10^{-1}	0.039	0.472	-	-
7	3.14×10^{-1}	0.035	0.204	-	-
10	3.25×10^{-1}	-	-	-	-
15	3.31×10^{-1}	-	-	-	-
20	3.8×10^{-1}	-	-	-	-
25	3.85×10^{-1}	-	-	-	-
30	3.85×10^{-1}	-	-	-	-

Table A4.36b DATA PERTAINING TO PHOTOREACTIVATION OF AB2480 GROWN AT 30°C (Expt. 36b)

PR TIME (min)	SURVIVING FRACTION	CORRECTED (1-P)	h_t	$h_2e^{-\alpha_2 t}$	$h_t - h_2e^{-\alpha_2 t}$
0	2.86×10^{-4}	-	-	-	-
FLASH	1.21×10^{-3}	0.80/1.00	-	-	-
0.25	1.26×10^{-2}	0.58	3.422	2.682	0.736
0.50	2.31×10^{-2}	0.472	2.816	2.438	0.378
1.0	4.56×10^{-2}	0.350	2.136	2.008	0.128
2.0	1.01×10^{-1}	0.210	1.341	-	-
3.0	1.63×10^{-1}	0.122	0.862	-	-
4	1.90×10^{-1}	0.094	0.709	-	-
5	2.56×10^{-1}	0.041	0.411	-	-
7	3.18×10^{-1}	0.002	0.194	-	-
10	3.22×10^{-1}	-	-	-	-
15	3.01×10^{-1}	-	0.249	-	-
20	2.96×10^{-1}	-	0.265	-	-
25	3.86×10^{-1}	-	-	-	-
30	3.2×10^{-1}	-	-	-	-

Table A4.37a DATA PERTAINING TO PHOTOREACTIVATION OF AS44 GROWN AT 26° (EXPT 37a)

PR TIME (min)	SURVIVING FRACTION	CORRECTED (1-P)	h_t	$h_2e^{-\alpha_2 t}$	$ht-h_2e^{-\alpha_2 t}$
0	7.27×10^{-5}	-	-	-	-
FLASH	1.08×10^{-3}	0.66/1.0	-	-	-
0.5	6.47×10^{-3}	0.66	3.451	1.776	1.675
1	9.64×10^{-3}	0.582	3.052	1.662	1.390
2	1.83×10^{-2}	0.460	2.411	1.455	0.956
3	3.23×10^{-2}	0.352	1.843	1.274	0.569
4	5.22×10^{-2}	0.260	1.363	1.116	0.247
6	9.03×10^{-2}	0.156	0.815	0.9774	0.1666
8	1.12×10^{-1}	0.114	0.600	-	-
10	1.21×10^{-1}	0.099	0.522	-	-
15	1.51×10^{-1}	-	-	-	-
20	1.67×10^{-1}	-	0.125	-	-
25	1.87×10^{-1}	-	-	-	-
30	1.93×10^{-1}	-	-	-	-
45	2.04×10^{-1}	-	-	-	-
60	1.93×10^{-1}	-	-	-	-

Table A4.37b DATA PERTAINING TO PHOTOREACTIVATION OF AS44 GROWN AT 26° (EXPT 37b)

PR TIME (min)	SURVIVING FRACTION	CORRECTED (1-P)	h_t	$h_2e^{-\alpha_2 t}$	$h_t-h_2e^{-\alpha_2 t}$
0	9.26×10^{-5}	-	-	-	-
FLASH	1.20×10^{-2}	0.68/1.0	-	-	-
0.5	2.70×10^{-3}	0.85	4.4	2.52	1.88
1	6.10×10^{-3}	0.70	3.58	2.34	1.24
2	1.56×10^{-2}	0.52	2.65	2.03	0.62
3	3.68×10^{-2}	0.36	1.79	1.762	0.028
4	4.79×10^{-2}	0.31	1.52	-	-
6	6.56×10^{-2}	0.25	1.21	-	-
8	1.02×10^{-1}	0.17	0.77	-	-
10	1.2×10^{-1}	0.14	0.61	-	-
15	1.64×10^{-1}	-	0.29	-	-
20	1.76×10^{-1}	-	0.22	-	-
30	2.13×10^{-1}	-	0.03	-	-
45	2.16×10^{-1}	-	0.02	-	-
60	2.52×10^{-1}	-	-	-	-

Table A4.38a DATA PERTAINING TO PHOTOREACTIVATION OF AS44 GROWN AT 30°C (Expt. 38a)

PR TIME (min)	SURVIVING FRACTION	CORRECTED (1-P)	h_t	$h_2e^{-\alpha_2 t}$	$h_t-h_2e^{-\alpha_2 t}$
0	5.10×10^{-5}	-	-	-	-
FLASH	3.30×10^{-4}	0.77/1.00	-	-	-
1	5.57×10^{-4}	0.82	5.85	2.82	3.03
2	1.11×10^{-3}	0.73	5.16	2.59	2.57
3	2.98×10^{-3}	0.59	4.17	2.37	1.80
4	5.75×10^{-3}	0.49	3.52	2.18	1.34
6	1.53×10^{-2}	0.36	2.54	1.83	0.71
8	2.92×10^{-2}	0.27	1.89	1.54	0.35
10	5.20×10^{-2}	0.19	1.32	-	-
15	8.49×10^{-2}	-	0.83	-	-
20	1.01×10^{-1}	-	0.56	-	-
30	1.52×10^{-1}	-	-	-	-
45	1.69×10^{-1}	-	-	-	-
60	1.94×10^{-1}	-	-	-	-

Table A4.38b DATA PERTAINING TO PHOTOREACTIVATION OF AS44 GROWN AT 30°C (Expt. 38b)

PR TIME (min)	SURVIVING FRACTION	CORRECTED (1-P)	h_t	$h_2e^{-\alpha_2 t}$	$h_t-h_2e^{-\alpha_2 t}$
0	8.7×10^{-5}	-	-	-	-
FLASH	2.31×10^{-4}	0.87/1.0	-	-	-
0.5	3.41×10^{-4}	0.94	6.13	2.78	2.33
1	9.42×10^{-4}	0.78	5.11	2.49	1.74
2	2.27×10^{-3}	0.65	4.23	2.24	1.18
3	5.10×10^{-3}	0.53	3.42	2.00	0.88
4	8.77×10^{-3}	0.44	2.88	1.62	0.50
6	1.87×10^{-2}	0.33	2.12	1.30	0.23
8	3.38×10^{-2}	0.24	1.53	-	-
10	5.68×10^{-2}	0.16	1.01	-	-
15	8.41×10^{-2}	0.09	0.61	-	-
20	9.74×10^{-2}	-	0.35	-	-
25	1.14×10^{-1}	-	0.24	-	-
30	1.40×10^{-1}	-	-	-	-
45	1.36×10^{-1}	-	-	-	-
60	1.56×10^{-1}	-	-	-	-

Table A4.39a DATA PERTAINING TO PHOTOREACTIVATION OF DY326 GROWN AT 26°C (Expt. 39a)

PR TIME (min)	SURVIVING FRACTION	CORRECTED (1-P)	h_t	$h_2e^{-\alpha_2 t}$	$h_t-h_2e^{-\alpha_2 t}$
0	4.00×10^{-5}	-	-	-	-
10	1.25×10^{-4}	0.84	3.1	2.27	0.83
20	3.20×10^{-4}	0.74	2.17	1.81	0.36
30	5.30×10^{-4}	0.66	1.66	1.44	0.22
40	8.00×10^{-4}	0.62	1.25	1.153	0.097
60	1.35×10^{-3}	0.55	0.73	-	-
80	1.76×10^{-3}	0.54	0.46	-	-
100	2.05×10^{-3}	0.495	0.31	-	-
120	2.3×10^{-3}	0.49	0.196	-	-
150	2.55×10^{-3}	0.47	0.93	-	-
180	2.8×10^{-3}	-	-	-	-

Table A4.39b DATA PERTAINING TO PHOTOREACTIVATION OF DY326 GROWN AT 26°C (Expt. 39b)

PR TIME (min)	SURVIVING FRACTION	CORRECTED (1-P)	h_t	$h_2e^{-\alpha_2 t}$	$h_t-h_2e^{-\alpha_2 t}$
0	3.99×10^{-5}	-	-	-	-
10	1.01×10^{-4}	0.88	3.34	1.06	2.28
20	3.91×10^{-4}	0.74	1.99	0.873	1.12
30	6.8×10^{-4}	0.64	1.44	0.716	0.724
40	1.07×10^{-3}	0.58	0.98	0.59	0.39
60	1.43×10^{-3}	0.55	0.69	-	-
80	2.06×10^{-3}	0.50	0.33	-	-
100	2.42×10^{-3}	0.48	0.17	-	-
120	2.55×10^{-3}	0.47	0.115	-	-
150	2.62×10^{-3}	0.471	-	-	-
180	2.79×10^{-3}	0.463	-	-	-

Table A4.39c DATA PERTAINING TO PHOTOREACTIVATION OF DY326 GROWN AT 26°C (Expt. 39c)

PR TIME (min)	SURVIVING FRACTION	CORRECTED (1-P)	h_t	$h_2e^{-\alpha_2 t}$	$h_t-h_2e^{-\alpha_2 t}$
0	2.11×10^{-5}	-	-	-	-
10	8.20×10^{-5}	0.84	3.20	1.98	1.22
20	2.00×10^{-4}	0.73	2.30	1.53	0.77
30	4.20×10^{-4}	0.65	1.56	1.19	0.37
40	7.00×10^{-4}	0.59	1.05	0.92	0.13
60	1.20×10^{-3}	0.52	0.51	-	-
80	1.51×10^{-3}	0.49	0.29	-	-
100	1.65×10^{-3}	0.48	0.19	-	-
120	1.77×10^{-3}	0.477	0.13	-	-
150	1.81×10^{-3}	0.474	-	-	-
180	2.08×10^{-3}	0.457	-	-	-

Table A4.40 DATA PERTAINING TO THE PHOTOREACTIVATION OF DY326 GROWN AT 30°C (EXPT 40a,b)

PR TIME	Expt. 40a			Expt. 40b		
(min)	S/So	(1-P)	h_t	S/So	(1-P)	h_t
0	7.01×10^{-5}	-	-	8.60×10^{-5}	-	-
20	1.11×10^{-4}	0.84	2.31	1.36×10^{-4}	0.94	1.95
40	2.20×10^{-4}	0.76	1.63	4.23×10^{-4}	0.77	0.82
60	4.00×10^{-4}	0.68	1.03	6.76×10^{-4}	0.71	0.35
80	6.05×10^{-4}	0.62	0.62	8.26×10^{-4}	0.68	0.15
100	7.75×10^{-4}	0.58	0.37	9.04×10^{-4}	0.67	0.06
120	9.19×10^{-4}	0.57	0.22	9.34×10^{-4}	0.66	0.026
150	1.07×10^{-3}	0.55	0.05	9.6×10^{-5}	0.66	-
180	1.12×10^{-3}	-	-	9.5×10^{-5}	0.66	-

Table A4.41 DATA PERTAINING TO THE PHOTOREACTIVATION OF AS46 GROWN AT 26°C (EXPT 41a,b)

PR TIME	Expt. 41a			Expt. 41b		
(min)	S/So	(1-P)	h_t	S/So	(1-P)	h_t
0	3.2×10^{-5}	-	-	3.92×10^{-5}	-	-
20	6.5×10^{-5}	0.915	2.22	5.26×10^{-5}	0.96	2.21
40	1.5×10^{-4}	0.82	1.39	7.41×10^{-5}	0.92	1.86
60	3.1×10^{-4}	0.737	0.66	3.49×10^{-4}	0.72	0.33
80	4.6×10^{-4}	0.690	0.27	4.04×10^{-4}	0.70	0.17
120	5.6×10^{-4}	0.688	-	3.7×10^{-4}	0.71	0.23
150	5.8×10^{-4}	0.670	-	4.78×10^{-4}	0.68	-
180	5.7×10^{-4}	-	-	4.35×10^{-4}	0.69	-

Table A4.42 DATA PERTAINING TO THE SURVIVOR CURVES OBTAINED WHEN AB2480 WAS IRRADIATED AT 313 nm IN THE PRESENCE OF 0.1% ACETOPHENONE AT 0°C, THE INACTIVATION PARAMETERS OF WHICH ARE GIVEN IN TABLE 3.12

EXPT No.	INITIAL VIABLE COUNT (ml^{-1})	CORRECTED FLUENCE (Jm^{-2})	SURVIVING FRACTION 313 nm	SURVIVING FRACTION FLASH
42a	8.5×10^{6}	15.78	$\underline{1.90 \times 10^{-1}}$	6.35×10^{-1}
		31.54	1.90×10^{-1}	$\underline{2.98 \times 10^{-1}}$
		47.32	7.02×10^{-1}	1.14×10^{-1}
Fluence rate ~ 1.99 Wm^{-2}		62.93	2.16×10^{-2}	6.20×10^{-2}
		78.66	6.78×10^{-3}	2.1×10^{-2}
		94.39	2.36×10^{-3}	2.38×10^{-2}
		125.86	3.53×10^{-4}	4.86×10^{-3}
		157.32	5.65×10^{-5}	1.43×10^{-3}
42b	1.17×10^{6}	16.8	$\underline{6.96 \times 10^{-1}}$	6.00×10^{-1}
		33.6	1.46×10^{-1}	$\underline{2.61 \times 10^{-1}}$
		50.4	4.92×10^{-2}	1.22×10^{-1}
Fluence rate ~ 1.96 Wm^{-2}		67.2	1.67×10^{-2}	5.85×10^{-2}
		84.0	1.89×10^{-3}	2.68×10^{-2}
		100.8	1.89×10^{-3}	1.40×10^{-2}
		117.6	6.37×10^{-4}	7.52×10^{-3}
42c	1.04×10^{6}	14.98	$\underline{4.57 \times 10^{-1}}$	-
		29.95	1.76×10^{-1}	-
		44.93	7.27×10^{-2}	-
Fluence rate ~ 1.64 Wm^{-2}		59.75	2.62×10^{-2}	-
		74.69	9.42×10^{-3}	-
		89.60	3.51×10^{-3}	-
		104.56	1.54×10^{-3}	-
42d	9.7×10^{6}	32.38	$\underline{1.39 \times 10^{-1}}$	-
		66.76	1.78×10^{-2}	-
		97.15	3.3×10^{-3}	-
		129.53	2.76×10^{-4}	-
Fluence rate ~ 1.97 Wm^{-2}				

Table A4.43 DATA PERTAINING TO THE SURVIVOR CURVES OBTAINED WHEN AS44 WAS IRRADIATED AT 313 nm IN THE PRESENCE OF 0.1% ACETOPHENONE AT 0 °C, THE INACTIVATION PARAMETERS OF WHICH ARE GIVEN IN TABLE 3.12

EXPT No.	INITIAL VIABLE COUNT (ml^{-1})	CORRECTED FLUENCE (Jm^{-2})	SURVIVING FRACTION 313 nm	FLASH
43a	7.43×10^{6}	12.2	4.93×10^{-1}	6.32×10^{-1}
		24.4	1.53×10^{-1}	2.15×10^{-2}
		36.6	4.98×10^{-2}	7.17×10^{-2}
Fluence rate ~ 2.00 Wm^{-2}		48.8	1.51×10^{-2}	1.57×10^{-2}
		61.0	5.56×10^{-3}	1.13×10^{-2}
		73.2	1.82×10^{-3}	4.46×10^{-3}
		97.6	3.77×10^{-4}	7.18×10^{-4}
		122.0	6.37×10^{-5}	-
43b	8.9×10^{6}	12.15	3.7×10^{-1}	5.2×10^{-1}
		24.29	1.34×10^{-1}	2.31×10^{-2}
		36.44	4.72×10^{-2}	8.52×10^{-2}
Fluence rate ~ 2.00 Wm^{-2}		48.47	1.72×10^{-2}	2.21×10^{-2}
		60.58	6.16×10^{-3}	1.11×10^{-2}
		72.69	2.21×10^{-3}	3.81×10^{-3}
		96.92	2.83×10^{-4}	3.76×10^{-4}
		121.16	3.62×10^{-5}	-
43c	5.7×10^{6}	25.62	1.00×10^{-1}	-
		51.24	1.08×10^{-2}	-
Fluence rate ~ 1.75 Wm^{-2}		76.86	1.23×10^{-3}	-
		102.48	1.48×10^{-4}	-
43d	7.7×10^{6}	26.15	2.32×10^{-1}	-
		52.30	2.43×10^{-1}	-
Fluence rate ~ 1.75 Wm^{-2}		78.45	1.97×10^{-1}	-
		105.60	2.43×10^{-4}	-

Table A4.44 DATA PERTAINING TO THE SURVIVOR CURVES OBTAINED WHEN DY326 WAS IRRADIATED AT 313 nm IN THE PRESENCE OF 0.1% ACETOPHENONE AT 0 °C, THE INACTIVATION PARAMETERS OF WHICH ARE GIVEN IN TABLE 3.12

EXPT No.	INITIAL VIABLE COUNT (ml^{-1})	CORRECTED FLUENCE (Jm^{-2})	SURVIVING FRACTION 313 nm	FLASH
44a	1.38×10^{7}	12.2	$\underline{4.75 \times 10^{-1}}$	5.16×10^{-1}
		24.4	2.45×10^{-1}	$\underline{2.44 \times 10^{-1}}$
Fluence rate ~ 2.00 Wm^{-2}		36.6	1.0×10^{-1}	1.11×10^{-1}
		48.8	4.63×10^{-2}	4.60×10^{-2}
		61.0	2.2×10^{-2}	2.19×10^{-2}
		73.2	1.02×10^{-2}	1.03×10^{-2}
		97.6	2.23×10^{-3}	3.83×10^{-3}
		122.0	5.23×10^{-4}	-
44b	5.73×10^{6}	23.05	$\underline{3.32 \times 10^{-1}}$	2.61×10^{-1}
		46.10	6.43×10^{-2}	$\underline{6.41 \times 10^{-2}}$
Fluence rate ~ 1.99 Wm^{-2}		69.16	1.25×10^{-2}	1.23×10^{-2}
		92.20	2.42×10^{-3}	2.50×10^{-3}
		115.25	4.70×10^{-4}	4.68×10^{-4}
44c	6.87×10^{6}	33.00	$\underline{1.81 \times 10^{-1}}$	-
		66.00	2.15×10^{-2}	-
Fluence rate ~ 2.1 Wm^{-2}		99.00	1.90×10^{-3}	-
		132.00	2.62×10^{-4}	-
44d	1.47×10^{7}	23.00	$\underline{1.44 \times 10^{-1}}$	-
		46.12	4.35×10^{-2}	-
Fluence rate ~ 1.99 WM^{-2}		69.20	8.15×10^{-3}	-
		92.23	1.53×10^{-3}	-

Table A4.45 DATA PERTAINING TO THE SURVIVOR CURVES OBTAINED WHEN AS46 WAS IRRADIATED AT 313 nm IN THE PRESENCE OF 0.1% ACETOPHENONE AT 0 °C, THE INACTIVATION PARAMETERS OF WHICH ARE GIVEN IN TABLE 3.12

EXPT No.	INITIAL VIABLE COUNT (ml^{-1})	CORRECTED FLUENCE (Jm^{-2})	SURVIVING FRACTION 313 nm	SURVIVING FRACTION FLASH
45a	5.87×10^{6}	13.1	2.30×10^{-1}	2.41×10^{-1}
		26.2	6.25×10^{-2}	6.61×10^{-2}
Fluence rate ~ 2.01 Wm^{-2}		39.3	1.65×10^{-2}	1.56×10^{-2}
		52.4	4.01×10^{-3}	4.30×10^{-3}
		65.5	7.50×10^{-4}	7.69×10^{-4}
		78.6	2.32×10^{-4}	2.90×10^{-4}
		91.7	5.60×10^{-5}	6.04×10^{-5}
45b	4.80×10^{6}	11.4	3.68×10^{-1}	4.03×10^{-1}
		22.8	1.06×10^{-1}	9.30×10^{-2}
Fluence rate ~ 1.99 Wm^{-2}		35.0	3.28×10^{-2}	3.79×10^{-2}
		56.9	2.84×10^{-3}	3.09×10^{-3}
		68.4	7.96×10^{-4}	8.05×10^{-4}
		79.8	9.16×10^{-5}	-
45c	6.17×10^{6}	23.1	8.72×10^{-2}	-
		46.2	7.27×10^{-3}	-
Fluence rate ~ 2.1 Wm^{-2}		69.3	6.07×10^{-4}	-
		92.4	5.06×10^{-5}	-

Table A4.46 DATA PERTAINING TO PHOTOREACTIVATION OF ACP/313 nm UV IRRADIATED AB2480 (Fig. 3.36)

PR TIME (min)	SURVIVING FRACTION	CORRECTED (1-P)	h_t	$h_2e^{-\alpha_2 t}$	$h_t-h_2e^{-\alpha_2 t}$
0	2.76×10^{-4}	-	-	-	-
FLASH	2.95×10^{-3}	0.66/1.00	-	-	-
0.25	4.86×10^{-3}	0.89	4.19	2.25	1.94
0.50	7.97×10^{-3}	0.79	3.70	2.17	1.53
0.75	1.10×10^{-2}	0.72	3.37	2.09	1.28
1.50	4.21×10^{-2}	0.43	2.37	1.86	0.51
3	6.34×10^{-2}	0.35	1.62	1.48	0.14
5	1.1×10^{-1}	0.23	1.23	-	-
9	1.80×10^{-1}	0.16	0.58	-	-
14	2.52×10^{-1}	0.05	0.24	-	-
20	2.18×10^{-1}	0.08	-	-	-
30	3.21×10^{-1}	-	-	-	-

ACP ~ Acetophenone

Table A4.47 DATA PERTAINING TO PHOTOREACTIVATION OF ACP/313 nm UV IRRADIATED AS44 (Fig.3.36)

PR TIME (min)	SURVIVING FRACTION	CORRECTED (1-P)	h_t	$h_2e^{-\alpha_2 t}$	$h_t-h_2e^{-\alpha_2 t}$
0	1.48×10^{-4}	-	-	-	-
FLASH	2.21×10^{-4}	0.75/1.0	-	-	-
1	7.94×10^{-4}	0.81	4.84	2.33	2.51
2	1.50×10^{-3}	0.72	4.20	2.18	2.02
3	3.18x103	0.61	3.45	2.05	1.40
4	4.53×10^{-3}	0.56	3.09	1.92	1.17
8	1.81×10^{-2}	0.35	1.71	1.48	0.23
14	3.71×10^{-2}	0.25	0.99	-	-
20	5.10×10^{-2}	0.20	0.67	-	-
30	6.94×10^{-2}	0.16	0.37	-	-
45	8.59×10^{-2}	0.12	0.19	-	-
60	1.29×10^{-1}	-	-	-	-

ACP ~ Acetophenone

Table A4.48 DATA PERTAINING TO PHOTOREACTIVATION OF ACP/313 nm UV IRRADIATED DY326 (Fig. 3.36)

PR TIME (min)	SURVIVING FRACTION	1-P	h_t
0	1.86×10^{-4}	-	-
20	2.15×10^{-4}	0.978	0.883
40	2.35×10^{-4}	0.965	0.794
60	2.85×10^{-4}	0.936	0.601
80	3.20×10^{-4}	0.919	0.486
100	3.80×10^{-4}	0.893	0.314
120	4.20×10^{-4}	0.878	0.214
150	5.00×10^{-4}	0.850	0.039
180	5.20×10^{-4}	0.846	-

ACP ~ Acetophenone

Table A4.49 DATA PERTAINING TO THE SURVIVOR CURVES OBTAINED WHEN AS46/pBR322 GROWN AT 37°C WAS IRRADIATED AT 254 nm. THE SURVIVAL PARAMETERS ARE INCLUDED IN TABLE 4.3

EXPT No.	INITIAL VIABLE COUNT (ml^{-1})	254 nm FLUENCE RATE (Wm^{-2})	FLUENCE (Jm^{-2})	SURVIVING FRACTION
49a	1.5×10^{7}	0.053	0.07	3.13×10^{-1}
			0.141	9.47×10^{-2}
			0.211	3.30×10^{-2}
			0.281	6.40×10^{-3}
			0.351	1.51×10^{-3}
			0.422	4.43×10^{-4}
			0.492	1.15×10^{-4}
49b	2.9×10^{6}	0.061	0.08	1.90×10^{-1}
			0.162	5.86×10^{-2}
			0.242	1.07×10^{-2}
			0.324	2.24×10^{-3}
			0.404	2.93×10^{-4}
			0.485	1.08×10^{-4}
			0.565	3.62×10^{-5}

Table A4.50 DATA PERTAINING TO THE SURVIVOR CURVES OBTAINED WHEN AS46/pBR322 GROWN AT 26°C WAS IRRADIATED AT 254 nm. THE SURVIVAL PARAMETERS ARE INCLUDED IN TABLE 4.3

EXPT No.	INITIAL VIABLE COUNT (ml^{-1})	254 nm FLUENCE RATE (Wm^{-2})	FLUENCE (Jm^{-2})	SURVIVING FRACTION
50a	1.71×10^{7}	0.052	0.069	3.70×10^{-1}
			0.138	1.04×10^{-1}
			0.207	2.30×10^{-2}
			0.276	6.65×10^{-3}
			0.345	1.69×10^{-3}
			0.414	3.70×10^{-4}
			0.484	1.09×10^{-4}
50b	1.37×10^{7}	0.052	0.069	2.08×10^{-1}
			0.138	1.27×10^{-1}
			0.207	3.54×10^{-2}
			0.277	9.12×10^{-3}
			0.347	2.36×10^{-3}
			0.417	5.62×10^{-4}
			0.487	1.27×10^{-4}

Table A4.51 DATA PERTAINING TO THE SURVIVOR CURVES OBTAINED WHEN AS46/pASO1 GROWN AT 37°C WAS IRRADIATED AT 254 nm. THE SURVIVAL PARAMETERS ARE INCLUDED IN TABLE 4.3

EXPT No.	INITIAL VIABLE COUNT (ml^{-1})	254 nm FLUENCE RATE (Wm^{-2})	FLUENCE (Jm^{-2})	SURVIVING FRACTION
51a	2.2×10^{7}	0.061	0.084	3.4×10^{-1}
			0.169	3.70×10^{-2}
			0.254	1.21×10^{-2}
			0.337	2.05×10^{-3}
			0.420	5.91×10^{-4}
			0.504	1.09×10^{-4}
			0.588	2.27×10^{-4}
51b	5.1×10^{6}	0.061	0.082	3.04×10^{-1}
			0.164	6.47×10^{-2}
			0.246	9.40×10^{-3}
			0.328	1.47×10^{-3}
			0.407	3.04×10^{-4}
			0.487	9.51×10^{-5}
			0.568	2.45×10^{-5}

Table A4.52 DATA PERTAINING TO THE SURVIVOR CURVES OBTAINED WHEN AS46/pASO1 GROWN AT 26°C WAS IRRADIATED AT 254 nm. THE SURVIVAL PARAMETERS ARE INCLUDED IN TABLE 4.3

EXPT No.	INITIAL VIABLE COUNT (ml^{-1})	254 nm FLUENCE RATE (Wm^{-2})	FLUENCE (Jm^{-2})	SURVIVING FRACTION
52a	8.2×10^{6}	0.059	0.08	1.59×10^{-2}
			0.159	5.67×10^{-2}
			0.237	1.14×10^{-2}
			0.315	2.32×10^{-3}
			0.394	5.24×10^{-4}
			0.472	1.33×10^{-4}
			0.551	2.80×10^{-5}
52b	7.1×10^{6}	0.059	0.08	3.62×10^{-1}
			0.159	7.23×10^{-2}
			0.238	2.04×10^{-2}
			0.317	4.18×10^{-3}
			0.396	1.37×10^{-3}
			0.476	1.67×10^{-4}
			0.555	5.67×10^{-5}

Table A4.53 DATA PERTAINING TO THE SURVIVOR CURVES OBTAINED WHEN DY326/pBR322 GROWN AT 37°C WAS INACTIVATED AT 254 nm. THE SURVIVAL PARAMETERS ARE INCLUDED IN TABLE 4.3

EXPT No.	INITIAL VIABLE COUNT (ml^{-1})	254 nm FLUENCE RATE (Wm^{-2})	FLUENCE (Jm^{-2})	SURVIVING FRACTION
53a	1.4×10^{7}	0.053	0.07	3.21×10^{-1}
			1.41	8.14×10^{-2}
			0.212	2.00×10^{-2}
			0.283	6.25×10^{-3}
			0.353	1.50×10^{-3}
			0.424	4.50×10^{-4}
			0.495	1.10×10^{-4}
53b	1.4×10^{7}	0.053	0.072	3.10×10^{-1}
			0.142	9.20×10^{-2}
			0.214	2.19×10^{-2}
			0.285	6.76×10^{-3}
			0.356	2.10×10^{-3}
			0.428	4.32×10^{-4}
			0.499	1.31×10^{-4}

Table A4.54 DATA PERTAINING TO THE SURVIVOR CURVES OBTAINED WHEN DY326/pASO1 GROWN AT 37°C WAS IRRADIATED AT 254 nm. THE SURVIVAL PARAMETERS ARE INCLUDED IN TABLE 4.3

EXPT No.	INITIAL VIABLE COUNT (ml^{-1})	254 nm FLUENCE RATE (Wm^{-2})	FLUENCE (Jm^{-2})	SURVIVING FRACTION
54a	6.7×10^{6}	0.053	0.072	3.28×10^{-1}
			0.143	9.90×10^{-2}
			0.215	2.50×10^{-2}
			0.286	5.75×10^{-3}
			0.358	1.66×10^{-3}
			0.428	5.07×10^{-4}
			0.499	1.28×10^{-4}
54b	5.7×10^{6}	0.053	0.072	2.74×10^{-1}
			0.144	8.67×10^{-2}
			0.214	2.32×10^{-2}
			0.285	6.02×10^{-3}
			0.356	1.70×10^{-3}
			0.427	4.16×10^{-4}
			0.497	9.99×10^{-5}

Table A4.55 DATA PERTAINING TO THE PHOTOREACTIVATION OF 254 nm UV-INACTIVATED AS46/pBR322 GROWN AT 37°C

PR TIME	Experiment 55a			Experiment 55b		
(Min)	S/So	(1-P)	h_t	S/So	(1-P)	h_t
0	2.6×10^{-5}	-	-	8.04×10^{-5}	-	-
30	2.41×10^{-5}	-	-	7.3×10^{-5}	-	-
60	2.65×10^{-5}	0.99	-	6.81×10^{-5}	-	-
90	2.70×10^{-5}	0.98	-	8.02×10^{-5}	-	-
120	2.50×10^{-5}	-	-	8.48×10^{-5}	-	-
150	2.50×10^{-5}	-	-	-	-	-
180	3.0×10^{-5}	0.96	-	7.33×10^{-5}	-	-

Table A4.56 DATA PERTAINING TO THE PHOTOREACTIVATION OF 254 nm UV-INACTIVATED AS46/pBR322 GROWN AT 26°C. THE RATE PARAMETERS ARE INCLUDED IN TABLES 4.45

PR TIME	Experiment 56a			Experiment 56b		
(Min)	S/So	(1-P)	h_t	S/So	(1-P)	h_t
0	1.09×10^{-4}	-	-	1.27×10^{-4}	-	-
30	0.69×10^{-4}	0.94	0.98	2.85×10^{-4}	0.89	0.74
60	2.86×10^{-4}	0.867	0.45	3.39×10^{-4}	0.86	0.57
80	3.40×10^{-4}	0.481	0.28	4.52×10^{-4}	0.82	0.28
120	4.17×10^{-4}	0.815	0.03	5.33×10^{-4}	0.80	0.12
150	4.49×10^{-4}	0.805	-	5.70×10^{-4}	0.76	0.05
180	4.49×10^{-4}	0.805	-	6.0×10^{-4}	-	-

Table A4.57 DATA PERTAINING TO THE PHOTOREACTIVATION OF AS46/pASO1 GROWN AT 37°C. THE RATE PARAMETERS ARE INCLUDED IN TABLES 4.4-5.

PR TIME	Experiment 57a			Experiment 57b		
(Min)	S/So	(1-P)	h_t	S/So	(1-P)	h_t
0	2.45×10^{-5}	-	-	2.27×10^{-5}	-	-
30	2.70×10^{-5}	0.99	1.41	3.97×10^{-5}	0.93	1.20
60	3.14×10^{-5}	0.97	12.5	5.53×10^{-5}	0.89	0.87
90	4.22×10^{-5}	0.93	0.96	6.28×10^{-5}	0.88	0.63
120	7.65×10^{-5}	0.86	0.36	8.38×10^{-5}	0.84	0.45
150	8.33×10^{-5}	0.85	0.28	9.51×10^{-5}	0.83	0.33
180	1.10×10^{-4}	0.82	-	1.32×10^{-4}	0.79	-

Table A4.58 DATA PERTAINING TO THE PHOTOREACTIVATION OF AS46/pASO1 GROWN AT 26°C. THE RATE PARAMETERS ARE INCLUDED IN TABLES 4.4-5.

PR TIME	Experiment 58a			Experiment 58b		
(Min)	S/So	(1-P)	h_t	S/So	(1-P)	h_t
0	2.8×10^{-5}	-	-	5.67×10^{-5}	-	-
30	6.58×10^{-5}	0.90	2.03	1.41×10^{-4}	0.88	1.09
60	1.44×10^{-4}	0.80	1.24	2.55×10^{-4}	0.80	0.50
90	2.85×10^{-4}	0.72	0.56	3.08×10^{-4}	0.78	0.31
120	3.36×10^{-4}	0.70	0.40	3.60×10^{-4}	0.76	0.15
150	4.82×10^{-4}	0.66	0.04	4.0×10^{-4}	0.75	0.05
180	5.00×10^{-4}	0.64	-	4.2×10^{-4}	0.74	-

Table A4.59 DATA PERTAINING TO THE PHOTOREACTIVATION OF DY326/pBR322 GROWN AT 37°C. THE RATE PARAMETERS ARE INCLUDED IN TABLES 4.4-5.

PR TIME	Experiment 59a			Experiment 59b		
(Min)	$\bar{S}/So$	(1-P)	h_t	$\bar{S}/So$	(1-P)	h_t
0	1.10×10^{-4}	-	-	1.31×10^{-4}	-	-
30	2.46×10^{-4}	0.89	0.65	2.51×10^{-4}	0.91	0.65
60	3.50×10^{-4}	0.84	0.29	3.45×10^{-4}	0.86	0.33
90	3.96×10^{-4}	0.82	0.17	3.90×10^{-4}	0.84	0.21
120	4.20×10^{-4}	0.81	0.11	4.36×10^{-4}	0.83	0.09
150	4.4×10^{-4}	0.80	0.06	3.41×10^{-4}	-	-
180	4.7×10^{-4}	0.79	-	3.17×10^{-4}	-	-

Table A4.60 DATA PERTAINING TO THE PHOTOREACTIVATION OF DY326/pASO1 GROWN AT 37°C. THE RATE PARAMETERS ARE INCLUDED IN TABLES 4.4-5.

PR TIME	Experiment 60a			Experiment 60b		
(Min)	$\bar{S}/So$	(1-P	h_t	$\bar{S}/So$	(1-P)	h_t
0	1.28×10^{-4}	-	-	9.91×10^{-5}	-	-
30	1.51×10^{-4}	0.98	1.09	2.55×10^{-4}	0.87	0.63
60	2.13×10^{-4}	0.88	0.46	4.26×10^{-4}	0.80	0.11
120	3.14×10^{-4}	0.87	0.33	4.14×10^{-4}	0.80	0.14
150	3.82×10^{-4}	0.84	0.17	4.77×10^{-4}	0.78	-
180	4.53×10^{-4}	0.82	-	4.66×10^{-4}	0.78	-

Table A4.61 DATA PERTAINING TO UV INACTIVATION AND FLASH PHOTREACTIVATION SURVIVAL CURVES FOR AS44/pBR322 SHOWN IN FIG. 4.8 (PARAMETERS IN TABLE 4.6)

EXPT No.	INITIAL VIABLE COUNT (ml^{-1})	FLUENCE (Jm^{-2})	SURVIVING FRACTION 254 nm	FLASH
60a	1.58×10^{7}	0.069	$\underline{3.56 \times 10^{-1}}$	-
		0.139	9.49×10^{-2}	$\underline{2.10 \times 10^{-1}}$
FLUENCE RATE ~ 0.053 Wm^{-2}		0.210	1.65×10^{-2}	8.52×10^{-2}
		0.278	5.36×10^{-3}	2.33×10^{-2}
		0.347	1.49×10^{-3}	6.19×10^{-3}
		0.417	3.27×10^{-4}	2.35×10^{-3}
		0.486	9.49×10^{-5}	7.21×10^{-4}
60b	1.23×10^{7}	0.069	$\underline{3.66 \times 10^{-1}}$	5.08×10^{-1}
		0.138	9.47×10^{-2}	$\underline{2.36 \times 10^{-1}}$
FLUENCE RATE ~ 0.056 Wm^{-2}		0.208	2.85×10^{-2}	6.83×10^{-2}
		0.293	5.69×10^{-3}	2.44×10^{-2}
		0.347	1.33×10^{-3}	6.87×10^{-3}
		0.415	3.09×10^{-4}	1.94×10^{-3}
		0.485	9.07×10^{-5}	5.37×10^{-4}
60c	3.67×10^{6}	0.062	$\underline{3.27 \times 10^{-1}}$	4.18×10^{-1}
		0.126	1.15×10^{-1}	$\underline{2.36 \times 10^{-1}}$
FLUENCE RATE ~ 0.043 Wm^{-2}		0.189	4.24×10^{-2}	1.27×10^{-1}
		0.251	1.38×10^{-2}	5.22×10^{-2}
		0.315	4.31×10^{-3}	1.79×10^{-2}
		0.378	1.05×10^{-3}	6.18×10^{-3}
		0.442	2.65×10^{-4}	1.80×10^{-3}

Table A4.62 DATA PERTAINING TO UV INACTIVATION AND FLASH PHOTREACTIVATION SURVIVAL CURVES FOR AS44/pASO1 SHOWN IN FIG. 4.9 (PARAMETERS IN TABLE 4.6)

EXPT No.	INITIAL VIABLE COUNT (ml^{-1})	FLUENCE (Jm^{-2})	SURVIVING FRACTION 254 nm	SURVIVING FRACTION FLASH
61a	8.9×10^{6}	0.070	$\underline{4.61 \times 10^{-1}}$	7.53×10^{-1}
		0.139	1.12×10^{-1}	2.92×10^{-1}
FLUENCE RATE ~ 0.053 Wm^{-2}		0.208	2.97×10^{-2}	1.19×10^{-1}
		0.278	5.84×10^{-3}	4.49×10^{-2}
		0.348	1.73×10^{-3}	1.62x102
		0.418	3.54×10^{-4}	4.72×10^{-3}
		0.488	1.07×10^{-4}	1.46×10^{-3}
61b	1.97×10^{7}	0.075	$\underline{3.357 \times 10^{-1}}$	6.65×10^{-1}
		0.150	9.70×10^{-2}	$\underline{3.07 \times 10^{-1}}$
		0.225	2.26×10^{-2}	7.36×10^{-2}
FLUENCE RATE ~ 0.053 Wm^{-2}		0.300	5.48×10^{-3}	3.15×10^{-2}
		0.374	1.20×10^{-3}	9.31×10^{-3}
		0.450	2.66×10^{-4}	2.99×10^{-3}
		0.525	5.36×10^{-5}	6.85×10^{-4}

Table A4.63a DATA PERTAINING TO PHOTOREACTIVATION OF AS44/pBR322 (Figs. 4.10-12, Tables 4.7-8)

PR TIME (Min)	SURVIVING FRACTION	(1-P)	h_t	$h_2e^{-\alpha_2 t}$	$h_t-h_2e^{-\alpha_2 t}$
0	2.65×10^{-4}	-	-	-	-
F	3.94×10^{-3}	0.72/1.0	-	-	-
1	8.24×10^{-3}	0.69	3.46	1.41	2.05
2	1.17×10^{-2}	0.61	3.11	1.35	1.76
3	2.14×10^{-2}	0.49	2.51	1.28	1.23
4	3.02×10^{-2}	0.42	2.16	1.22	0.94
5	4.41×10^{-2}	0.34	1.79	1.17	0.62
6	4.79×10^{-2}	0.32	1.70	1.14	0.56
8	7.13×10^{-2}	0.24	1.31	1.01	0.30
10	8.45×10^{-2}	0.20	1.13	0.92	0.21
15	1.21×10^{-2}	0.13	0.78		
20	1.51×10^{-2}	-	0.56		
30	1.88×10^{-2}	-	0.34		
40	2.00×10^{-2}	-	0.27		
50	2.28×10^{-2}	-	0.14		
60	2.63×10^{-2}	-	-		

Table A4.63b DATA PERTAINING TO PHOTOREACTIVATION OF AS44/pBR322 (Tables 4.7-8)

PR TIME (Min)	SURVIVING FRACTION	(1-P)	h_t	$h_2e^{-\alpha_2 t}$	$h_t-h_2e^{-\alpha_2 t}$
0	4.09×10^{-5}	-	-	-	-
F	1.25×10^{-4}	0.86/11.0	-	-	-
1	7.22×10^{-4}	0.75	5.17	1.68	3.49
2	1.66×10^{-3}	0.63	4.34	1.59	2.75
3	3.23×10^{-3}	0.53	3.67	1.51	2.16
4	4.89×10^{-3}	0.47	3.26	1.44	1.82
5	8.17×10^{-3}	0.40	2.74	1.36	1.38
6	1.10×10^{-2}	0.35	2.44	1.29	1.15
8	1.55×10^{-2}	0.31	2.10	1.17	0.93
10	2.52×10^{-2}	0.24	1.62	1.05	0.57
15	4.60×10^{-2}	0.15	1.01		
20	6.50×10^{-2}	-	0.67		
30	8.90×10^{-2}	-	0.36		
40	1.04×10^{-1}	-	0.20		
50	1.20×10^{-1}	-	0.144		
60	1.27×10^{-1}	-	-		

Table A4.64a DATA PERTAINING TO PHOTOREACTIVATION OF AS44/pASO1 (Figs. 4.10-12, Tables 4.7-8)

PR (Min)	TIME SURVIVING FRACTION	(1-P)	h_t	$h_2e^{-\alpha_2 t}$	$h_t-h_2e^{-\alpha_2 t}$
0	3.40×10^{-4}	-	-	-	-
F	4.72×10^{-3}	0.69/1.0	-	-	-
1	1.05×10^{-2}	0.65	2.83	1.40	1.43
2	2.98×10^{-2}	0.41	1.79	1.22	0.57
3	4.87×10^{-2}	0.30	1.30	1.06	0.24
4	6.76×10^{-2}	0.22	0.97	0.93	0.04
5	7.76×10^{-2}	0.19	0.83	0.81	0.02
6	8.43×10^{-2}	0.17	0.75	-	-
8	8.82×10^{-2}	0.16	0.48	-	-
10	9.90×10^{-2}	0.14	0.39	-	-
15	1.40×10^{-1}	0.08	0.24	-	-
20	1.50×10^{-1}	-	0.11	-	-
30	1.73×10^{-1}	-	0.03	-	-
40	1.78×10^{-1}	-	-	-	-
50	1.68×10^{-1}	-	-	-	-
60	1.47×10^{-1}	-	-	-	-

Table A4.64b DATA PERTAINING TO PHOTOREACTIVATION OF AS44/pASOl (Tables 4.7-8)

PR (Min)	TIME SURVIVING FRACTION	(1-P)	h_t	$h_2e^{-\alpha_2 t}$	$h_t-h_2e^{-\alpha_2 t}$
0	2.7×10^{-4}	-	-	-	-
F	4.10×10^{-3}	0.57/1.0	-	-	-
1	9.88×10^{-3}	0.76	2.72	1.07	1.65
2	3.38×10^{-2}	0.41	1.49	0.96	0.53
3	5.36×10^{-2}	0.29	1.03	0.86	0.17
4	6.60×10^{-2}	0.23	0.82	0.77	0.05
5	7.43×10^{-2}	0.20	0.70	0.69	0.01
6	8.12×10^{-2}	0.19	0.61	-	-
8	9.20×10^{-2}	0.17	0.49	-	-
10	1.01×10^{-2}	0.14	0.39	-	-
15	1.20×10^{-1}	0.11	0.22	-	-
20	1.32×10^{-1}	0.06	0.13	-	-
30	1.44×10^{-1}	0.03	0.04	-	-
40	1.48×10^{-1}	-	0.01	-	-
50	1.51×10^{-1}	-	-	-	-
60	1.50×10^{-1}	-	-	-	-

APPENDIX 5

ANALYSIS OF COVARIANCE AND USE OF DUMMY (1,0) VARIABLES

All data were analysed by least squares linear regression analysis, and fitted to the form:-

$$y' = a + bx \qquad \ldots. 1$$

where y' is a prediction of the observed value y for the corresponding value of x, a is the intercept and b is the slope.

$$b = \frac{\Sigma xy - (\Sigma x)(\Sigma y)/n}{\Sigma x^2 - (\Sigma x)^2/n} \qquad \ldots. 2$$

$$a = \bar{y} - b\bar{x} \qquad \ldots. 3$$

The variance of y is given by:-

$$Sy^2 = \frac{\Sigma(y - \bar{y})^2}{n - 1} \qquad \ldots. 4$$

and

$$Sx^2 = \frac{\Sigma(x - \bar{x})^2}{n - 1} \qquad \ldots. 5$$

The sample correlation coefficient r is given by:-

$$r = \frac{1}{(n - 1)} \sum \left[\frac{(x - \bar{x})}{Sx}\right] \left[\frac{(y - \bar{y})}{Sy}\right]$$

and the sample covariance Sxy is given by:-

$$Sxy = \frac{1}{(n-1)} \sum (x - \bar{x})(y - \bar{y})$$

The total deviation, that is, $(y-\bar{y})$, is the sum of the explained deviation, $(y'-\bar{y})$, where y' is the predicted value of y at a given x knowing the regression of y on x, and the unexplained deviation, $(y-y')$:-

$$\Sigma(y - \bar{y}) = \Sigma(y' - \bar{y}) + \Sigma(y - y')$$

Total Dev. Explained Unexplained

Since, $(y' - \bar{y}) = bx$, the total variation is given by:-

$$\sum(y - \bar{y})^2 = b^2 \sum x^2 + \sum(y - y')^2$$

Since the variance is the variation divided by the number of degrees of freedom, and the F-ratio is the variance explained by the regression divided by the unexplained variance, F may be calculated from:-

$$F = \frac{b^2 \Sigma x^2 / 1}{\Sigma(y - y')^2 / n-2}$$

The coefficient of determination r^2, is given by:-

$$r^2 = \frac{\text{Explained variation of y}}{\text{Total variation of y}} \qquad \frac{\Sigma(y' - \bar{y})^2}{\Sigma(y - \bar{y})^2}$$

Using the example of having two sets of data (e.g. two survival curves for the same organism), where the logarithm of the surviving fraction is linearly related to the inactivating fluence, a third 'dummy' variable (1 or 0) is assigned to test the hypothesis that one survivor curve was affected by an additional factor, such as the day of the experiment, or variation in culture conditions.

Using the example set out below, two experiments are grouped together to form one regression model, but in addition, separate lines are calculated using the dummy variables x_2 and x_3.

To test the intercept location:-

$$y' = a + b_1x_1 + b_2x_2$$

if $x_2 = 1$, then $y' = a + b_1x_1 + b_2$

if $x_2 = 0$ then $y' = a + b_1x_1$

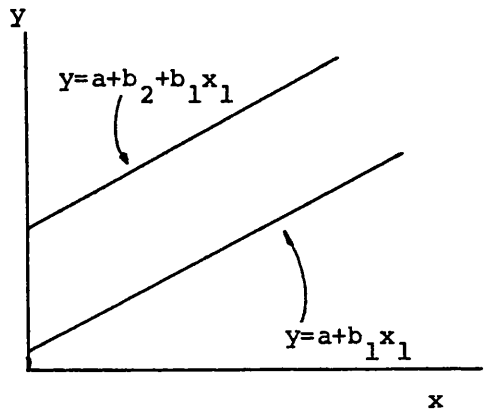

To test the slope location:-

$$y' = a + (b_1 + cx_3)x_1$$

if $x_3 = 1$, then $y' = a + (b_1 + c)x_1$

if $x_3 = 0$, then $y' = a + b_1x_1$

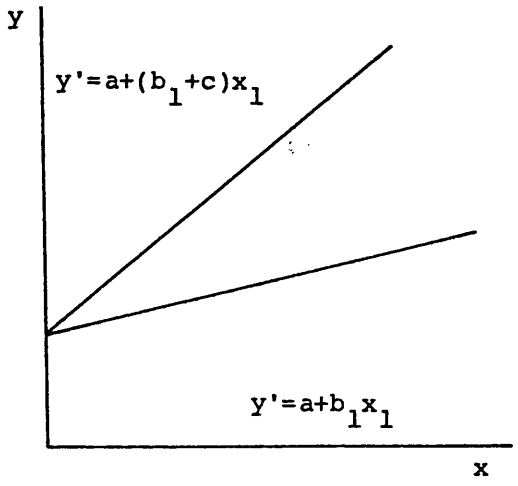

Having calculated the 'sums of squares and products' (SSP) matrix, including the 'dummy' variables, an F-value was calculated:-

$$F_{(j,n-m-1)} = \frac{(SSE_s - SSE)\ /j}{SSE\ /\ (n-m-1)}$$

where SSE_s is the sum of the squares of the errors of the grouped data only, and SSE is the amount of unexplained variation when all of the variables in the equation are included. J is the number of 'dummy' variables; n, the number of observations and m, the number sets of data. A dummy variable was assigned to the slope and intercept for each set of data, and the two parameters of each set were compared with the regression model. The F-ratio tests whether Ho, the joint effect of the dummy varaibles is not significant versus Hi, the dummy variables as a group do contribute to the explanation of the variation in y. Therefore, if the F-value exceeds the critical value with j,n-m-1 degrees of freedom, then the individual data is significantly different at that confidence interval.

BIBLIOGRAPHY

Achey, P. M., A. D. Woodhead and R. B. Setlow (1979) Photoreactivation of pyrimidine dimers in DNA from thyroid cells of the teleost Poecilia formosa. Photochem. Photobiol. 29,307-310.

Adhya, S., P. Cleary and A. Campbell (1968) A deletion analysis of prophage lambda and adjacent genetic regions. Proc. Natl. Acad. Sci. USA. 61,956-962.

Ahmed, F. E and R. B. Setlow (1979) DNA repair in Xeroderma pigmentosum cells treated with combinations of ultraviolet radiation and n-acetoxy-2-acetylaminofluorine. Cancer Res. 39,471-479.

Ananthaswamy, H. N. and M. S. Fisher (1981) Photoreactivation of ultraviolet radiation-induced pyrimidine dimers in neonatal BALB/c mouse skin. Cancer Res. 41,1829-1833.

Anderson, E. H. (1946) Growth requirements of virus-resistant mutants of Escherichia coli B. Proc. Natl. Acad. Sci. USA. 32,120-128.

Appleyard, R. K. (1954) Segregation of new lysogenic types during growth of a doubly lysogenic strain derived from Escherichia coli K-12. Genetics. 39,440-452.

Arikan, E., M. S. Kulkarni, D. C. Thomas and A. Sancar (1986) Sequences of the E. coli uvrB gene and protein. Nuc. Ac. Res. 14,2637-2650.

Bachmann, B. J. Linkage map of Escherichia coli, Edition 7. Microbiol. Rev. 14,180-230.

Backendorf, C., H. Spaink, A. P. Barbeiro and P. van de Putte (1986) Structure of the uvrB gene of Escherichia coli. Homology with other DNA repair enzymes and characterization of the uvrB5 mutation. Nuc. Ac. Res. 14,2877-2890.

Beukers, R. and W. Berends (1960) Isolation and identification of the irradiation product of thymine. Biochim. Biophys. Acta. 41,550-551.

Boatwright, D. T., J. J. Madden, J. Denson and H. Werbin (1975) Yeast DNA photolyase: molecular weight, subunit structure, and reconstitution of active enzyme from its subunits. Biochemistry. 14,5418-5421.

Bose, S. M. and R. J. H. Davies (1984) The photoreactivation of T-A sequences in oligodeoxyribonucleotides and DNA. Nuc. Ac. Res. 12,7903-7914.

Boyce, R. P. and P. Howard-Flanders (1964) Release of ultraviolet-induced thymine dimers from DNA in E. coli. Proc. Natl. Acad. Sci. USA. 51,293-300.

Brash, D. E. and W. A. Haseltine (1982) UV-induced mutation hotspots occur at DNA damage hotspots. Nature. 298,189-192.

Brash, D. E., W. A. Franklin, G. B. Sancar, A. Sancar and W. A. Haseltine (1985) Escherichia coli DNA photolyase reverses cyclobutane pyrimidine dimers but not pyrimidine-pyrimidone [6-4] photoproducts. J. Biol. Chem. 260,11438-11441.

Brash, D. E. and W. A. Haseltine (1985) Photoreactivation of Escherichia coli reverses umuC induction by UV light. J. Bacteriol. 163,460-463.

Bridges, B. A. and R. Woodgate (1984) Mutagenic repair in Escherichia coli. X. The umuC gene product may be required for replication past pyrimidine dimers but not for the coding error in UV-mutagenesis. Mol. Gen. Genet. 193,364-366.

Bridges, B. A. and R. Woodgate (1985) The two-step model of baterial UV mutagenesis. Mutation Res. 150,133-139.

Brown, M. S. and R. B. Webb (1972) Photoreactivation of 365 nm inactivation in Escherichia coli. Mutation Res. 15,348-352.

Campbell, A. (1961) Sensitive mutants of bacteriophage lambda. Virology. 14,22-32.

Caron, P. R., S. R. Kushner and L. Grossman (1985) Involvement of helicase II (uvrD gene product) and DNA polymerase I in excision mediated by the UVR ABC protein complex. Proc. Natl. Acad. Sci. USA. 82,4925-4929.

Chan, G. L., M. J. Peak, J. G. Peak and W. A. Haseltine (1986) Action spectrum for the formation of endonuclease-sensitive sites and [6-4] photoproducts induced in a DNA fragment by ultraviolet radiation. Int. J. Radiat. Biol. 50,641-648.

Cimino, G. D. and J. C. Sutherland (1982) Photoreactivating enzyme from Escherichia coli: Isolated enzyme lacks absorption in its actinic wavelength region and its ribonucleic acid cofactor is partially double-stranded when associated with apoprotein. Biochemistry. 21,3914-3921.

Clark, J. M. and G. P. Beardsley (1986) Thymine glycol lesions terminate chain elongation by DNA polymerase I in vitro. Nuc. Ac. Res. 14,737-749.

Cleaver, J. E. (1966) Photoreactivation: a radiation repair mechanism absent from mammalian cells. Biochem. Biophys. Res. Commun. 24,569-576.

Cook, J. S. and J. R. McGrath (1967) Photoreactivating enzyme in metazoa. Proc. Natl. Acad. Sci. USA. 58,1359-1365.

Cook, J. S. and J. D. Regan (1969) Photoreactivation and photoreactivating enzyme in an order of mammals (Marsupialia). Nature. 223,1066-1067.

Cox, R. and H. P. Charles (1973) Porphyrin accumulating mutants of Escherichia coli. J. Bacteriol. 113,122-132.

Csonka, L. N. and A. J. Clark (1980) Construction of an Hfr strain useful for transferring recA mutations between Escherichia coli strains. J. Bacteriol. 143,529-530.

D'Ambrosio, S. M., J. W. Whetstone, L. Slazinski and E. Lowney (1981) Photorepair of pyrimidine dimers in human skin in vivo. Photochem. Photobiol. 34,461-464.

D'Ambrosio, S. M., E. Bisaccia, J. W. Whetstone, D. A. Scarborough and E. Lowney (1983) DNA repair in skin of lupus erythematosus following in vivo exposure to ultraviolet radiation. J. Inv. Dermatol. 81,452-454.

Davies, D. J. G., S. A. Tyler and R. B. Webb (1970) A sequential repair model of photoreactivation in bacteria. Photochem. Photobiol. 11,371-386.

Demple, B. and S. Linn (1982) 5,6-saturated thymine lesions in DNA: Production by ultraviolet light and hydrogen peroxide. Nuc. Ac. Res. 10, 3781.

DeWitt, S. K. and E. A. Adelberg (1962) The occurrence of genetic transposition in a strain of Escherichia coli. Genetics. 47,577-585.

Dulbecco, R. (1949) Reactivation of ultraviolet inactivated bacteriophage by visible light. Nature. 163,949-950.

Eker, A. P. M. (1978) Some properties of a DNA photoreactivating enzyme from Streptomyces griseus. ICN-UCLA Symp. Mol. Cell Biol. 9,129-132.

Eker, A. P. M. (1980) Photoreactivating enzyme from Streptomyces griseus. III. Evidence for the presence of an intrinsic chromophore. Photochem. Photobiol. 32,593-600.

Eker, A. P. M. (1985) Studies on a DNA photoreactivating enzyme from Streptomyces griseus. Part 5. Evidence for the presence of an essential arginine residue in photoreactivating enzyme from Streptomyces griseus. J. Biochem. 229,469,476.

Eker, A. P. M. and A. M. J. Fichtinger-Shepman (1975) Studies on a DNA photoreactivating enzyme from Streptomyces griseus. II. Purification of the enzyme. Biochim. Biophys. Acta. 378,54-63.

Eker A. P. M., A. Pol, P. van der Meyden and G. D. Vogels (1980) Purification and properties of 8-hydroxy-5-deazaflavin derivatives from Streptomyces griseus. FEMS Microbiol. Lett. 8,161-165.

Eker, A. P. M., R. H. Dekker and W. Berends (1981) Photoreactivating enzyme from Streptomyces giseus. IV. On the nature of the chromophoric cofactor in Streptomyces griseus. Photochem. Photobiol. 33,65-72.

Eker, A. P. M., J. K. C. Hessels and R. H. Dekker (1986) Photoreactivating enzyme from Sreptomyces griseus. VI. Action

spectrum and kinetics of photoreactivation. Photochem. Photobiol. 44,197-205.

Ellison, M. J. and J. D. Childs (1981) Pyrimidine dimers induced in Escherichia coli DNA by ultraviolet radiation present in sunlight. Photochem. Photobiol. 34,465-469.

Farland, W. H. and B. M. Sutherland (1979 A rapid DEAE disk assay for photoreactivation of pyrimidine dimers in [^{3}H] DNA. Anal. Biochem. 97,376-381.

Franklin, W. A., K. Lo and W. A. Haseltine (1982) Alkaline lability of fluorescent photoproducts in ultraviolet light-irradiated DNA. J. Biol. Chem. 257,13535-13543.

Franklin, W. A. and W. A. Haseltine (1986) The role of the [6-4] photoproduct in ultraviolet-induced transition mutations in E. coli. Mutation Res. 165,1-7.

Friedberg, E. C. (1984) DNA Repair. W. H. Freeman and Co., New York.

Fukui, A., K. Hieda and Y. Matsudaira (1978) Light flash analysis of the photoenzymic repair process in yeast cells. I. Determination of the number of photoreactivating enzyme molecules. Mutation Res. 51,435-439.

Fukui, A., K. Hieda and Y. Matsudaira (1981) Light flash analysis of the photoenzymic repair process in yeast cells. II. Determination of the rate constant for formation of photo-reactivating enzyme-pyrimidine dimer complexes and its activation energy term. Mutation Res. 81,27-36.

Fukui, A. and W. Laskowski (1984a) Modifying factors of the cellular concentration of photolyase molecules in Saccharomyces cerevisiae cells. I. Effects of temperature and light. Photochem. Photobiol. 39,613-617.

Fukui, A. and W, Laskowski (1984b) Modifying factors of the cellular concentration of photolayse molecules in Saccharomyces cerevisiae. II. Effects of pre-illumination with light flashes. Photochem. Photobiol. 40,227-230.

Fukui, A. and W. Laskowski (1985) Light-illumination effects on the cellular concentration of photolyse molecules in yeast. Radiat. Environ. Biophys. 24,251-258.

Gallagher, P. E. and N. J. Duker (1986) Detection of UV purine photoproducts in a defined sequence of Human DNA. Mol. Cell Biol. 6,707-709.

Gates, F. L. (1930) A study of the bactericidal action of UV light. III. The absorption of ultraviolet light by bacteria. J. Gen. Physiol. 14,31-42.

Glickman, B. W., R. M. Schaaper, W. A. Haseltine, R. L. Dunn and D. E. Brash (1986) The C-C [6-4] UV photoproduct is mutagenic in Escherichia coli. Proc. Natl. Acad. Sci. USA. 83,6945-6949.

Gordon, L. K. and W. A. Haseltine (1982) Quantitation of cyclobutane pyrimidine dimer formation in double- and single-stranded DNA fragments of defined sequence. Radiat. Res. 89,99-112.

Guyer, M. S. (1978) The γδ sequence of F is an insertion sequence. J. Mol. Biol. 126,347-365.

Harm, H. and C. S. Rupert (1968) Analysis of photoenzymatic repair of UV lesions in DNA by single light flashes. I. In vitro studies with Haemophilus influenzae transforming DNA and yeast photoreactivating enzyme. Mutation Res. 6,355-370.

Harm, H. and C. S. Rupert (1970a) Analysis of photoenzymatic repair of UV lesions by single light flashes. VI. Rate constants for enzyme-substrate binding in vitro between yeast photoreactivating enzyme and ultraviolet lesions in Haemophilus transforming DNA. Mutation Res. 10,291-306.

Harm, H. and C. S. Rupert (1970b) Analysis of UV lesions in DNA by single light flashes. VII. Photolysis of enzyme-substrate complexes in vitro. Mutation Res. 10,307-318.

Harm, H. and C. S. Rupert (1976) Analysis of photoenzymatic repair of UV lesions in DNA by single light flashes. XI. Light-induced activation of the yeast photoreactivating enzyme. Mutation Res. 34,75-92.

Harm, W. and B. Hillebrandt (1962) A non-photoreactivable mutant of E. coli B. Photochem. Photobiol. 1,271-272.

Harm, W. (1969) Analysis of the photoenzymatic repair of UV lesions in DNA by single light flashes. IV. Mutations affecting the number of photoreactivating enzyme molecules in E. coli cells. Mutation Res. 8,411-415.

Harm, W. (1970) Analysis of photoenzymatic repair of UV lesions in DNA by single light flashes. V. Determination of the reaction rate constants in E. coli cells. Mutation Res. 10,277-290.

Harm, W. (1975) Kinetics of Photoreactivation. In Molecular Mechanisms for Repair of DNA. (Edited by P. C. Hanawalt and R. B. Setlow) pp 89-101. Plenum, New York.

Harm, W. (1979) Analysis of photoenzymatic repair of UV lesions in DNA by single light flashes. XII. Evidence for enhanced photolysis of enzyme-substrate complexes by a 2-photon reaction. Mutation Res. 60,121-133.

Harm, W., H. Harm and C. S. Rupert (1968) Analysis of photoenzymatic repair of UV lesions in DNA by single light flashes. II. In vivo studies with Escherichia coli and bacteriophage. Mutation Res. 6,371-385.

Harm, W., C. S. Rupert and H. Harm (1971) The Study of Photoenzymatic Repair in DNA by Flash Photolysis. In Photophysiology Vol. VI (Edited by A. C. Giese) pp 279-324.

Academic Press, New York.

Hatchard, C. G. and C. A. Parker (1956) A new sensitive chemical actinometer. II. Potassium ferrioxalate as a standard chemical actinometer. Proc. Roy. Soc. (London) A235,518-536.

Haynes, R. H. (1966) The interpretation of microbial inactivation and recovery phenomenon. Radiat. Res. 6,1-29.

Haynes, R. H., F. Eckardt and B. A. Kunz (1984) The DNA damage-repair hypothesis in radation biology: Comparison with classical hit theory. Br. J. Cancer 49S,81-90.

Hays, J. B., S. J. Martin and K. Bhatia (1985) Repair of non-replicating UV irradiated DNA: Co-operative dark repair by Escherichia coli UVR and PHR functions. J. Bacteriol. 161,602-608,

Heelis, P. F. and A. Sancar (1986) Photochemical properties of Escherichia coli DNA photolyase: A flash photolysis study. Biochemistry. 25,8163-8166.

Helene, C. and M. Charlier (1977) Photosensitized splitiing of pyrimidine dimers by indole derivatives and by tryptophan-containing oligopeptides and proteins. Photochem. Photobiol. 25,429-434.

Hodges, N. D. M. (1979) Ph.D. Thesis. University of Bath.

Hodges, N. D. M., S. H. Moss and D. J. G. Davies (1980) The role of pyrimidine dimers and non-dimer damage in the inactivation of of E. coli by UV radiation. Photochem. Photobiol. 31,571-580.

Howard-Flanders, P. (1981) Inducible Repair. Scientific American 245,56-74.

Howard-Flanders, P. and L. Theriot (1966) Mutants of Escherichia coli K-12 defective in DNA repair and in genetic recombination. Genetics. 53,1137-1150.

Husain, I., B. van Houten, D. C. Thomas, M. Abel-Monem and A. Sancar (1985) Effect of DNA polymerase I and DNA helicase II on the turnover rate of UVR ABC excision nuclease. Proc. Natl. Acad. Sci. USA. 82,6774-6778.

Husain, I. and A. Sancar (1987a) Binding of E. coli DNA photolyase to a defined substrate containing a single T-T dimer. Nuc. Ac. Res. 15,1109-1120.

Husain, I. and A. Sancar (1987b) Photoreactivation in phr mutants of Escherichia coli K-12. J. Bacteriol. 169,2367-2372.

Ihara, M., K. Yamamoto and T. Ohnishi (1987) Induction of phr gene expression by ultraviolet light in Escherichia coli. Mol. Gen. Genet. In Press.

Ingledew, W. J. and R. K. Poole (1984) The respiratory chains of Escherichia coli. Microbiol. Rev. 48,222-271.

Iwatsuki, N., C. O. Joe and H. Werbin (1980) Evidence that deoxyribonucleic acid photolyase from bakers' yeast is a flavoprotein. Biochemistry. 19,1172-1176.

Jagger, J. (1967) Introduction to Research in Ultraviolet Photobiology. Prentice Hall, New Jersey.

Jagger, J. (1985) Solar-UV Actions on Living Cells. Praeger, New York.

Jagger, J., R. S. Stafford and J. M. Snow (1969) Thymine-dimer and action spectrum evidence for indirect photoreactivation in Escherichia coli. Photochem. Photobiol. 10,383-395.

Johnson, R. G. and R. H. Haynes (1986a) Kinetics of photoreactivation and liquid holding recovery in yeast cells. Photochem. Photobiol. 43,413-421.

Johnson, R. G. and R. H. Haynes (1986b) Evidence from photoreactivation kinetics for multiple DNA photolyases in yeast. Photochem. Photobiol. 43,423-428.

Jorns, M. S., G. B. Sancar and A. Sancar (1984) Identification of a neutral flavin radical and characterization of a second chromophore in Escherichia coli DNA photolyase. Biochemistry 23,2673-2679.

Jorns, M. S., G. B. Sancar and A. Sancar (1985) Identification of oligothymidylates as new simple substrates for Escherichia coli DNA photolyase and their use in a rapid spectrophotometric assay. Biochemistry 24,1856-1861.

Jorns, M. S., E. T. Baldwin, G. B. Sancar and A. Sancar (1987) Action mechanism of Escherichia coli DNA photolyase. II. Role of the chromophores in catalysis. J. Biol. Chem. 262,486-491.

Kelland, L. R. (1984) Ph.D. Thesis. University of Bath.

Kelner, A. (1949) Effect of visible light on the recovery of Streptomyces griseus conidia from ultraviolet irradiation injury. Proc. Nat. Acad. Sci. USA. 35,73

Kittler, L. and G. Lober (1977) Photochemistry of the nucleic acids. Photochem. Photobiol. Rev. 2,39.

Kondo, S. and T. Kato (1966) Action spectra of killing and mutation to prototrophy in UV-sensitive strains of Escherichia coli possessing and lacking photoreactivating enzyme. Photochem. Photobiol. 5,827-837.

Lamola, A. A. (1969) Specific formation of thymine dimers in DNA. Photochem. Photobiol. 9,291-294.

Lamola, A. A. and T. Yamane (1967) Sensitized photodimerization of thymine in DNA. Proc. Natl. Acad. Sci. USA. 58,443-446.

Langeveld, S. A., A. Yasui and A. P. M. Eker (1985) Expression of an Escherichia coli phr gene in the yeast Saccharomyces cerevisiae. Mol. Gen. Genet. 199,396-400.

Lennox, E. S. (1955) Transduction of linked genetic characters of the host by bacteriophage Pl. Virology. 1,190-206.

Ley, R. D. (1984) Photorepair of pyrimidine dimers in the marsupial Monodelphis domestica. Photochem. Photobiol. 41,141-143.

Ley, R. D. (1985) Photoreactivation of UV-induced pyrimidine dimers and erythema in the marsupial Monodelphis domestica. Proc. Natl Acad. Sci. USA. 82,2409-2411.

Ley, R. D., B. A. Sedita and D. D. Grube (1978) Absence of photoreactivation of pyrimidine dimers in the epidermis of hairless mice following exposure to ultraviolet light. Photochem. Photobiol. 27,483-485.

Ley, R. D. and L. A. Applegate (1985) Ultraviolet radiation-induced histopathological changes in the skin of the marsupial Monodelphis domestica. II. Quantitative studies of the photoreactivation of induced hyperplasia and sunburn cell formation. J. Inv. Dermatol. 85,365-367.

Lippke, J. A., L. K. Gordon, D. E. Brash and W. A. Haseltine (1981) Distribution of UV light-induced damage in a defined sequence of Human DNA: Detection of alkaline sensitive lesions at pyrimidine nucleoside-cytidine sequences. Proc. Natl. Acad. Sci. USA 78,3388-3392.

Little, J. W. and D. W. Mount (1982) The SOS regulatory system of Escherichia coli. Cell. 29,11-22.

MacQuillan, A. M., A. Herman, J. S. Coberly and G. Green (1981) A second photoreactivation-deficient mutant in Saccharomyces cerevisiae. Photochem. Photobiol. 34,673-677.

Madden, J. J., H. Werbin and J. Denson (1973) A rapid assay for DNA photolyase using a membrane-binding technique. Photochem. Photobiol. 18,441.

Madden, J. J., J. Denson and H. Werbin (1976) Purification from bakers' yeast of an activator of DNA photolyase. Biochim. Biophys. Acta. 454,222-229.

Maniatis, T., E. Fritsch and J. Sambrook (1982) Molecular Cloning, a Laboratory Manual. Cold Spring Harbour Press, Cold Spring Harbour, New York.

Matson, S. W. (1986) Escherichia coli helicase II (uvrD gene product) translocates unidirectionally in a 3' to 5' direction. J. Biol. Chem. 261,10169-10175.

Meechan, P. J., K. M. Milam and J. E. Cleaver (1986) Evaluation of homology between cloned Escherichia coli and yeast DNA photolyase genes and higher eukaryotic genomes. Mutation Res. 166,143-147.

Miller, J. H. (1972) Experiments in Molecular Genetics. Cold Spring Harbour Press. Cold Spring Harbour, New York.

Minato, S. and H. Werbin (1971) Spectral properties of the chromophoric material associated with the deoxyribonucleic acid photoreactivating enzyme isolated from bakers' yeast. Biochemistry. 10,4503-4508.

Moolenaar, G. F., C. A. van Sluis, C. Backendorf and P. van de Putte (1987) Regulation of the Escherichia coli excision repair gene uvrC. Overlap between the uvrC structural gene and the region coding for a 24-kDa protein. Nuc. Ac. Res. 15,4273-4289.

Morowitz, J. M. (1950) Absorption effects in volume irradiation in microorganisms. Science. 111,229-230.

Mortelmans, K., J. E. Cleaver, E. C. Friedberg, M. C. Paterson, B. P. Smith and G. H. Thomas (1977) Photoreactivation of thymine dimers in UV-irradiated human cells: unique dependence on culture conditions. Mutation Res. 44,433-446.

Moss, S. H. (1972) Ph.D. Thesis. University of Bath.

Myles, G. M., B. van Houten and A. Sancar (1987) Utilization of DNA photolyase, pyrimidine dimer endonucleases and alkali hydrolysis in the analysis of abberant ABC excinuclease incisions adjacent to UV-induced DNA photoproducts. Nuc. Ac. Res. 15,1227-1243.

Nishioka, H. and W. Harm (1972) Analysis of photoenzymatic repair of UV lesions in DNA by single light flashes. IX. Excess production of photoreactivating enzyme in E. coli B_{s-1} 160 under different growth conditions, and its suppression by adenine. Mutation Res. 16,121-131.

Oh, E. Y. and L. Grossman (1986) The effect of Escherichia coli UVR protein binding on the topology of supercoiled DNA. Nuc. Ac. Res. 14,8557-8571.

Pac, C., J. Majima and H. Sakurai (1982) Structure-reactivity relationships in redox-photosensitised splitting of pyrimidine dimers and unusual enhancing effect of molecular oxygen. Photochem. Photobiol. 36,273-282.

Patrick, M. H. and H. Harm (1973) Substrate specificity of a bacterial UV-endonuclease and the overlap with in vitro photoenzymic repair. Photochem. Photobiol. 18,371-386.

Peak, J. G., M. J. Peak, R. S. Sikorski and C. A. Jones (1985) Induction of DNA-protein crosslinks in human cells by ultraviolet and visible radiations: action spectrum. Photochem. Photobiol. 41,295-302.

Perry, K. L., S. J. Elledge, B. B. Mitchell, L. Marsh and G. C. Walker (1985) UmuDC and mucAB operons whose products are required for UV light- and chemical mutagenesis: UMUD, MUCA and LEXA proteins share homology. Proc. Natl. Acad. Sci. USA. 82,4331-4331.

Piessens, J. P. and A. P. M. Eker (1975) Photoreactivation of template activity of UV-irradiated DNA in an RNA-polymerase system. A rapid assay for photoreactivating enzyme. FEBS Lett. 50,125.

Plakidou, S., K. G. Moffat, G. P. C. Salmond and G. Mackinnon (1984) Convenient transduction of recA with bacteriophage T4GT7. J. Bacteriol. 159,1072-1073.

Porsche, K. (1973) A specific photoreaction in polyadenylic acid. Proc. Natl. Acad. Sci. USA. 70,2638-2686.

Ramabhadran, T. V. and J. Jagger (1976) Mechanism of growth delay induced in Escherichia coli by near ultraviolet radiation. Proc. Natl. Acad. Sci. USA. 73,59-63.

Redpath, J. L. (1986) UV-type damage associated with ionizing radiation: A review. Int. J. Radiat. Biol. 50,191-203.

Resnick, M. A. and J. K. Setlow (1972) Photoreactivation and gene dosage in yeast. J. Bacteriol. 109,1307-1309.

Rosner, J. L. (1972) Formation, induction and curing of bacteriophage lysogens. Virology. 46,679-689.

Ruiz-Rubio, M., R. Woodgate, B. A. Bridges, G. Herrera and M. Blanco (1986) New role for photoreversible pyrimidine dimers in induction of prototrophic mutations in excision-deficient Escherichia coli by UV light. J. Bacteriol. 166,1141-1143.

Rupert, C. S. (1960) Photoreactivation of transforming DNA by an enzyme from bakers' yeast. J. Gen. Physiol. 43,573-595.

Rupert, C. S. (1962a) Photoenzymatic repair of ultraviolet damage in DNA. I. Kinetics of the reaction. J. Gen. Physiol. 45,703-724.

Rupert, C. S. (1962b) Photoenzymatic repair of ultraviolet damage in DNA. II. Formation of an enzyme-substrate complex. J. Gen. Physiol. 45,725-741.

Rupert, C. S. (1975) Enzymatic Photoreactivation: An Overview. In Molecular Mechanisms for Repair of DNA (Edited by P. C. Hanawalt and R. B. Setlow) Part A p.73. Plenum Press. New York.

Rupert, C. S., S. H. Goodgal and R. M. Herriott (1958) Photoreactivation in vitro of ultraviolet inactivated Haemophilus influenzae transforming factor. J. Gen. Physiol. 41,451.

Rupp, W. D. and P. Howard-Flanders (1968) Discontinuities in the DNA synthesized in an excision-deficient strain of Escherichia coli following ultraviolet irradiation. J. Mol. Biol. 31,291-304.

Sabourin, C. L. K. and R. D. Ley (1987) Isolation and characterization of a marsupial DNA photolyase. Photochem. Photobiol. 45S,75.

Saito, N. and H. Werbin (1970) Purification of a blue-green algal deoxyribonucleic acid photoreactivating enzyme - an enzyme requiring light as a physical cofactor to perform its catalytic function. Biochemistry. 9,2610-2620.

Sancar, A. and C. S. Rupert (1978a) Correction of the map location for the phr gene in Escherichia coli K-12. Mutation Res. 51,139-143.

Sancar, A. and C. S. Rupert (1978b) Cloning of the phr gene and amplification of photolyase in Escherichia coli. Gene. 4,295-308.

Sancar, A. and C. S. Rupert (1979) Penicillin selection of Escherichia coli deoxyribonucleic acid repair mutants. J. Bacteriol. 138,779-782.

Sancar, A., N. D. Clarke, J. Griswold, W. J. Kennedy and W. D. Rupp (1981a) Identification of the uvrB gene product. J. Mol. Biol. 148,63-76.

Sancar, A., B. M. Kacinski, D. L. Mott and W. D. Rupp (1981b) Identification of the uvrC gene product. Proc. Natl. Acad. Sci. USA. 78,5450-5454.

Sancar, A., R. P. Wharton, S. Seltzer, B. M. Kacinski, N. D. Clarke and W. D. Rupp (1981c) Identification of the uvrA gene product. J. Mol. Biol. 148,45-62.

Sancar, A., G. B. Sancar, W. D. Rupp, J. W. Little and D. W. Mount (1982a) LEXA protein inhibits transcription of the E. coli gene in vitro. Nature. 289,96-98.

Sancar, A. and W. D. Rupp (1983) A novel repair enzyme: UVRABC excision nuclease of Escherichia coli cuts a DNA strand on both sides of the damaged region. Cell. 33,249-260.

Sancar, A., K. A. Franklin and G. B. Sancar (1984a) Proc. Natl. Acad. Sci. USA. Escherichia coli DNA photolyase stimulates UVRABC excision nuclease in vitro. 81,7397-7401.

Sancar, A. and G. B. Sancar (1984) Escherichia coli DNA photolyase is a flavoprotein. J. Mol. Biol. 172,223-227.

Sancar, A., F. W. Smith and G. B. Sancar (1984b) Purification of Escherichia coli DNA photolyase. J. Biol. Chem. 259,6028-6032.

Sancar, G. B. (1985a) Expression of a Saccharomyces cerevisiae photolyase gene in Escherichia coli. J. Bacteriol. 161,769-771.

Sancar, G. B. (1985b) Sequence of the Saccharomyces cerevisiae phr1 gene and homology of the PHR1 photolyase to E. coli photolyase. Nuc. Ac. Res. 13,8231-8246.

Sancar, G. B., A. Sancar, J. W. Little and W. D. Rupp (1982b) The

uvrB gene of E. coli has both LEXA and LEXA-independent promoters. Cell. 28,523-530.

Sancar, G. B., F. W. Smith and A. Sancar (1983) Identification and amplification of the E. coli phr gene product. Nuc. Ac. Res. 11,6667-6678.

Sancar, G. B., F. W. Smith, M. C. Lorence, C. S. Rupert and A. Sancar (1984c) Sequences of the Escherichia coli photolyase gene and protein. J. Biol. Chem. 256,6033-6038.

Sancar, G. B., F. W. Smith and A. Sancar (1985) Binding of Escherichia coli DNA photolyase to UV-irradiated DNA. Biochemistry. 24,1849-1855.

Sancar, G. B., M. S. Jorns, G. Payne, D. J. Fluke, C. S. Rupert and A. Sancar (1987a) Action mechanism of Escherichia coli DNA photolyase. I. Formation of the enzyme-substrate complex. J. Biol. Chem. 262,492-498.

Sancar, G. B., F. W. Smith, G. Payne, M. Levy and A. Sancar (1987b) Action mechanism of Escherichia coli DNA photolyase. III. Photolysis of the enzyme-substrate complex and the absolute action spectrum. J. Biol. Chem. 262,478-485.

Schild, D., J. Johnston, C. Chang and R. K. Mortimer (1984) Cloning and mapping of Saccharomyces cerevisiae photoreactivation gene phrl. Mol. Cell Biol. 4,1864-1870.

Sedgwick, S. G. and P A. Goodwin (1985) Interspecies regulation of the SOS response by the E. coli $lexA^+$ gene. Mutation Res. 145,103-106.

Setlow, J. K. (1964) Effects of UV on DNA: Correlations among biological changes, physical changes and repair mechanisms. Photochem. Photobiol. 3,405-413.

Setlow, J. K. and R.B. Setlow (1963) The nature of the photo-reactivable lesion in DNA. Nature. 197,560-562.

Setlow, R. B. and J. K. Setlow (1962) Evidence that ultra-violet-induced thymine dimers in DNA can cause biological damage. Proc. Natl. Acad. Sci. USA. 48,1250-1257.

Setlow, R. B. and W. L. Carrier (1964) The disappearance of thymine dimers from DNA: an error correcting mechanism. Proc. Natl. Acad. Sci. USA. 51,226.

Setlow, R. B. and W. L. Carrier (1966) Pyrimidine dimers in ultra-violet irradiated DNAs. J. Mol. Biol. 17,237-254.

Shine, J. and L. Dalgarno (1974) 3'-terminal sequence of Escherichia coli 16S ribosomal RNA ~ complementarity to nonsense triplets and ribosome binding sites. Proc. Natl. Acad. Sci. USA. 71,1342-1346.

Silhavy, T. J., S. A. Benson and S. D. Emr (1983) Mechanisms of protein localization. Microbiol. Rev. 47,313-344.

Silhavy, T. J., M. L. Berman and L. W. Enquist (1984) Experiments with Gene Fusions. Cold Spring Harbour Press. Cold Spring Harbour, New York.

Snapka, R. M. and C. O. Fuselier (1977) Photoreactivating enzyme from Escherichia coli. Photochem. Photobiol. 25,415-420.

Snapka, R. M. and B. M. Sutherland (1980) Escherichia coli photoreactivating enzyme: Purification and properties. Biochemistry. 19,4201-4208.

Sutherland, B. M. (1974) Photoreactivating enzyme in human leukocytes. Nature. 248,109-112.

Sutherland, B. M.,D. Court and M. J. Chamberlin (1972) Studies on the DNA photoreactivating enzyme from Escherichia coli. 1. Transduction of the phr gene by bacteriophage lambda. Virology. 48,87-93.

Sutherland, B. M. and M. J. Chamberlin (1973) A rapid and sensitive assay for pyrimidine dimers in DNA. Anal. Biochem. 53,168-176.

Sutherland, B. M., M. J. Chamberlin and J. C. Sutherland (1973) Deoxyribonucleic acid photoreactivating enzyme from Escherichia coli: Purification and properties. J. Biol. Chem. 248,4200-4205.

Sutherland, B. M., P. Runge and J. C. Sutherland (1974) DNA photoreactivating enzyme from placental mammals, origins and characteristics. Biochemistry. 13,4710-4715.

Sutherland, B. M. and R. Oliver (1975) Low levels of photoreactivating enzyme in Xeroderma pigmentosum variants. Nature. 257,132-143.

Sutherland, B. M., M. Rice and K. E. Wagner (1975) Xeroderma pigmentosum cells contain low levels of photoreactivating enzyme. Proc. Natl. Acad. Sci. USA. 72,103-107.

Sutherland, B. M. and R. Oliver (1976) Culture conditions affect photoreactivating enzyme levels in human fibroblasts. Biochim. Biophys. Acta. 442,358-367.

Sutherland, B. M. and S. C. Hausrath (1979) Multiple loci affecting photoreactivation in Escherichia coli. J. Bacteriol. 138,333-338.

Sutherland, B. M., L. C. Harber and I. E. Kochevar (1980) Pyrimidine dimer formation and repair in human skin. Cancer Res. 40,3181-3185.

Sutherland, B. M., O. M. Oliveira, G. Ciarrocchi, D. E. Brash, W. A. Haseltine, R. J. Lewis and P. C. Hanawalt (1986) Substrate range of the 40,000-Dalton photoreactivating enzyme from Escherichia coli. Biochemistry. 25,681-687.

Sutherland, J. C. and B. M. Sutherland (1975) Human photoreactivating enzyme: Action spectrum and safelight conditions. J. Biophys. 15,435-440.

Tang, M-S. and L. Ross (1985) Single-strand breakage of DNA in UV-irradiated uvrA, uvrB and uvrC mutants of Escherichia coli. J. Bacteriol. 161,933-938.

Tang, M-S., J. Herncir, D. Mitchell, J. Ross and J. Clarkson (1986) The relative cytotoxicity and mutagenicity of cyclobutane pyrimidine dimers and [6-4] photoproducts in Escherichia coli cells. Mutation Res. 161,9-17.

Thomas, D. C., M. Levy and A. Sancar (1985) Amplification and purification of the UVRA, UVRB and UVRC proteins of Escherichia coli. J. Biol. Chem. 260,9875-9883.

Tyrrell, R. M. (1971) Ph.D. Thesis. University of Bath.

Tyrrell, R. M. (1973a) Induction of pyrimidine dimers in bacterial DNA by 365 nm radiation. Photochem. Photobiol. 17,69-73.

Tyrrell, R. M. (1973b) Suppression of photoreactivating enzyme production in Escherichia coli grown under anaerobic conditions. J. Bacteriol. 115,450-452.

Tyrrell, R. M., S. H. Moss and D. J. G. Davies (1972) The variation in photoreactivating enzyme activity as a function of the stage of growth of three K-12 strains of Escherichia coli. Mutation Res. 16,345-352.

Tyrrell, R. M. and R. B. Webb (1973) Reduced dimer excision in bacteria following near-ultraviolet (365 nm) radiation. Mutation Res. 19,361-364.

Tyrrell, R. M., R. B. Webb and M. S. Brown (1973) Destruction of photoreactivating enzyme by 365 nm radiation. Photochem. Photobiol. 18,249-254.

Tyrrell, R. M. and D. J. G. Davies (1974) The kinetics of photoreactivation in the ultraviolet-sensitive mutant Escherichia coli K-12 AB2480. Mutation Res. 23,151-161.

Van de Putte, P., C. A. van Sluis, J. van Dillewijn and A. Rorsch (1965) The location of genes controlling radiation sensitivity in Escherichia coli. Mutation Res. 2,97-110.

Walker, G. C. (1984) Mutagenesis and inducible responses to deoxyribonucleic acid damage in Escherichia coli. Microbiol. Rev. 48,60-93.

Wang, S. Y. (1960) Reversible behaviour of the ultraviolet irradiated deoxyribonucleic acid and its apurinic acid. Nature. 188,844-846.

Wang, T. V. and K. C. Smith (1985a) Mechanism of sbcB-suppression of the recBC deficiency in post-replication repair in UV-irradiated Escherichia coli K-12. Mol. Gen. Genet.

201,186-191.

Wang, T. V. and K. C. Smith (1985b) Role of the umuC gene in post-replication repair in UV-irradiated Escherichia coli B. Mutation Res. 145,107-112.

Wang, T. V. and K. C. Smith (1986) Post replication formation and repair of double-strand breaks in UV-irradiated Escherichia coli uvrB cells. Mutation Res. 165,39-44.

Werbin, H. and J. J. Madden (1977) The subunit structure of yeast DNA photolyase and the purification of a fluorescent activator of the enzyme. Photochem. Photobiol. 25,421-427.

Whittaker, D. M. (1942) Counteracting the retarding and inhibitory effects of strong ultraviolet on Fucus eggs by white light. J. Gen. Physiol. 25,391-397.

Witkin, E. M. (1976) Ultraviolet mutagenesis and inducible DNA repair in Escherichia coli. Bacteriol. Rev. 40,869.

Woodhead, A. D. and P. M. Achey (1979) Photoreactivating enzyme in the blind cavefish, Anoptichthys jordani. Comp. Biochem. Physiol. 63,73-76.

Wulff, D. L. and C. S. Rupert (1962) Disappearance of thymine photodimers in ultraviolet-irradiated DNA upon treatment with a photoreactivating enzyme from bakers' yeast. Biochem. Biophys. Res. Commun. 7,237-240.

Wun, K. L., A. Gih and J. C. Sutherland (1977) Photoreactivating enzyme from Escherichia coli: Appearance of new absorption on binding to ultraviolet irradiated DNA. Biochemistry. 16,921-924.

Yamamoto, K. (1985) Photoreactivation reverses ultraviolet radiation-induced pre-mutagenic lesions leading to frameshift mutations in Escherichia coli. Mol. Gen. Genet. 201,141-145.

Yamamoto, K., Y. Fujiwara and H. Shinagawa (1983a) Evidence that the phr$^+$ gene enhances the ultraviolet resistance of Escherichia coli recA strains in the dark. Mol. Gen. Genet. 192,282-284.

Yamamoto, K., M. Satake, H. Shinagawa and Y. Fujiwara (1983b) Amelioration of the ultraviolet sensitivity of an Escherichia coli recA mutant in the dark by photoreactivating enzyme. Mol. Gen. Genet. 190,511-515.

Yamamoto, K., M. Satake and H. Shinagawa (1984) A multi-copy phr- plasmid increases the ultraviolet resistance of a recA strain of Escherichia coli. Mutation Res. 131,11-18.

Yamamoto, K., H. Shinagawa and T. Ohnishi (1985) Photoreactivation of UV damage in Escherichia coli uvrA6: Lethality is more effectively reversed than either pre-mutagenic lesions or SOS induction. Mutation Res. 146,33-42.

Yasui, A. and S. A. Langeveld (1985) Homology between the photoreactivation genes of Saccharomyces cerevisiae and Escherichia coli. Gene. 36,349-355.

Yeung, A. T., W. B. Mattes and L. Grossman (1986) Protein complexes formed during the incision reaction catalyzed by the Escherichia coli UVRABC endonuclease. Nuc. Ac. Res 14,2567-2582.

Youngs, D. A. and K. C. Smith (1978) Genetic location of the phr gene of Escherichia coli K-12. Mutation Res. 51,131-137.

Zwetsloot, J. C., W. Vermeulen, J. H. J. Hoeijmakers, A. Yasui, A. P. M. Eker and D. Bootsma (1985) Microinjected photoreactivating enzyme from Anacystis and Saccharomyces monomerize dimers in chromatin of human cells. Mutation Res. 146,71-77.

Zwetsloot, J. C. M., J. H. J. Hoeijmakers, W. Vermeulen, A. P. M. Eker and D. Bootsma (1986) Unscheduled DNA synthesis in Xeroderma pigmentosum cells after microinjection of yeast photoreactivating enzyme. Mutation Res. 165,109-115.